Some studies of the reactions of amines with aldehydes and with aromatic nitro - compounds in acetonitrile

Simon D. Lord

SOME STUDIES OF THE REACTIONS OF AMINES WITH ALDEHYDES AND WITH AROMATIC NITRO - COMPOUNDS IN ACETONITRILE

by

Simon D. Lord, B.Sc. (Dunelm)

Hatfield College

A thesis submitted for the degree of Doctor of Philosophy in the Department of Chemistry, University of Durham
1996

SOME STUDIES OF THE REACTIONS OF AMINES WITH ALDEHYDES AND WITH AROMATIC NITRO - COMPOUNDS IN ACETONITRILE

by Simon D. Lord

A thesis submitted for the degree of Doctor of Philosophy in the Department of Chemistry, University of Durham, 1996

ABSTRACT

Kinetic and equilibrium studies of the reactions between three trinitroaromatic species, 1,3,5-trinitrobenzene, ethyl 2,4,6-trinitrophenyl ether and phenyl 2,4,6-trinitrophenyl ether and the aliphatic amines n-butylamine, pyrrolidine and piperidine, in acetonitrile were undertaken. It was found that the reactions between 1,3,5-trinitrobenzene and each amine were too fast to measure. However kinetic information was gained from the decomposition of the σ-adducts formed from 1,3,5-trinitrobenzene and both pyrrolidine and piperidine. Both the 3-adduct and the 1-adduct are observed as intermediates in the reaction of the ethyl ether with each amine, though formation of the 3-adduct was too fast to measure by stopped flow spectrometry. Formation of the picramides is subject to general acid catalysis due to the poor leaving group ability of the ethoxide ion. Only the 3-adduct intermediate was observed in the formation of each picramide from the phenyl ether. The fact that the 1-adduct is not seen is attributed to the phenoxide ion being a weaker base and hence a much superior leaving group to the ethoxide ion. The equilibrium constants $K_{c,3}^{o}$ and $K_{c,1}^{o}$ are a factor of ca. 10^4 smaller in acetonitrile than dimethyl sulphoxide. This is due to acetonitrile being inferior to dimethyl sulphoxide in its ability to solvate charged species. The value of k_{Am} for reaction at an unsubstituted position approaches the diffusion controlled limit of acetonitrile.
The reactions of propanal, 2-chloroethanal, 2,2-dichloroethanal and 2,2,2-trichloroethanal (chloral) with ammonia and several primary amines were studied. Only the reactions of ammonia with propanal and 2-chloroethanal produced the corresponding 2,4,6-trisubstituted-1,3,5-hexahydrotriazine.
Reactions of the aldehydes with primary amines yield propylidene imines as relatively stable species. Trimerisation was not observed however the imine may undergo dimerisation together with elimination of amine.
Kinetic and equilibrium studies are reported on the formation in acetonitrile of 2,4,6-triethyl-1,3,5-hexahydrotriazine, (TEHT), from propanal and ammonia, and also the corresponding decomposition reaction. The equilibrium constant was found to decrease with increasing water content in the acetonitrile which can be attributed to stabilisation of ammonia by the water. Good correlation was achieved for values of the equilibrium constant calculated directly from absorbance measurements and from combination of rate constants obtained from the formation and decomposition reactions.

DECLARATION

The material in this thesis is the result of research undertaken in the Department of Chemistry, University of Durham between October 1992 and October 1995. It is the original work of the author except where acknowledged by reference and has not been submitted for any other degree.

STATEMENT OF COPYRIGHT

ACKNOWLEDGEMENTS

I would like to express my thanks to my supervisor, Dr. M.R. Crampton, for his time, guidance and friendship throughout my time in Durham.

I also wish to thank my industrial supervisor Dr. R. W. Millar and the Defence Research Agency for funding this project.

I am grateful for the friendship and support of my colleagues and close friends Alex, Ian, Andy, Rachel, Helen, Gaynor, Jonathan, John, Pablo, Kathryn, Andrew, E, Sahab, Ana, Sarah, Stumpy, Christian, Tom, Marky, Archie, Ginger, Sam, Rob, Tim, Paddy and Pecky. I would also like to express my gratitude all members of department staff for their assistance, but especially Colin Greenhalgh for his help with maintaining all our machines and Hazel and Jean for keeping my lab in order and the amusing chats during the production of this thesis.

In addition I would like to thank Nick, Dave and all those who I have played basketball with, the Grad. Soc. and University Staff footy lads, Lenny, Durham City Football Club and Newcastle Eagles Basketball Club (as well as their predecessors) for making my time in Durham so enjoyable.

Thanks also to Audrey and Brian for the paper and chat each morning, Mick for all his help at Maiden Castle, Lynne for making sure I was fit for sport, Martin for his beer and the staff at Hatfield College including Eric, Pam, Linda, Lynne and especially Joe who I sorely miss.

Finally I feel the numbers 6, 34 and 113 need a mention!

To the memory of my Nan
and to my parents who made it all possible.

CONTENTS

Chapter 1

Introduction to Nucleophilic Aromatic Substitution

1.1 Nucleophilic Aromatic Substitution

Nucleophilic displacements at an unsubstituted aromatic ring position rarely occur due to the fact that the hydride ion (H^-) is a very poor leaving group[1]. However the presence of a good leaving group on the ring allows nucleophilic aromatic substitution to take place by one of the following mechanisms.

1.1.1 S_NAr

An aromatic ring that contains strong electron withdrawing groups and a good leaving group, can undergo nucleophilc displacement via the S_NAr mechanism as in equation 1.1.

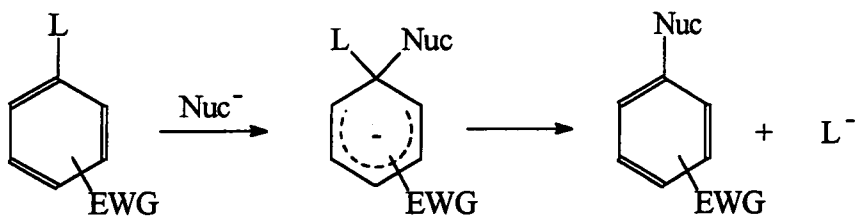

1.1 1.2

Equation 1.1

L^- = good leaving group or nucleofuge, e.g. Cl^-
Nuc^- = anionic or neutral nucleophile, e.g. RO^-, RNH_2
EWG = one or more electron withdrawing groups, e.g. NO_2

Non electron-deficient benzene derivatives tend not to undergo nucleophilic addition due to repulsion between the nucleophile and the π-electron system. The introduction of electron withdrawing groups (e.g. NO_2) has the effect of reducing the electron density of the benzenoid ring and thus promoting nucleophilic attack.
The first step in this addition-elimination mechanism is formation of a negatively charged Meisenheimer complex, or σ-complex, 1.1. The second is expulsion of the leaving group and rearomatisation of the ring in formation of the product, 1.2. This nucleophilic substitution mechanism is analogous to that of electrophilic substitution, where a positively charged intermediate is formed and the reaction is promoted by electron releasing groups.

Evidence for the S_NAr mechanism first came from work by Jackson[2] and Meisenheimer[3]. Meisenheimer proved that σ-complexes of the form 1.1 existed by isolating 1.3 from the reaction between 1-ethoxy-2,4,6-trinitrobenzene with methoxide.[3]

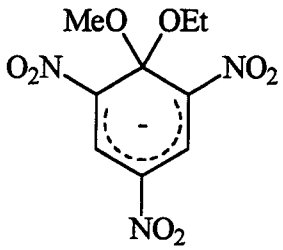

1.3

The stability of Meisenheimer complexes is enhanced by the use of protic - dipolar aprotic cosolvent systems, e.g. H_2O - DMSO or ROH - DMSO. The use of DMSO as a cosolvent has greatly increased the range of adducts to be studied. This has yielded more information on the kinetics of the formation and decomposition of σ-complexes and hence the mechanism of S_NAr processes.[4-9] The kinetic measurements have been obtained by use of U.V./Visible spectroscopy. However this method gives very little structural information. NMR has been found to be a much improved technique to determine the structure of intermediates.

The reaction between picryl chloride and methoxide was initially believed to form the 1-adduct, 1.4[10] when followed by U.V./Visible techniques. However the use of NMR proved the observable species to be the 3-adduct 1.5. 1.4 is a low concentration intermediate which will rapidly lose chloride ions and be converted to the substitution product. The energy diagram is shown in figure 1.1.

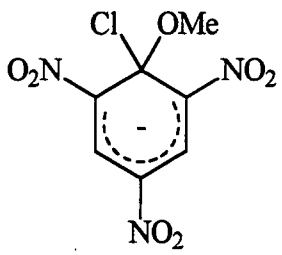

1.4

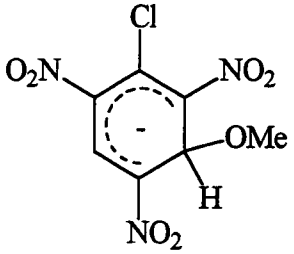

1.5

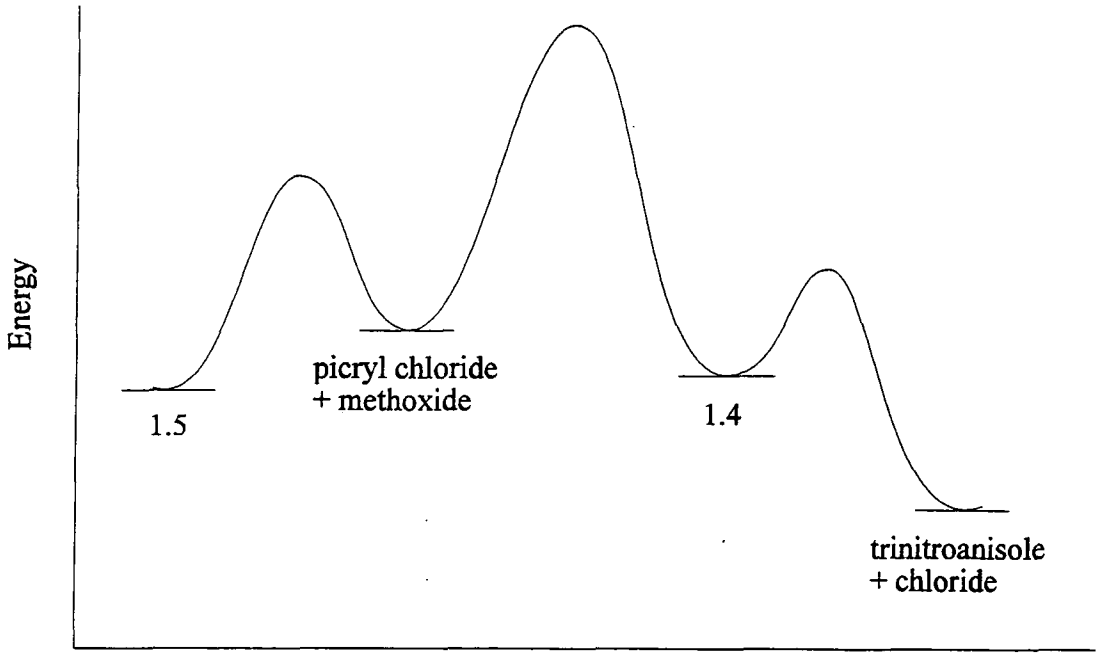

Figure 1.1

1.1.2 The Benzyne Mechanism

The reaction of iodo-, bromo-, or chloro-benzene with potassium amide yields aniline.[11] These compounds have no strong electron withdrawing groups and hence the S_NAr mechanism cannot be operating. The reaction of chlorobenzene-1-^{14}C with potassium amide[11] yields aniline in which roughly half of the ^{14}C is present in the 1-position and half in the 2-position as shown in equation 1.2.

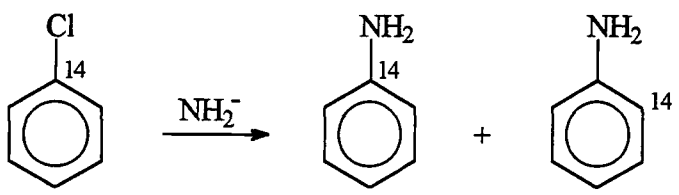

Equation 1.2

Therefore the overall substitution must proceed via an elimination-addition mechanism in which the highly strained intermediate benzyne is formed.[13-15] The symmetrical benzyne can then be attacked by ammonia at either of two positions, explaining why half of the labelled carbon is at the 2-position.

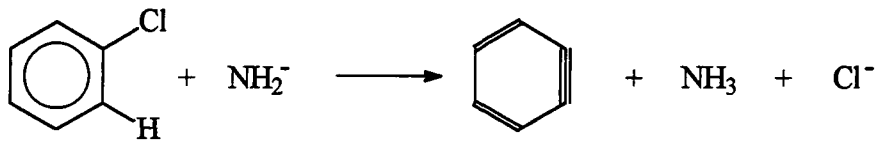

1.6

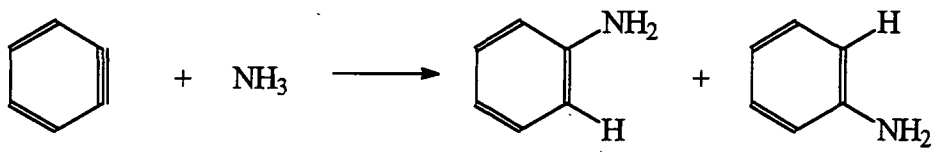

Comparison of the rate constants of formation of aniline from bromobenzene and bromobenzene-2-d gives a $k_H / k_D = 5.5$. This shows that proton abstraction is involved in the rate determining step.[14] Fluorobenzene-2-d exchanges its deuterium with solvent a million times faster than deuterobenzene, but no aniline is formed.[16] Apparently when the halogen is weakly electron withdrawing but a good leaving group, hydrogen abstraction is the slow step; though, when the halogen is strongly electron withdrawing but unreactive as a leaving group, its expulsion is the slow step. Further proof of benzyne being the intermediate in these reactions has been gained from trapping experiments. Generation of benzyne in the presence of anthracene gives the Diels-Alder adduct triptycene, 1.7.[17,18]

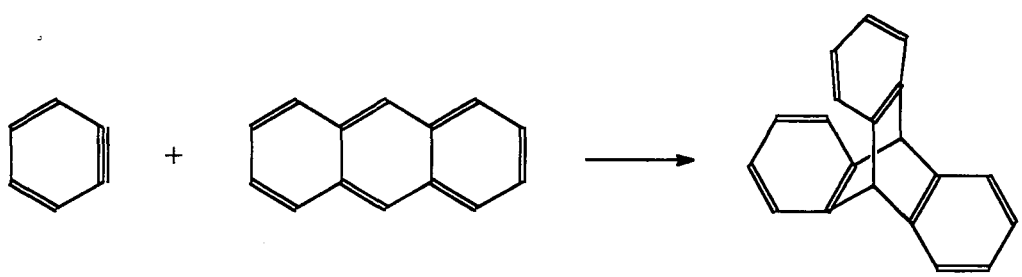

1.7

1.1.3 Nucleophilic Substitution on Aromatic Diazonium Compounds

A nucleophilic aromatic substitution mechanism, specific for substitution on aromatic diazonium salts is shown in equation 1.3.

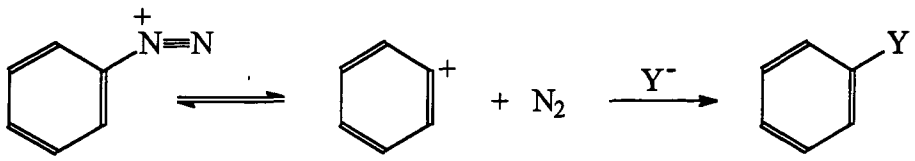

1.8

Equation1.3

There is excellent evidence that 1.8 is the intermediate.[19-22] The diazonium salt reacts with D_2O to give only 1.9; no 1.10 is formed. Hence the benzyne mechanism can be ruled out.

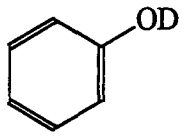

1.9

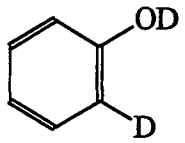

1.10

Labelling experiments have also provided evidence for 1.8 being the intermediate. When the starting material is selectively labelled with ^{15}N, the rearrangement shown in equation 1.4 occurs.

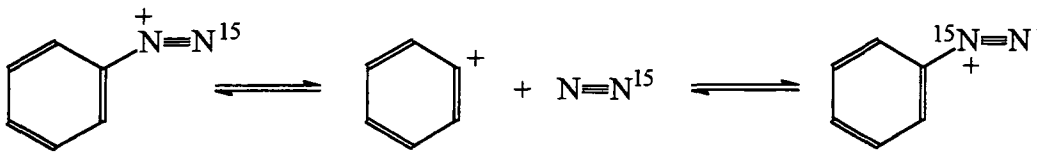

1.11

Equation 1.4

A proportion of 1.11 must procede via 1.8 and not via the intermediate 1.12, as when the experiment is carried out under 300 atm of unlabelled nitrogen, 2.5% of unlabelled nitrogen is incorporated into the diazonium cation.[22]

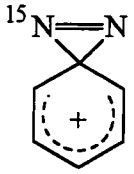

1.12

1.1.4 Single Step Mechanism for Nucleophilic Aromatic Substitution

Generally nucleophilic aromatic substitutions occur by one of the mechanisms shown in scheme 1.1. Either addition then elimination, path A, or elimination followed by addition, path B, occurs. This suggests that such conditions might exist, by suitable manipulation of the structures of solvent, nucleophile, leaving group and aromatic substrate to favour a concerted mechanism.

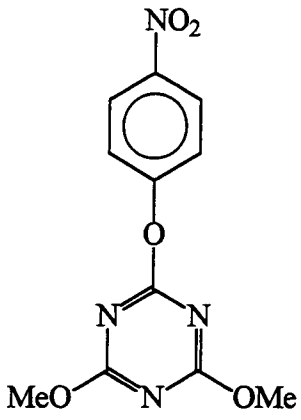

1.13

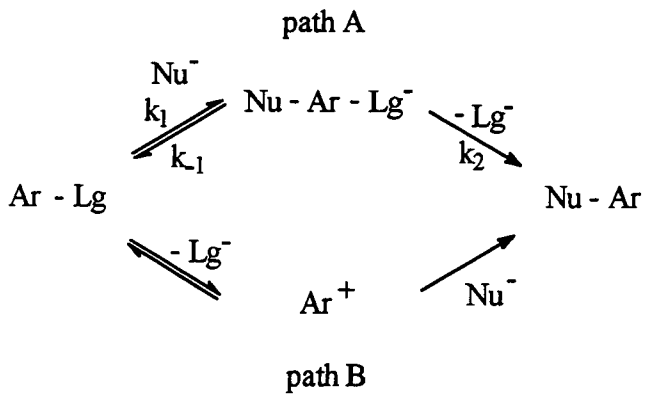

Scheme1.1

Recent work has been published indicating that displacement of the 4-nitrophenolate ion from 2-(4-nitrophenoxy)-4,6-dimethoxy-1,3,5-triazine, 1.13, by a series of substituted phenolate ions, proceeds via a single step mechanism rather than a two step one involving an intermediate.[23] The Bronsted plot shows an absence of curvature over a range of pK_{ArOH} values well above and well below that for 4-nitrophenol. This linearity is consistent with a concerted process having a single transition state, or at least a borderline mechanism between stepwise and concerted. The stepwise mechanism would have predicted a change in rate limiting step at $\Delta pK=0$ where forward, k_2, and reverse, k_{-1}, rate constants would be the same.

1.1.5 Radical Mechanisms, $S_{RN}1$ and $S_{RN}2$

Nucleophilic substitution reactions can occur through a chain process with radicals and radical anions as intermediates. Two possibilities for the propagation step involve fragmentation of the radical anion to give a radical, which reacts with the nucleophile ($S_{RN}1$) or reaction of the radical anion with the nucleophile to give the substitution product ($S_{RN}2$).

The reaction of 5-chloro-1,2,4-trimethylbenzene with potassium in liquid ammonia yields 5-amino- and 6-amino-1,2,4-trimethylbenzene in a ratio[24] of 0.68 : 1, as shown in equation 1.5. The reaction of the 6-chloro-isomer gave an identical ratio of products. The bromo compounds give similar results. These amination reactions must then proceed via a benzyne intermediate.

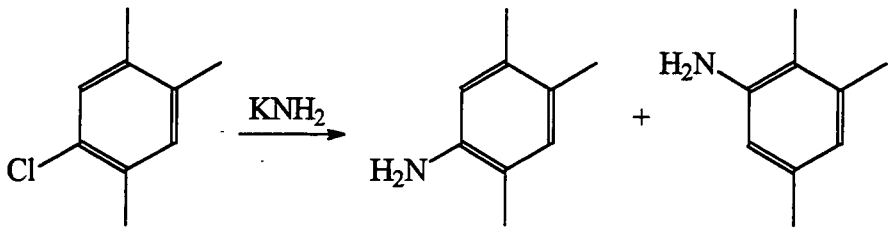

Equation 1.5

The iodo compounds give similar results only in the presence of a radical scavenger.[24] In the absence of a radical scavenger, the 5-iodo- isomer gives the 5-amino- and 6-amino- products in a ratio of 15.9 : 1 respectively. Similarly the 6-iodo- isomer yields mainly the 6-amino- product. Bunnett proposed the following $S_{RN}1$ (reductively initiated nucleophilic substitution, unimolecular) mechanism for the major radical component of the reaction shown in scheme 1.2.

$$ArI \xrightarrow{e^-} ArI^{\cdot -} \qquad \text{initiation step}$$

$$ArI^{\cdot -} \longrightarrow Ar^{\cdot} + I^- \qquad \text{chain propagation 1}$$

$$Ar^{\cdot} + NH_2^- \longrightarrow ArNH_2^{\cdot -} \qquad \text{chain propagation 2}$$

$$ArNH_2^{\cdot -} + ArI \longrightarrow ArNH_2 + ArI^{\cdot -} \qquad \text{chain propagation 3}$$

termination steps

Scheme 1.2

The electrons in the initiation step were provided from the potassium in ammonia.

The $S_{RN}2$ mechanism involves reaction of the radical anion with the nucleophile to give the radical anion of the substitution product and the anion of the leaving group. Generally, though, it is thought that the reaction of radical anions with nucleophiles cannot compete kinetically with their fragmentation.[25] However for reactions involving relatively stable radical anions which may fragment slowly, the $S_{RN}2$ mechanism may operate.

1.1.6 $S_{ON}2$ Mechanism

The $S_{ON}2$ (oxidatively initiated nucleophilic substitution, bimolecular) mechanism[26] is another example of an electron-transfer chain process. The reaction of p-fluoroanisole with ethanoate ion is an example as shown in equation 1.6

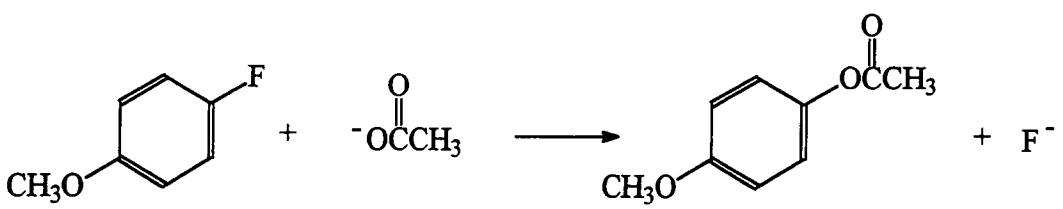

Equation 1.6

This reaction requires anodic initiation. The mechanism is shown in scheme 1.3.

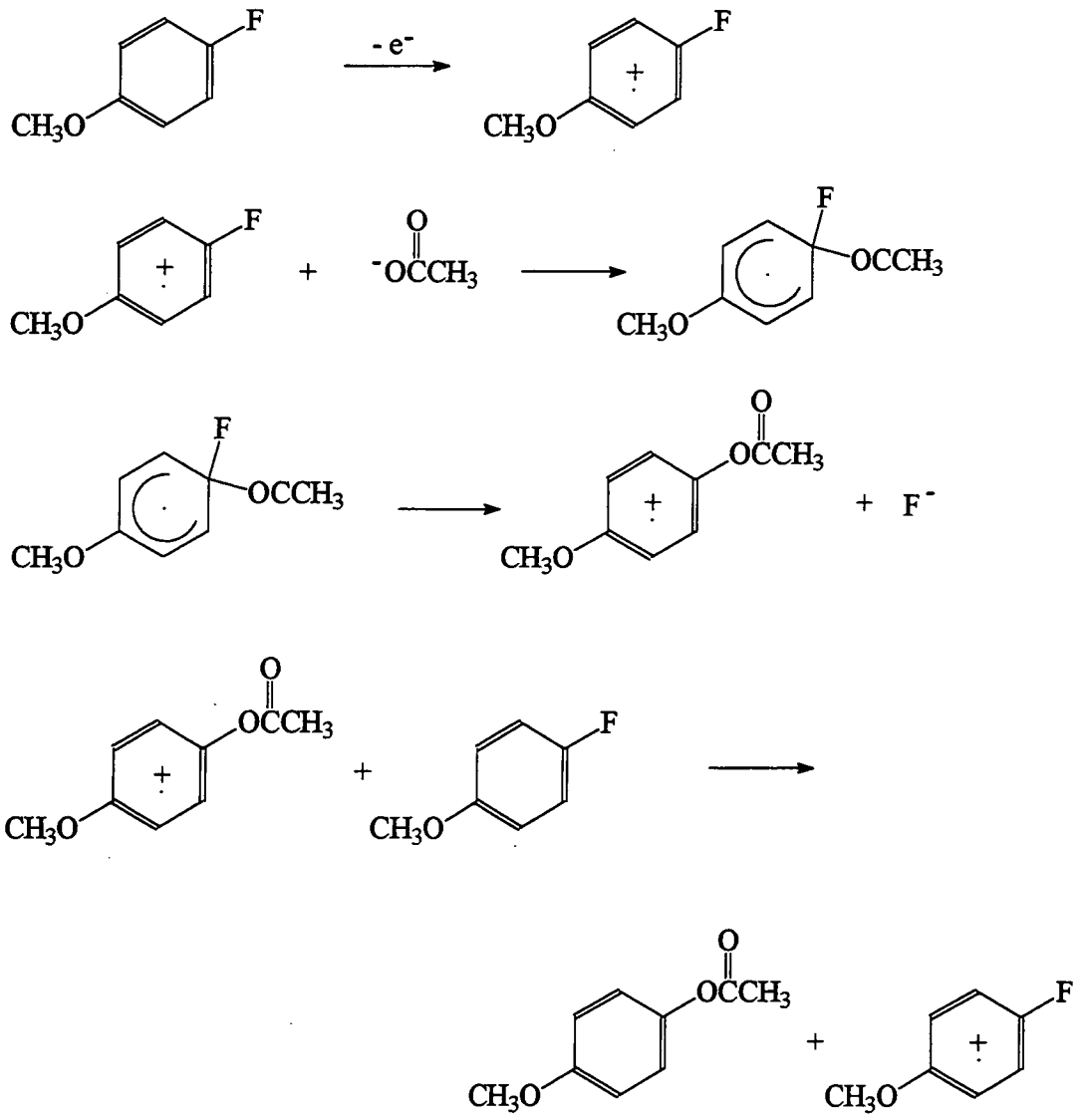

Scheme 1.3

The number of possible starting materials that react by this mechanism is limited. Both the leaving group and the nucleophile must be difficult to oxidize, and the product must be less oxidizable than the starting material or else the last step is inhibited.

1.1.7 Vicarious Nucleophilic Substitution VS_NArH

Nucleophilic substitution of hydrogen via the S_NAr mechanism is not a common process since the hydride (H^-) ion has a very low stability and is thus a poor leaving group.[26-28] However reactions are known in which an aromatic hydrogen atom is replaced by the attacking nucleophile. These involve σ-complex type intermediates that can decompose via oxidation pathways[29] as in equation 1.7.

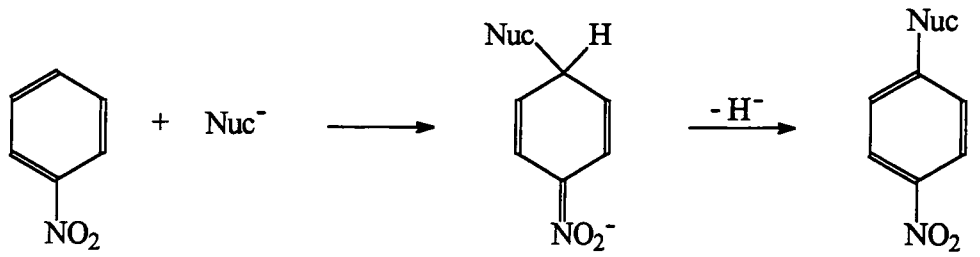

Equation 1.7

Alternatively, rearomatization of the intermediate can occur via a series of chemical transformations not involving an oxidation step. An example of this is vicarious nucleophilic substitution. Here rearomatization is afforded by the intermediate eliminating a nucleofugal group, initially present at the reaction centre of the attacking nucleophile.[1,5,30,31] as shown in equation 1.8.

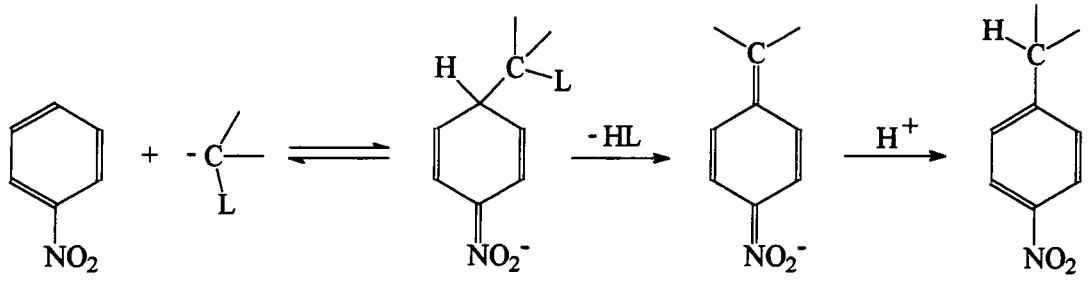

Equation 1.8

Many VS_NArH reactions have been developed by Makosza and co-workers. They found that carbanions containing leaving groups at the reaction centre react rapidly with nitroarenes, replacing the hydrogen atom para- or ortho- to the nitro group.[32,32] Scheme 1.4 shows this behaviour in the reaction of nitrobenzene with the carbanion of chloromethyl phenyl sulphone in the presence of a strong base (KOH, NaOH or t-BuOK) in DMSO[33,34] to give 4-nitrobenzyl phenyl sulphone, 1.14a, or 2-nitrobenzyl phenyl sulphone, 1.15.

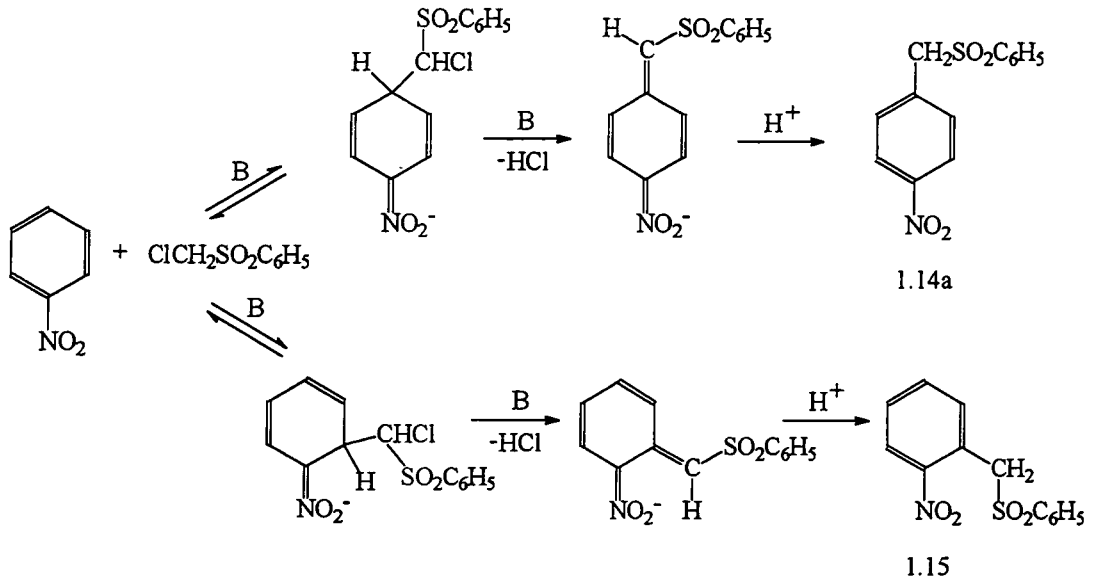

Scheme 1.4

A major feature of the VS_NArH reaction is its applicability to many substituted nitroarenes, including those that possess a good leaving group.[35] 4-Chloro-, 4-bromo- and 4-iodo-nitrobenzenes react with the anion of chloromethyl phenyl sulphone as shown in scheme 1.5 to give exclusively the corresponding 3-halo-6-nitrobenzyl phenyl sulphones, 1.16. No α-chloro-4-nitrobenzyl phenyl sulphone, 1.14b, which would be formed in the S_NAr substitution of halogen atoms could be detected. This shows that the overall vicarious substitution pathway proceeds at a much faster rate than that of S_NAr substitution.

However, with the greater electronegativity of F and NO_2 relative to Cl, Br and I, in the reaction of the carbanion with p-fluoronitrobenzene and p-dinitrobenzene, the S_NAr process becomes competitive with the VS_NArH one, and both sulphones are produced.

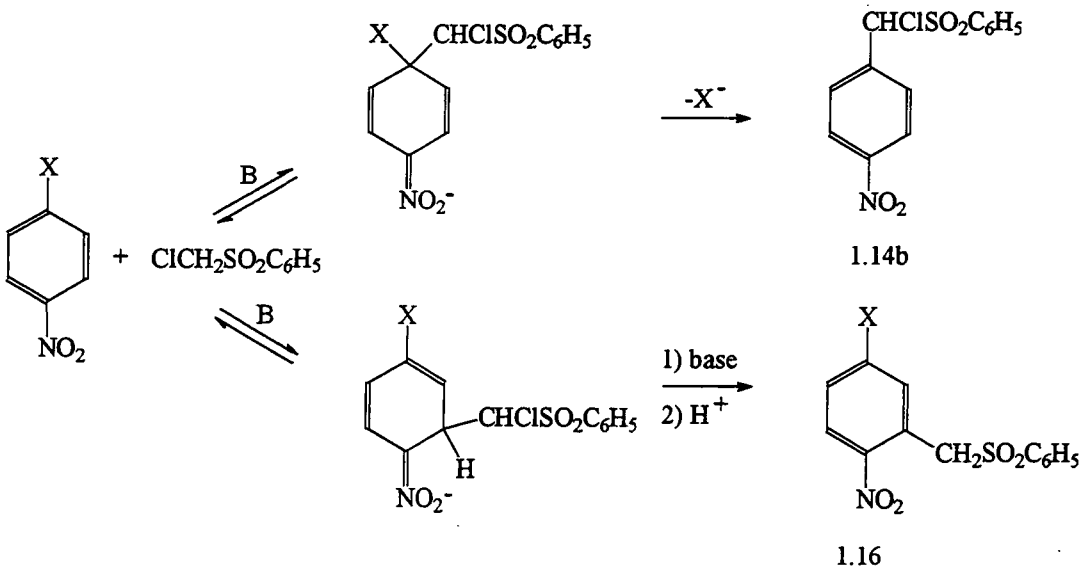
X
B
+ ClCH2SO2C6H5
B
NO2
X
CHClSO2C6H5
NO2-
-X-
CHClSO2C6H5
NO2
1.14b
X
CHClSO2C6H5
H
NO2-
1) base
2) H+
X
CH2SO2C6H5
NO2
1.16

Scheme 1.5

1.2 S_NAr Reactions with Amines

The reaction with anionic nucleophiles proceeds as in equation 1.1 (p.2). The rate-limiting step may be either formation or decomposition of the Meisenheimer complex, 1.1, depending on the energy of the two transition states. The reaction with neutral nucleophiles, e.g. primary or secondary amines, requires a slightly modified mechanism as shown in equation 1.9.

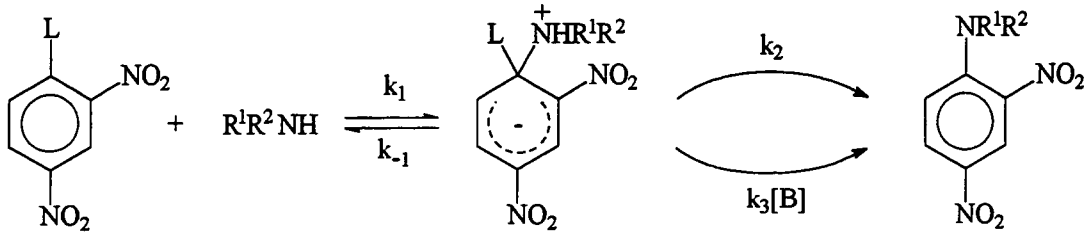

1.17 (ZH)

Equation 1.9

In this case the Meisenheimer complex, 1.17, is a zwitterionic adduct containing an NH proton which can be removed by base. Hence decomposition of the intermediate is susceptible to base catalysis and can proceed to products either directly (k_2) or via pathways afforded by removal of the NH proton ($k_3[B]$). The latter process generally has a much lower activation energy than the uncatalysed one and hence should be relatively favoured. The base may be the nucleophilic amine reactant or another base added to the reaction mixture.[36,37]
The rate expression for systems as in equation 1.9 is of the form:

$$\frac{\text{rate}}{[ArL][R^1R^2NH]} = \frac{k_{obs}}{[R^1R^2NH]} = k'_{obs} = \frac{k_1k_2 + k_1k_3[B]}{k_{-1} + k_2 + k_3[B]} \qquad \text{equation 1.10}$$

Three cases of interest arise from equation 1.10.

i) $k_2 + k_3[B] >> k_{-1}$

In this instance equation 1.10 reduces to $k'_{obs} = k_1$ and formation of the intermediate becomes rate limiting, with no possibility of base catalysis.

ii) $k_2 + k_3[B] << k_{-1}$

Under this condition equation 1.10 reduces to equation 1.1

$$k'_{obs} = \frac{k_1 k_2}{k_{-1}} + \frac{k_1 k_3 [B]}{k_{-1}} \qquad \text{equation 1.11}$$

This corresponds to the intermediate ZH being formed in a rapidly established equilibrium and decomposition of ZH being rate limiting. This predicts the occurrence of base catalysis with k'_{obs} being linearly dependent on base concentration.

iii) $k_2 + k_3[B] \approx k_{-1}$

At low base concentrations a situation as in case ii) arises where $k_2 + k_3[B] < k_{-1}$ and k'_{obs} shows a linear dependence on concentration of base. At increasing base concentrations the dependence of k'_{obs} changes in curvilinear fashion until at high base concentrations where $k_2 + k_3[B] > k_{-1}$ as in case i), no base catalysis is observed due to formation of ZH being rate limiting.

All three cases have been observed in the multitude of kinetic studies probing the reaction in equation 1.9.[36-40] These studies have shown whether base catalysis is or is not in operation, or how effective it is depends on the nature of amine, the leaving group, the base added and the solvent.

Generally base catalysis is most commonly observed with secondary rather than primary amines, with poor leaving groups and in less polar solvents.

The last two observations are the simplest to account for. The condition that $k_{-1} >> k_2 + k_3[B]$ for base catalysis will be most easily fulfilled with poor (F, OR, SR) than with good (Cl, Br, I) leaving groups. Non-polar solvents are much better at solvating uncharged species than charged ones. Since reversion of the zwitterionic intermediates to reactants leads to charge neutralization, k_{-1} is expected to be much larger in non-polar solvents, thus satisfying the above condition.

The reason for base catalysis being more prominent with secondary rather than with primary amines is seemingly due to the role of the ortho-NO_2 group. Evidence has been presented for the stabilization of zwitterionic intermediates from intramolecular hydrogen bonding between the ammonio proton and the ortho-nitro group.[41] For both adducts of the primary amine, 1.18, and the secondary amine, 1.19, the reduction of the k_{-1} value should be similar.

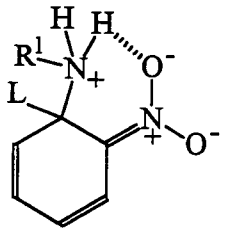

1.18

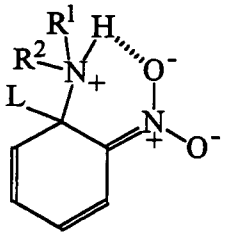

1.19

However the influence on the value of k_2 should be markedly different. Structure 1.18 has a non-hydrogen bonded proton that is readily transferred to the leaving group. Structure 1.19 has its only transferrable proton tied up through hydrogen bonding. This must be broken before it can be transferred. This will lead to a large decrease in the ratio of $(k_2 + k_3[B]) / k_{-1}$ for secondary amines but will have little effect for primary amines.

It should nevertheless be remembered that the ring carbon at the position of substitution is sp^3 hybridised. Hence the ammonium group will not be in the ring plane. This will render difficult potential hydrogen-bonding as shown in 1.18 and 1.19. Further, dimethyl sulphoxide, in which many studies have been carried out, is an excellent hydrogen bond acceptor, so it is likely that hydrogen-bonding with solvent can compete effectively with intramolecular hydrogen-bonding.

In the reactions where decomposition of the intermediate is rate limiting, the understanding of the mode of operation of base catalysis has greatly improved in recent years. There are now two recognised mechanisms, specific base - general acid (SB-GA), and rate limiting proton transfer (RLPT) mechanisms. In both of these deprotonation of ZH leads to the ionic adduct Z^- and then decomposition of this affords the product.

1.2.1 Specific Base - General Acid Mechanism

This mechanism involves rapid equilibrium deprotonation of the zwitterionic adduct, ZH, followed by rate limiting, acid catalysed expulsion of the leaving group from the anionic σ-complex, Z^-, via a concerted transition state as in 1.22. The SB-GA mechanism was first proposed in the 1960's[42-44], but was widely accepted in 1970 after a study of the reaction of 2,4-dinitro-1-naphthyl ethyl ether with n-butylamine and t-butylamine in DMSO[45] which is shown in scheme 1.6. This was

the first study in which both formation and decomposition of the σ-complex could be separately followed.

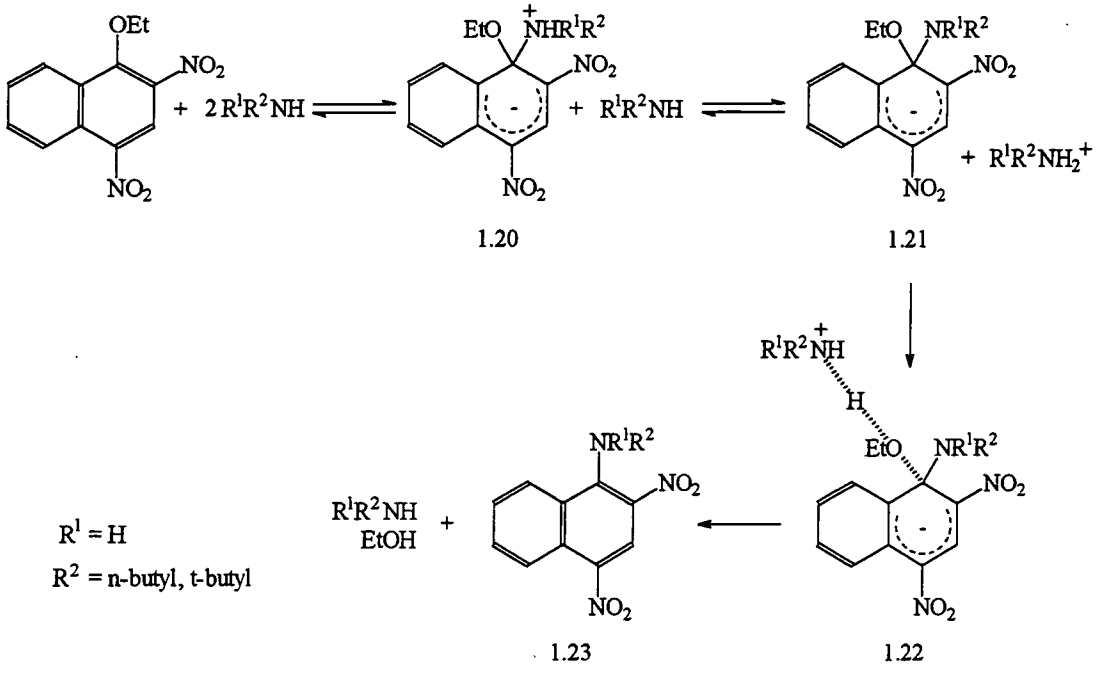

Scheme 1.6

Orvik and Bunnett showed the first stage to be nucleophilic attack of the amine to give 1.20, which is in rapid equilibrium with its conjugate base, 1.21. Subsequent flow NMR reactions[46,47] proved this equilibrium to lie strongly on the side of the deprotonated adduct. The second stage is expulsion of the leaving group to yield the product naphthylamine, 1.23. They found this to be first order in butylammonium ion but independent of amine concentration, an observation consistent with general acid catalysed expulsion of the leaving group. The product was found to be in equilibrium with its conjugate base since the NH proton is known to be relatively acidic in DMSO. There has also been evidence for the SB-GA mechanism in solvents other than DMSO, such as acetone and acetonitrile.[48,49] However in protic solvents its occurrence has been questioned after the discovery that the RLPT mechanism may be favoured in such media.

1.2.2 Rate Limiting Proton Transfer

In the RLPT mechanism the zwitterionic adduct ZH undergoes rate limiting base induced deprotonation followed by rapid uncatalysed or acid catalysed leaving group departure from the anionic adduct, Z^-. This mechanism was first proposed by Bunnett and Randall[50] in 1958. It was initially rejected when evidence that proton transfer between 'normal' (O, N) acids generally proceeds at a rate approaching diffusion control,[51] came to light. However it is now established that proton transfer steps can become rate limiting[52,53] in a multistep process where the species being deprotonated is present in a highly unfavourable equilibrium, or where reversion to reactants is rapid.[37]

The general reaction can be expressed by equation 1.12.

$$ArL + R^1R^2NH \underset{k_{-1}}{\overset{k_1}{\rightleftharpoons}} ZH \underset{k_{-d}}{\overset{k_d}{\rightleftharpoons}} Z^- \xrightarrow{k_4} Product$$

Equation 1.12

Here k_d refers to the deprotonation of ZH by the general bases, k_{-d} refers to the reprotonation of Z^- by general acids, and k_4 refers to unassisted or general acid catalysed leaving group departure.

For deprotonation of ZH to be rate limiting the following conditions must be met. $k_4 >> k_{-d}$ and $k_{-1} >(>) k_d$. No base catalysis would be observed if the first but not the second condition were met.[36,37]

Temperature-jump studies on reactions such as in equation 1.13 have afforded much of the evidence for the RLPT mechanism.[54-57] They have revealed that amine departure from zwitterionic complexes such as 1.24 is remarkably fast. Consequently, deprotonation of these species, although thermodynamically favoured and hence diffusion controlled, becomes rate limiting ($k_d << k_{-1}$), or partially so ($k_d < k_{-1}$) at low pH and low buffer concentrations.[36,37]

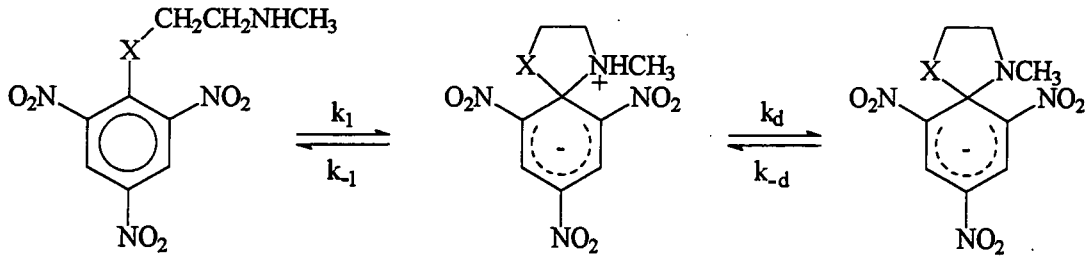

X = O, NCH_3 1.24

Equation 1.13

Other results have concluded that the condition $k_4 >> k_{-d}$ is probably met in many cases. Values of $k_4^{H_2O}$ for spontaneous or solvent assisted departure of typical leaving groups were found to be very high by extrapolation of the k_4 values for alkoxide and phenoxide ion departure from complexes such as 1.25 and 1.26 in aqueous solution.

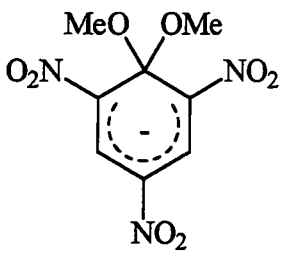

1.25

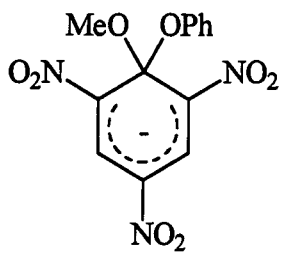

1.26

Studies of the reactions in equation 1.13 have shown that the basicity of the amino group in the anionic adducts like 1.24 is much less than the basicity of the parent amine ($\Delta pK \geq 2$). As a consequence the k_{-d} step refers to a thermodynamically unfavourable proton transfer under all conditions. This implies that $k_4 >> k_{-d}$ will hold for all reactions involving good leaving groups.

1.3 S_NAr Reactions of Trinitroaromatics in Dimethyl Sulphoxide

It is known that the reaction of 1,3,5-trinitrobenzene, 1.27, with aliphatic amines in dipolar solvents yields anionic σ-adducts[27,58,59], 1.29, by the process shown in equation 1.14.

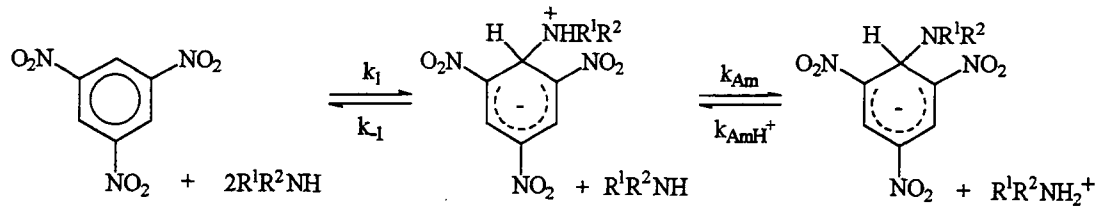

1.27 1.28 1.29

Equation 1.14

Kinetic studies of these reactions in dimethyl sulphoxide[57,60] (DMSO) and in mixed aqueous solvents[56] have shown that the proton transfer step may be rate determining. In DMSO the value of k_{Am} is ca. 10^7 dm^3 mol^{-1} s^{-1} for reaction with n-butylamine, 10^6 for the reaction with pyrrolidine and 10^5 for piperidine. These values are considerably lower than that expected for diffusion controlled reaction even though the proton transfers from zwitterions, 1.28, to amines are thermodynamically downhill. The greater acidities of 1.28 than the parent ammonium ions can be attributed to the electron-withdrawing effect of the trinitroaromatic moiety.[61,62]

The rate expression for formation of the σ-adducts , 1.29, is given in equation 1.15.

$$k_{fast} = \frac{k_1 k_{Am}[Am]^2 + k_{-1}k_{AmH^+}[AmH^+]}{k_{-1} + k_{Am}[Am]} \qquad \text{equation 1.15}$$

When the forward reaction dominates (in the absence of salt) this simplifies to equation 1.16.

$$k_{fast} = \frac{k_1 k_{Am}[Am]^2}{k_{-1} + k_{Am}[Am]} \qquad \text{equation 1.16}$$

For proton transfer to be the rate-limiting the condition $k_{-1} >> k_{Am}[Am]$ must be fulfilled. This holds for the reaction of 1.28 with the secondary amines pyrrolidine[60] and piperidine.[57,60] For n-butylamine[57] $k_{-1} \approx k_{Am}[Am]$, though at

high amine concentrations $k_{Am}[Am] > k_{-1}$ and k_{fast} linearly increases with [Am]. This is indicative of a change in the rate determining step to nucleophilic attack. Table 1.1 contains values for k_{Am} / k_{-1}, k_1, and $K_{c,1}$ relating to the overall equilibrium shown in equation 1.17.

Table 1.1

Amine	k_{Am} / k_{-1} / $dm^3\ mol^{-1}$	$K_{c,1}$ / $dm^3\ mol^{-1}$	k_1 / $dm^3\ mol^{-1}\ s^{-1}$
n-butylamine	1200	1000	4.5×10^4
piperidine	< 10	2140	$> 2 \times 10^5$
pyrrolidine	14	3500	7.5×10^5

$$K_{c,1} = \frac{[1.29][R^1R^2NH_2{}^+]}{[1.27][R_1R_2NH]^2} = \frac{k_1}{k_{-1}} \cdot \frac{K_{Am}}{K_{AmH^+}} \qquad \text{equation 1.17}$$

In nucleophilic substitution reactions the observation of general base catalysis is also an indication of rate determining proton transfer. Several detailed studies have been reported in DMSO.[27,59] The overall mechanism is shown in scheme 1.8.

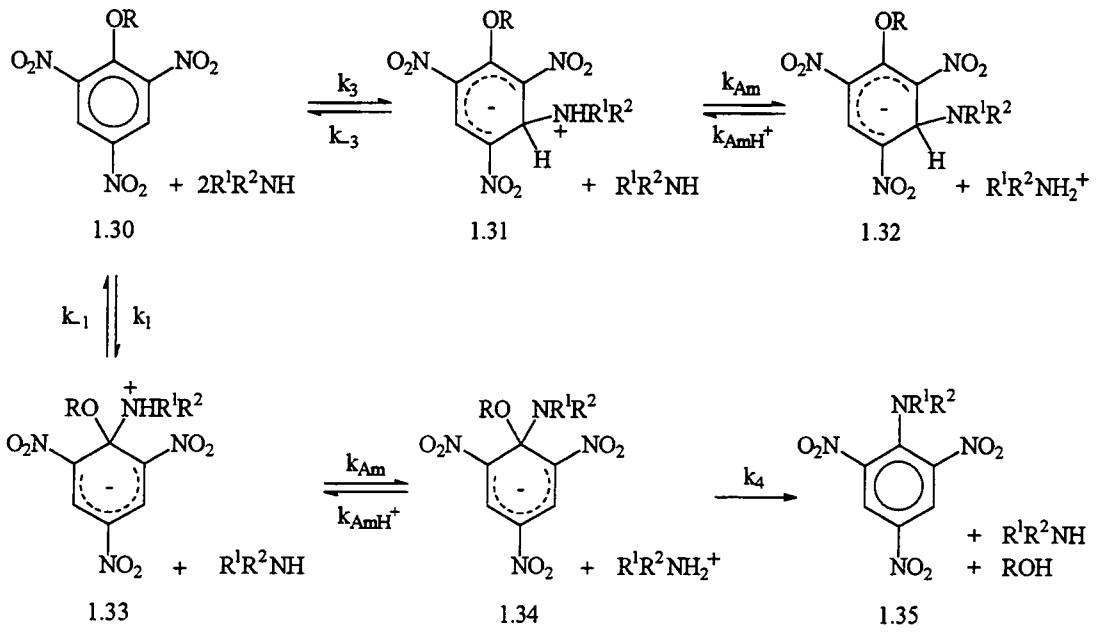

1.30a R = Et

1.30b R = Ph

scheme1.8

The base catalysed pathway may in an analogous fashion to that shown in scheme 1.7, involve rate limiting proton transfer from the zwitterionic intermediate, 1.33, to base (the $k_{Am}[Am]$ step). Alternatively leaving group departure (the k_4 step) may be general acid catalysed. The latter SB-GA mechanism has been shown to apply to substrates such as alkyl ethers, e.g. 1.30a, carrying poor leaving groups.[45,63-65] However, for substrates carring good leaving groups such as phenyl ethers, e.g. 1.30b, and phenyl sulphides, base catalysis may result from rate limiting proton transfer from zwitterion to base [66,67] (the RLPT mechanism).

In the reaction between ethyl 2,4,6-trinitrophenyl ether, 1.30a, and aliphatic amines in DMSO three separate rate processes are observed. The first is very rapid reversible formation of the 3-adducts, 1.32, for which the general rate expression is give by equation 1.18. In the absence of salt this reduces to equation 1.19 which can be more conveniently written as equation 1.20 to obtain values for k_{Am} / k_{-3}.

$$k_{fast} = \frac{k_3 k_{Am}[Am]^2 + k_{-3} k_{AmH^+}[AmH^+]}{k_{-3} + k_{Am}[Am]} \qquad \text{equation 1.18}$$

$$k_{fast} = \frac{k_3 k_{Am}[Am]^2}{k_{-3} + k_{Am}[Am]} \qquad \text{equation 1.19}$$

$$k_{fast} = \frac{K_3 k_{Am}[Am]^2}{1 + \frac{k_{Am}}{k_{-3}}[Am]} \qquad \text{equation 1.20}$$

For the reaction with n-butylamine the k_{Am} / k_{-3} value is large (> 200 $dm^3\ mol^{-1}$) so that at higher amine concentrations $k_{Am}[Am] > k_{-3}$. Thus the rate expression simplifies to equation 1.21 and the rate determining step becomes nucleophilic attack.

$$k_{fast} = k_3[Am] \qquad \text{equation 1.21}$$

In the reaction with piperidine the k_{Am} / k_{-3} value is small (< 5 dm^3 mol^{-1}) and thus $k_{-3} >> k_{Am}[Am]$. Equation 1.19 simplifies to equation 1.22 in which k_{fast} shows a linear dependence on the square of the amine concentration and proton transfer becomes rate limiting.

$$k_{fast} = K_3 k_{Am}[Am]^2 \qquad \text{equation 1.22}$$

With pyrrolidine k_{Am} / k_{-3} has an intermediate value of 15 dm^3 mol^{-1}, $k_{Am}[Am] \approx k_{-3}$ and proton transfer becomes partially rate limiting, especially at lower amine concentrations.

The major factor here is the reduction in the value of k_{Am} in changing from primary to secondary amines and is a reflection of the increase in steric hindrance to amine approach. A similar effect will also be found on the values of $k_{AmH}+$, since the value of k_{Am} / $k_{AmH}+$ (ca. 500) reflecting the much higher acidities of the zwitterionic adducts than the corresponding ammonium ions, is not expected to vary greatly with the nature of the amine or the trinitroaromatic substrate.[56,57]

The equilibrium constants $K_{c,3}$ and rate constants k_3 follow the trend pyrrolidine > piperidine > n-butylamine. This reflects the greater basicity of pyrrolidine with respect to piperidine and n-butylamine. For all three amines the $K_{c,3}$ and k_3 values are much smaller than the corresponding ones for reaction with 1,3,5-trinitrobenzene. This is due to the steric bulk of the 1-substituent which has the effect of twisting the 2- and 6-nitro groups out of the ring plane[71] and reducing their electron-withdrawing capabilities.

Table 1.2 contains values for k_{Am} / k_{-3}, k_3 and $K_{c,3}$ for the reactions of 1.30a with n-butylamine, piperidine and pyrrolidine.

Table 1.2

Amine	k_{Am} / k_{-3} / dm^3 mol^{-1}	$K_{c,3}$ / dm^3 mol^{-1}	k_3 / dm^3 mol^{-1} s^{-1}
n-butylamine	> 200	3200	15
piperidine	< 5	4.3×10^4	27
pyrrolidine	15	5×10^4	70

Reaction at the 1-position of 1.30a leading to the substitution of the ethoxy group occurs in two stages, so that the anionic σ-adducts are observable intermediates. As observed in the formation of 1.32, the rate limiting step in the formation of 1.34, changes from being nucleophilic attack with n-butylamine to proton transfer with pyrrolidine and piperidine.

$K_{c,1}$ values no longer reflect the basicities of the amines but follow the trend n-butylamine > pyrrolidine > piperidine. This is seemingly due to the adverse steric interactions between the ethoxy and amine functionalities in the 1-adducts, 1.34, which increase with the increasing bulk of the amine group. However, the k_1 values still follow the same order pyrrolidine > piperidine > n-butylamine.

It is seen that the k_3 values are larger than the corresponding k_1 values, which are shown in table 1.3, by roughly an order of magnitude, but, $K_{c,1} >> K_{c,3}$. This indicates that attack at the 3-position is kinetically preferred, though attack at the 1-position is thermodynamically preferred.

Table 1.3

Amine	$K_{c,1}$ / $dm^3\ mol^{-1}$	k_1 / $dm^3\ mol^{-1}\ s^{-1}$	k_{Am} / k_{-1} / $dm^3\ mol^{-1}$	k_4 / $dm^3\ mol^{-1}\ s^{-1}$
n-butylamine	5×10^4	250	$>1 \times 10^4$	8.3
piperidine	600	1800	3	N/A
pyrrolidine	2000	4000	30	0.25

The rate expression for substitution product formation is given by equation 1.23 from which values of k_4 can be obtained.

$$k_{slow} = \frac{k_4 K_{c,1}[Am]^2[AmH^+]}{K_{c,1}[Am]^2 + [AmH^+]} \qquad \text{equation 1.23}$$

For both n-butylamine and pyrrolidine $k_{AmH}+ > k_4$ showing that proton transfer is faster to the amino group in the adducts, 1.34, than to the ethoxy group. Hence the k_4 step becomes rate determining in the substitution process which is consistent with theSB-GA mechanism. Piperidine does not undergo the substitution reaction.

In the reaction between phenyl 2,4,6-trinitrophenyl ether, 1.30b, with n-butylamine, pyrrolidine and piperidine in DMSO[66] two different rate processes are observed. Initial fast formation at the 3-position is followed by much slower formation of the N-substituted picryl derivatives, 1.35. There is no accumulation of the 1-adduct intermediates, 1.34.

The rate constant, k_{fast}, for reaction of n-butylamine with 1.30b at the 3-position shows a linear dependence with amine concentration in the absence of salt. This indicates that $k_{Am}[Am] >> k_{-3}$ and that the rate determining step is nucleophilic attack. For piperidine $k_{-3} > k_{Am}[Am]$ and proton transfer from the zwitterion, 1.31, to amine becomes rate limiting. With pyrrolidine $k_{Am}[Am] \approx k_{-3}$ so proton transfer becomes partially rate limiting.

$K_{c,3}$ and k_3 values, shown in table 1.4, follow the same pattern as for the reactions of 1.30a, reflecting the basicities of the amines.

Table 1.4

Amine	$K_{c,3}$ / $dm^3\ mol^{-1}$	k_3 / $dm^3\ mol^{-1}\ s^{-1}$
n-butylamine	210	8000
piperidine	400	N/A
pyrrolidine	1300	1×10^5

Failure to observe the 1-adducts, 1.34, on the substitution pathway when it has been shown[66] that they should be thermodynamically more favoured with respect to reactants than the corresponding adducts of the ethyl ether, provides strong evidence against the SB-GA mechanism. Thus making the assumption that k_4 is not the rate determining step, then the rate expression for formation of the n-substituted picramide products is given by equation 1.24.

$$k_{sub} = \frac{k_1 k_{Am}[Am]^2}{k_{-1} + k_{Am}[Am]\left(1 + K_{c,3}\frac{[Am]^2}{[AmH^+]}\right)} \qquad \text{equation 1.24}$$

Incorporating the modification for the rapid reversible reaction at the three position into k_{sub} yields equation 1.25.

$$k'_{sub} = \frac{k_1 k_{Am}[Am]^2}{k_{-1} + k_{Am}[Am]} \qquad \text{equation 1.25}$$

$$\text{where } k'_{sub} = k_{sub}\left(1 + K_{c,3}\frac{[Am]^2}{[AmH^+]}\right) \qquad \text{equation 1.26}$$

For the reaction with n-butylamine k'_{sub} shows a linear dependence on amine concentration indicating that $k_{Am}[Am] >> k_{-1}$ so that nucleophilic attack is the rate-determining step in the substitution process. In the reaction with piperidine k'_{sub} has a linear dependence on the square of the amine concentration. This indicates $k_{-1} >> k_{Am}[Am]$ with proton transfer from zwitterion, 1.33, to amine being rate limiting. Pyrrolidine shows intermediate behaviour with proton transfer being partly rate limiting.

These results are consistent with the RLPT mechanism whereas those for the ethyl ether, 1.30a, conform to the SB-GA mechanism.

1.4 References

1. M. Makosza, J. Golinski and J. Baran, *J. Org. Chem.*, 1984, **49**, 1488.
2. C. J. Jackson and F. H. Gazzolo, *J. Am. Chem. Soc.*, 1900, **23**, 376.
3. J. Meisenheimer, *Justus Liebigs Ann. Chem.*, 1902, **323**, 205.
4. M. R. Crampton, *Adv. Phys. Org. Chem.*, 1969, **7**, 211.
5. M. J. Strauss, *Acc. Chem. Res.*, 1978, **11**, 147.
6. R. Foster and C. A. Fyfe, *Rev. Pure Appl. Chem.*, 1966, **16**, 61.
7. E. Buncel, A. R. Norris and K. E. Russell, *Q. Rev. Chem. Soc*, 1968, **22**, 123.
8. M. R. Crampton and V. Gold, *J. Chem. Soc.*, 1964, 4293.
9. M. R. Crampton and V. Gold, *J. Chem. Soc. B*, 1966, 893.
10. R. Graboiaud and R. Schaal, *Bull. Soc. Chem. Fr.*, 1969, 2683.
11. D. M. Brevis, N. B. Chapman, J. S. Paine, J. Shorter and D. J. Wright, *J. Chem. Soc. Perkin Trans. 2*, 1900, 1787.
12. D. M. Brevis, N. B. Chapman, J. S. Paine and J. Shorter, *J. Chem. Soc. Perkin Trans. 2*, 1900, 1787.
13. J. D. Roberts, H. E. Simmons Jr., L. A. Carlsmith and C. W. Vaughan, *J. Am. Chem. Soc.*, 1953, **75**, 3290.
14. J. D. Roberts, D. A. Semenow, H. E. Simmons Jr. and L. A. Carlsmith, *J. Am. Chem. Soc.*, 1956, **78**, 601.
15. J. D. Roberts, C. W. Vaughan, L. A. Carlsmith and D. A. Semenow, *J. Am. Chem. Soc.*, 1956, **78**, 611.
16. G. E. Hall, R. Piccolini and J. D. Roberts, *J. Am. Chem. Soc.*, 1955, **77**, 4540.
17. G. Wittig and K. Niethammer, *Chem. Ber.*, 1960, **93**, 944.
18. G. Wittig, H. Härle, E. Knauss and K. Niethammer, *Chem. Ber.*, 1960, **93**, 951.
19. C. G. Swain, J. E. Sheets and K. G. Harbison, *J. Am. Chem. Soc.*, 1975, **97** , 783.
20. C. G. Swain, J. E. Sheets, D. G. Gorenstein and K. G. Harbison, *J. Am. Chem. Soc.*, 1975, **97**, 791.
21. C. G. Swain, J. E. Sheets and K. G. Harbison, *J. Am. Chem. Soc.*, 1975, **97**, 796.
22. R. G. Bergstrom, R. G. M. Landells, G. W. Whal Jr and H. Zollinger, *J. Am. Chem. Soc.*, 1976, **98**, 3301.
23. A. H. M. Renfew, J. A. Taylor, J. M. J. Whitmore and A. Williams, *J. Chem. Soc. Perkin Trans. 2*, 1973, 1703.

24. J. F. Bunnett, *J. Am. Chem. Soc.*, 1970, **92**, 7463.
25. R. A. Rossi and S. M. Palacios, *Tetrahedron*, 1993, **49**, 4485.
26. J. Miller, "Aromatic Nucleophilic Substitution", Elsevier, Amsterdam, 1968.
27. E. Buncel, M. R. Crampton, M. J. Strauss and F. Terrier, "Electron Deficient Aromatic and Heteroaromatic - Base Interactions", Elsevier, New York, 1984.
28. J. F. Bunnett and R. E. Zahler, *Chem. Rev.*, 1957, **49**, 273.
29. F. Terrier, "Nucleophilic Aromatic Displacement", VCH, New York, 1991, p. 258.
30. M. Makosza and J. Winiarski, *Acc. Chem. Res.*, 1987, **20**, 282.
31. M. Makosza "Current Trends in Organic Synthesis", Pergamon Press, New York, 1983, p. 401.
32. M. Makosza, *Pol. J. Chem.*, 1992, **3**, 66.
33. J. Golinski and M. Makosza, *Tetrahedron Letters*, 1978, 3495.
34. M. Makosza and T. Glinka, *J. Org. Chem*, 1983, **48**, 3860.
35. F. Terrier, "Nucleophilic Aromatic Displacement", VCH, New York, 1991, p. 251.
36. C. F. Bernasconi, *Acc. Chem. Res.*, 1978, **11**, 147.
37. C. F. Bernasconi, *Chimia*, 1980, **34**, 1.
38. C. F. Bernasconi, *M. T. P. Int. Rev. Sci.: Org. Chem. Ser. one*, Butterworths, London, 1973, **3**, 33.
39. J. F. Bunnett and C. F. Bernasconi, *J. Am. Chem. Soc.*, 1965, **87**, 5209.
40. J. F. Bunnett and C. F. Bernasconi, *J. Org. Chem.*, 1970, **35**, 70.
41. C. F. Bernasconi, *J. Phys. Chem.*, 1971, **75**, 3636.
42. A. J. Kirby and W. D. Jencks, *J. Am. Chem. Soc.*, 1965, **87**, 3217.
43. J. F. Bunnett and R. H. Garst, *J. Am. Chem. Soc.*, 1965, **87**, 3879.
44. J. F. Bunnett and G. T. Davies, *J. Am. Chem. Soc.*, 1960, **82**, 665.
45. J. A. Orvik and J. F. Bunnett, *J. Am. Chem. Soc.*, 1970, **92**, 2417.
46. C. A. Fyfe, A. Koll, S. W. H. Damji, C. D. Malkiewich and P. E. Forte, *J. Chem. Soc. Chem. Comm.*, 1977, 335.
47. C. A. Fyfe, A. Koll, S. W. H. Damji, C. D. Malkiewich and P. E. Forte, *Can. J. Chem*, 1977, **55**, 1468.
48. R. H. de Rossi and R. A. Rossi, *J.Org. Chem.*, 1974, **39**, 3486.
49. T. O. Bamkole, J. Hirst and J. Onyido, *J. Chem. Soc. Perkin Trans. 2*, 1982, 889.
50. J. F. Bunnett and J. J. Randall, *J. Am. Chem. Soc.*, 1958, **80**, 6020.
51. M. Eigen, *Angew. Chem., Int. Ed. Engl.*, 1964, **3**, 1.

52. W. P. Jencks, *Chem. Rev.*, 1972, **72**, 705.
53. R. E. Barnett, *Acc. Chem. Res.*, 1973, **6**, 41.
54. C. F. Bernasconi, C. L Gehriger and R. H. de Rossi, *J. Am. Chem. Soc.*, 1976, **98**, 8451.
55. C. F. Bernasconi and F. Terrier, *J. Am. Chem. Soc*, 1975, **97**, 7458.
56. C. F. Bernasconi, M. C. Muller and P. Schmid, *J. Org. Chem*, 1979, **44**, 3189.
57. M. R. Crampton and B. Gibson, *J. Chem. Soc. Perkin Trans. 2*, 1981, 533.
58. M. R. Crampton and V. Gold, *Chem. Comm*, 1965, 549: *J. Chem. Soc. B*, 1967, 23
59. F. Terrier, "Nucleophilic Aromatic Displacement", VCH, New York, 1991.
60. M. R. Crampton and C. Greenhalgh, *J. Chem. Soc. Perkin Trans. 2*, 1981, 1175.
61. M. R. Crampton, *J. Chem. Soc. B*, 1971, 2112.
62. E. Buncel and J. G. K. Webb, *Can. J. Chem*, 1981, **52**, 533.
63. J. F. Bunnett, S. Sekiguchi and L. A. Smith, *J. Am. Chem. Soc.*, 1981, **103**, 4865.
64. M. R. Crampton and P. Routledge, *J. Chem. Soc. Perkin Trans. 2*, 1984, 573.

Chapter 2

Kinetic and Equilibrium Studies on the Reactions Between Trinitroaromatics and Amines in Acetonitrile

2.1 Acetonitrile as a Solvent

Many of the studies on reactions between nitroaromatics and amines have used dimethyl sulphoxide, DMSO, or DMSO-water solvent systems. However, acetonitrile has also been extensively used as a solvent for the examination of base catalysis in S_NAr reactions,[1-4] though the substrates previously studied have been less activated than the phenyl and ethyl 2,4,6-trinitrophenyl ethers, 2.2 and 2.3, so that intermediates were not observed. The only quantitative measurement of a trinitroaromatic-amine interaction in acetonitrile was a determination of the equilibrium constant[5] for σ-adduct formation between 1,3,5-trinitrobenzene, 2.1, and piperidine. Also d_3-acetonitrile has been previously used as a solvent for obtaining NMR spectra of σ-adducts.[6-10]

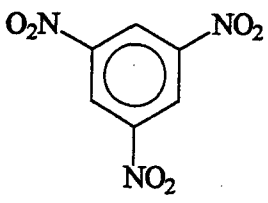

2.1

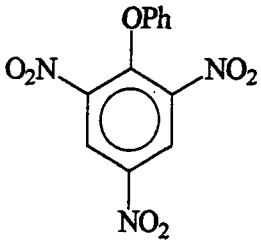

2.2

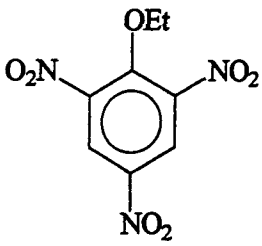

2.3

The dielectric constant of acetonitrile is comparable with that of DMSO, the values[11] being 36 and 46.6 respectively. However, acetonitrile is a much less basic solvent and pK_a values for aliphatic ammonium ions are ca. 8 units larger than in DMSO.[11,12] Nevertheless extensive studies of acid-base behaviour have been carried out in acetonitrile and it is a sufficiently basic solvent to fully dissociate perchloric acid.[13,14] This is the reason for the use of perchloric acid in these studies.

A major difference between the two solvents are their hydrogen-bonding properties. DMSO is known to be a strong hydrogen-bond acceptor while acetonitrile forms only weak hydrogen-bonds[16,17] as shown in figure 2.1.

Figure 2.1. Solvent-ammonium ion hydrogen bonding.

strong interaction weak interaction

Hence ammonium ions are much more poorly solvated in acetonitrile. As a result of this, in solutions containing aliphatic amines and their corresponding perchlorate salts, an interaction arises producing homoconjugates,[15] as shown in the equilibrium in equation 2.1. The values of the equilibrium constants are ca. 20 - 30 $dm^3\ mol^{-1}$.

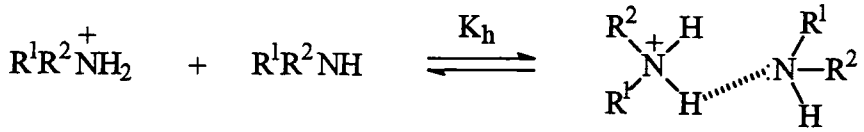

Equation 2.1

In DMSO, amines and their corresponding ammonium salts are solvated to a greater extent and the formation of homoconjugates is not observed.

2.2 Reaction of Aliphatic Amines with 1,3,5-Trinitrobenzene

The reaction of 1,3,5-trinitrobenzene, 2.1, with the aliphatic amines n-butylamine, piperidine and pyrrolidine, resulted in the rapid formation of σ-adducts via the process shown in equation 2.2.

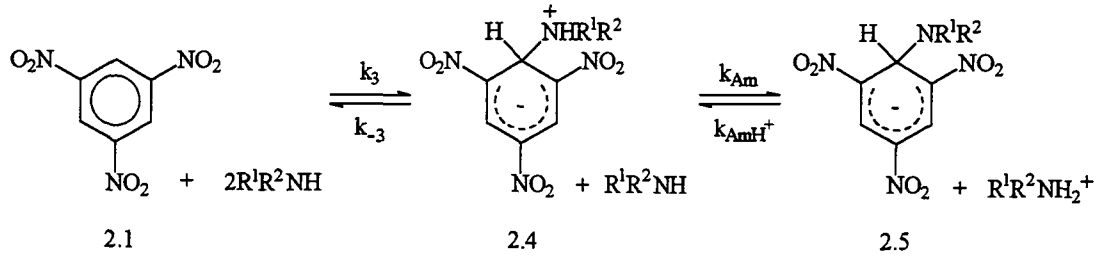

2.1 2.4 2.5

Equation 2.2

The final spectra had characteristic absorption maxima at ca. 450 and 530 nm. An example is shown in fig2.2.

Figue 2.2. The spectrum of the σ-adduct formed between 1,3,5-trinitrobenzene and pyrrolidine.

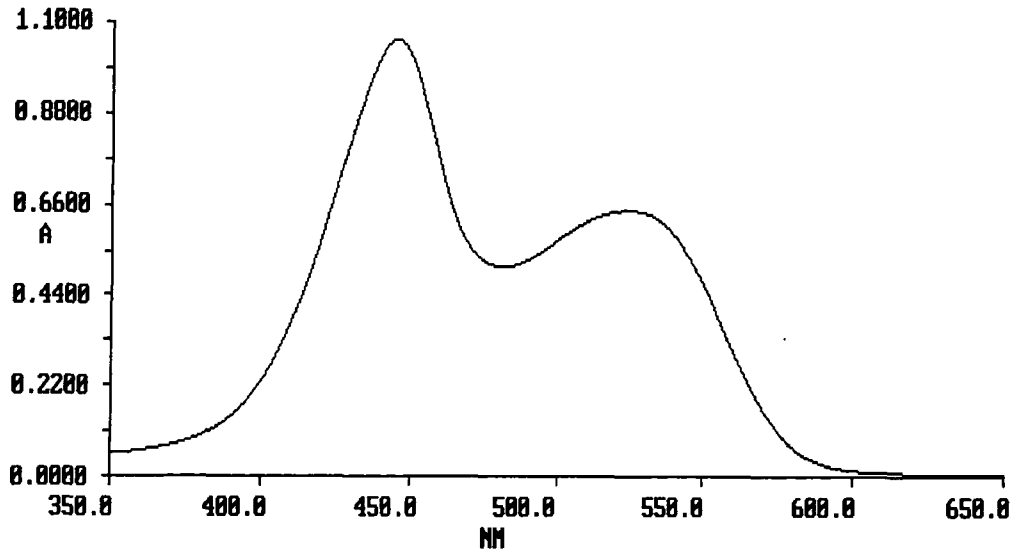

For each different amine, virtually identical spectra were obtained at high amine concentrations ($\geq$ 0.1 mol dm^{-3}), in the absence of salt, indicating complete conversion to 2.5. This allowed the determination of values for extinction coefficients which are given in table 2.1.

Table 2.1. Extinction coefficients of the σ-adducts, 2.5, in acetonitrile.

Amine	λ_{max} of 2.5 / nm	ε / dm^3 mol^{-1} cm^{-1}
n-butylamine	450	2.8×10^4
	534	1.6×10^4
piperidine	446	2.8×10^4
	524	1.6×10^4
pyrrolidine	445	2.7×10^4
	524	1.6×10^4

Measurement of absorbance values in solutions containing 0.001 mol dm^{-3} of the corresponding ammonium perchlorate salt with various concentrations of amine allowed the calculation of the values of $K_{c,3}$ as defined in equation 2.3.

$$K_{c,3} = \frac{[2.5]}{[2.1]} \cdot \frac{[R_1R_2NH_2{}^+]_{stoich}}{[R_1R_2NH]^2} \qquad \text{equation 2.3}$$

The data for all three amines, that are shown in tables 2.2, 2.3 and 2.4, show that the values of $K_{c,3}$ increase with increasing amine concentration. This is attributed to stabilisation of the ammonium cations by association with the large excess of amine in the formation of homoconjugates as shown in equation 2.1. Hence $K_{c,3}°$ is defined in terms of the free, unassociated cations as in equation 2.4.

$$K_{c,3}° = \frac{[2.5]}{[2.1]} \cdot \frac{[R_1R_2NH_2{}^+]_{free}}{[R_1R_2NH]^2} \qquad \text{equation 2.4}$$

$K_{c,3}$ and $K_{c,3}°$ are related to the equilibrium constant, K_h, for homoconjugation, by equation 2.5. It can be seen that $K_{c,3}$ approaches the value of $K_{c,3}°$ as the amine concentration tends to zero.

$$K_{c,3} = K_{c,3}°\left(1 + K_h[R^1R^2NH]\right) \qquad \text{equation 2.5}$$

A plot, shown in figure 2.3, of $K_{c,3}$ versus pyrrolidine concentration gave values of $K_{c,3}°$ 0.20 $dm^3\ mol^{-1}$ and K_h 27 $dm^3\ mol^{-1}$. Similar plots, shown in figures 2.4 and 2.5, give values of $K_{c,3}°$ 0.055 $dm^3\ mol^{-1}$ and K_h 25 $dm^3\ mol^{-1}$ for piperidine, and $K_{c,3}°$ 0.0025 $dm^3\ mol^{-1}$ and K_h 20 $dm^3\ mol^{-1}$ for n-butylamine.

Figure 2.3. A plot of $K_{c,3}$ versus pyrrolidine concentration.

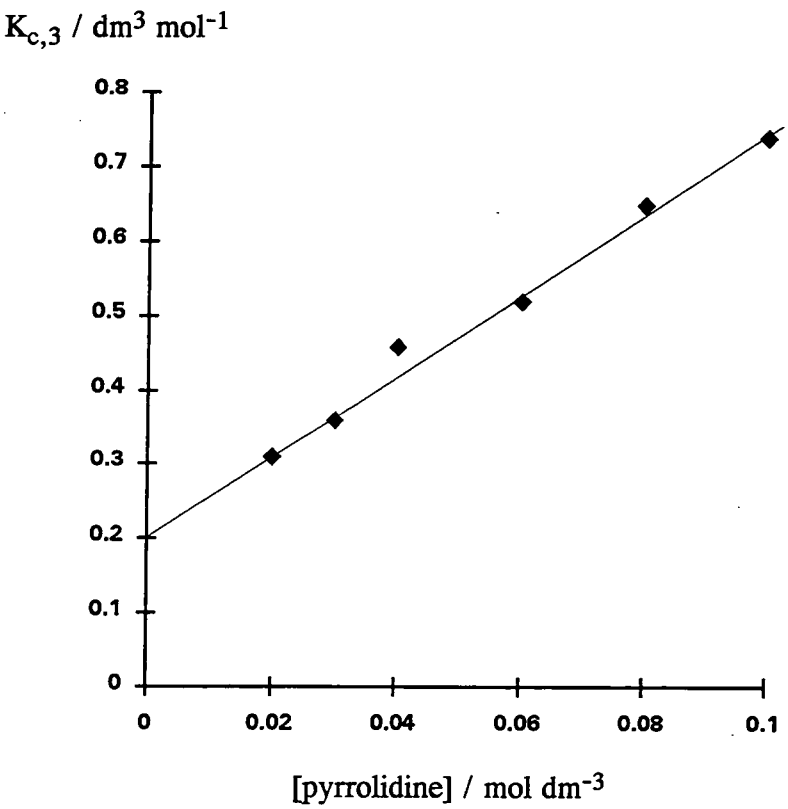

Figure 2.4. A plot of $K_{c,3}$ versus piperidine concentration.

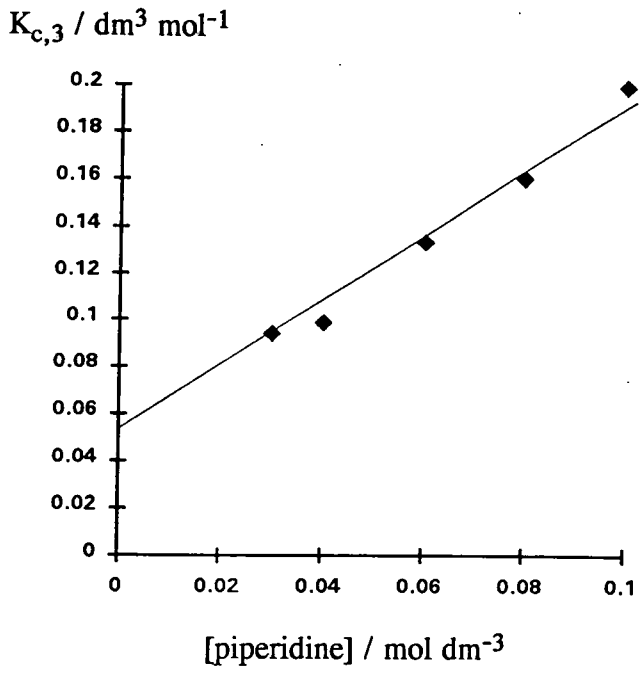

Figure 2.5. A plot of $K_{c,3}$ versus n-butylamine concentration.

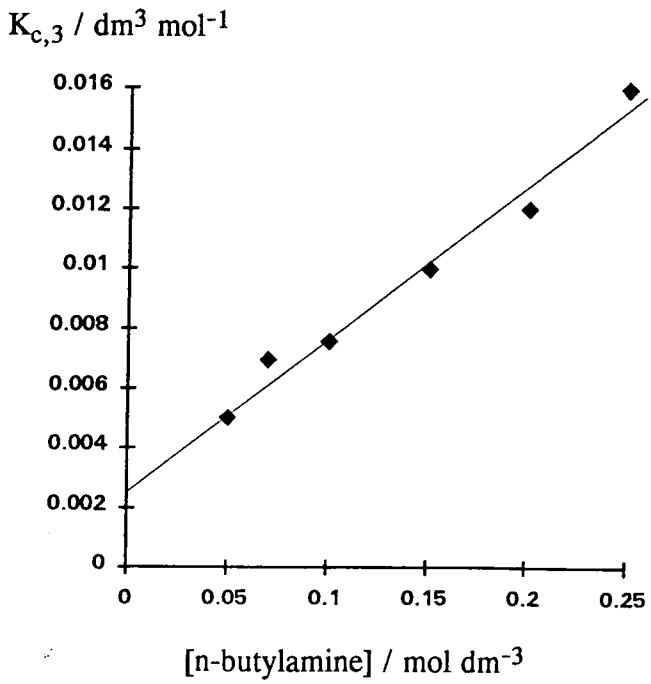

Table 2.2. Equilibrium data for the formation of 2.5 from 1,3,5-trinitrobenzene[a] and pyrrolidine in acetonitrile at 25°C.

[pyrrolidine] / mol dm^{-3}	[pyrrolidineH^+] / mol dm^{-3}	Abs @ 445 nm	$K_{c,3}$[b] / dm^3 mol^{-1}	$K_{c,3}$[c] / dm^3 mol^{-1}
0.01	0.001	0.028	0.26	0.25
0.02	0.001	0.120	0.31	0.31
0.03	0.001	0.267	0.36	0.36
0.04	0.001	0.46	0.46	0.42
0.06	0.001	0.71	0.52	0.52
0.08	0.001	0.88	0.65	0.63
0.10	0.001	0.96	0.74	0.74
0.10	-	1.08	-	-
0.20	-	1.09	-	-
0.03	0.002	0.153	0.36	0.37
0.03	0.004	0.087	0.38	0.37

a. Concentration is 4×10^{-5} mol dm^{-3}.

b. Calculated as $\left(\frac{\text{Abs}}{1.09 - \text{Abs}}\right)\frac{[\text{pyrrolidineH}^+]_{\text{stoich}}}{[\text{pyrrolidine}]^2}$.

c. Calculated from equation 2.5 with $K_{c,3}°$ 0.20 dm^3 mol^{-1} and K_h 27 dm^3 mol^{-1}.

Table 2.3. Equilibrium data for the formation of 2.5 from 1,3,5-trinitrobenzene[a] and piperidine in acetonitrile at 25°C.

[piperidine] / mol dm^{-3}	[piperidineH$^+$] / mol dm^{-3}	Abs @ 446 nm	$K_{c,3}$[b] / dm^3 mol^{-1}	$K_{c,3}$[c] / dm^3 mol^{-1}
0.03	0.001	0.0872	0.094	0.096
0.04	0.001	0.154	0.099	0.110
0.06	0.001	0.364	0.134	0.137
0.08	0.001	0.565	0.16	0.16
0.10	0.001	0.752	0.20	0.19
0.08	0.002	0.386	0.16	0.16
0.08	0.004	0.252	0.18	0.16
0.20	-	1.12	-	-

a. Values quoted for 4 x 10^{-5} mol dm^{-3} although some measurements were made with 1 x 10^{-4} mol dm^{-3}.

b. Calculated as $\left(\frac{\text{Abs}}{1.12 - \text{Abs}}\right)\frac{[\text{piperidineH}^+]_{\text{stoich}}}{[\text{piperidine}]^2}$.

c. Calculated from equation 2.5 with $K_{c,3}°$ 0.055dm^3 mol^{-1} and K_h 25 dm^3 mol^{-1}.

Table 2.4. Equilibrium data for the formation of 2.5 from 1,3,5-trinitrobenzene[a] and n-butylamine in acetonitrile at 25°C.

[n-butylamine] / mol dm^{-3}	[n-butylamineH^+] / mol dm^{-3}	Abs @ 450 nm	$K_{c,3}$[b] / dm^3 mol^{-1}	$K_{c,3}$[c] / dm^3 mol^{-1}
0.05	0.001	0.0141	0.0050	0.0050
0.07	0.001	0.0374	0.0070	0.0060
0.10	0.001	0.080	0.0076	0.0075
0.15	0.001	0.21	0.010	0.010
0.20	0.001	0.37	0.012	0.012
0.25	0.001	0.57	0.016	0.015
0.50	-	1.11	-	-
1.00	-	1.13	-	-

a. Values quoted for 4 x 10^{-5} mol dm^{-3} although some measurements were made with 1 x 10^{-4} mol dm^{-3}.

b. Calculated as $\left(\frac{\text{Abs}}{1.13 - \text{Abs}}\right)\frac{[\text{n-butylamine}H^+]_{\text{stoich}}}{[\text{n-butylamine}]^2}$.

c. Calculated from equation 2.5 with $K_{c,3}°$ 0.0025dm^3 mol^{-1} and K_h 20 dm^3 mol^{-1}.

$K_{c,3}°$ values in acetonitrile and the corresponding $K_{c,3}$ values in DMSO are summarised in table 2.5.

Table 2.5. Equilibrium constants for the reaction of 2.1 with aliphatic amines in acetonitrile and DMSO at 25°C.

Amine	$K_{c,3}°(CH_3CN)$ / $dm^3\ mol^{-1}$	$K_{c,3}(DMSO)$ / $dm^3\ mol^{-1}$	$K_{c,3}(DMSO) / K_{c,3}°(CH_3CN)$
n-butylamine	0.002	1000	5×10^5
piperidine	0.055	2140	4×10^4
pyrrolidine	0.20	3000	1.5×10^4

The same trend is seen in $K_{c,3}°(CH_3CN)$ as for $K_{c,3}(DMSO)$, for the three amines, with pyrroldine > piperidine > n-butylamine reflecting the decreasing basicity of the parent amine. However the values are 10^4-10^5 times smaller in acetonitrile. This is a reflection on each solvent's capability to solvate the charged products. DMSO strongly solvates all species, especially the ammonium cations, being a strong hydrogen-bond acceptor. Acetonitrile, on the other hand, is a poor hydrogen-bonding solvent, and thus solvates these species to a much reduced extent than DMSO. The 10-fold increase in value of the ratio $K_{c,3}(DMSO) / K_{c,3}°(CH_3CN)$ for n-butylamine over piperidine and pyrrolidine maybe due to the stronger solvent-solute interactions of its protonated species. The n-butylammonium cation has three centres capable of hydrogen-bonding whereas the piperidinium and pyrrolidinium cations only have two.

Assuming that the zwitterionic adducts, 2.4, may be treated as steady state intermediates, then the rate constant for equilibration of 2.1 and 2.5 is given by equation 2.6. The complete derivation is given in chapter 7 pp 209 - 212.

$$k_{obs} = \frac{k_3 k_{Am}[Am]^2}{k_{-3} + k_{Am}[Am]} + \frac{k_{-3} k_{AmH^+}[AmH^+]_{stoich}}{(k_{-3} + k_{Am}[Am])(1 + K_h[Am])} \qquad \text{equation 2.6}$$

This differs from the rate constant for reaction in DMSO (chapter 1 equation 1.18) by the factor 1 / (1 + K_h) in the reverse decomposition term. This allows for the observation that only the free, unhomoconjugated ammonium ions will participate in the protonation of the σ-adduct. The relationship between the concentrations of free and stoichiometric ammonium ions is given by equation 2.7.

$$[AmH^+]_{free} = \frac{[AmH^+]_{stoich}}{1 + K_h[Am]}$$ equation 2.7

In the absence of salt ($[AmH^+] = 0$), complex kinetics[18] are expected, due to mixed first order (forward) and second order (reverse) reactions. If a sufficiently large concentration of amine is used, so that virtually complete conversion to product is attained, then the forward term dominates and first order kinetics are predicted. If, in addition , $k_{Am}[Am] >> k_{-3}$ then equation 2.8 will apply.

$$k_{obs} = k_3[Am]$$ equation 2.8

However with this condition fulfilled the rate constants proved too rapid for measurement using the stopped-flow techniques available. This problem was overcome in the reactions of piperidine and pyrrolidine by the measuring reverse, decomposition reactions of the σ-adducts. In the case of the adduct formed with n-butylamine both forward and reverse rate constants were too fast for measurement. Thus pre-formed solutions of each adduct were reacted with the appropriate ammonium salt and the rate constants of decomposition (colour-fading) reactions were measured. If the conditions are chosen so that >90% reversion of the σ-adduct to parent is achieved, then the decomposition reaction dominates. This is represented by the second term in equation 2.6, so that the observed rate expression becomes that in equation 2.9.

$$k_{obs} = \frac{k_{-3}k_{AmH}+[AmH^+]_{stoich}}{(k_{-3} + k_{Am}[Am])(1 + K_h[Am])}$$ equation 2.9

At the amine concentrations (0.001 and 0.002 mol dm^{-3}) used in tables 2.6 and 2.7 and using K_h values of between 20 and 27 dm^3 mol^{-1} then the condition $1 >> K_h[Am]$ is always met. Hence the $1 + K_h[Am]$ term disappears. Also the results in tables 2.6 and 2.7 show that the observed rate constants for the decomposition reactions are linearly dependent on the ammonium salt concentration. This proves that at the amine concentrations used $k_{-3} >> k_{Am}[Am]$. Hence equation 2.9 may be condensed to equation 2.10.

$$k_{obs} = k_{AmH}+[AmH^+]_{stoich}$$ equation 2.10

Hence at the low amine concentrations used the proton transfer step is rate-determining in the equilibration of 2.1 and 2.5. The values obtained for $k_{AmH}+$ are 9×10^6 dm^3 mol^{-1} s^{-1} for the pyrrolidine reaction, and 2.5×10^6 dm^3 mol^{-1} s^{-1} for piperidine. These values, summarised in table 2.8, are nearly 10^4 times faster than the corresponding values[18-20] in DMSO which are 3000 and 280 dm^3 mol^{-1} s^{-1} respectively. This 10^3-10^4 fold increase in values in acetonitrile can be explained by the reduced solvation of the ammonium cations in this solvent. Thus the approach of the cation to the σ-adduct is less hindered by the solvation shell in acetonitrile, leading to the increased values of $k_{AmH}+$.

Table 2.6. Rate data for the colour fading decomposition reaction of the pyrrolidino σ-adduct[a] with pyrrolidinium perchlorate in acetonitrile at 25°C.

[pyrrolidine] / mol dm^{-3}	[pyrrolidineH$^+$] / 10^{-5} mol dm^{-3}	k_{obs}[b] / s^{-1}	$k_{AmH}+$[c] / 10^6 dm^3 mol^{-1} s^{-1}
0.001	2	160 ± 20	8
0.001	3	260 ± 20	9
0.001	4	330 ± 40	8
0.002	2	175 ± 15	9
0.002	3	255 ± 20	9

a. The concentration of 1,3,5-trinitrobenzene is 1×10^{-4} mol dm^{-3}. The estimated concentration of σ-adduct, 2.5, before reaction with salt is $\leq 9 \times 10^{-6}$ mol dm^{-3}.

b. Measured at 445 nm.

c. Calculated from $k_{AmH}+ = \frac{k_{obs}}{[AmH^+]}$.

Table 2.7. Rate data for the colour fading decomposition reaction of the piperidino σ-adduct[a] with piperidinium perchlorate at 25°C.

[piperidine] / mol dm^{-3}	[piperidineH$^+$] / mol dm^{-3}	k_{obs}[b] / s^{-1}	k_{AmH^+}[c] / dm^3 mol^{-1} s^{-1}
0.001	2×10^{-5}	52 ± 2	2.6×10^6
0.001	3×10^{-5}	75 ± 4	2.5×10^6
0.001	4×10^{-5}	110 ± 4	2.7×10^6
0.001	5×10^{-5}	130 ± 5	2.6×10^6
0.001	8×10^{-5}	200 ± 7	2.5×10^6
0.002	2×10^{-5}	55 ± 2	2.7×10^6
0.002	3×10^{-5}	73 ± 3	2.4×10^6
0.002	4×10^{-5}	105 ± 3	2.6×10^6
0.002	5×10^{-5}	125 ± 5	2.5×10^6
0.002	8×10^{-5}	200 ± 10	2.5×10^6

a. The concentration of 1,3,5-trinitrobenzene is 1×10^{-4} mol dm^{-3}. The estimated concentration of σ-adduct, 2.5, before reaction with salt is $\leq 5 \times 10^{-6}$ mol dm^{-3}.

b. Measured at 446 nm.

c. Calculated from $k_{AmH^+} = \frac{k_{obs}}{[AmH^+]}$.

Since values of $K_{c,3}°$ are known from the equilibrium measurements, values of k_3k_{Am}/k_{-3} ($\equiv k_{AmH}+.K_{c,3}°$) could be calculated and are given in table 2.8.

Table 2.8. Summary of rate data for equilibration of 2.1 and 2.5 in acetonitrile[a] at 25°C.

Amine	$k_{AmH}+$ / $dm^3\ mol^{-1}\ s^{-1}$	K_3k_{Am} / $dm^6\ mol^{-2}\ s^{-1}$
n-butylamine	$>> 10^7$ (6×10^4)	$> 3.6 \times 10^6$ (6×10^7)
piperidine	2.5×10^6 (280)	1.4×10^5 (6×10^5)
pyrrolidine	9×10^6 (3000)	2×10^6 (1.1×10^7)

a. Figures in parentheses are corresponding values in DMSO.[24]

The results show a 10^3 - 10^4 fold increase in the value of $k_{AmH}+$ in changing the solvent from DMSO to acetonitrile. This indicates how poorly solvated the ammonium cations are in acetonitrile as compared to DMSO.

2.3 Reaction of Aliphatic Amines with Ethyl 2,4,6-Trinitrophenyl Ether

The reactions of ethyl 2,4,6-trinitrophenyl ether, 2.3, with the aliphatic amines n-butylamine, piperidine and pyrrolidine, shown in scheme 2.1, were qualitatively similar to the corresponding reactions in DMSO.[21,22]

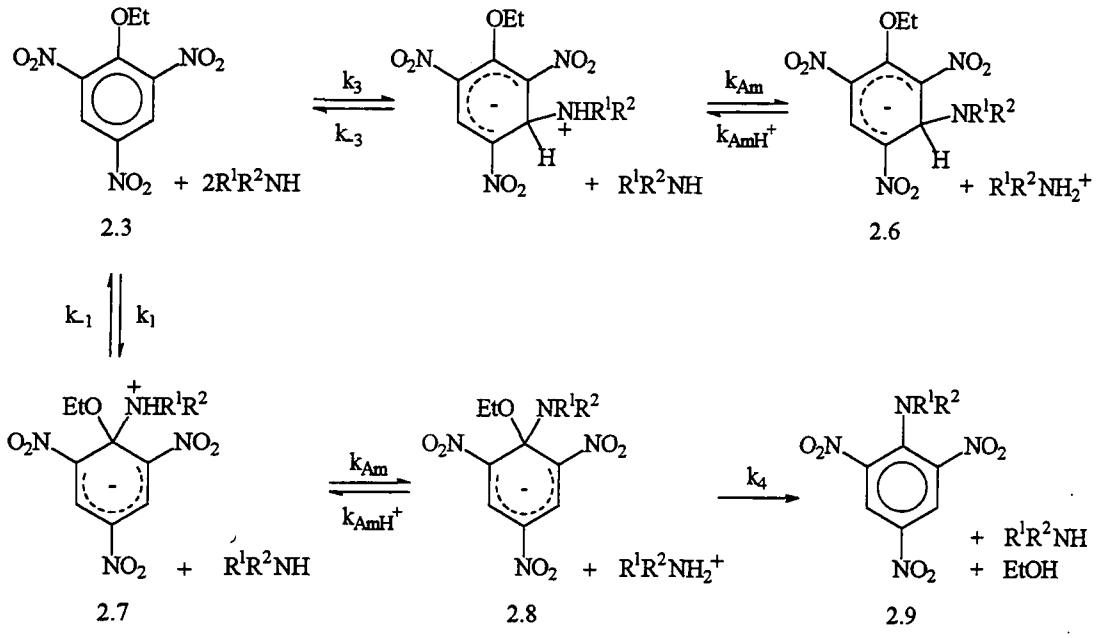

Scheme 2.1

With each amine a very rapid reversible reaction with low amplitude was observed. This was attributed to the equilibration of 2.3 with 2.6, the σ-adduct formed from attack at the 3-position. However the rate of this process in acetonitrile was too fast for measurement by stopped-flow techniques.

This was followed by another rapid, but measurable, reaction giving rise to a species absorbing at 430 and 500 nm. This process is attributed to the equilibration with the 1-adduct on the substitution pathway. Extinction coefficients for these species at 430nm are shown in table 2.9. Isolating the 1-adducts and obtaining absorbance spectra was not possible due to their short lifetimes in acetonitrile. However, figure 2.6 contains the spectrum of the reaction between 2.3 and n-butylamine ca. 15 seconds after mixing. The peaks at 430 and 500 nm are due to the 1-adduct, whilst the peak at 340 nm (and a small percentage of the peak at 430 nm) is due to the substitution product whose spectrum can be seen in figure 2.7.

Table 2.9. Extinction coeffients at 430 nm for species 2.6.[a]

Amine	Absorbance	ε / $dm^3\ mol^{-1}\ cm^{-1}$
n-butylamine	0.189	2.3×10^4
piperidine	0.194	2.4×10^4
pyrrolidine	0.20	2.5×10^4

a. Values measured by stopped-flow spectrophotometry.

Figure 2.6. Spectrum of the reaction between 2.3 and n-butylamine showing the 1-adduct (430 and 500 nm) and the substitution product (340 and 430 nm).

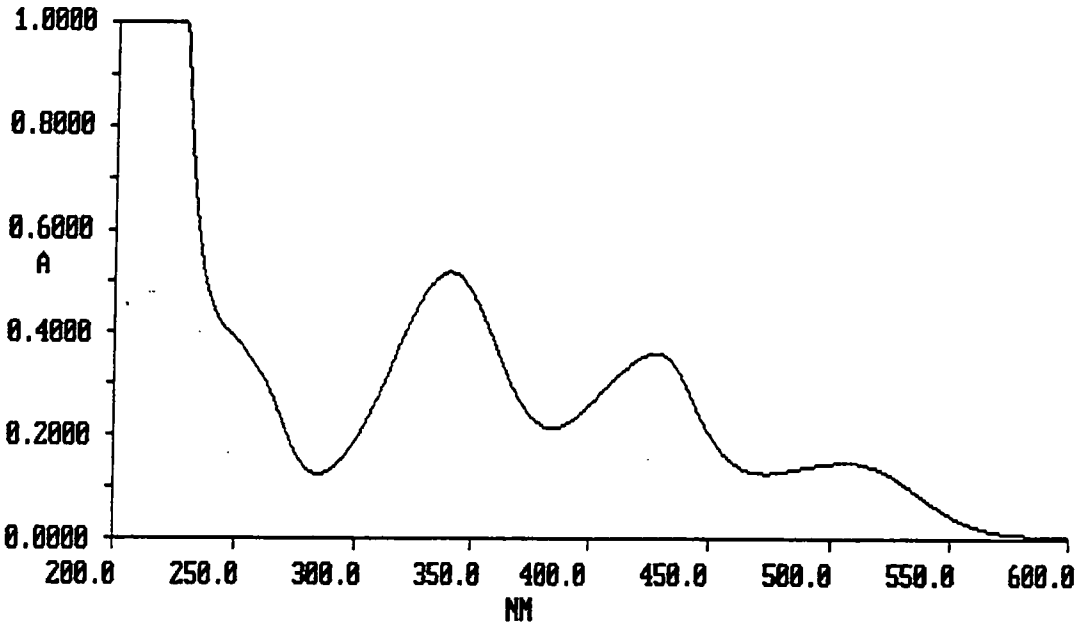

The general rate expression for the formation of these adducts is shown in equation 2.10, where $K_1 \equiv k_1 / k_{-1}$ and $K_{c,3}$ is the equilibrium constant for formation of 2.6 from 2.3. The complete derivation is given in chapter 7 pp 213 - 217.

$$k_{fast} = \frac{K_1 k_{Am}[Am]^2}{\left(1+\frac{k_{Am}}{k_{-1}}[Am]\right)\left(1+K_{c,3}\frac{[Am]^2}{[AmH^+]}\right)} + \frac{k_{AmH}+[AmH^+]_{stoich}}{\left(1+\frac{k_{Am}}{k_{-1}}[Am]\right)(1+K_h[Am])} \quad \text{equation 2.10}$$

If the condition $k_{Am}[Am] >> k_{-1}$ applies then equation 2.10 reduces to equation 2.11.

$$k_{fast} = \frac{k_1[Am]}{1+K_{c,3}\frac{[Am]^2}{[AmH^+]}} + \frac{k_{-1}k_{AmH}+[AmH^+]_{stoich}}{k_{Am}[Am](1+K_h[Am])} \quad \text{equation 2.11}$$

In the reactions of 2.3 with both n-butylamine and pyrrolidine a third reaction, k_{slow}, was observed yielding the substitution product picramides, 2.9. Examples of the product spectra are given in figures 2.7 and 2.8 showing peaks at 340 and 415 nm for the n-butylamine reaction and 362 nm for the pyrrolidine reaction.

Figure 2.7. Spectrum of the picramide formed from 2.3 and n-butylamine.

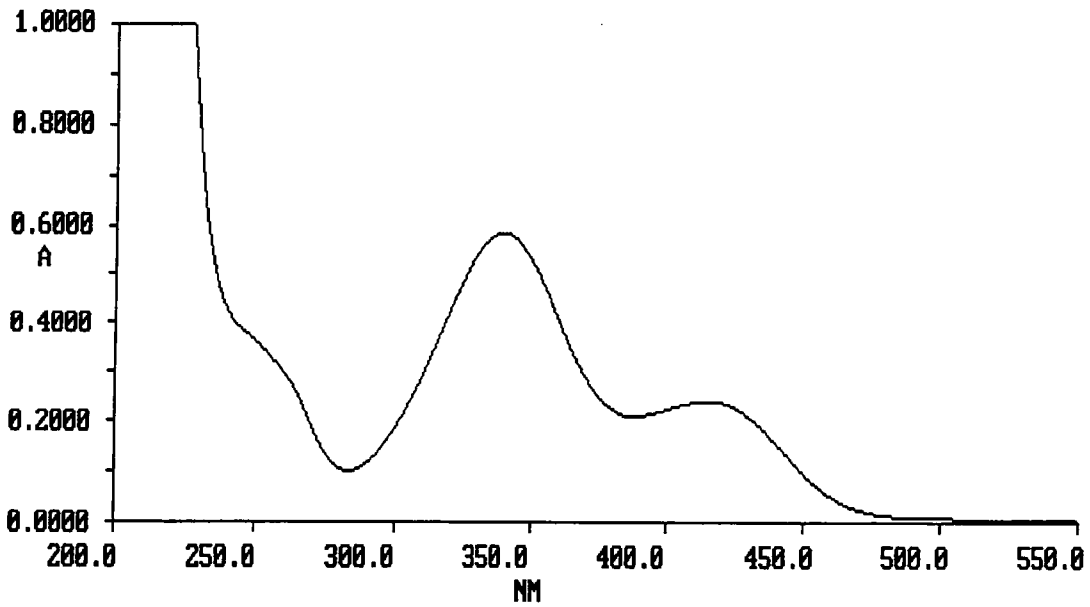

Figure 2.8. Spectrum of the picramide formed from 2.3 and pyrrolidine.

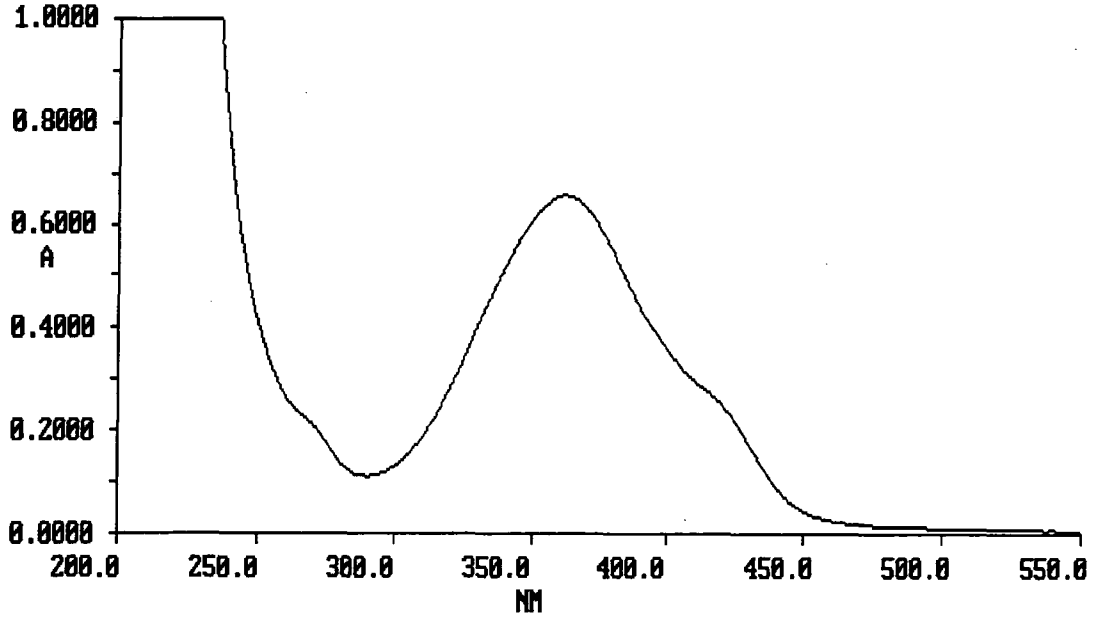

At high amine concentrations the product spectra were shifted to slightly longer wavelength, consistent with the known[23] rapid equilibration of 2.9 with excess amine yielding of the 3-adducts, 2.10. With n-butylamine this reaction is complemented by the loss of a side chain proton resulting in the formation of 2.11.

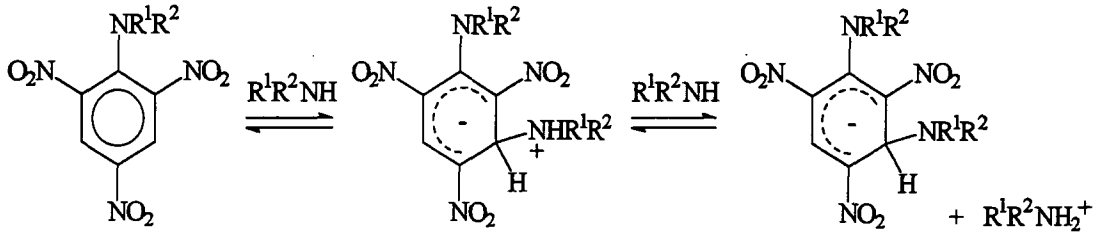

2.9 2.10

Equation 2.12

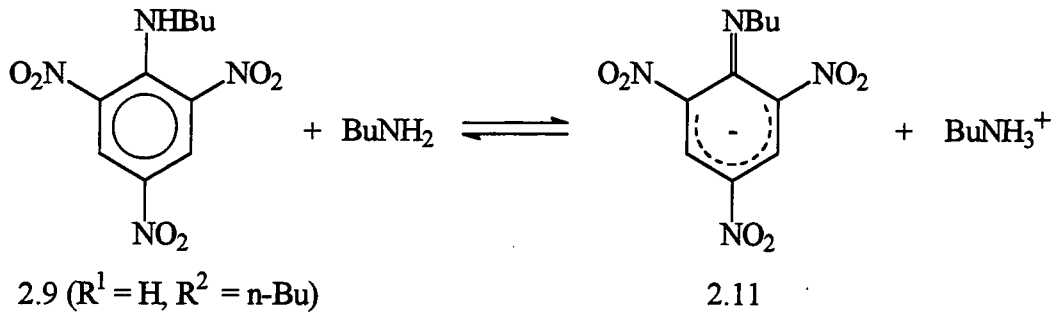

2.9 (R^1 = H, R^2 = n-Bu) 2.11

Equation 2.13

Figure 2.9 shows how the spectrum of the pyrrolidino picramide (1-pyrrolidino-2,4,6-trinitrobenzene) changes in the presence of 0.1 mol dm^{-3} pyrrolidine. Figure 2.10 shows how the spectrum of the N-(n-butyl) picramide changes in the presence of added n-butylamine.

Figure 2.9. Spectra of the pyrrolidino picramide (a), and with 0.1 mol dm^{-3} added pyrrolidine (b).

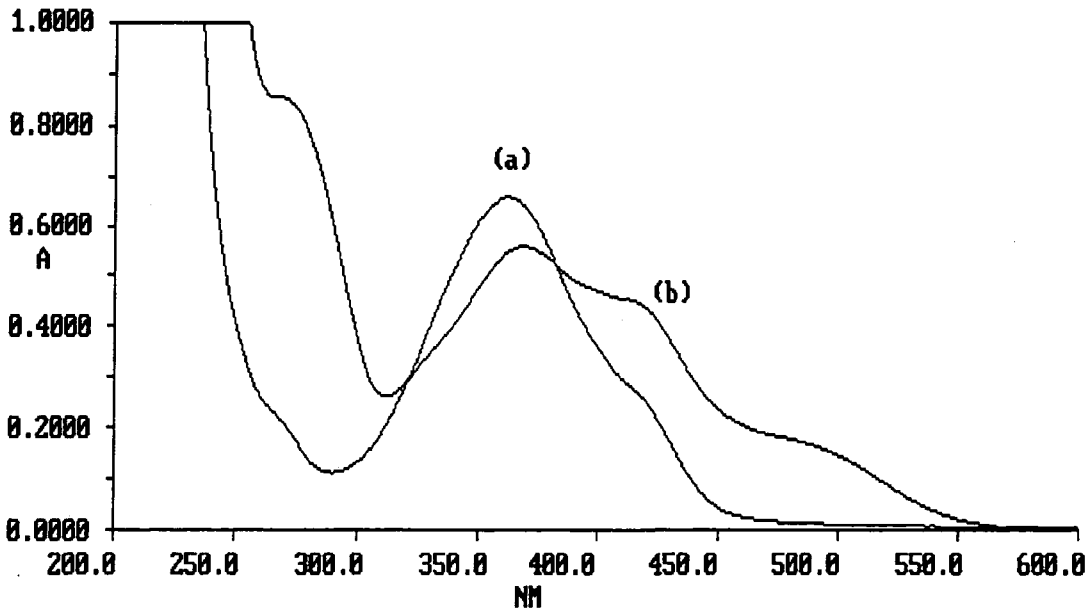

Figure 2.10. Spectra of the N-(n-butyl) picramide (a), with 0.1 mol dm^{-3} added n-butylamine (b), and with 1.0 mol dm^{-3} added n-butylamine (c).

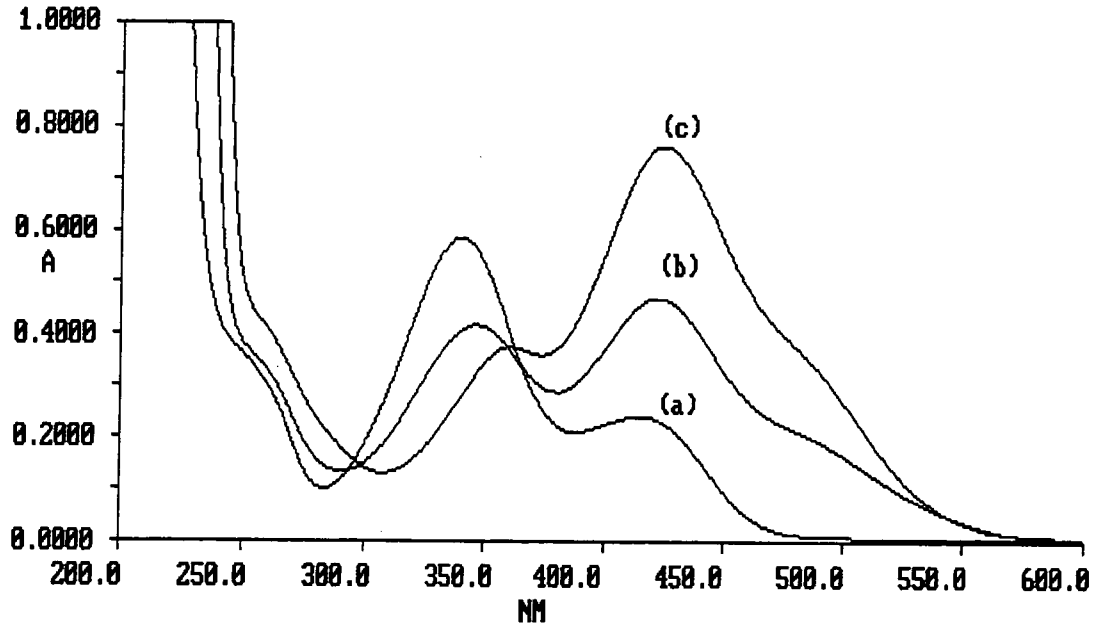

For reactions with pyrrolidine and n-butylamine final spectra at completion of the substitution reactions were identical to those of authentic samples of previously prepared product in the same reaction medium.

Although reaction of 2.3 with piperidine led to the formation of both the 3-adduct, 2.6, and the 1-adduct, 2.8, the subsequent reaction was very slow and did not lead to the expected substitution product, 2.9. This slow reaction was not investigated further.

The rate expression for formation of the picramides is given in equation 2.14, where $K_{c,1}°$ is defined in equation 2.15. The complete derivation of equation 2.14 is given in chapter 7 pp 218 - 220.

$$k_{slow} = \frac{k_4 K_{c,1}°[Am]^2[AmH^+]_{stoich}}{K_{c,1}°[Am]^2(1+K_h[Am])+[AmH^+]_{stoich}} \qquad \text{equation 2.14}$$

$$K_{c,1}° = \frac{[2.9]}{[2.3]} \cdot \frac{[AmH+]_{free}}{[Am]^2} \qquad \text{equation 2.15}$$

The products from the reactions between 2.3 and all three amines have also been characterised using ^1H NMR spectroscopy. Spectral data for the three previously prepared picramide samples are given later in table 2.18. The reaction between 2.3 (0.1 mol dm^{-3}) and n-butylamine (0.2 mol dm^{-3}) in d_3-acetonitrile yielded a spectrum that contained peaks for the picramide (8.92 ppm, s; 3.08 ppm, t; 1.68 ppm, p; 1.38 ppm, sextet; 0.91 ppm, t), n-butylamine (2.61 ppm, t; 1.3 ppm, m; 0.90 ppm, t), and ethanol (3.53 ppm, q; 1.11 ppm, t). The broad peak at δ 3.3 is attributed to slowly exchanging hydroxyl and amino protons. This is shown in figure 2.11. The corresponding reaction with pyrrolidine gave a spectrum containing peaks for the picramide (8.77 ppm, s; 3.30 ppm, t; 1.98 ppm, m), pyrrolidine (2.78 ppm, t(broad); 1.64 ppm, m(broad)) and ethanol (3.53 ppm, q; 1.11 ppm, t) and is shown in figure 2.12. The ^1H NMR results for the reaction of 2.3 with piperidine support the UV/Visible evidence that there is no clean reaction forming the picramide. The spectrum, shown in figure 2.13, contains two sets of quartets and triplets from the original ethoxy functionality and two distinct aromatic peaks pointing towards the possibility of two competing reactions. However, one of these quartets appears at 2.44 ppm indicating the presence of an NCH_2CH_3 grouping rather than an OCH_2CH_3 one.

Figure 2.11. ^1H NMR spectrum of the reaction products from the reaction of 2.3 and n-butylamine in d_3-acetonitrile.

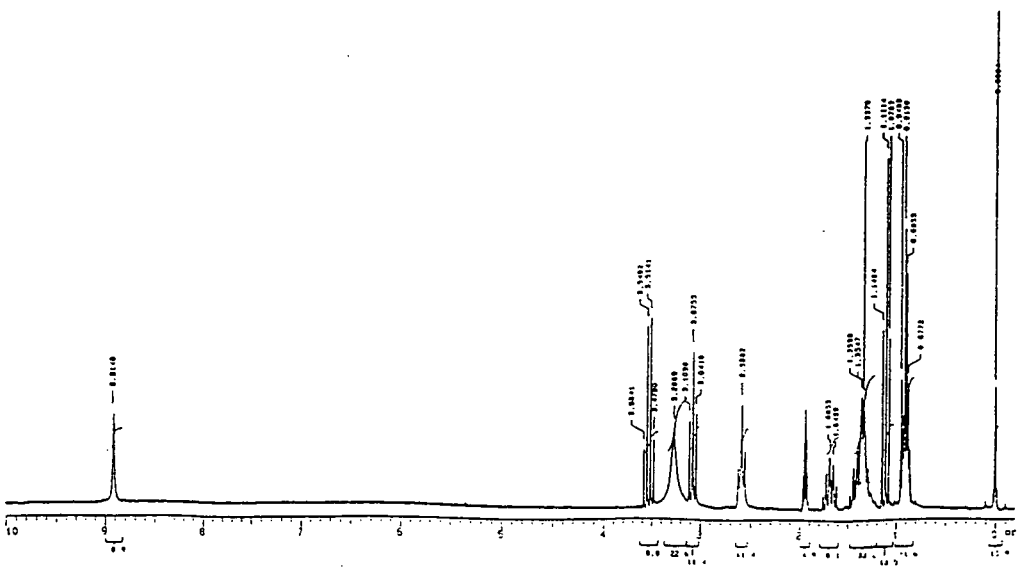

Figure 2.12. ^{1}H NMR spectrum of the reaction products from the reaction of 2.3 and pyrrolidine in d_3-acetonitrile.

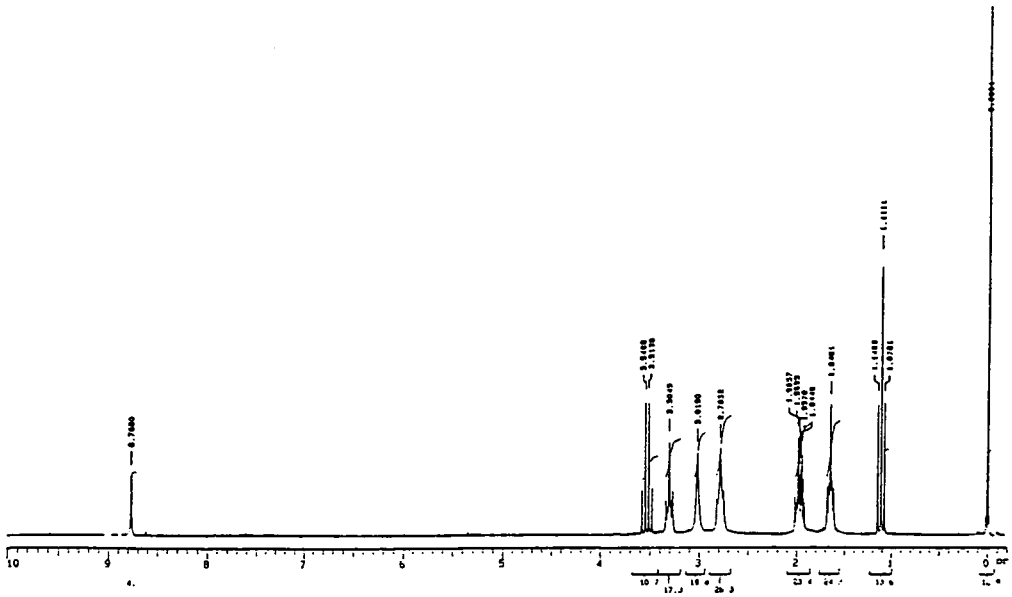

Figure 2.13. ^{1}H NMR spectrum of the reaction products from the reaction of 2.3 and piperidine in d_3-acetonitrile.

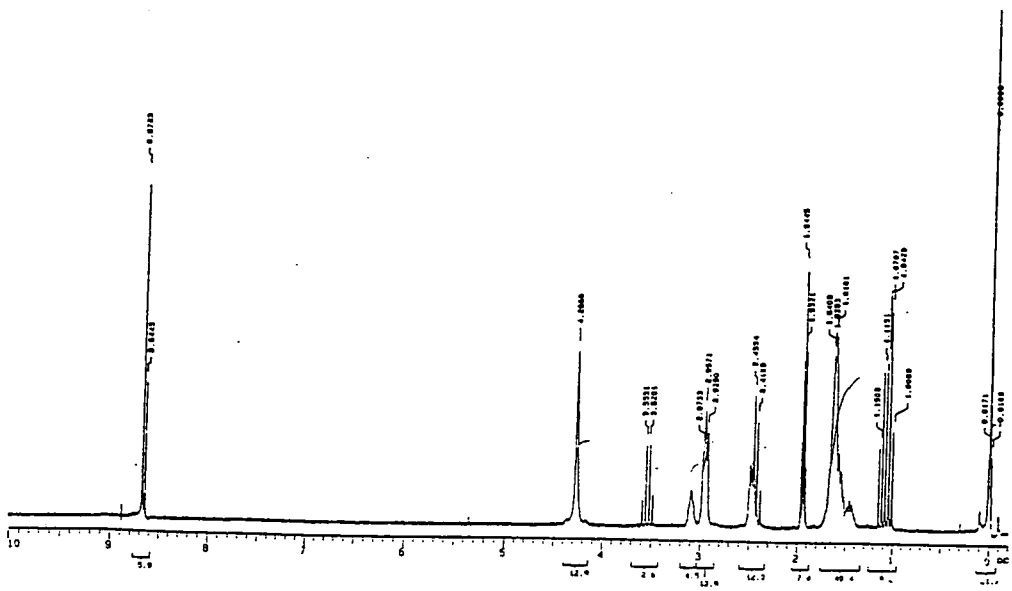

Tables 2.10 and 2.11 contain the results for the reaction of 2.3 with pyrrolidine both with and without added pyrrolidinium perchlorate salt. In solutions containing no added salt the concentration of pyrrolidinium ions produced should ideally be equal to that of the anionic adduct. These concentrations may be calculated from absorbance data. However if the solvent is not perfectly neutral then these concentrations may not be exactly equal. Hence there exists a slight uncertainty in the final salt concentration. For this reason all results calculated are from runs containing 0.001 mol dm^{-3} added salt.

Table 2.10. Kinetic and equilibrium results for the reaction of 2.3[a] with pyrrolidine in acetonitrile at 25°C.

[pyrrolidine] / mol dm^{-3}	Absorbance[b] at 430 nm	Absorbance[b] at 500 nm	k_{fast}[c] / s^{-1}
0.003	0.0269	0.0210	8.3
0.005	0.0557	0.0356	11.4
0.01	0.1096	0.0639	15.4
0.02	0.1610	0.1032	20.9
0.03	0.2354	0.1174	25.1
0.05	0.2607	0.1228	27.5
0.07	0.2769	0.1277	23.1
0.10	0.2782	-	16.4

a. Concentration of 2.3 is 4 x 10^{-5} mol dm^{-3}.

b. Measurement at completion of 1-adduct formation.

c. Measured as a colour forming reaction; identical values were obtained at 430 and 500 nm.

Table 2.11. Kinetic and equilibrium results for the reaction of 2.3[a] with pyrrolidine in acetonitrile containing 0.001 mol dm^{-3} pyrrolidinium perchlorate at 25°C.

[Amine] / mol dm^{-3}	k_{fast}[b] / s^{-1}	k_{calc}[c] / s^{-1}	Abs[d] at 430 nm	$K_{c,1}$[e] / dm^3 mol^{-1}	k_{slow}[f] /10^{-2} s^{-1}	k_4[g] / dm^3 mol^{-1} s^{-1}
0.004	-	-	-	-	0.082	184
0.005	-	-	-	-	0.13	187
0.006	-	-	-	-	0.20	201
0.008	-	-	-	-	0.35	200
0.01	-	-	-	-	0.55	203
0.02	-	-	0.027	0.39	2.0	209
0.03	90	87	0.054	0.41	3.9	225
0.05	78	81	0.125	0.67	6.0	227
0.07	85	87	0.162	0.87	6.2	201
0.10	95	97	0.183	1.08	5.2	211
0.15	97	94	0.195	-	3.9	203
0.20	80	77	0.198	-	2.9	188

a. Concentration of 2.3 is 4×10^{-5} mol dm^{-3}.

b. Measured as a colour forming reaction; identical values were obtained at 430 and 500 nm.

c. Calculated from equation 2.10 using the values K_1k_{Am} 1.1×10^5 dm^6 mol^{-2} s^{-1}, k_{Am} / k_{-1} 86 dm^3 mol^{-1}, $k_{AmH}+$ 3.9×10^5 dm^3 mol^{-1} s^{-1}, K_h 27 dm^3 mol^{-1} and with $K_{c,3} = 0.009(1 + 27[Am])$.

d. Measurement at completion of 1-adduct formation.

e. Calculated as $\frac{Abs}{0.20 - Abs} \cdot \frac{[AmH^+]}{[Am]^2}$.

The data fit the expression $K_{c,1} = 0.28(1 + 27[Am])$

f. Identical results were obtained for measurement of colour forming reaction at 362 nm or fading reaction at 500 nm.

g. Calculated from equation 2.14 with $K_{c,1}°$ 0.28 dm^3 mol^{-1} and K_h 27 dm^3 mol^{-1}.

The absorbance values at completion of the reaction forming the 1-adduct allow the calculation of values for $K_{c,1}$. These lead to a value for $K_{c,1}°$ of 0.28 $dm^3\ mol^{-1}$ through equation 2.16 with K_h 27 $dm^3\ mol^{-1}$.

$$K_{c,1} = K_{c,1}°(1 + K_h[Am])$$ eqaution 2.16

As amine concentration increases, values of k_{fast} decrease before rising to a maximum and then falling again. This behaviour is predicted by equation 2.10 and a good fit is achieved when the following values are inserted.

K_1k_{Am} 1.1 x 10^5 $dm^6\ mol^{-2}\ s^{-1}$, k_{Am} / k_{-1} 86 $dm^3\ mol^{-1}$, $K_{c,3}°$ 0.009 $dm^3\ mol^{-1}$, $k_{AmH}+$ 3.9 x 10^5 $dm^3\ mol^{-1}\ s^{-1}$ and K_h 27 $dm^3\ mol^{-1}$.

This set of values allows calculation of a value for k_1 ($\equiv K_1k_{Am}$. k_{-1} / k_{Am}) of 1280 $dm^3\ mol^{-1}\ s^{-1}$.

$$k_{fast} = \frac{K_1k_{Am}[Am]^2}{\left(1+\frac{k_{Am}}{k_{-1}}[Am]\right)\left(1+K_{c,3}\frac{[Am]^2}{[AmH^+]}\right)} + \frac{k_{AmH}+[AmH^+]}{\left(1+\frac{k_{Am}}{k_{-1}}[Am]\right)(1+K_h[Am])}$$ equation 2.10

At low pyrrolidine concentration ($\leq$ 0.03 mol dm^{-3}) the contribution from the reverse (second) term dominates, though this becomes increasingly less important at concentrations $\geq$ 0.05 mol dm^{-3}. The forward term becomes significant at $\geq$ 0.03 mol dm^{-3} and starts to dominate at $\geq$ 0.07 mol dm^{-3}, climbing to a maximum between 0.10 and 0.15 mol dm^{-3} and then tailing off at $\geq$ 0.20 mol dm^{-3}. The figures are shown in table 2.12.

Table 2.12. Contributions from $k_{forward}$ and $k_{reverse}$ in the theoretically calculated rate constant for the reaction between 2.3 and pyrrolidine.

[Amine] / mol dm^{-3}	$k_{forward}$ / s^{-1}	$k_{reverse}$ / s^{-1}	k_{calc} / s^{-1}
0.03	27.2	60.2	87.4
0.05	49.3	31.3	80.6
0.07	68.1	29.2	87.3
0.10	86.0	11.0	97.0
0.15	88.0	5.6	93.6
0.20	73.2	3.3	76.5

Values of k_{slow}, the product forming reaction, go through a maximum with increasing amine concentration. Substitution of the known values of $K_{c,1}°$ 0.28 dm^3 mol^{-1} s^{-1} and K_h 27 dm^3 mol^{-1} into equation 2.14 yields an average value for k_4 of 203 dm^3 mol^{-1}.

The data for reaction of 2.3 with piperidine are given in table 2.13. The rate data give an excellent fit to equation 2.10 when the following values are inserted.

K_1k_{Am} 6200 dm^6 mol^{-2} s^{-1}, k_{Am} / k_{-1} 8 dm^3 mol^{-1}, $K_{c,3}°$ 0.0015 dm^3 mol^{-1}, $k_{AmH}+$ 2.4 x 10^5 dm^3 mol^{-1} s^{-1} and K_h 25 dm^3 mol^{-1}.

This yields a value for k_1 ($\equiv K_1k_{Am} \cdot k_{-1} / k_{Am}$) of 780 dm^3 mol^{-1} s^{-1}. From the absorbance data $K_{c,1}$ is calculated as 0.025 dm^3 mol^{-1}, which is in good accord with that obtained from the combination of values for K_1k_{Am} and $k_{AmH}+$ using equation 2.15.

Table 2.13. Kinetic and equilibrium results for the reaction of 2.3[a] with piperidine in acetonitrile containing 0.001 mol dm^{-3} piperidinium perchlorate at 25 C.

[Amine] / mol dm^{-3}	k_{fast}[b] / s^{-1}	k_{calc}[c] / s^{-1}	Abs[d] at 430 nm	$K_{c,1}$[e] / dm^3 mol^{-1}
0.03	106	114	-	-
0.05	90	89	0.0239	0.056
0.07	77	75	0.0478	0.067
0.10	70	70	0.0902	0.087
0.15	75	77	0.141	0.12
0.20	84	85	0.169	0.17
0.25	87	88	0.183	-
0.30	85	85	0.189	-
0.40	69	69	0.194	-

a. Concentration of 2.3 is 4×10^{-5} mol dm^{-3}.

b Measured as a colour forming reaction; identical values were obtained at 430 and 500 nm.

c. Calculated from equation 2.10 using the values K_1k_{Am} 6200 dm^6 mol^{-2} s^{-1}, k_{Am} / k_{-1} 8 dm^3 mol^{-1}, $k_{AmH}+$ 2.4×10^5 dm^3 mol^{-1} s^{-1}, K_h 25 dm^3 mol^{-1} and with $K_{c,3} = 0.0015(1 + 25[Am])$.

d. Measurement at completion of 1-adduct formation.

e. Calculated as $\frac{Abs}{0.194 - Abs} \cdot \frac{[AmH^+]}{[Am]^2}$.

The data fit the expression $K_{c,1} = 0.025(1 + 25[Am])$

The data for the reaction of 2.3 with n-butylamine both with and without added n-butylamine perchlorate salt is given in tables 2.14 and 2.15. As in the case with pyrrolidine, calculations are only made on the results containing added salt. At all amine concentrations used the condition $k_{Am}[Am] >> k_{-1}$ is fulfilled and hence equation 2.11 is applicable. An excellent fit is obtained when the values below are inserted.

k_1 130 $dm^3\ mol^{-1}\ s^{-1}$ and $k_{-1}k_{AmH}+ / k_{Am}$ 360 s^{-1}.

Combination of these via equation 2.15 yields a value for $K_{c,1}°$ of 0.36 $dm^3\ mol^{-1}$. Substitution of this and K_h 20 $dm^3\ mol^{-1}$ into equation 2.14 leads to calculation of k_4 8.7 x 10^3 $dm^3\ mol^{-1}\ s^{-1}$. The data indicates that $k_{Am} / k_{-1} > 500\ dm^3\ mol^{-1}$ so that $k_{AmH}+ > 1.8 \times 10^5\ dm^3\ mol^{-1}\ s^{-1}$.

Table 2.14. Kinetic and equilibrium results for the reaction of 2.3[a] with n-butylamine in acetonitrile at 25 C.

[Amine] / mol dm^{-3}	Abs[b] at 430 nm	k_{fast}[c] / s^{-1}
0.02	0.176	2.81
0.03	0.186	3.76
0.05	0.184	5.63
0.07	0.186	7.47
0.10	0.193	10.31
0.15	0.196	13.98
0.20	0.196	16.33
0.25	0.197	16.13
0.30	0.198	15.33

a. Concentration of 2.3 is 4 x 10^{-5} mol dm^{-3}.

b. Measurement at completion of 1-adduct formation.

c. Measured as a colour forming reaction at 430 nm.

Table 2.15. Kinetic and equilibrium results for the reaction of 2.3[a] with n-butylamine in acetonitrile containing 0.001 mol dm^{-3} piperidinium perchlorate at 25 C.

[Amine] / mol dm^{-3}	k_{fast}[b] / s^{-1}	k_{calc}[c] / s^{-1}	Absorbance[d] at 430nm	k_{slow}[e] / s^{-1}	k_4[f] /10^3 dm^3 mol^{-1} s^{-1}
0.02	14	15	0.0312	1.1	9.2
0.03	12	11	0.056	1.8	8.7
0.05	11	10	0.107	2.8	8.7
0.07	11	11	-	3.1	9.3
0.10	14	14	0.162	2.8	9.3
0.15	18	19	0.186	2.1	8.8
0.20	23	24	0.189	1.7	8.3
0.25	28	29	0.186	1.4	8.1
0.30	32	31	0.185	1.1	8.0

a. Concentration of 2.3 is 4×10^{-5} mol dm^{-3}.

b. Measured as a colour forming reaction at 430 nm.

c. Calculated from equation 2.11 with k_1 130 dm^3 mol^{-1} s^{-1}, $k_{-1}k_{AmH^+} / k_{Am}$ 360 s^{-1}, K_h 20 dm^3 mol^{-1} and $K_{c,3} = 0.0004(1 + 20[Am])$ dm^3 mol^{-1}.

d. Measurement at completion of 1-adduct formation.

e. Identical values obtained at 340 and 430 nm.

f. Calculated from equation 2.14 with $K_{c,1}°$ 0.36 dm^3 mol^{-1} and K_h 20 dm^3 mol^{-1}.

Equilibrium data for the formation of both the 1- and 3-adducts are summarised in table 2.16.

Table 2.16. Equilibrium data for the reaction of 2.3 with aliphatic amines in acetonitrile[a] at 25°C.

Amine	$K_{c,3}°$ / $dm^3\ mol^{-1}$	$K_{c,3}^b$ / $K_{c,3}°$	$K_{c,1}°$ / $dm^3\ mol^{-1}$	$K_{c,1}^b$ / $K_{c,1}°$
n-butylamine	0.0004 (15)	4×10^4	0.36 (5×10^4)	1×10^5
piperidine	0.0015 (27)	2×10^4	0.025 (600)	2.4×10^4
pyrrolidine	0.0090 (70)	8×10^3	0.28 (2000)	7×10^3

a. Values for reaction in DMSO[24] in parentheses.

b. Equilibrium constant for reaction in DMSO.[24]

$K_{c,3}°$ values, which increase with the increasing basicity of each amine, are much lower than for the reactions of the amines at an unsubstituted position of 1,3,5-trinitrobenzene. They reflect the ethoxy group's disruption of the planarity of the ortho nitro groups and thus the reduction of their electron withdrawing capabilities. The order of $K_{c,1}°$ values in acetonitrile is qualitatively similar to that in DMSO. It is interesting that the value with n-butylamine is the largest in each solvent. In the 1-adduct, steric interactions between the two groups at the 1-position are important. This steric crowding is likely to be smaller in the n-butylamino-adduct than in adducts formed from secondary amines. All the values in acetonitrile are about 10^4 times smaller than for those in DMSO. This was also seen in the $K_{c,3}°$ values for the reaction with 1,3,5-trintrobenzene and reflects the much reduced ability of acetonitrile in solvating the ionic products compared to DMSO.

Rate data for the reaction of 2.3 with the three amines is given in table 2.17. Compared with corresponding reactions in DMSO slight increases are seen in k_{Am} / k_{-1} for piperidine and pyrrolidine. Both the individual rate constants k_{Am} and k_{-1} are expected to be greater in acetonitrile, so the change in k_{Am} must be slightly greater than that in k_{-1}. As observed in reactions with 1,3,5-trinitrobenzene the values of $k_{AmH}+$ are 10^3 - 10^4 fold higher in acetonitrile than in DMSO.

Table 2.17. Rate data for the reaction of 2.3 with aliphatic amines in acetonitrile[a] at 25°C.

Amine	k_{Am} / k_{-1} / $dm^3\ mol^{-1}$	$k_{AmH}+$ / $dm^3\ mol^{-1}\ s^{-1}$	k_1 / $dm^3\ mol^{-1}\ s^{-1}$
n-butylamine	> 500 (> 1 x 10^4)	> 1.8 x 10^5 (> 50)	130 (250)
piperidine	8 (3)	2.4 x 10^5 (9)	780 (2000)
pyrrolidine	86 (30)	3.9 x 10^5 (60)	1280 (4000)

a. Values for reaction in DMSO in parentheses.[24]

These data will be discussed further after results for substitution reaction of phenyl 2,4,6-trinitrophenyl ether have been presented.

2.4 Reaction of Aliphatic Amines with Phenyl 2,4,6-Trinitrophenyl Ether

In the reactions between phenyl 2,4,6-trinitrophenyl ether, 2.2, and aliphatic amines in acetonitrile, only two time dependent processes are observed, as is the case for reaction in DMSO. Initially, there is a rapid, reversible equilibration with the 3-adducts, 2.13. This is followed by the slower product forming substitution process. The 1-adducts, 2.15, on this latter pathway are not observed. This is attributed to the phenoxide ion's much reduced basicity compared with methoxide, thus rendering it a much superior leaving group. It is known[25] that phenoxide departure from 2.12 is 10^6 times more rapid than methoxide departure. The pK_a values for phenol and methanol in water are shown below in figure 2.14.

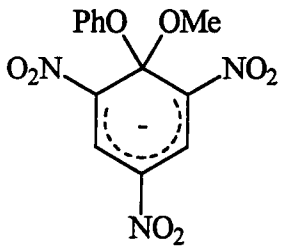

2.12

Figure 2.14. pK_a values[26,27] for phenol and methanol in water.

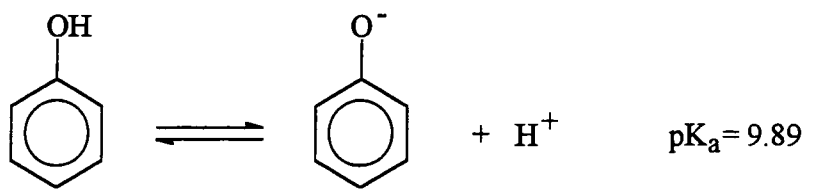

In the series of reactions between amines and 2.2, $k_4 >> k_{AmH}+$, which is a reversal of the case in the reactions with 2.3. This results in a subtle change in the reaction scheme, with the formation of the 1-adducts effectively becoming an irreversible process. This is shown in scheme 2.2.

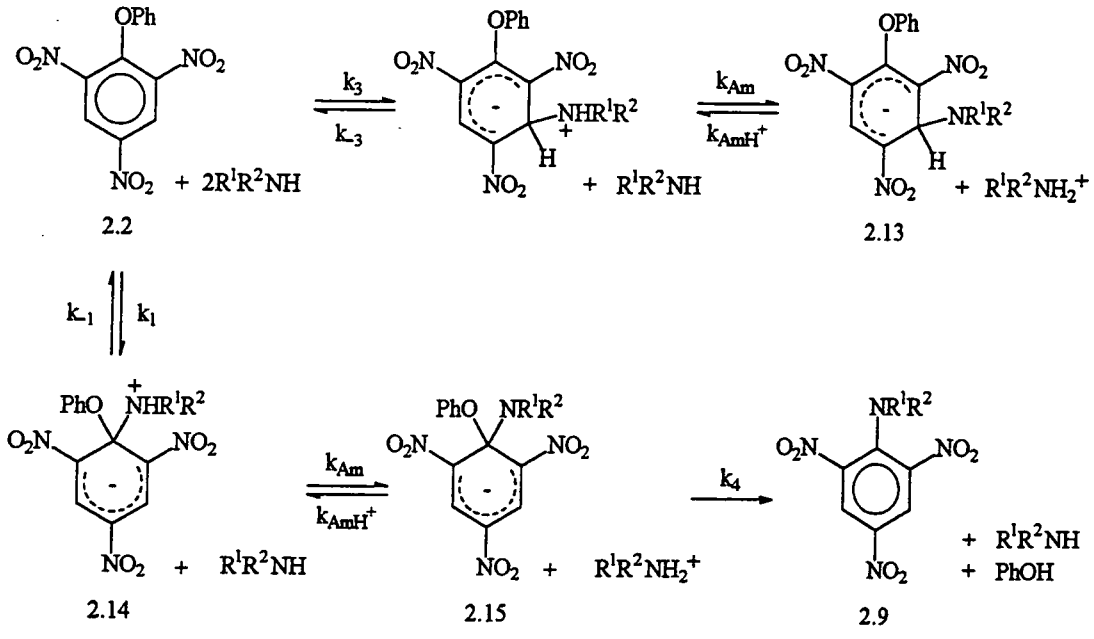

Scheme 2.2

The formation of the 3-adducts, 2.13, can only be followed in the absence of added ammonium salt. This is due to the $K_{c,3}$ values in acetonitrile being very small (< 1 dm^3 mol^{-1}, cf. > 200 dm^3 mol^{-1} in DMSO[24]). Hence, with salt present, only small concentrations of 2.13 are formed, even at the highest amine concentrations used.

Most measurements were made in buffered solutions where concentrations of both amine and amine salt were in large excess of substrate concentration. The general rate expression for formation of the 3-adduct is given in equation 2.17.

$$k_{obs} = \frac{k_3 k_{Am}[Am]^2}{k_{-3} + k_{Am}[Am]} + \frac{k_{-3} k_{AmH} + [AmH^+]_{stoich}}{(k_{-3} + k_{Am}[Am])(1 + K_h[Am])} \qquad \text{equation 2.17}$$

Some measurements were made in the presence of excess amine but in the absence of added ammonium ions. Here complex kinetic behaviour is expected. This is because in the equilibration with the adducts 2.13 the forward reaction is first order but the reverse reaction is second order. Some rate constants obtained under these conditions are quoted in the following tables. However the data here were forced to fit first order curves, which will not strictly apply under the conditions used. Hence data obtained in the absence of added salt are of limited usefulness.

In DMSO[24] the rate constants for reaction at the 3-positions of both the phenyl and ethyl 2,4,6-trinitrophenyl ethers are quite close in value. This is presumably the case in acetonitrile as well. However the formation of the 3-adducts, 2.6, of the ethyl ether could not be followed in acetonitrile. Using the reactions of pyrrolidine with both 2.2 and 2.3 as examples, it can be seen there are two contributing factors in this observation.

i) at amine concentrations < 0.01 mol dm^{-3}, where measurements of the reaction with 2.3 were made, there is only a very low concentration of the 3-adduct, 2.6. Hence only a negligible absorbance change is produced; and

ii) at amine concentrations > 0.01 mol dm^{-3}, at which point appreciable concentrations of 2.6 are formed, the reaction has become too fast to measure.

The subsequent substitution reaction is quite fast in acetonitrile. This results in the spectra of the 3-adducts being unobtainable. They are however expected to be similar to those obtained in DMSO[24] with λ_{max} 430-435 nm and 505nm.

Since the expulsion of the phenoxy leaving group is the most rapid stage of the substitution reaction, the rate expression for formation of the picramides is given by that for the formation of the 1-adducts. This is given in equation 2.18 which is similar to equation 2.10, given previously, but without the reverse term relating to reprotonation of the 1-adducts, 2.15.

$$k_{sub} = \frac{K_1 k_{Am}[Am]^2}{\left(1+\frac{k_{Am}}{k_{-1}}[Am]\right)\left(1+K_{c,3}\frac{[Am]^2}{[AmH^+]}\right)}$$ equation 2.18

For the case when $k_{Am}[Am] >> k_{-1}$ then equation 2.18 simplifies to equation 2.19.

$$k_{sub} = \frac{k_1[Am]}{\left(1+K_{c,3}\frac{[Am]^2}{[AmH^+]}\right)}$$ equation 2.19

Comparison of the uv/vis spectra obtained at completion of the reactions with those of the corresponding picramide derivatives, prepared independently, show that substitution proceeded as expected. The product spectra were identical to those obtained from the reaction of 2.3 with n-butylamine and pyrrolidine, as shown previously in figures 2.7 and 2.8. The reaction between piperidine and 2.2 does lead to the formation of the picramide, 1-piperidino-2,4,6-trinitrobenzene, which was not produced in the corresponding reaction of 2.3. The spectrum of the piperidino picramide is given in figure 2.15. The spectral information for the three picramides produced is given in table 2.18.

Figure 2.15. Spectrum of the picramide formed from 2.2 and piperidine.

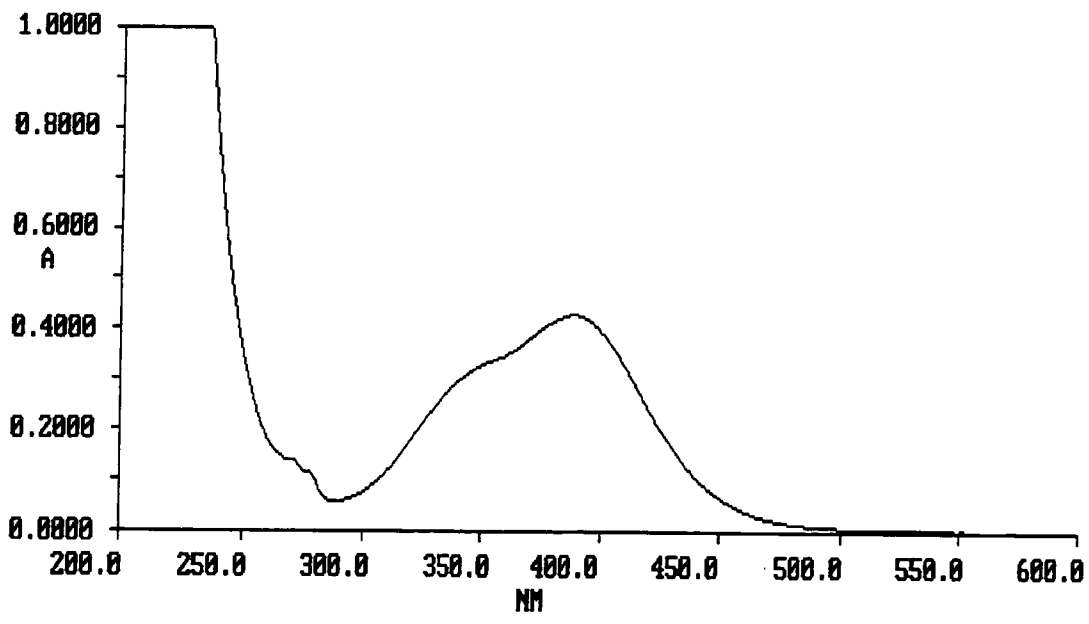

The product spectrum of the piperidino picramide was shifted to higher wavelength at high piperidine concentrations, as shown in figure 2.16, in similar fashion to the corresponding reactions with pyrrolidine and n-butylamine shown in figures 2.9 and 2.10. The peak at 407 nm and shoulder at 480 nm are characteristic[23] of the picramide's 3-adduct. The equilibrium constant for this process is small, however, as in the presence of 0.0005 mol dm^{-3} piperidinium perchlorate the UV/Vis spectrum gives evidence for the sole presence of the parent picramide.

Figure 2.16. Spectra of the piperidino picramide (a), and with 0.1 mol dm^{-3} added piperidine (b).

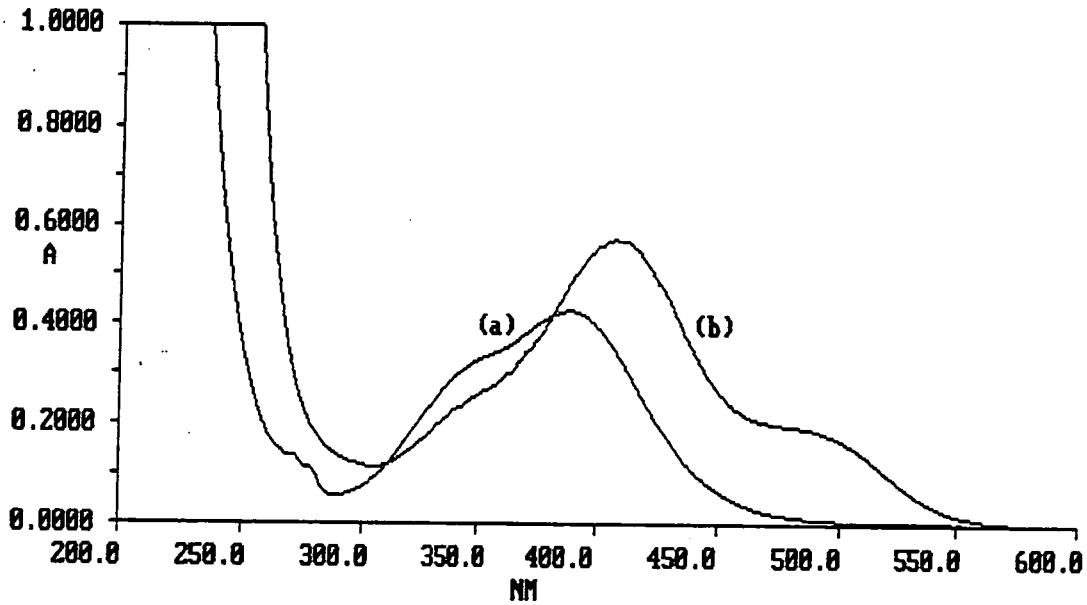

The products from the reactions between 2.2 and all three amines have also been characterised using ^1H NMR spectroscopy. The reaction between 2.2 (0.1 mol dm^{-3}) and n-butylamine (0.2 mol dm^{-3}) in d_3-acetonitrile yielded a spectrum that contained peaks for the picramide (8.93 ppm, s; 3.07 ppm, t; 1.68 ppm, p; 1.38 ppm, sextet; 0.91 ppm, t), n-butylamine (2.63 ppm, t; 1.3 ppm, m; 0.90 ppm, t), and phenol (6.77 ppm, d; 6.79 ppm, t; 7.17 ppm, t). The broad band at δ 4.2 is attributed to slowly exchanging hydroxyl and amino protons. This is shown in figure 2.17. The corresponding reaction with pyrrolidine gave a spectrum containing peaks for the picramide (8.77 ppm, s; 3.30 ppm, t; 1.98 ppm, m), pyrrolidine (2.81 ppm, t(broad); 1.67 ppm, m(broad)) and phenol (6.77 ppm, d; 6.79 ppm, t; 7.17 ppm, t) and is shown in figure 2.18. The reaction of 2.2 with piperidine similarly gave peaks for the picramide (8.63 ppm, s; 3.09 ppm, t(broad); 1.64 ppm, s(v. broad)), piperidine (2.76 ppm, t(broad); 1.52 ppm, m(broad)) and phenol (6.77 ppm, d; 6.79 ppm, t; 7.17 ppm, t). This spectrum is shown in figure 2.19.

Figure 2.17. ^1H NMR spectrum of the reaction products from the reaction of 2.2 and n-butylamine in d_3-acetonitrile.

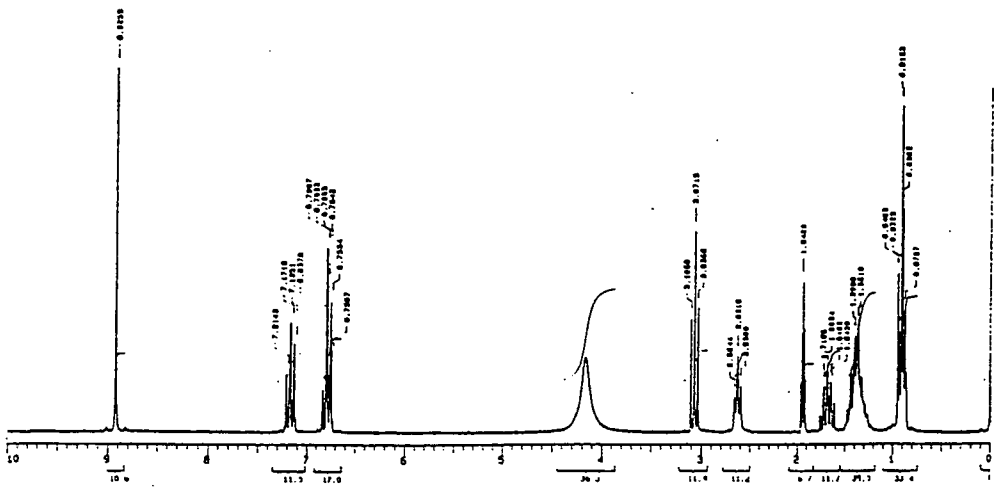

Figure 2.18. ^1H NMR spectrum of the reaction products from the reaction of 2.2 and pyrrolidine in d_3-acetonitrile.

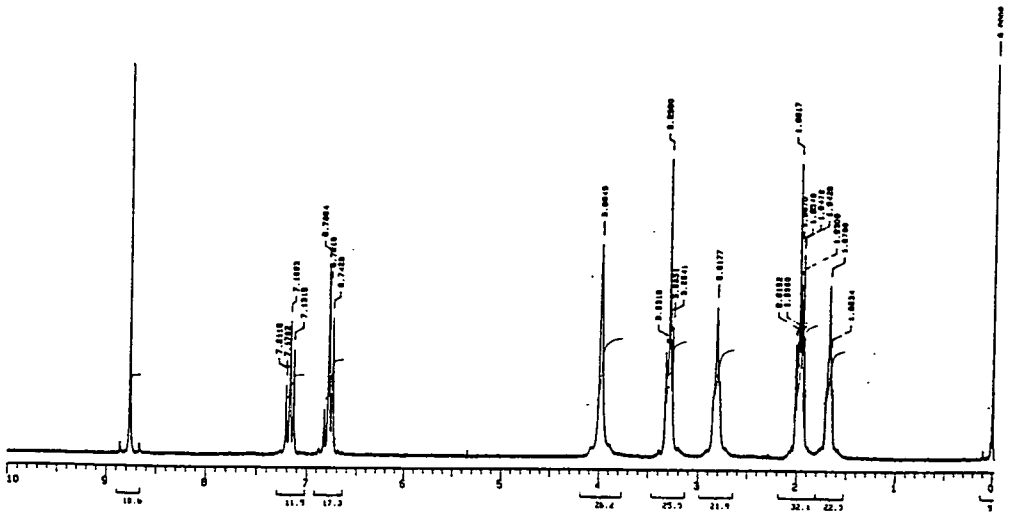

Figure 2.19. ^1H NMR spectrum of the reaction products from the reaction of 2.2 and piperidine in d_3-acetonitrile.

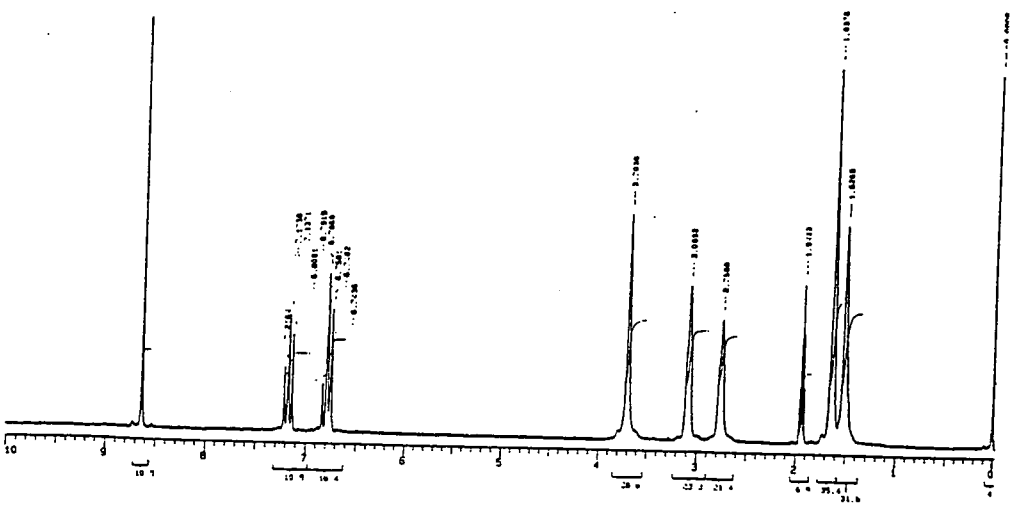

Table 2.18. Spectral information for the N-(n-butylamino), piperidino and pyrrolidino picramides.

Structure	λ_{max} / nm	ε / $dm^3\ mol^{-1}\ cm^{-1}$	^1H NMR signals / ppm (in CD_3CN)
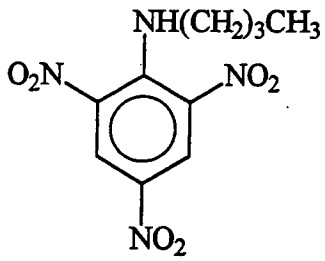 1-(n-butylamino)-2,4,6-trinitrobenzene	340 415	1.53×10^4 6.23×10^3	0.91 (triplet J = 7.0 Hz) 1.38 (sextet) 1.68 (pentet) 3.07 (triplet J = 6.9 Hz) 8.94 (singlet)
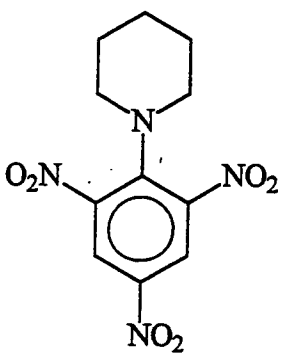 1-piperidino-2,4,6-trinitrobenzene	389	1.08×10^3	1.64 (v. broad singlet) 3.09 (v. broad triplet) 8.65 (singlet)
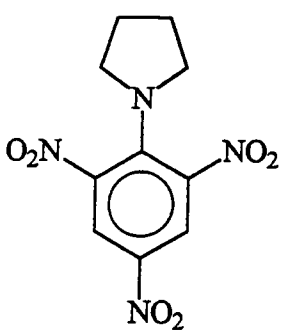 1-pyrrolidino-2,4,6-trinitrobenzene	362	1.63×10^3	1.98 (triplet) 3.30 (triplet) 8.78 (singlet)

Tables 2.19 and 2.20 contain the results for the reaction of 2.2 with pyrrolidine in the absence and in the presence of added pyrrolidinium perchlorate. Rate and equilibrium data were calculated from the reactions carried out in the presence of added salt.

Table 2.19. Kinetic and equilibrium results for the reaction of 2.2[a] with pyrrolidine in acetonitrile at 25°C.

[pyrrolidine] / mol dm^{-3}	k_{fast}[b] / s^{-1}	Absorbance[c]	k_{sub}[b] / s^{-1}	k_{sub}[d] / s^{-1}
0.004	64	0.030	1.23	1.32
0.005	83	0.035	1.69	1.89
0.006	104	0.039	2.08	2.5
0.008	138	0.050	2.87	3.6
0.01	173	0.060	3.43	4.6
0.02	-	-	3.88	-
0.03	-	-	3.29	-
0.05	-	0.128	1.88	-
0.07	-	-	1.36	-
0.10	-	0.135	0.91	-

a. Concentration of 2.2 is 4×10^{-5} mol dm^{-3}.

b. Measured as a colour forming reaction at 415nm.

c. Measured at completion of 3-adduct formation.

d. Calculated from equation 2.20 using the values K_1k_{Am} 1.3×10^5 dm^6 mol^{-2} s^{-1} and k_{Am} / k_{-1} 55 dm^3 mol^{-1}.

Table 2.20. Kinetic and equilibrium results for the reaction of 2.2[a] with pyrrolidine in acetonitrile containing 0.001 mol dm^{-3} pyrrolidinium perchlorate at 25°C.

[pyrrolidine] / mol dm^{-3}	k_{sub}[b] / s^{-1}	k_{calc}[c] / s^{-1}	Absorbance[d]	$K_{c,3}$[e] / dm^3 mol^{-1}
0.004	1.72	1.70	-	-
0.005	2.56	2.54	-	-
0.006	3.52	3.50	-	-
0.008	5.89	5.72	-	-
0.01	8.29	8.23	-	-
0.02	22.5	22.6	-	-
0.03	35.6	35.3	-	-
0.05	46.4	45.5	0.064	0.361
0.07	42.0	41.1	0.090	0.408
0.10	28.7	29.6	0.115	0.575

a. Concentration of 2.2 is 4×10^{-5} mol dm^{-3}.

b. Measured at 415nm as a colour forming reaction for amine concentrations $\leq$ 0.03 mol dm^{-3} and a colour fading reaction for amine concentrations $\geq$ 0.05 mol dm^{-3}.

c. Calculated from equation 2.18 using the values K_1k_{Am} 1.3×10^5 dm^6 mol^{-2} s^{-1}, k_{Am} / k_{-1} 55 dm^3 mol^{-1} and $K_{c,3} = 0.155(1 + 27[Am])$ dm^3 mol^{-1}.

d. Measured at the start of the substitution reaction. Final absorbances at the end of the substitution reaction are ca. 0.056 for all amine concentrations

e. Calculated as $\frac{Abs}{0.135 - Abs} \cdot \frac{[AmH^+]}{[Am]^2}$.

The absorbance values at completion of the reaction forming the 3-adduct allow the calculation of values of $K_{c,3}$. Use of the known value of K_h 27 $dm^3\ mol^{-1}$ allowed the calculation of $K_{c,3}°$ 0.155 $dm^3\ mol^{-1}$.

As amine concentration increases, values of k_{sub} increase, reaching a maximum at a concentration of 0.05 mol dm^{-3}, after which point they begin to decrease due to a stengthening contribution of $K_{c,3}$. A good fit was obtained when the following values were inserted into equation 2.18.

K_1k_{Am} 1.3 x 10^5 $dm^6\ mol^{-2}\ s^{-1}$, k_{Am} / k_{-1} 55 $dm^3\ mol^{-1}$ and $K_{c,3}°$ 0.155 $dm^3\ mol^{-1}$.

The results in table 2.19 show that in the absence of added salt there is greater initial formation of the 3-adduct. The measurements at higher amine concentrations, where the reaction proceeds to virtual completion, allow the determination of a value of 0.135 for the absorbance of this adduct. It is interesting to compare the values for k_{sub} in tables 2.19 and 2.20. The results show that in the absence of added salt, AmH^+, values are, at a given amine concentration, lower than those in the presence of salt. Also the maximum value of k_{sub} is reached at a lower amine concentration. This is the expected result of the greater contribution of the $K_{c,3}$ term in equation 2.18. Since

$$K_{c,3} = \frac{[3\text{-Adduct}]}{[\text{Parent}]} \cdot \frac{[AmH^+]}{[Am]^2}$$

it is possible to reformulate equation 2.18 in the form of equation 2.20 where absorbance values are those at the completion of the reaction forming the 3-adduct. Using these values, and the values previously calculated for K_1k_{Am} and for k_{Am} / k_{-1}, yielded values for k_{sub} which are in reasonable agreement with the experimental results. However these data are judged to be less reliable than those obtained in buffered solutions.

$$k_{sub} = \frac{K_1k_{Am}[Am]^2}{\left(1+\frac{k_{Am}}{k_{-1}}[Am]\right)\left(1+\frac{Abs}{(Abs)_\infty - Abs}\right)} \qquad \text{equation 2.20}$$

The data for reaction of 2.2 with piperidine both in the absence and presence of added piperidinium perchlorate salt are given in tables 2.21 and 2.22. The absorbances at completion of the reaction forming the 3-adduct, in the absence of added salt, allow calculation of $K_{c,3}$ values. Extrapolation back to zero amine concentration gives $K_{c,3}°$ 0.016 dm^3 mol^{-1}. Rate constants were calculated from the reactions carried out in the presence of added salt.

Table 2.21. Kinetic and equilibrium results for the reaction of 2.2 with piperidine in acetonitrile at 25°C.

[piperidine] / mol dm^{-3}	k_{fast}[a] / s^{-1}	Absorbance[b]	$K_{c,3}$[c] dm^3 mol^{-1}	k_{sub}[d] / s^{-1}
0.01	-	-	-	0.356
0.0125	44.16	0.1278	0.0188	0.551
0.015	50.59	0.1524	0.0197	0.693
0.0175	58.71	0.1926	(0.0258)	0.828
0.02	69.01	0.2072	0.0239	0.907
0.03	102.5	0.2890	0.0274	1.371
0.05	211.5	0.3960	0.0323	1.488
0.07	365.5	0.4570	0.0380	1.437
0.10	-	0.5100	-	1.276
0.15	-	-		0.942
0.20	-	-		0.792
0.25	-	-		0.604

a. Measured as colour forming reaction at 430 nm.

b. Measured at the end of the reaction forming the 3-adduct.

c. Calculated as $\frac{Abs}{0.54 - Abs} \cdot \frac{[AmH^+]}{[Am]^2}$ where [AmH+] = [Adduct].

d. Measured as colour forming reaction at 353 nm. The product spectra have a shoulder peak at this wavelength with $\varepsilon = 8.4 \times 10^3$ dm^3 mol^{-1} cm^{-1}.

Table 2.22. Kinetic and equilibrium results for the reaction of 2.2[a] with piperidine in acetonitrile containing 0.001 mol dm^{-3} piperidinium perchlorate at 25°C.

[piperidine] / mol dm^{-3}	k_{sub}[b] / s^{-1}	k_{calc}[c] / s^{-1}
0.01	0.47	0.48
0.0125	0.73	0.74
0.015	1.03	1.04
0.0175	1.40	1.39
0.02	1.78	1.77
0.03	3.81	3.69
0.05	9.2	8.6
0.07	14.4	13.8
0.10	19.0	19.5

a. Concentration of 2.2 is $4x10^{-5}$ mol dm^{-3}.

b. Measured as a colour forming reaction at 353 nm.

c. Calculated from equation 2.18 using the values K_1k_{Am} 5200 dm^6 mol^{-2} s^{-1}, k_{Am} / k_{-1} 8 dm^3 mol^{-1}, $K_{c,3}°$ 0.016 dm^3 mol^{-1}.

Values of k_{sub} show a linear dependence on the square of piperidine concentration up to 0.0175 mol dm^{-3}. They still keep increasing at concentrations greater than this. It should be noted that the contribution from $K_{c,3}$ doesn't become large enough at the amine concentrations used to start reducing k_{sub}. A good fit was obtained when the following values were inserted into equation 2.18.

K_1k_{Am} 5200 dm^6 mol^{-2} s^{-1}, k_{Am} / k_{-1} 8 dm^3 mol^{-1}, $K_{c,3}°$ 0.016 dm^3 mol^{-1}.

The results in the absence of added salt, in table 2.21, show that k_{sub} reaches a maximum value as the amine concentration is increased, reflecting the enhanced contribution of the $K_{c,3}$ term under these conditions.

Tables 2.23 and 2.24 contain the results for the reaction of 2.2 with n-butylamine both with and without added n-butylammonium perchlorate. Absorbances at the end of the 3-adduct formation, in the absence of salt allow calculation of $K_{c,3}$ values. This gives $K_{c,3}°$ 9.4 x 10^{-4} dm^3 mol^{-1}. Rate constants were calculated from the reactions carried out in the presence of added salt.

Table 2.23. Kinetic and equilibrium results for the reaction of 2.2[a] with n-butylamine in acetonitrile at 25°C.

[n-butylamine]	Absorbance[b]	10^3 x $K_{c,3}$[c] / dm^3 mol^{-1}	k_{sub}[d] / s^{-1}
0.004			0.727
0.005			0.907
0.006			1.08
0.008			1.42
0.01	0.0086	0.96	1.77
0.015	0.0137	1.11	2.54
0.02	0.0185	1.18	3.35
0.03	0.0318	1.68	4.48
0.04	0.044	1.98	5.72
0.05	0.057	2.35	6.76
0.07	0.079	2.80	-[e]
0.10	0.109	3.72	5.92
0.15	0.140	4.84	5.04
0.20	0.158	6.30	3.63
0.50	0.181	-	-

a. Concentration of 2.2 is $4x10^{-5}$ mol dm^{-3}.

b. Measured at the end of the formation of the 3-adduct at 430 nm.

c. Calculated as $\frac{Abs}{0.18 - Abs} \cdot \frac{[AmH^+]}{[Am]^2}$ where $[AmH+] = \frac{Abs}{0.18} \cdot 4 \times 10^{-5}$.

d. Measured as a colour forming reaction for 0.05 mol dm^{-3} ≥ [n-butylamine] ≥ 0.004 mol dm^{-3} or a colour fading reaction for 0.2 mol dm^{-3} ≥ [n-butylamine] ≥ 0.1 mol dm^{-3}.

e. Absorbance of adduct is equal to absorbance of product, hence no rate measurable.

Table 2.24. Kinetic and equilibrium results for the reaction of 2.2[a] with n-butylamine in acetonitrile containing 0.001 mol dm^{-3} n-butylammonium perchlorate at 25°C.

[n-Butylamine]	k_{sub}[b] / s^{-1}	k_{calc}[c] / s^{-1}
0.01	1.81	1.83
0.02	3.65	3.66
0.05	9.20	9.10
0.07	12.66	12.64
0.10	17.49	17.64

a. Concentration of 2.2 is $4x10^{-5}$ mol dm^{-3}.

b. Measured as a colour forming reaction at 418 nm.

c. Calculated from equation 2.19 using the values k_1 183 dm^3 mol^{-1} s^{-1} and $K_{c,3}°$ 9.4 x 10^{-4} dm^3 mol^{-1}.

The data in table 2.24 show, that in the presence of added salt, the rate constant for the substitution process increases in nearly linear fashion with increasing amine concentration. This indicates that equation 2.19 is applicable and in terms of scheme 2.2, is compatible with attack by n-butylamine at the 1-position being the rate determining step in the substitution process. The value calculated for k_1 is 183 dm^3 mol^{-1} s^{-1}. The rate constants for the substitution process in the absence of added salt in table 2.23 are, at low amine concentrations, similar to those in the presence of salt. However at higher amine concentrations, where the denominator of equation 2.19 becomes important, values of k_{sub} reach a maximum and then decrease.

The data for reaction of the phenyl ether, 2.2, are collected in table 2.25 where they are compared with corresponding data for reaction in DMSO. As observed for reaction with 1,3,5-trinitrobenzene, 2.1, and the ethyl ether, 2.3, values of $K_{c,3}°$ are ca. 10^4 smaller in acetonitrile compared to those in DMSO. This is likely to reflect the much better ability of DMSO to solvate the ionic products. Values of k_1 are only slightly smaller (between 2 and 7 times) in acetonitrile than in DMSO.

Table 2.25. Summary of results for the reaction of 2.2 with aliphatic amines in acetonitrile[a] at 25°C.

Amine	$K_{c,3}^{\circ}$ / $dm^3\ mol^{-1}$	K_1k_{Am} / $dm^3\ mol^{-1}\ s^{-1}$	k_{Am} / k_{-1} / $dm^3\ mol^{-1}$	k_1 / $dm^3\ mol^{-1}\ s^{-1}$
n-butylamine	9.4×10^{-4}	-	-	183
	(210)	-	-	(410)
piperidine	0.016	5200	55	2400
	(1300)	(3000)	(20)	(1×10^4)
pyrrolidine	0.155	1.3×10^5	8	650
	(400)	(2×10^5)	(0.6)	(5000)

a. Results for reaction in DMSO[24] given in parentheses.

2.5 Discussion

Table 2.26 contains all the data for the reactions of 1,3,5-trinitrobenzene, 2.1, and both the phenyl and ethyl 2,4,6-trinitrophenyl ethers, 2.2 and 2.3, with aliphatic amines in acetonitrile.

Table 2.26. Summary of results for the reactions of 2.1, 2.2 and 2.3, with aliphatic amines in acetonitrile at 25°C.

	2.1	2.2	2.3
Reaction with n-butylamine			
$K_{c,3}°$ / dm^3 mol^{-1} s^{-1}	0.002	0.00094	0.0004
K_3k_{Am} / dm^3 mol^{-1} s^{-1}	$> 3.6 \times 10^6$	-	-
$k_{AmH}+$/ dm^3 mol^{-1} s^{-1}	$> 10^7$	-	-
$K_{c,1}°$ / dm^3 mol^{-1}	-	-	0.36
k_1 / dm^3 mol^{-1} s^{-1}	-	183	130
k_{Am} / k_{-1} / dm^3 mol^{-1}	-	-	> 500
$k_{AmH}+$ / dm^3 mol^{-1} s^{-1}	-	-	$> 1.8 \times 10^5$
k_4 / dm^3 mol^{-1} s^{-1}	-	-	8.7×10^3
Reaction with piperidine			
$K_{c,3}°$ / dm^3 mol^{-1} s^{-1}	0.055	0.016	0.0015
K_3k_{Am} / dm^3 mol^{-1} s^{-1}	1.4×10^5	-	-
$k_{AmH}+$/ dm^3 mol^{-1} s^{-1}	2.5×10^6	-	-
$K_{c,1}°$ / dm^3 mol^{-1}	-	-	0.025
k_1 / dm^3 mol^{-1} s^{-1}	-	650	780
k_{Am} / k_{-1} / dm^3 mol^{-1}	-	8	8
$k_{AmH}+$ / dm^3 mol^{-1} s^{-1}	-	-	2.4×10^5
k_4 / dm^3 mol^{-1} s^{-1}	-	-	-
Reaction with pyrrolidine			
$K_{c,3}°$ / dm^3 mol^{-1} s^{-1}	0.20	0.155	0.009
K_3k_{Am} / dm^3 mol^{-1} s^{-1}	2×10^6	-	-
$k_{AmH}+$/ dm^3 mol^{-1} s^{-1}	9×10^6	-	-
$K_{c,1}°$ / dm^3 mol^{-1}	-	-	0.28
k_1 / dm^3 mol^{-1} s^{-1}	-	2400	1280
k_{Am} / k_{-1} / dm^3 mol^{-1}	-	55	86
$k_{AmH}+$ / dm^3 mol^{-1} s^{-1}	-	-	3.9×10^5
k_4 / dm^3 mol^{-1} s^{-1}	-	-	203

2.5.1 Comparisons of Parent Compounds

For attack at 3-position, $K_{c,3}°$ follows the trend 2.1 > 2.2 > 2.3 with each amine. The reduction of the values of 2.2 and 2.3 compared to 2.1 reflects the steric disruption of the ortho- nitro groups in the parent compound. Forcing the nitro groups out of the ring plane has the effect of reducing their electron-withdrawing capacity and hence decreasing the overall equilibrium constant. The σ_{meta} values for phenoxy and ethoxy groups are 0.25 and 0.10 respectively, so both have a favourable electronic effect for reaction at the 3-position.

For attack at 1-position there is little difference in the ratios k_1 (2.2) : k_1 (2.3), with values of 1.9 for reaction with pyrrolidine and 0.8 with piperidine. In this case there is a combination of two factors with inductive withdrawal virtually balancing the steric hindrance to nucleophilic attack.

All these results are similar to those for the reactions made using DMSO.

2.5.2 Comparison of Amines

The pK_a values for the three aliphatic amines n-butylamine, piperidine and pyrrolidine are given in table 2.27.

Table 2.27. pK_a values for n-butylamine, piperidine and pyrrolidine in acetonitrile.[12,15]

	n-butylamine	piperidine	pyrrolidine
pK_a	18.26	18.92	19.58

$K_{c,3}°$ values follow the trend pyrrolidine > piperidine > n-butylamine with each substrate, reflecting the basicity of the reacting amine. Values are between 4 and 10 times larger for reaction with pyrrolidine than for piperidine, and between 100 and 165 times larger for reaction with pyrrolidine than for n-butylamine.

Values of k_1 also reflect the the basicities of each amine. However, amine basicity is not the major factor in the trend in $K_{c,1}°$ values in which n-butylamine > pyrrolidine > piperidine. The dominant factor here is internal steric congestion. The 1-adduct formed from 2.3 and the primary amine n-butylamine, suffers from less internal congestion than the 1-adducts formed from the secondary amines pyrrolidine and piperidine. Hence the n-butylamino adduct has the largest equilibrium constant. A similar effect would be expected with the 1-adducts of 2.2 if they were observable on the substitution pathway. The structures of 1-adducts of n-butylamine, pyrrolidine and piperidine are shown in 2.16, 2.17 and 2.18.

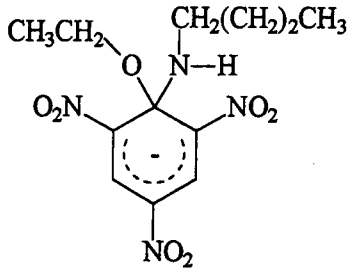

2.16

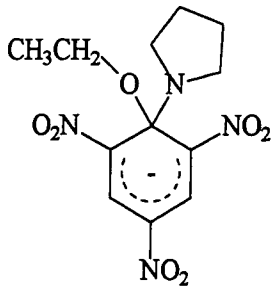

2.17

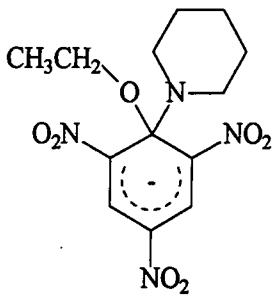

2.18

$K_{c,1}°$ values are always larger than those for $K_{c,3}°$. Ratios of $K_{c,1}°$: $K_{c,3}°$ for 1-adducts of 2.3 are 900 for n-butylamine, 31 for pyrrolidine and 17 for piperidine. This shows a thermodynamic preference for attack at the 1-position for all three amines, though especially so for n-butylamine.

2.5.3 Mechanism of Substitution

In the reaction of the ethyl ether, 2.3, with aliphatic amines, the 1-adduct intermediates are observable on the substitution pathway. Since $k_{AmH}+ > k_4$, the anionic intermediates, 2.8, revert to the zwitterions, 2.7, more rapidly than they are converted to product. Hence loss of the ethoxy group becomes rate determining and subject to acid catalysis. This conforms to the SB-GA mechanism.

Results in tables 2.11 and 2.15 show that k_4 (n-butylamine) > k_4 (pyrrolidine). This is probably a reflection of the n-butylammonium ion having a higher acidity than the pyrrolidinium ion (a reversal of the basicities of the parent amines). There may also be a steric factor as well, with approach of the n-butylammonium ion to 2.16 being less hindered than the approach of the pyrrolidinium ion to 2.17.

For the reaction of the phenyl ether, 2.2, with aliphatic amines, there was no evidence for the build-up in concentration of intermediates formed by attack at the 1-position. With the phenoxide ion being a much superior leaving group to the ethoxide ion, the case now arises that $k_4 > k_{AmH}+$ and formation of the anionic intermediates becomes the rate determining step in the substitution mechanism. Results show that in the reaction of 2.2 with n-butylamine nucleophilic attack is rate limiting as $k_{Am}[Am] >> k_{-1}$. However in the reactions with pyrrolidine and piperidine proton transfer is rate limiting or partially rate limiting, as $k_{-1} \geq k_{Am}[Am]$. This is most probably the consequence of lower values of k_{Am} expected for reaction with the secondary amines resulting from the greater steric hindrance to proton transfer. Values of k_{-1} for the reaction of secondary amines may also be higher due to the steric strain in the anionic adducts, 2.14, which results in their more rapid reversion to reactants. Similarly in the formation of the anionic adducts, 2.8, from 2.3, the rate limiting step may change from nucleophilic attack to proton transfer as the amine is changed from n-butylamine to a secondary amine.

2.5.4 Solvent Effects

It is interesting to compare the data for reaction in acetonitrile with the corresponding results in DMSO to see how changes in solvent alter the values of both equilibrium and rate constants.

Values of the overall equilibrium constants $K_{c,3}°$ and $K_{c,1}°$ are ca. 10^4 - 10^5 times lower in acetonitrile than in DMSO. For 2.1 the ratio $K_{c,3}°$ (DMSO) : $K_{c,3}°$ (CH_3CN) is 5 x 10^5 for reaction with n-butylamine, 4 x 10^4 for piperidine and 1.5 x 10^4 for pyrrolidine. For reaction with 2.2 the ratios are 2.2 x 10^5, 2.5 x 10^4 and 8.4 x 10^3, and with 2.3 they are 4 x 10^4, 2 x 10^4 and 7.8 x 10^3 for each respective amine. We can also get the ratio $K_{c,1}°$ (DMSO) : $K_{c,1}°$ (CH_3CN) for the reaction of 2.3. Values are 1.2 x 10^5 for n-butylamine, 2.4 x 10^4 for piperidine and 7.1 x 10^3 for pyrrolidine. In all these reactions charged species are produced from neutral reactants.

This 10^4 - 10^5 fold reduction in values of $K_{c,3}°$ and $K_{c,1}°$ in acetonitrile can be interpretted in terms of the improved ability of DMSO to solvate charged species than acetonitrile. The trend in the ratios shows that n-butylamine > piperidine > pyrrolidine, which follows the acidities of the substituted ammonium ions. DMSO is known to be a particularly good hydrogen-bond acceptor and this trend may reflect the much improved stability of these ions in this solvent. The need for stabilization of the substituted ammonium ions in acetonitrile is evidenced by the observation of homoconjugation with the parent amines. This interaction is not observed in DMSO.

Results in acetonitrile lead to the direct determination of values of $k_{AmH}+$, the rate constant for protonation of anionic adducts by ammonium ions. The values obtained are ca. 10^4 times larger in acetonitrile than those in DMSO and are compared in table 2.28.

Table 2.28. Comparison of $k_{AmH}+$ values for the reactions 2.1 and 2.3 with aliphatic amines in acetonitrile and DMSO[18,21].

Amine		$k_{AmH}+$ / dm^3 mol^{-1} s^{-1}	
		2.1[a]	2.3[b]
n-butylamine	CH_3CN	$> 10^7$	$>1.8 \times 10^5$
	DMSO	6×10^4	> 50
	ratio	$> 2 \times 10^2$	-
piperidine	CH_3CN	2.5×10^6	2.4×10^5
	DMSO	280	9
	ratio	8.9×10^3	2.7×10^4
pyrrolidine	CH_3CN	9×10^6	3.9×10^5
	DMSO	3×10^3	60
	ratio	3×10^3	6.5×10^3

a. Attack at an unsubstituted ring position.

b. Attack at the 1-position.

Values of k_{Am} / k_{-1} were obtained for the reactions of 2.2 and 2.3 with piperidine and pyrrolidine. In acetonitrile a value of 8 was obtained for the reactions of piperidine with both 2.2 and 2.3 compared to 0.6 and 3 in DMSO. For the reactions of pyrrolidine with 2.2 and 2.3, values are 55 and 86 respectively in acetonitrile and 20 and 30 in DMSO. Hence these ratios show little change on transferring between the two solvents. The ratio of k_{Am} / k_{-3} would also be expected to show similar behaviour.

Table 2.29 contains the values of k_1 for the reactions of 2.2 and 2.3 with n-butylamine, piperidine and pyrrolidine.

Table 2.29. Comparison of k_1 values for the reactions 2.2 and 2.3 with aliphatic amines in acetonitrile and DMSO[24].

Amine		k_1 / dm^3 mol^{-1} s^{-1}	
		2.1	2.3
n-butylamine	CH_3CN	130	183
	DMSO	250	410
	ratio	0.5	0.4
piperidine	CH_3CN	780	650
	DMSO	(2000)	(5000)
	ratio	0.4	0.1
pyrrolidine	CH_3CN	1280	2400
	DMSO	4000	10000
	ratio	0.3	0.24

Values are generally about a factor of 2 - 4 smaller in acetonitrile, though there are no major differences.

The results show that decreases of ca. 10^4 in values of $K_{c,1}°$ and $K_{c,3}°$, shown below, are largely due to the increases in value of $k_{AmH}+$.

$$K_{c,1}° = \frac{k_1}{k_{-1}} \cdot \frac{k_{Am}}{k_{AmH}+} \qquad K_{c,3}° = \frac{k_3}{k_{-3}} \cdot \frac{k_{Am}}{k_{AmH}+}$$

However, it is interesting to speculate on the solvent dependence of k_{Am}, the rate constant for proton transfer from zwitterionic adducts to amine. It has been shown that the ratio k_{Am} / k_{-1} has only little solvent dependence. Nevertheless, values of both k_{Am} and k_{-1} may be much larger in acetonitrile than in DMSO.

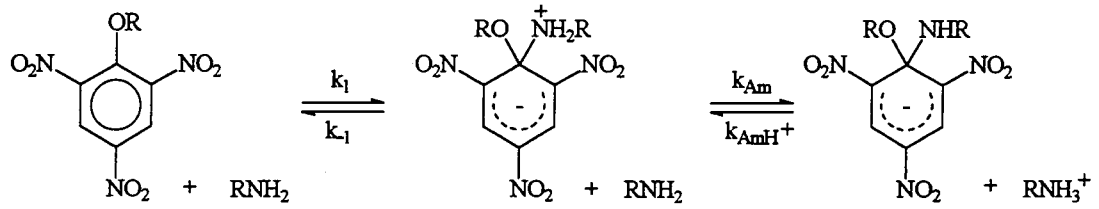

Equation 2.21

The first step in the mechanism of equation 2.21, zwitterion formation, involves charge formation. It is reasonable to expect that the equilibrium constant for this process, K_1, should be strongly solvent dependent, whereas the equilbrium constant for the second step, proton transfer, should show little dependence on solvent. It has been argued previously[18] that in DMSO the equilibrium constant for the second step should have a value of ca. 500 which reflects the greater acidity of the zwitterion than the parent ammonium ion. This greater acidity is due to the electron withdrawing capability of the trinitroaromatic moiety, even though it is negatively charged. Since values of $k_{AmH}+$ are much larger in acetonitrile than in DMSO this implies that the value of k_{Am} will also be much larger in acetonitrile. Using the factor of 500 for the ratio k_{Am} / $k_{AmH}+$ yields values for k_{Am} of 10^9 - 5 x 10^9 dm^3 mol^{-1} s^{-1} for reaction at an unsubstituted ring position and 10^8 - 2 x 10^8 dm^3 mol^{-1} s^{-1} for reaction at a substituted ring position. The former values are close to the diffusion controlled limit, which is consistent with proton transfers that are in the thermodynamically favoured direction. There is most likely some steric hindrance to proton transfer when reaction involves attack at a 1-substituted position, accounting for the somewhat lower values observed for the reaction of 2.3. The values for reaction with different amines are in the trend n-butylamine > pyrrolidine > piperidine which agrees with the known increasing steric requirements of this sequence.

The conclusion is that both values of $k_{AmH}+$ and k_{Am} are considerably greater in acetonitrile than in DMSO. The reduction in values in the latter solvent probably reflects the strong hydrogen bonding between the proton to be transferred and the DMSO.

If k_{Am} values are higher in acetonitrile, while the ratio of k_{Am} / k_{-1} are only slightly changed, then the inference is that values of k_{-1} must be much higher in acetonitrile as well. Hence the reduction in values of K_1 reflect the slightly smaller values of k_1 with much higher values k_{-1}.

2.5.5 Diffusion Controlled Reactions in Acetonitrile

Making the assumption that reacting molecules can be treated as spheres undergoing Brownian motion in a viscous liquid, then the diffusion controlled limit[28] for bimolecular reactions between molecules with radii r_A and r_B is given by equation 2.22 where η is the viscocity of the solvent.

$$k_2 = \frac{2000 L k_B T}{3\eta}\left(2 + \frac{r_A}{r_B} + \frac{r_B}{r_A}\right) \qquad \text{equation 2.22}$$

For molecules of similar size ($r_A \approx r_B$) the second order rate constant tends to a value independent of the reactants.

$$k_2 = \frac{8000 L k_B T}{3\eta} = \frac{8000 RT}{3\eta} \qquad \text{equation 2.23}$$

The viscocity of acetonitrile[29] is quite low (η = 3.45 x 10^{-4} Pa s) leading to a value for k_2 of 1.9 x 10^{10} dm^3 mol^{-1} s^{-1}, compared to 3.3 x 10^9 dm^3 mol^{-1} s^{-1} for DMSO[28] (η = 2.0 x 10^{-3} Pa s).

Even if the ratio r_A : r_B were to change to 2 : 1, then equation 2.22 would yield a value for k_2 of 2.1 x 10^{10} dm^3 mol^{-1} s^{-1} in acetonitrile, which is little changed from that where the reactants have identical radii.

2.6 References

1. D. Ayediran, T. O. Bamkole, J. Hirst and I. Onyido, *J. Chem. Soc. Perkin Trans. 2*, 1977, 597; *ibid.* 1977, 1580.
2. T. O. Bamkole, J. Hirst and I. Onyido, *J. Chem. Soc. Perkin Trans. 2*, 1979, 1317.
3. T. A. Emokpae,P. U. Uwakwe and J. Hirst, *J. Chem. Soc. Perkin Trans. 2*, 1993, 125.
4. T. O. Bamkole, J. Hirst and I. Onyido, *J. Chem. Soc. Perkin Trans. 2*, 1982, 889.
5. G. Briegleb, W. Liptay and M. Canter, *Z. Phys. Chem. N. F.*, 1960, **26**, 55.
6. M. R. Crampton and V. Gold, *J. Chem. Soc.*, 1964, 4293.
7. R. Foster and R. K. Mackie, *Tetrahedron*, 1965, **21**, 3363.
8. P. Caveny and H. Zollinger, *Helv. Chim. Acta.*, 1967, **50**, 861.
9. E. Buncel and R. A. Manderville, *J. Am. Chem. Soc.*, 1993, **115**, 8985.
10. E. Buncel and R. A. Manderville, *J. Phys. Org. Chem*, 1993, **6**, 71.
11. J. F. Coetzee and C. D. Ritchie, "Solute - Solvent Interactions", Marcel Dekker, New York, 1969.
12. J. F. Coetzee, *Progr. Phys. Org. Chem*, 1967, **4**, 45.
13. I. M. Kolthoff, S, Bruckenstein and M. K. Chatooni, *J. Am. Chem. Soc.*, 1961, **83**, 3927.
14. I. M. Kolthoff and M. K. Chatooni, *J. Am. Chem. Soc.*, 1965, **87**, 4428.
15. J. F. Coetzee and G. R. Padmanabhan, *J. Am. Chem. Soc.*, 1965, **87**, 5005.
16. M. J. Kamlet and R. W. Taft, *J. Am. Chem. Soc.*, 1976, **98**, 377.
17. L. Morris, J. Mitsky and R. W. Taft, *J. Am. Chem. Soc.*, 1972, **94**, 3438.
18. M. R. Crampton and B. Gibson, *J. Chem. Soc. Perkin Trans. 2*, 1981, 533.
19. M. R. Crampton and C. Greenhalgh, *J. Chem. Soc. Perkin Trans. 2*, 1983, 1175.
20. R. Chamberlin and M. R. Crampton, *J. Chem. Soc. Perkin Trans. 2*, 1994, 425.
21. M. R. Crampton and P. Routledge, *J. Chem. Soc. Perkin Trans. 2*, 1984, 573.
22. R. Chamberlin, M. R. Crampton and I. A. Robotham, *J. Chem. Res*, 1994, (S) 408; (M) 2232.
23. R. Chamberlin and M. R. Crampton, *J. Chem. Res*, 1993, (S) 106; (M) 811.

24. R. Chamberlin and M. R. Crampton, *J. Chem. Soc. Perkin Trans. 2*, 1995, 1831.
25. C. F. Bernasconi and M. C. Muller, *J. Am. Chem. Soc.*, 1978, **100**, 5530.
26. R. C. Weast and M. J. Astle, "CRC Handbook of Chemistry and Physics", 63rd. Edition, 1981, CRC Press Inc., Boca Raton, Florida, D-172.
27. J. McMurry, "Organic Chemistry", 2nd Ed., Brooks/Cole Publishing Company, Pacific Grove, Califoria, p. 585.
28. B. G. Cox, "Modern Liquid Phase Kinetics", Oxford University Press, 1994, p. 59.
29. R. C. Weast and M. J. Astle, "CRC Handbook of Chemistry and Physics", 63rd. Edition, 1981, CRC Press Inc., Boca Raton, Florida, F-41.

Chapter 3

Introduction to Condensation Reactions Between Carbonyl Compounds and Amines

3.1 Reaction with Ammonia

The first stage in the reaction between aliphatic aldehydes and ammonia is the formation of 1-amino-1-alkanols, 3.1.

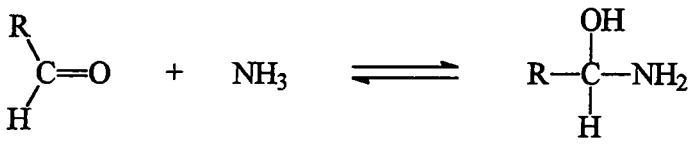

3.1

These are generally unstable though Nielsen and co-workers[1] have managed to isolate and characterise a few such compounds derived from a range of aldehydes. 1-aminobutanol is a typical example being a white solid melting at low temperature.

The next stage in the reaction is loss of water resulting in the formation of imines, 3.2.

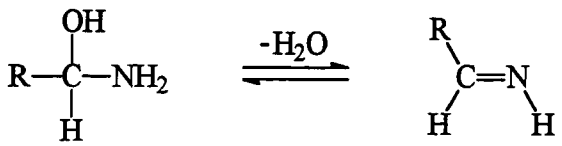

3.1 3.2

Imines from 1-amino-1-alkanols are often unstable and can undergo further reaction to form 2,4,6-trialkyl-1,3,5-hexahydrotriazines.

Initially the imine forms a dimer, 3.3, and then a trimer, 3.4 both of which are acyclic. Cyclisation of 3.4 affords the 2,4,6-trialkyl-1,3,5-hexahydrotriazine, 3.5,[1,2] in which the alkyl groups take up equatorial positions to minimise steric interactions. This is shown in scheme 3.1.

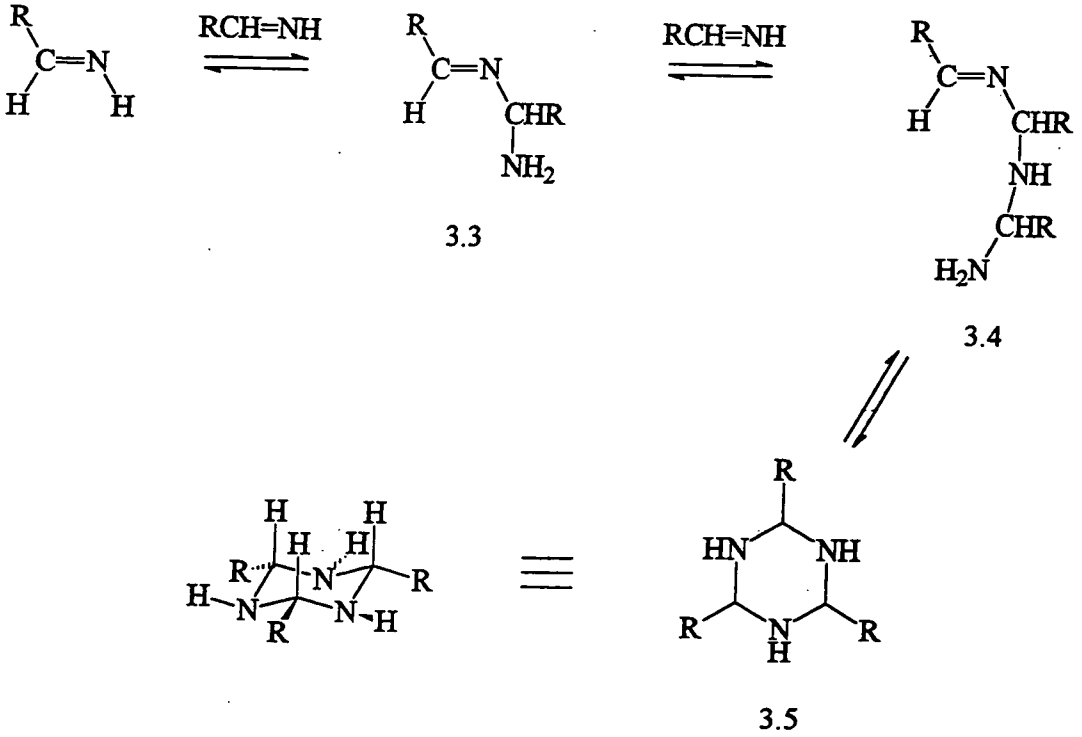

Scheme 3.1

These 2,4,6-trialkyl-1,3,5-hexahydrotriazines can be obtained with or without water of crystalization. The processes for converting between the two forms are simple, but are dependent on which trialkyl derivative is used. They have been discussed by Nielsen.[1]

3.2 Reaction with Primary Amines

As seen with the addition of ammonia to aldehydes, addition of primary amines initially affords a carbinolamine.

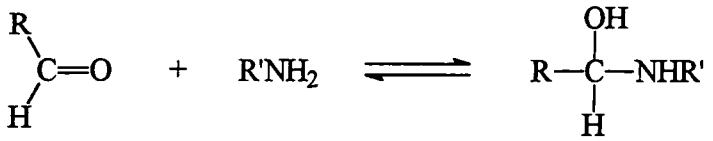

These carbinolamines, like their 1-amino-1-alkanol counterparts are unstable and undergo elimination of water to form imines.[3]

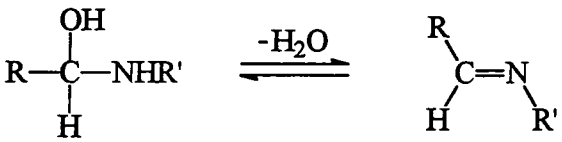

Imines formed from methanal are known[4-8] to trimerise readily. For example N-methylmethylidinamine, 3.6, trimerises to 1,3,5-trimethyl-1,3,5-hexahydrotriazine, 3.7.

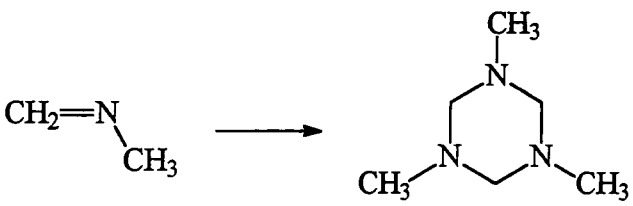

3.6 3.7

However, the more substituted an imine, the more stable it becomes to further reaction. Thus substituted imines can be detected by I.R. and ^{1}H N.M.R. techniques, etc., unlike the less substituted imines of formula RCH=NH. Extra stabilization is achieved when one or more aryl groups are attached to the carbon or nitrogen atoms. Addition of a hydroxyl group, or second nitrogen functional group, to the imine nitrogen also enhances stability. Hence oximes 3.8, semicarbazones 3.9 and hydrazones 3.10 are stable structures.[9]

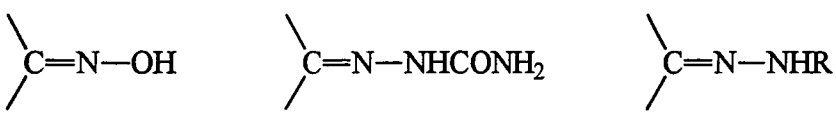

3.8 3.9 3.10

Another reaction of the carbinolamine, observed in the addition of amide or urea, is the substitution of the hydroxyl group by a second molecule of the nucleophile.[9]

3.2.1 Mechanism of Imine Formation from Primary Amines

Jencks and co-workers[10] have extensively studied the addition of primary amines to carbonyl compounds, in which the most striking feature is the characteristic maximum in the graph of rate constant as a function of pH. Figure 3.1 shows the dependence of rate constant on pH for the reaction between acetone and hydroxylamine shown in equation 3.1.

Figure 3.1. Plot showing the dependence of rate constant on pH for the reaction between acetone and hydroxylamine.

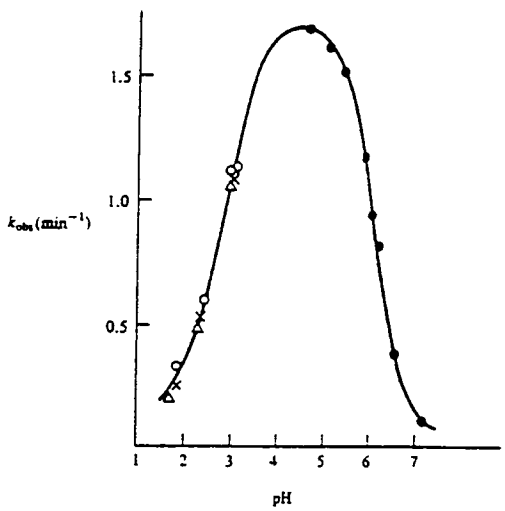

Equation 3.1

The overall mechanism for imine formation from carbonyl compounds and strongly basic amines is given in scheme 3.2.

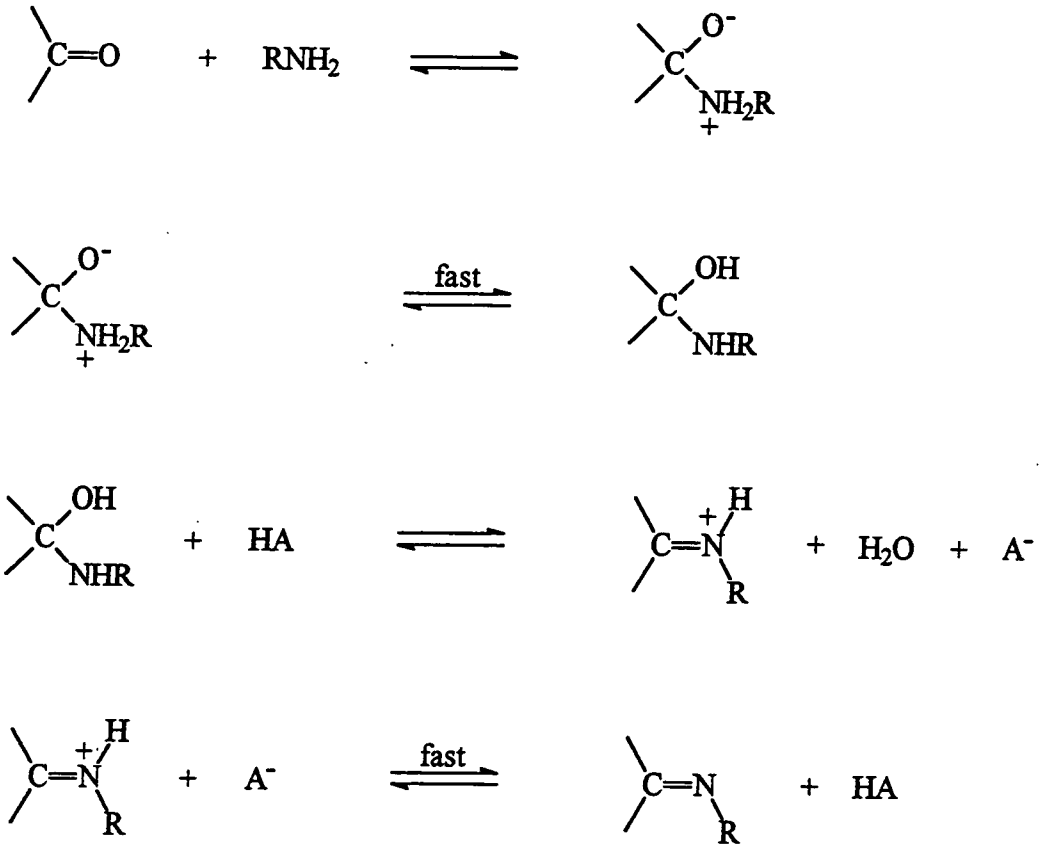

Scheme 3.2

In solution with pH above 5, the dehydration step is hindered, due to lack of acid catalyst. This step becomes rate-determining and is subject to general acid catalysis.

When the solution is below pH 5 dehydration becomes rapid. However, we still see a decrease in rate constant and this is due to protonation of the amine. Thus addition becomes the rate-determining step since only unprotonated amine is reactive.

More weakly basic nitrogen nucleophiles, e.g. aryl amines and semicarbazides, react in a similar manner, with the rate-determining step changing from addition to dehydration at virtually the same pH as for strongly basic amine. However, the electron withdrawing group hinders :-

i) the attack on the carbonyl group by the nitrogen lone pair; and

ii) the lone pair's assistance in the expulsion of the hydroxyl group.

Hence weaker nitrogen bases require more help from general acid catalysis in both the addition and dehydration steps as can be seen in scheme 3.3.

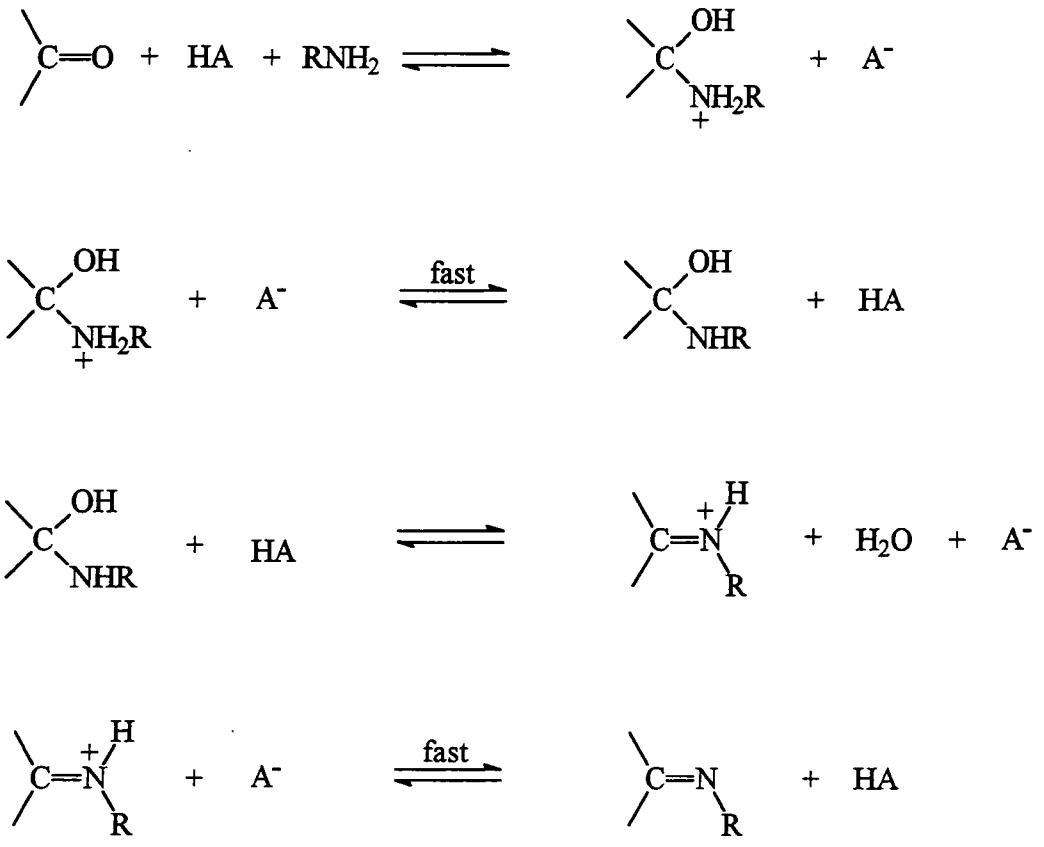

Scheme 3.3

3.3 Reaction with Secondary Amines

Carbinolamine formation is also the first stage in the reaction between carbonyl compounds and secondary amines.

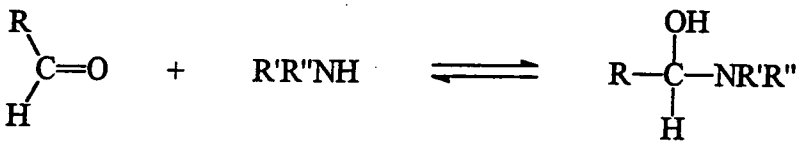

This is followed by expulsion of the hydroxyl group by the nitrogen's lone pair leading to formation of an iminium ion 3.11.

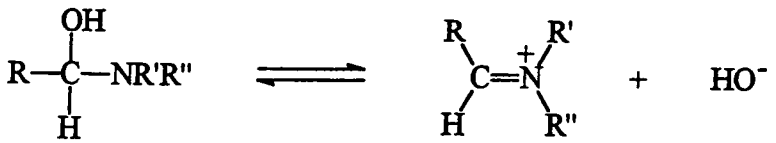

3.11

This expulsion step can also be acid catalysed,[11] involving protonation of the hydroxyl group.

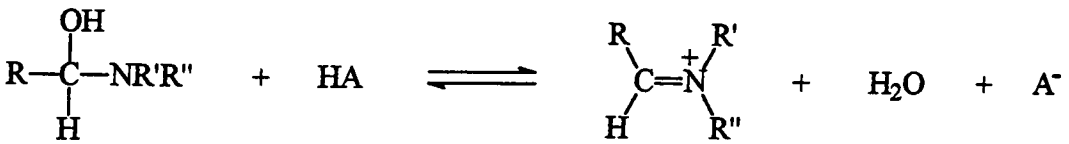

Iminium ions have no proton on the nitrogen that can be lost, so no neutral imine can be formed. If there is a hydrogen present on the α - carbon atom then loss of this proton leads to the formation of a vinyl - amine structure, an enamine (3.12).[11,12]

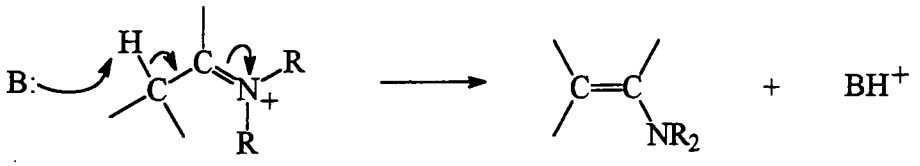

3.12

A resonance canonical structure leads to a carbanion equivalent.

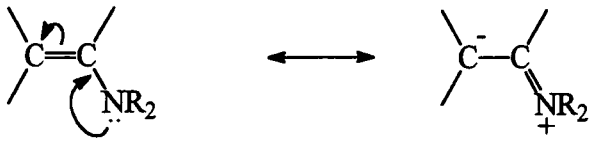

Hence enamines are useful as synthetic intermediates[11-13] and are also important biochemical intermediates.

3.4 Reaction with Tertiary Amines

Addition of tertiary amines to carbonyl compounds leads to the formation of zwitterionic carbinolamines. No neutral addition product can be formed and the carbinolamine generally reverts to the reactants. There are a few instances though where the carbinolamine is stable. This happens when the amine and carbonyl groups are in the same molecule and can form a ring of favourable size. 3,3-Dimethyl-4-dimethylaminobutanal (3.13)[14] also exists as the free base (3.14) and in aqueous solution as the conjugate acid (3.15).

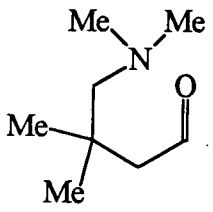

3.13

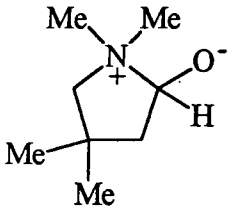

3.14

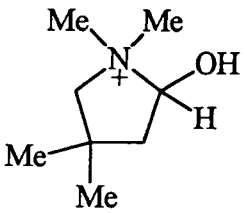

3.15

Transannular nitrogen - carbonyl interactions also facilitate the formation of the carbinolamine, as in 1-benzyl-1-azacyclooctan-5-one, 3.16.[15]

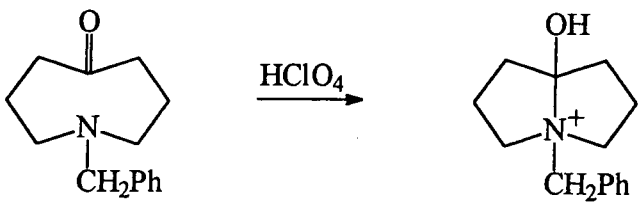

3.16

3.5 Condensation Reactions Leading to Polycyclic Amine Cage Structures

Many cage structures are known which incorporate one or more amine functionalities within the main framework of the molecule. 2-Azaadamantane, 3.17, is one such example. This compound was first prepared by Stetter[16,17] in 1964 by the synthetic route shown in equation 3.2.

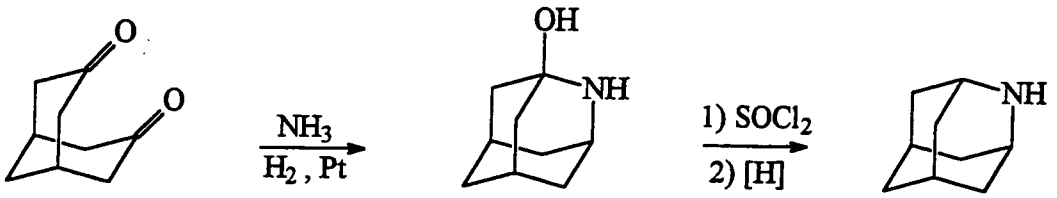

3.17

Equation 3.2

3,5,12-Triazawurtzitane, 3.19a, and 3,5,12-trisubstituted-3,5,12-triazawurtzitanes, 3.19b-f, are also examples, but derive from the wurtzitane parent cage structure rather than to the adamantane one. Nielsen[18] has synthesised 3.19a-f from cis,cis-1,3,5-triformylcyclohexane, 3.18. This is shown in scheme 3.4.

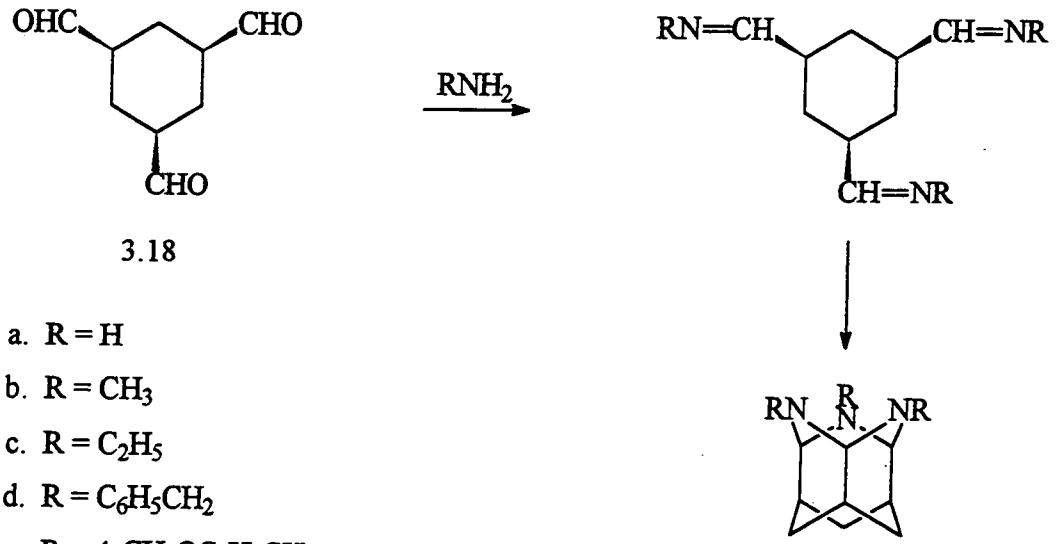

3.18

a. R = H
b. R = CH_3
c. R = C_2H_5
d. R = $C_6H_5CH_2$
e. R = 4-$CH_3OC_6H_4CH_2$
f. R = 4-$(CH_3)_2NC_6H_4CH_2$

3.19a-f

Scheme 3.4

If these polycyclic amine cage molecules are to react further then the nitrogen atoms are required to be at bridge, as opposed bridgehead, positions. This is the case in both 3.17 and 3.19a.

However these compounds are not synthesised solely by condensation reactions. There are only two known cage structures for which this is the case, hexamine, 3.20, and hexabenzylhexaazaisowurtzitane, 3.21.

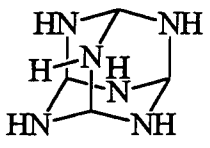

3.20

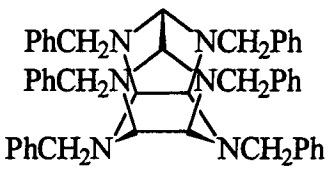

3.21

3.5.1 Hexamine

Hexamine, 3.20, or 1,3,5,7-tetraazabicyclo[3.3.1.1^{3,7}]decane , to properly name the molecule, is also known as 1,3,5,7-tetraazaadamantane, hexamethylenetetramine, methenimine, aminoform and urotropine. It was first synthesised by Butlerow[19] who demonstrated[20] that the empirical formula was $C_6H_{12}N_4$. He did not however correctly assign the structure. Duden and Scharff[21] are credited with being the first to postulate the now commonly accepted structure, 3.20, in 1895.

Hexamine is readily formed from the condensation of formaldehyde (methanal) and ammonia. Nielsen[22] has performed the most recent work on the mechanism of formation of 3.20. He has shown there to be two major, intermediates, 1,3,5-hexahydrotriazine, 3.23, and 1,3,5,7-tetraazabicyclo[3.3.0]nonane, 3.24, and has proposed a mechanism that is shown in scheme 3.5.

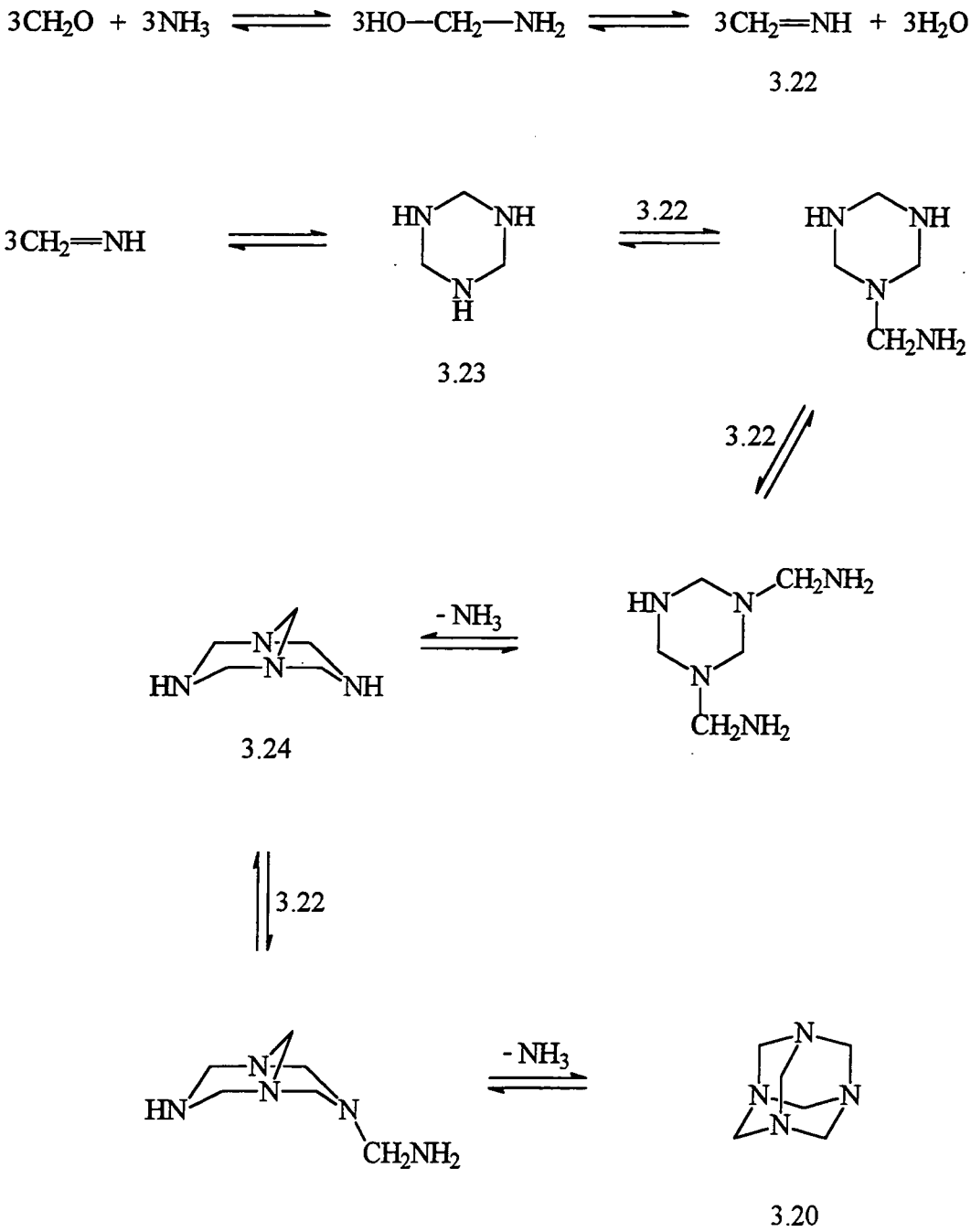
3CH2O + 3NH3
3HO—CH2—NH2
3CH2=NH + 3H2O
3.22
3CH2=NH
HN
NH
N
H
3.22
HN
NH
N
CH2NH2
3.23
3.22
HN
N
CH2NH2
N
CH2NH2
- NH3
N
N
HN
NH
3.24
3.22
N
N
HN
N
CH2NH2
- NH3
N
N
N
3.20

Scheme 3.5

Hexamine being a tertiary amine shows characteristic properties of such amines forming[23] many salts, addition compounds and complexes. Some of its more important and extensively studied reactions are nitration, nitrosation and acetylation. Nitration has been especially studied due to the formation of two highly explosive compounds 1,3,5-trinitro-1,3,5-hexahydrotriazine, 3.25, also called RDX (Research Department Explosive) and 1,3,5,7-tetranitro-1,3,5,7-tetraazacyclooctane, 3.26, also called HMX (High Melting Explosive). Altering the nitrating conditions dictates whether RDX[24,25] or HMX[26,27] is principally formed. Close examination of the hexamine ring structure shows that the parent 1,3,5-hexahydrotriazine and 1,3,5,7-tetraazacyclooctane ring structures exist within the cage. In the nitration process the bonds are cleaved selectively leading to either RDX or HMX.

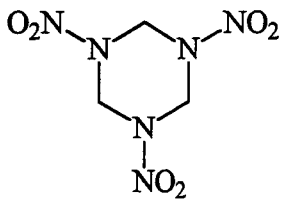

3.25

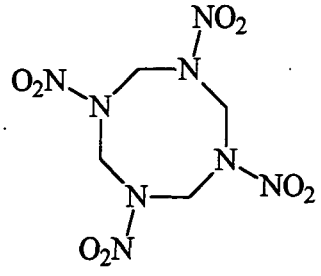

3.26

The nitration of hexamine also leads to the formation of 3,7-dinitro-1,3,5,7-tetraazabicyclo[3.3.1]nonane, 3.27, which is more commonly named dinitropentamethylenetetramine, DPT.

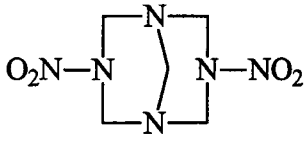

3.27

3.5.2 Hexabenzylhexaazaisowurtzitane

Hexabenzylhexaazaisowurtzitane, 3.21, or 2,4,6,8,10,12-hexabenzyl-2,4,6,8,10,12-hexaazatetracyclo[5.5.0.0^{5,9}.0^{3,11}]decane, as the compound is properly named, was first prepared by Nielsen.[28,29] The condensation[30] of glyoxal (40 % aqueous solution) and benzylamine in acetonitrile with a trace of acid catalyst yields the cage structure. Monomeric glyoxal, 3.28, readily polymerises on standing, but is stable as a 40 % solution in water. It can also be obtained in a "water - free" environment from 2,3-dihydroxy-1,4-dioxane, 3.29, which releases ethylene glycol as the sole by-product.

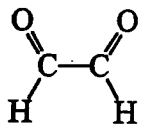

3.28

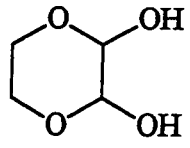

3.29

It has been shown that certain phenyl - substituted benzylamines also react with glyoxal to produce the cage structure, though primary aliphatic amines and anilines only form the dicarbinolamine, RNHCH(OH)CH(OH)NHR, or diimine, RN=CH-CH=NR, intermediates.[32-36]

The mechanism of formation of HBIW is shown in scheme 3.6. The initial addition product is the dicarbinolamine N,N'-dibenzyl-1,2-diamino-1,2-ethanediol, 3.30, which loses two molecules of water to form the diimine, N,N'-dibenzyl-1,2-ethanediimine, 3.31. It is believed[28] this trimerises via the pathway shown. This involves formation of a cyclic dimer, 3.32, and then a bicyclic trimer, 3.33, which then rearranges to the cage structure, 3.21.

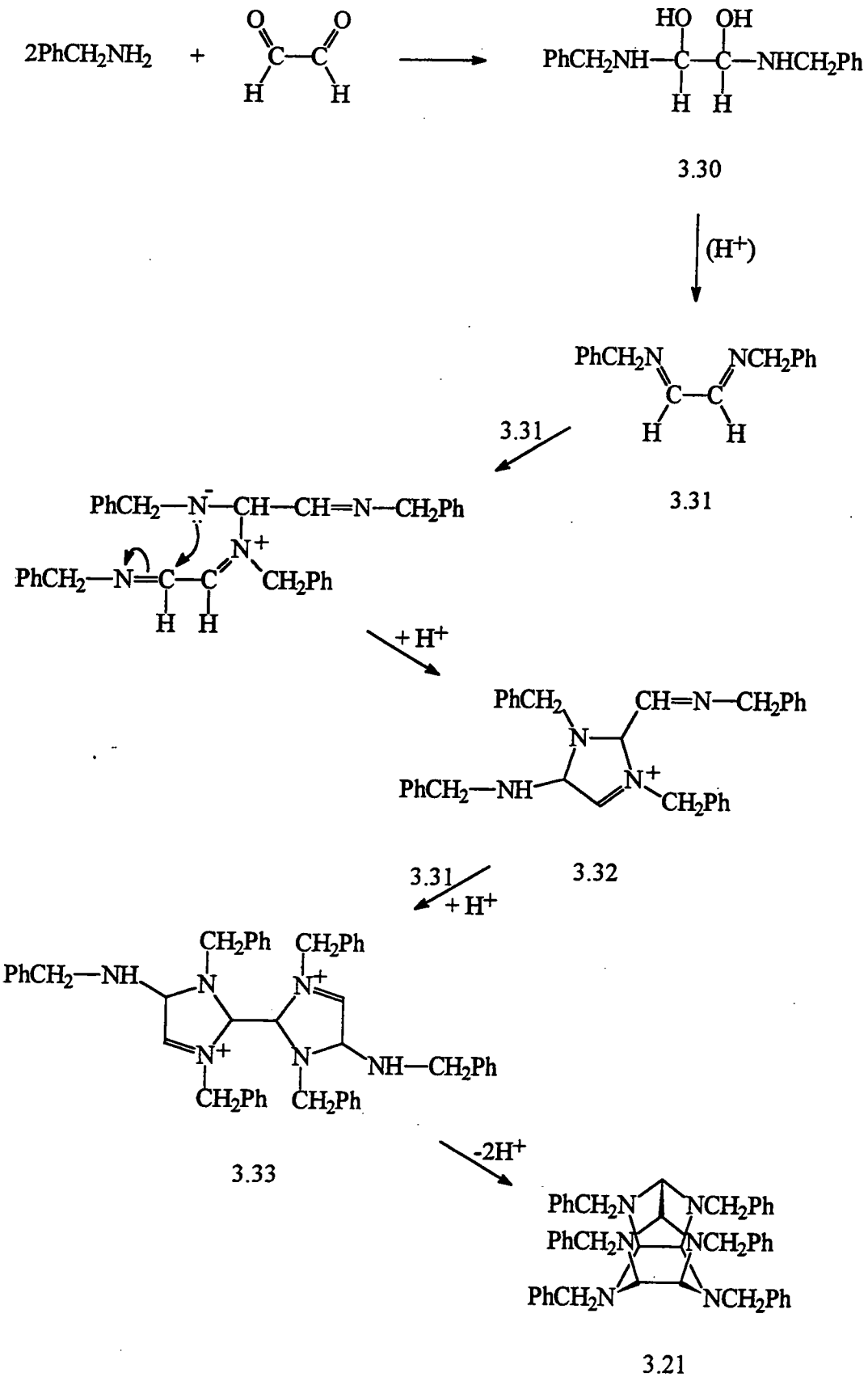

Scheme 3.6

Much of the interest in HBIW has arisen due to the possibility of replacing the benzyl groups with nitro functionalities, forming hexanitrohexaazaisowurtzitane, HNIW, 3.34. Two other highly sought after compounds are hexanitrohexaazawurtzitane, 3.35, and hexanitrohexaazaadamantane, 3.36.

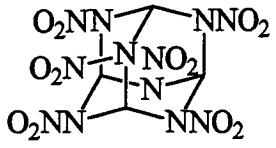

3.34

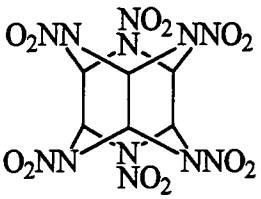

3.35

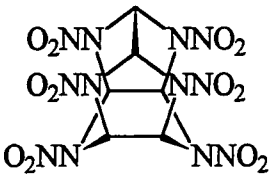

3.36

These polycyclic nitramines have greater densities than their monocyclic nitramine counterparts leading to increased detonation pressures and hence have far superior explosive capabilities.

3.6 Imines

Imines have structures that are isoelectronic with carbonyl compounds, though the oxygen atom has been replaced with an N-R group. This gives rise to the possibility of geometrical isomerisation. In aldimines the syn isomer has the nitrogen substituent (R') cis to the proton on the carbon, though in the anti isomer they are trans to each other.

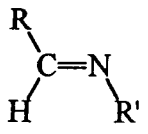

syn

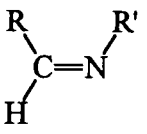

anti

The syn isomers have the greater thermodynamic stabilities which is explained in terms of the non-bonded interactions across the double bond.[37]

One of the most common methods of preparing imines is the reaction of carbonyl compounds with ammonia or amines as shown in equation 3.3. This method was first discovered by Schiff.[38]

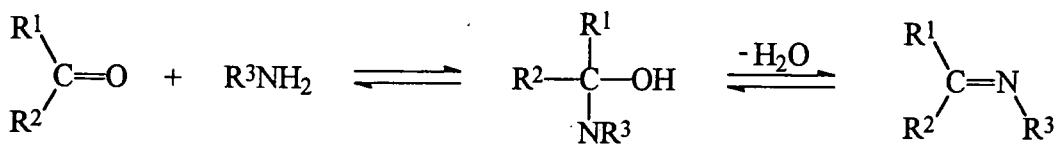

Equation 3.3

However, other methods have been used to prepare imines. Diethyl ketals[39,40] when refluxed with amines also yield imines, especially with aromatic amines.

Equation 3.4

Another route involves dehydrogenation of amines.[41-43] Ritter[44,45] found that isobornylaniline, 3.37, is readily dehydrogenated with sulphur at 220 °C to yield the anil of camphor. This is shown in equation 3.5.

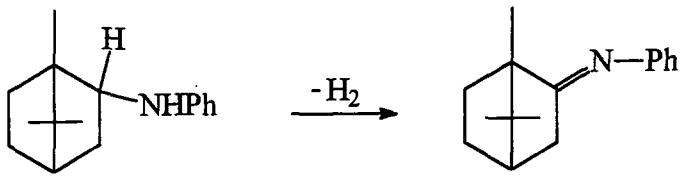

3.37

Equation 3.5

Hydrogenation of nitriles over nickel or platinum catalyst can also yield imines,[46] though one problem with this method is further reduction to amines as shown in equation 3.6.

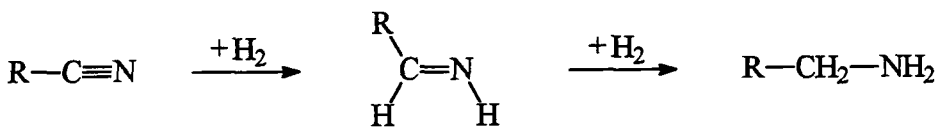

Equation 3.6

The reactions of a nitrile with phenols,[47-49] equation 3.7, or with alkyl or aryl Grignards,[50-52] equation 3.8, lead to the formation of imines. However the latter route requires careful hydrolysis of the organometallic intermediate so that the imine isn't hydrolysed also. The imine formed from the reaction between 2,2,6-trimethylcyclohexyl cyanide, 3.38, and phenyl magnesium bromide, equation 3.9, is rather stable towards hydrolysis.[53]

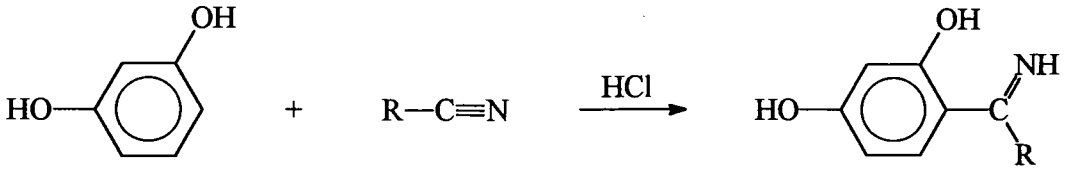

Equation 3.7

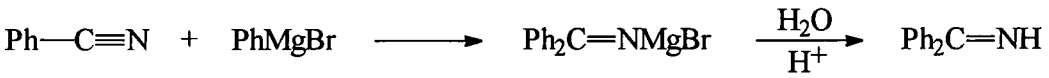

Equation 3.8

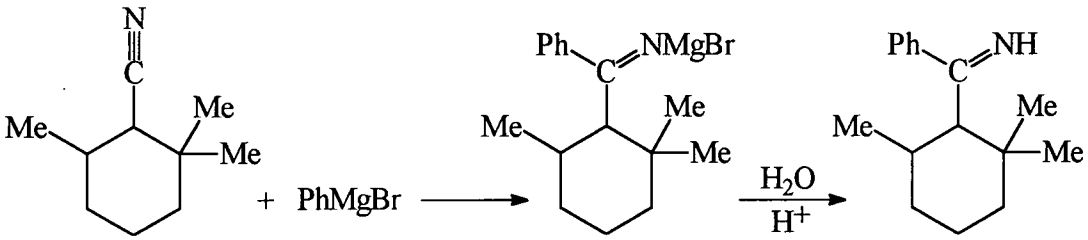

3.38

Equation 3.9

Imines are generally rather unstable compounds, especially those of little substitution. They are, however, very useful "building blocks" in organic reactions. As well as undergoing self-trimerisation to the 1,3,5-hexahydrotriazines, shown ealier in scheme 3.1, they can react with other compounds to form 3, 4, 5 or 6 membered rings. For example imines react with carbenes[54-57] to form aziridines, equation 3.10, with ketenes[58-63] to form β-lactams, equation 3.11, with diazomethane[64-67] to form 1,2,3-triazolines, equation 3.12, and with various dienes and heterodienes,[68-75] equation 3.13.

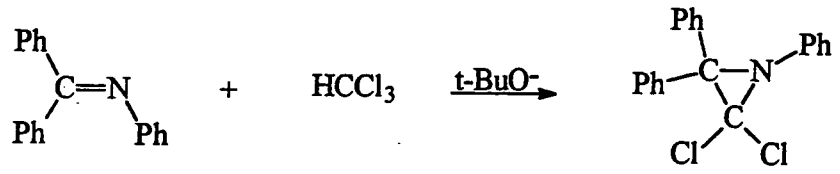

Equation 3.10

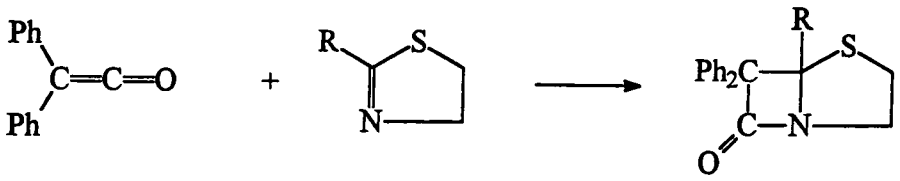

Equation 3.11

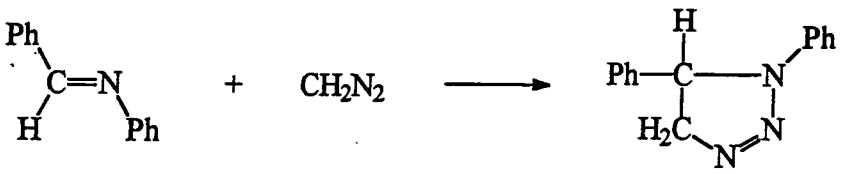

Equation 3.12

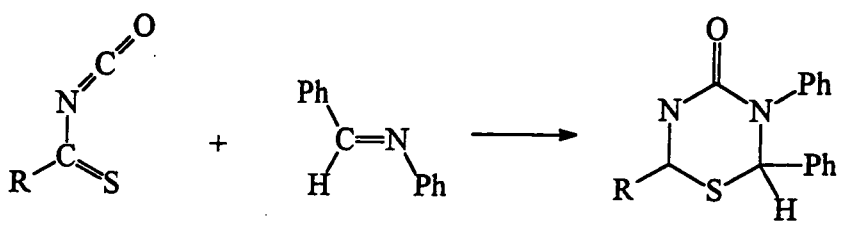

Equation 3.13

One or more aryl substituents at either the carbon or the nitrogen atoms of an imine creates a stabilising effect through conjugation of the double bond with the aromatic π-system. These compounds are called Schiff's bases and are easily isolated.[76,77]

Alkyl substitution at the nitrogen atom also has a stabilising effect, though at the carbon atom is destabilising. This is explained[77] in terms of the charge separation across the double bond, with increased polarity resulting in a decrease in stabilisation. The inductive effect of an alkyl substituent on the nitrogen atom reduces the charge separation in the double bond. However, an alkyl substituent on the carbon atom reduces the electron charge density from the double bond at the carbon atom while increasing it at the nitrogen atom. Hence, nitrogen substituents decrease the polarisation of the double bond, increasing stabilisation, while carbon substituents increase the polarisation, leading to destabilisation of the imine. An example of this is that compounds 3.9 and 3.11 are unstable in air at room temperature, though 3.10 is stable.

$Bu^tHC{=}NH$	$CH_2{=}NBu^t$	$Bu^tCH{=}NBu^t$
3.9	3.10	3.11

3.7 References

1. A. T. Nielsen, R. L. Atkins, A. T. Moore, R. Scott, D. Mallory and J. M. LaBerge, *J. Org. Chem.*, 1973, **38**, 3288.
2. Y. Ogata, and A. Kawasaki, *Tetrahedron*, 1964, **20**, 855, 1573.
3. R. A. Y. Jones, "Physical and Mechanistic Organic Chemistry", 2nd. Edition, 1984, p. 254.
4. E. M. Smolin and L. Rapoport, "The Chemistry of Heterocyclic Compounds; S - Triazines and Derivatives", A. Wiessberger, Ed., Interscience, New York, 1959, Volume 13, p. 476.
5. A. G. Giumanini, G. Verardo, E. Zangrando and L. Lassiani, *J. Prakt. Chem.*, 1987, **329**, 1087.
6. B. Mauzé J. Pornet, M. -L. Martin and L. Miginiac, *C. R. Acad. Sci. Paris Ser. C,*, 1970, **270**, 562.
7. J. Graymore, *J. Chem. Soc.*, 1932, 1353.
8. A. G. Giumanini, G. Verardo, L. Randaccio, N. Bresciani-Pahor and P. Traldi, *J. Prakt. Chem.*, 1985, **327**, 739.
9. T. H. Lowry and K. S. Richardson, "Mechanism and Theory in Organic Chemisty", Harper and Row, New York, 3rd. Edition, 1987, p. 703.
10. W. P. Jencks, *J. Am. Chem. Soc.*, 1969, **81**, 475.
11. S. F. Dyke, "The Chemistry of Enamines", 1973, p. 1.
12. P. W. Hicknott, *Tetrahedron*, 1982, **38**, 1975, 3363.
13. J. Szmuszkovicz, *Adv. Org. Chem. : Methods and Results*, vol 4, 1963, 1.
14. R. McCrindle and A. J. McAlees, *J. Chem. Soc. Chem. Comm.*, 1983, 61.
15. N. J. Leonard and J. A. Klainer, *J. Org. Chem.*, 1968, **33**, 4269.
16. H. Stetter, P. Tacke and J. Gärtner, *Chem. Ber.*, 1964, **97**, 3480.
17. H. Stetter and K. Heckel, *Chem. Ber.*, 1973, **106**, 339.
18. A. T. Nielsen, S. L. Christian, D. W. Moore, R. D. Gilardi and C. F. George, *J. Org. Chem.*, 1987, **52**, 1656.
19. A. Butlerow, *Ann. Chem.*, 1859, **111**, 250.
20. A. Butlerow, *Ann. Chem.*, 1860, **115**, 322.
21. P. Duden and M. Scharff, *Ann. Chem.*, 1895, **288**, 218.
22. A. T. Nielsen, D. W. Moore, M. D. Ogan and R. L. Atkins, *J. Org. Chem.*, 1979, **44**, 1678.
23. J. F. Walker, "Formaldehyde", Reinhold, New York, Chapter 18, p. 1944.
24. G. C. Hale, *J. Am. Chem. Soc.*, 1925, **47**, 2754.
25. W. J. Chute, D. C. Downing, A. F. McKay, R. H. Meen, G. S. Myers and G. F. Wright, *Can. J. Res.*, 1949, **27B**, 218.

26. W. E. Bachmann and J. C. Sheehan, *J. Am. Chem. Soc.*, 1949, **71**, 1842.
27. M. R. Crampton, M. Jones, J. K. Scranage and P. Golding, *Tetrahedron*, 1988, **44**, 1679.
28. A. T. Nielsen, R. A. Nissan, D. J. Venderah, C. L. Coon, R. D. Gilardi, C. F. George and J. Flippen-Anderson, *J. Org. Chem.*, 1990, **55**, 1459.
29. A. T. Nielsen, R. A. Nissan, A. P. Chafin, R. D. Gilardi and C. F. George, *J. Org. Chem.*, 1992, **57**, 6756.
30. M. R. Crampton, J. Hamid, R. Millar and G. Ferguson, *J. Chem. Soc. Perkin Trans. 2*, 1993, 923.
31. A. Batsanov, J. C. Cole, M. R. Crampton, J. Hamid, J. A. K. Howard and R. Millar, *J. Chem. Soc. Perkin Trans. 2*, 1994, 421.
32. J. M. Kliegman and R. K. Barnes, *Tetrahedron*, 1970, **26**, 2555.
33. J. M. Kliegman and R. K. Barnes, *J. Org. Chem.*, 1970, **35**, 3140.
34. H. tom Dieck and I. W. Renk, *Chem. Ber.*, 1971, **104**, 92.
35. M. D. Hurvitz, U.S. Patent 2,582,128, 1952; *Chem. Abstr.*, 1952, **46**, 8146f.
36. H. tom Dieck and J. Dietrich, *Chem. Ber.*, 1984, **117**, 694.
37. G. K. Karabatsos and S. S. Lande, *Tetrahedron*, 1968, **24**, 2555.
38. H. Schiff, *Ann.*, 1964, **131**, 118.
39. L. Claisen, *Ber.*, 1896, **29**, 2931.
40. J. Hoch, *Compt. rend.*, 1934, **199**, 1428.
41. A. A. Balandin and N. A. Vasyunina, *Dokl. Akad. Nauk SSSR*, 1955, **103**, 831; *Chem. Abstr.*, 1956, **50**, 9283.
42. R. Greeve, German Patent 923,010; *Chem. Abstr.*, 1958, **52**, 1222.
43. J. C. Duff and V. I. Furness, *J. Chem. Soc.*, 1951, 1512.
44. J. J. Ritter, *J. Am. Chem. Soc.*, 1953, **55**, 3322.
45. C. M. Rosser and J. J. Ritter, *J. Am. Chem. Soc.*, 1957, **59**, 2179.
46. V. Grignard and R. Escourrou, *Compt. rend.*, 1925, **180**, 1883.
47. K. Hoesch, *Ber.*, 1915, **48**, 1122.
48. K. Hoesch, *Ber.*, 1917, **50**, 462.
49. J. Houben and J. Fischer, *J. Prakt. Chem.*, 1929, **123**, 89.
50. C. Moureau and G. Mignonac, *Compt. rend.*, 1913, **156**, 1801.
51. P. L. Pickard and D. J. Vaughan, *J. Am. Chem. Soc.*, 1950, **72**, 876.
52. P. L. Pickard and C. W. Young, *J. Am. Chem. Soc.*, 1951, **73**, 42.
53. H. L. Lochte, J. Horeczy, P. L. Pickard and A. D. Barton, *J. Am. Chem. Soc.*, 1948, **70**, 2012.
54. E. K. Fields and J. M. Sandri, *Chem. Ind. (London)*, 1959, 1216.
55. A. G. Gook and E. K. Fields, *J.Org. Chem.*, 1962, **27**, 3686.

56. D. H. Deyrup and R. B. Grunwald, *Tetrahedron letters*, 1965, 32.
57. D. H. Deyrup and R. B. Grunwald, *J. Am. Chem. Soc.*, 1965, **87**, 4538.
58. H. Staudinger, *Ber.*, 1917, **50**, 1035.
59. H. Staudinger and J. Engel, *Ber.*, 1917, **50**, 1042.
60. W. Kirmse and L. Horner, *Chem. Ber.*, 1956, **89**, 2759.
61. R. P. Pfleger and A. Jäger, *Chem. Ber.*, 1957 **90**, 2460.
62. H. T. Clarke, J. R. Johnson and R. Robinson, Eds., "The Chemistry of Penicillin", Princeton University Press, Princeton, New Jersey, 1949, p. 849, 973.
63. A. D. Holley and R. W. Holley, *J. Am. Chem. Soc.*, 1951, **73**, 3172.
64. G. K. Buckley, *J. Chem. Soc.*, 1954, 1850.
65. P. K. Kabada and O. J. Edwards, *J. Org. Chem.*, 1961, **26**, 2631.
66. P. K. Kabada, *Tetrahedron*, 1966, **22**, 2453.
67. H. Hoberg, *Ann. Chem.*, 1967, **707**, 147
68. G. Kresze and R. Albrecht, *Chem. Ber.*, 1964, **97**, 490.
69. R. Albrecht and G. Kresze, *Chem. Ber.*, 1965, **98**, 1431.
70. W. J. Middleton and C. G. Krespan, *J. Org. Chem.*, 1965, **30**, 1398.
71. J. Geordeler and H. Schenk, *Chem. Ber.*, 1965, **98**, 383.
72. H. Schenk, *Chem. Ber.*, 1966, **99**, 1258.
73. J. Geordeler and K. Jonas, *Chem. Ber.*, 1966, **99**, 3572.
74. J. Geordeler and R. Sappelt, *Chem. Ber.*, 1967, **100**, 2064.
75. J. Geordeler and R. Wiess, *Chem. Ber.*, 1967, **100**, 1627.
76. D. G. Anderson and G. Wettermark, *J. Am. Chem. Soc.*, 1965, **87**, 1433.
77. M. D. Colle, G. Distefano, D. Jones, A. Guerrino, G. Seconi and A. Mordelli, *J. Chem. Soc. Perkin Trans. 2*, 1994, 789.

Chapter 4

Reactions of Carbonyl Compounds with Ammonia and Primary Amines

4.1 Reactions of Simple Aldehydes with Ammonia and Primary Amines

It is known[1-4] that mono-substituted imines of the form RCH=NH, 4.1, and CH_2=NR, 4.2, undergo trimerisation, producing 2,4,6- or 1,3,5-trisubstituted-1,3,5- hexahydrotriazines 4.3 and 4.4 respectively.

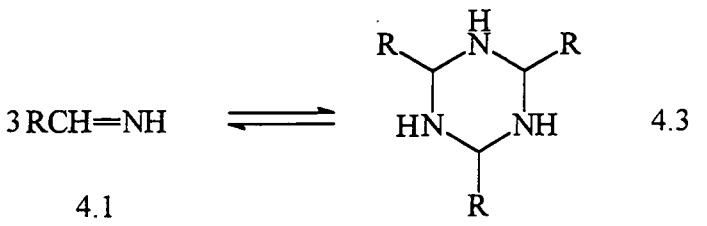

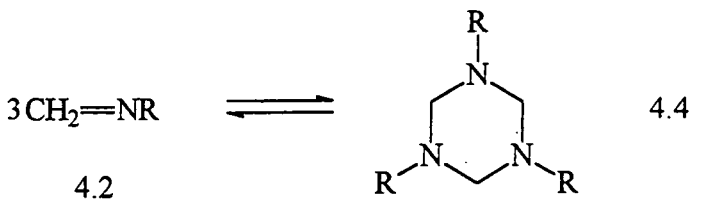

The imines, 4.1, are formed from the reactions of aldehydes with ammonia. However they are not isolable and trimerise rapidly, as shown in scheme 4.1. The imines, 4.2, are produced from the reaction of formaldehyde with various primary amines.

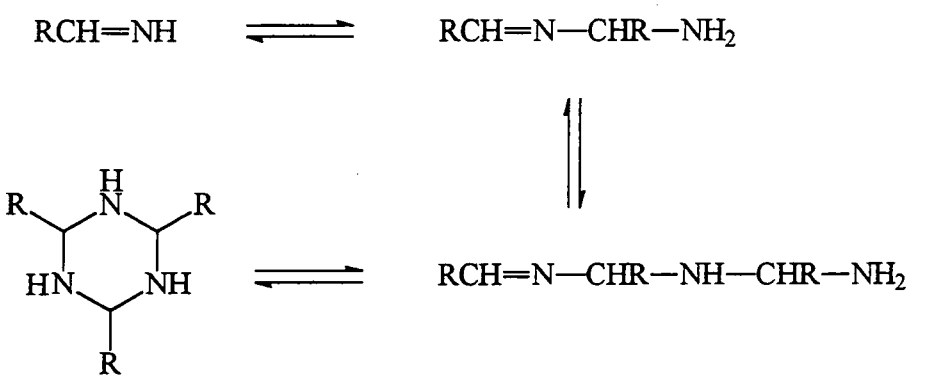

Scheme 4.1

4.1.1 The Reaction of Propanal and Ammonia

The reaction between propanal and ammonia leads to the formation of 2,4,6-triethyl-1,3,5-hexahydrotriazine, 4.5 via the mechanism shown in scheme 4.1. This compound has been synthesised by two different routes. The first, in water as solvent, was based on the procedure by Nielsen and co-workers.[1] However, in a method developed in Durham it was found that the reaction could be carried out conveniently in anhydrous acetonitrile. The ^1H NMR spectrum of the product, 4.5, is given in figure 4.1. The ring proton, CH, shows a characteristic peak at 3.44 ppm (triplet, J=6.1 Hz), the CH_2 peak appears at 1.38 ppm (pentet), and the CH_3 is observed at 0.92 ppm (triplet, J=7.4). Identical spectra were obtained from the products prepared using the two different methods.

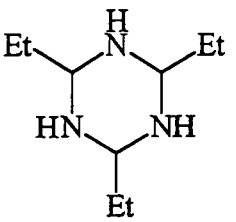

4.5

Figure 4.1. ^1H NMR spectrum of 4.5 in d_3-acetonitrile.

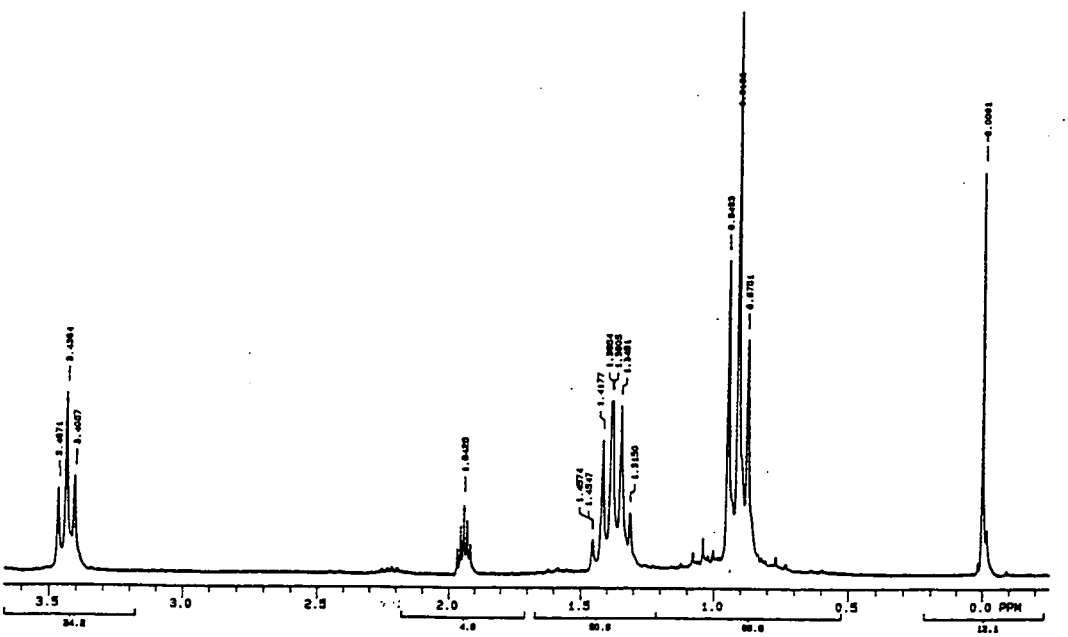

4.1.1.1 Synthesis of 2,4,6-triethyl-1,3,5-hexahydrotriazine, 4.5

a. In water

This method, as used by Nielsen and co-workers,[1] involved slow addition (30 mins) of 58 g propanal (1.0 mol) to 250 ml concentrated (16 mol dm^{-3}) aqueous ammonia solution (4 mol), maintaining the temperature below 5 °C with ice-bath cooling. The resultant clear solution was then stored at 0 °C for 5 days. Sodium chloride was added and the mixture stirred at room temperature for one hour, followed by extraction with four 100 ml portions of ether. The combined ether extracts were dried with magnesium sulphate, filtered and the solvent removed by rotary evaporator. The resulting liquid was pumped at 0.1 mbar for 1 hour affording 41.6 g (71 % yield) of clear colourless liquid. A temperature of below 25 °C was maintained during work-up.

b. In acetonitrile

The second synthetic approach, developed in Durham, involved slow bubbling of dry ammonia gas into 400 ml acetonitrile over 2½ hours. During this period 0.5 mol ammonia gas dissolved in the acetonitrile. To this solution 6.0 g propanal was then added and the mixture left for 15 hours. The solution was dried using magnesium sulphate, filtered and then pumped at 0.1 mbar for 1 hour affording 3.03 g (50 % yield) of product, 4.5.

This synthetic approach has also been carried out using the concentrated (16 mol dm^{-3})aqueous ammonia solution dissolved in acetonitrile. However this gave a very unsatisfactory yield.

More recently it has been found that ammonia gas dissolves more efficiently in solvents at temperatures below -33 °C, the boiling point of ammonia. However it must be noted that the freezing point of acetonitrile is -48 °C.

The reaction between propanal (0.1 mol dm^{-3}) and an excess of ammonia (1.0 mol dm^{-3}) in d_3-acetonitrile was also followed by ^1H NMR spectroscopy. Upon the addition of ammonia the signals for propanal at 9.71 ppm (CHO, triplet, J=1.3 Hz), 2.43 ppm (CH_2, quartet of doublets, ^3J = 7.3 and 1.3 Hz) and 1.02 ppm (CH_3, triplet, ^3J = 7.3 Hz) gradually decrease. Peaks at 3.46 ppm (triplet), 1.45 ppm (pentet) and 0.92 ppm (triplet) begin to appear. These correspond well with those of synthesised 4.5. After one day only a very small concentration of propanal is observable. Mixing this solution with an equal concentration of previously prepared 4.5 gave no extra bands in the spectrum, thus proving the product to have the expected structure. Acidification of this solution resulted in the re-emergence of the bands due to propanal indicating the reversibility of the reaction when the ammonia is converted to its ammonium salt. No other peaks were observed during the experiment, indicating that the intermediates are only present in very small concentrations, undetectable by ^1H NMR spectroscopy. This is in good agreement with the literature reports[1,5] on the instability of 1-amino-propanol and its corresponding imine.

Analysis of 4.5 by GC-Mass spectroscopy did not afford a mass peak of 171. However, it is known[1] that 2,4,6-trialkyl-1,3,5-hexahydrotriazines are unstable at higher temperatures (> 40 °C) and lose ammonia in forming N,N'-dialkylidene-1,1-diaminoalkanes. The major component had a mass peak of 154 which corresponds to that of N,N'-dipropylidine-1,1-diaminopropane, 4.6. The mechanism of formation of 4.6 is believed to be that contained in scheme 4.2.

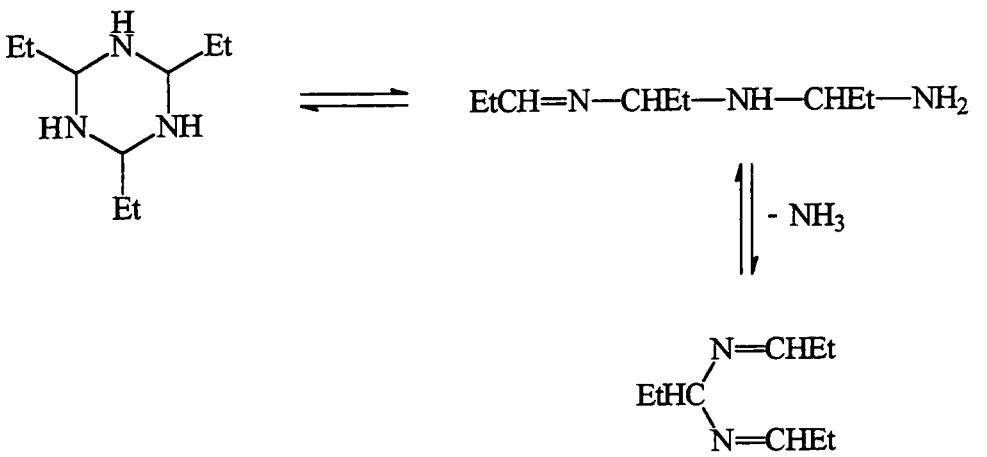

4.6

Scheme 4.2.

4.1.2 The Reaction Between Propanal and Primary Amines

Propanal has been reacted with a series of primary amines in an attempt to show whether imines of the form EtCH=NR can trimerise to 2,4,6-triethyl-1,3,5-trisubstitutedhexahydrotriazines, 4.7, for which no literature references could be found.

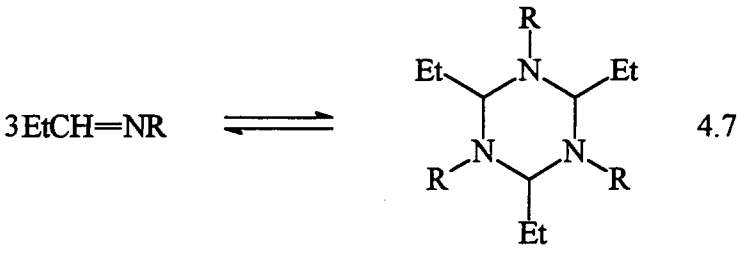

4.7

These reactions were followed by ^1H NMR spectroscopy in d_3-acetonitrile using equimolar concentrations, usually 0.2 mol dm^{-3}, of propanal, and each of the amines n-butylamine, t-butylamine, isopropylamine, benzylamine and aniline. Spectra were taken immediately upon mixing and then regularly until no further change occurred.

Benzylamine, isopropylamine and n-butylamine react rapidly and quantitatively with propanal to form the imines, N-substituted-propylidenamines, 4.9b-d, which are stable at room temperature for several hours before slowly reacting further. They are easily identifiable by ^1H NMR spectroscopy due to their characteristic CHN bands observed between 7.5 and 8.0 ppm. Spectra of 4.9c and 4.9d are shown in figures 4.2 and 4.3. There is no evidence for any of the carbinolamine intermediates, 4.8, forming in observable concentrations. 1-(t-Butylamino)-1-propanol, 4.8a, may suffer from some internal crowding due to the bulky tertiary-butyl group, hindering the conformation required for expulsion of the hydroxyl group to be achieved. However, the quantitative formation of the imine, 4.9b, does occur slowly and was complete after one day.

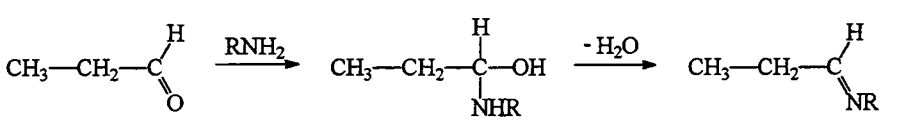

4.8 4.9

a. R = t-butyl
b. R = n-butyl
c. R = isopropyl
d. R = benzyl
e. R = phenyl

Equation 4.1

Figure 4.2. ^{1}H NMR Spectrum of 4.9c in d_3-acetonitrile.

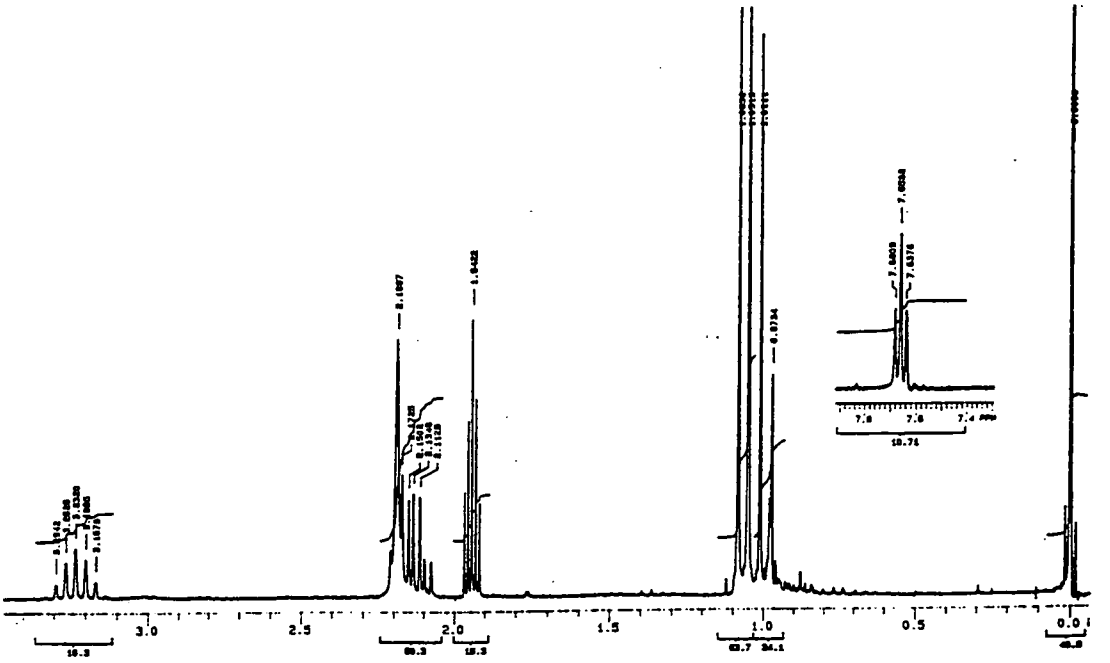

Figure 4.3. ^{1}H NMR Spectrum of 4.9d in d_3-acetonitrile.

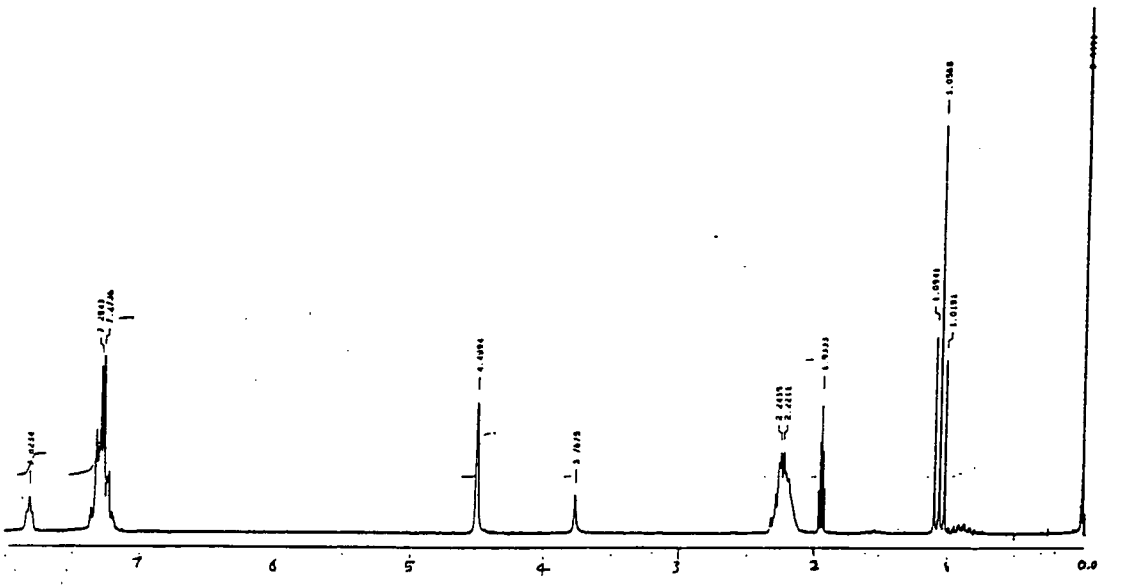

The imine 4.8e, N-phenylpropylidenamine, resulting from the reaction of propanal and aniline is not quantitatively formed. Instead an equilibrium is reached over a three hour period in which roughly equal concentrations of the imine and propanal are present. The imine 4.9e is a Schiff's base since the double bond is in conjugation with phenyl group. This leads to 4.9e having substantially greater stability than 4.9a-d, so much so that no further reaction occurs. In the presence of a five-fold excess of aniline the dianiline-substituted product, N,N'-diphenyl-1,1-diaminopropane, 4.10, forms together with 4.9e in a 2:1 ratio.

Figure 4.4 contains the ^1H NMR spectrum for the reaction of propanal with excess aniline in which peaks for 4.9e and 4.10 and propanal can be seen. Table 4.1 contains the ^1H NMR peak assignments for 4.9e and 4.10.

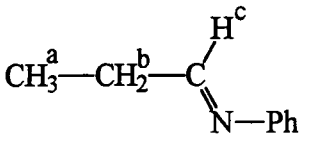

4.9e

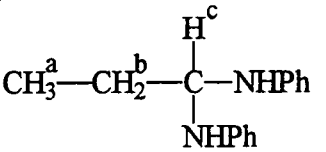

4.10

Table 4.1. ^1H NMR peak assignments for 4.9e and 4.10 in d_3-acetonitrile.

Compound		δ value / ppm	Splitting pattern	Coupling constant
4.9e	H^a	1.14 ppm	triplet	^3J = 7.5 Hz
	H^b	2.40 ppm	quartet of	^3J = 7.5 Hz
			doublets	^3J = 4.2 Hz
	H^c	7.85 ppm	triplet	^3J = 4.2 Hz
	Phenyl	7.0 - 7.4 ppm		
4.10	H^a	1.00 ppm	triplet	^3J = 7.4 Hz
	H^b	1.76 ppm	pentet	^3J = 7.4 Hz
	H^c	4.74 ppm	broad triplet	
	Phenyl	6.6 - 7.2 ppm		

Figure 4.4. The ^1H NMR spectrum of the reaction between propanal and excess aniline in d_3-acetonitrile.

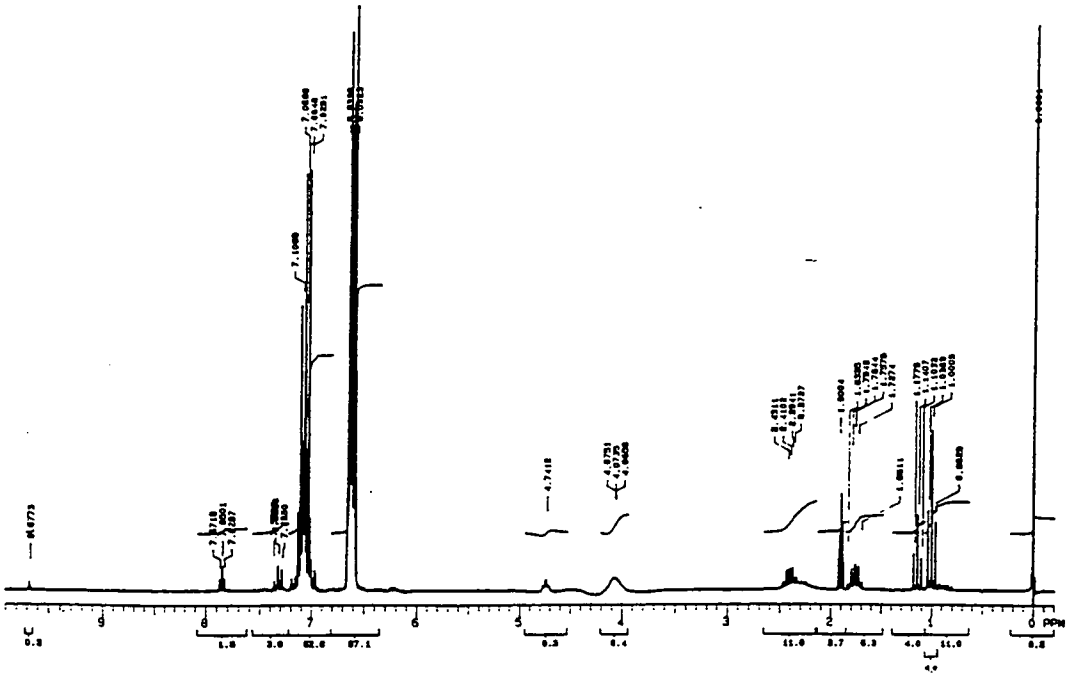

The imines 4.9a-d slowly react further. There is, however, no evidence for the trimerisation through to the 2,4,6-triethyl-1,3,5-trisubstitutedhexahydrotriazines in an analogous reaction to that shown in scheme 4.1. They form the series of N-substituted-2-methylpent-2-ene-1-ylidenamines 4.11a-d, via a reaction[6] equivalent to the aldol condensation. A possible mechanistic route is shown in scheme 4.3.

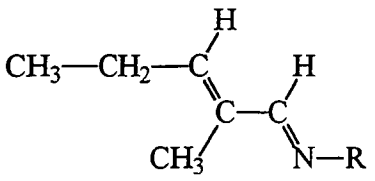

4.11

a. R = t-butyl
b. R = n-butyl
c. R = isopropyl
d. R = benzyl

This reaction involves tautomerisation of the imine, 4.9, to the corresponding enamine, 4.12, which reacts with another imine unit to give the equivalent of the aldol compound, an enamine, 4.13. This then loses one unit of the amine in forming the product, 4.11.

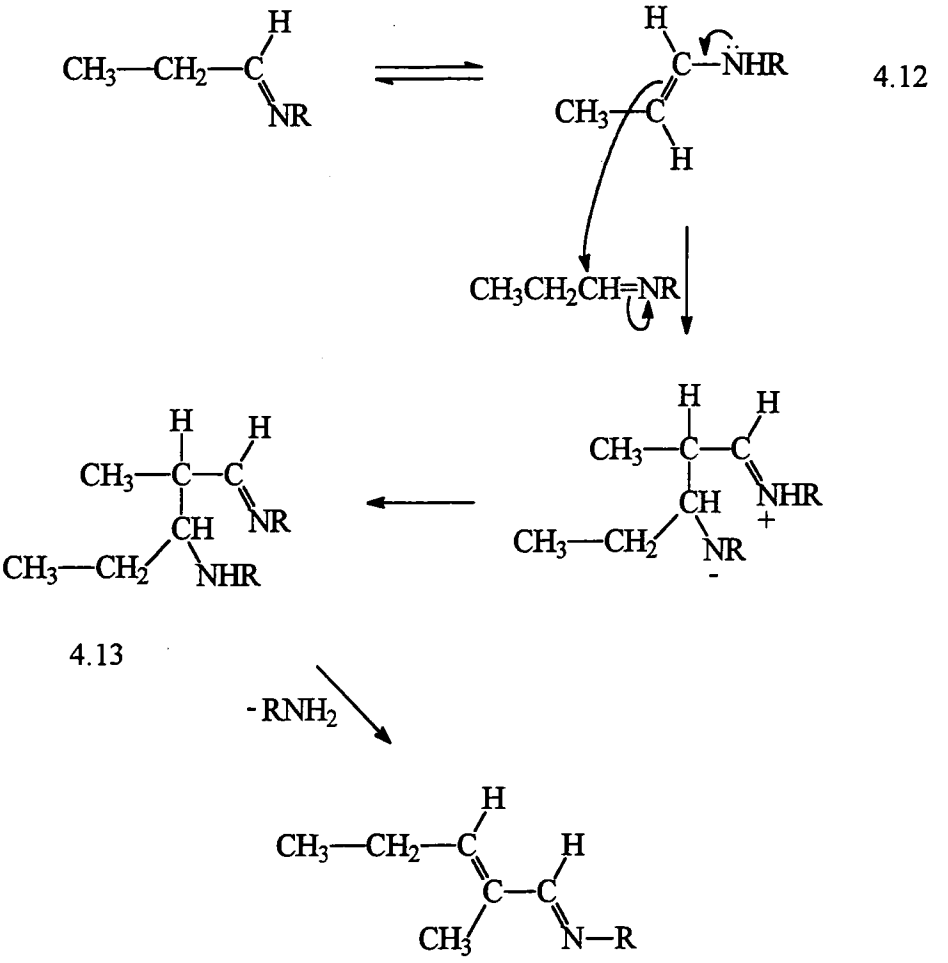

Scheme 4.3

In the following sections details are given of the reactions of propanal with a series of primary amines. These reactions were followed *in situ* by ^{1}H NMR spectroscopy in d_3-acetonitrile.

4.1.2.1 The Reaction Between Propanal and t-Butylamine

The imine 4.9a, N-(t-butyl)-propylidenamine, forms slowly as previously explained. The final product of this reaction, N-(t-butyl)-2-methylpent-2-ene-1-ylidenamine, 4.11a, is gradually produced over the period of a week. Figure 4.5 shows the spectrum of the reaction at about 60 % completion and contains peaks for both 4.9a and 4.11a. The ^1H NMR peak assignments for 4.9a and 4.11a are given in table 4.2.

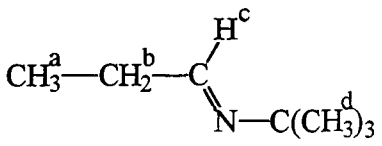

4.9a

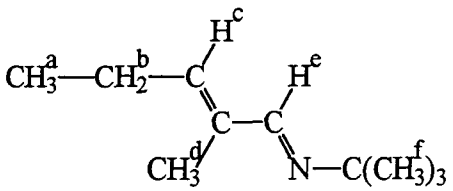

4.11a

Table 4.2. ^1H NMR peak assignments for 4.9a and 4.11a in d_3-acetonitrile.

Compound		δ value	Splitting pattern	Coupling constant
4.9a	H^a	1.01 ppm	triplet	^3J = 7.5 Hz
	H^b	2.17 ppm	quartet of doublets	^3J = 7.5 Hz ^3J = 4.6 Hz
	H^c	7.63 ppm	triplet	^3J = 4.6 Hz
	H^d	1.11 ppm	singlet	
4.11a	H^a	1.02 ppm	triplet	^3J = 7.5 Hz
	H^b	2.25 ppm	pentet	$^3J \approx$ 7.5 Hz
	H^c	5.89 ppm	triplet of quartets	^3J = 7.4 Hz ^4J = 1.4 Hz
	H^d	1.76 ppm	doublet of triplets	^4J = 1.4 Hz ^5J = 0.8 Hz
	H^e	7.84 ppm	singlet	
	H^f	1.16 ppm	singlet	

Figure 4.5. ^1H NMR spectrum in d_3-acetonitrile at 60 % completion.

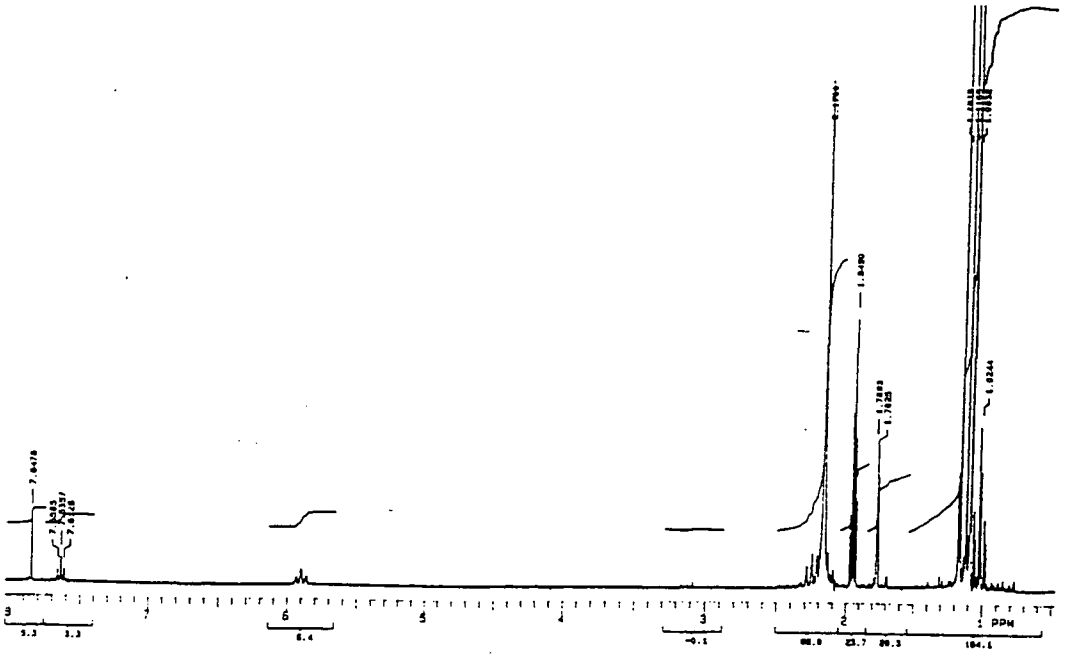

4.1.2.2 The Reaction Between Propanal and n-Butylamine

The imine 4.9b, N-(n-butyl)-propylidenamine, forms immediately. The final product of this reaction, N-(n-butyl)-2-methylpent-2-ene-1-ylidenamine, 4.11b, is produced over a similar timescale to 4.11a. Figure 4.6 shows the spectrum of the reaction at about 70 % completion and contains peaks for both 4.9b and 4.11b. The ^1H NMR peak assignments for 4.9b and 4.11b are given in table 4.3.

Figure 4.5. ^1H NMR spectrum in d_3-acetonitrile at 70 % completion.

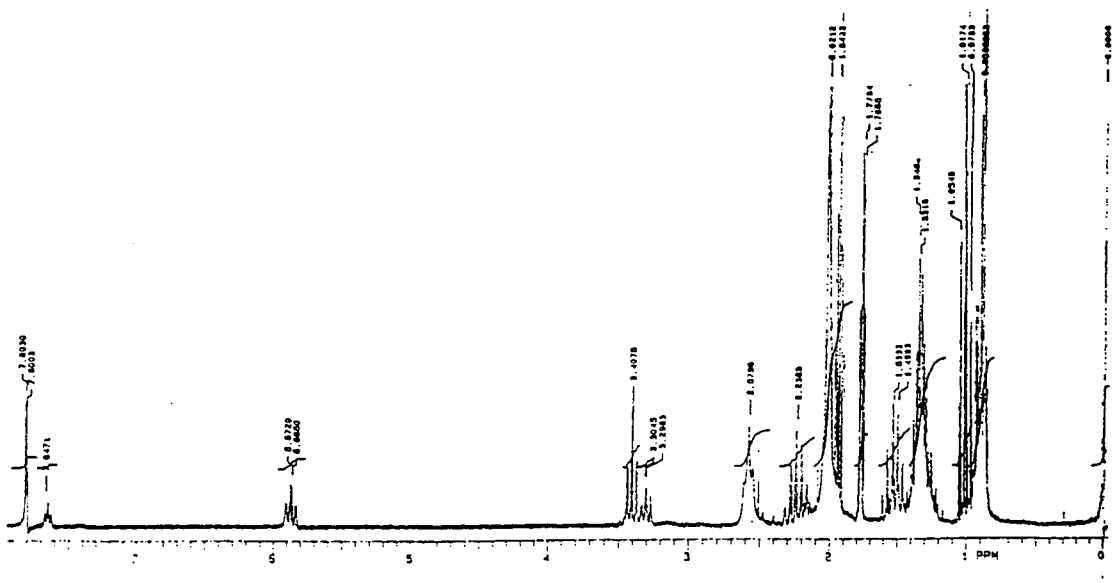

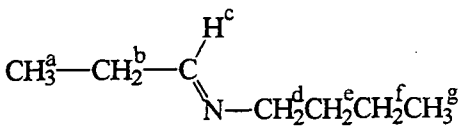

4.9b

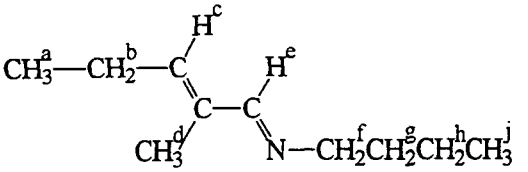

4.11b

Table 4.3. ^1H NMR peak assignments for 4.9b and 4.11b in d_3-acetonitrile.

Compound		δ value	Splitting pattern	Coupling constant
4.9b	H^a	1.01 ppm	triplet	^3J = 7.5 Hz
	H^b	2.17 ppm	quartet of	^3J = 7.5 Hz
			doublets	^3J = 4.6 Hz
	H^c	7.63 ppm	triplet	^3J = 4.6 Hz
	H^d	3.30 ppm	triplet	^3J = 6.6 Hz
	H^e	1.50 ppm	pentet	
	H^f	1.3 ppm	multiplet	
	H^g	0.90 ppm	triplet	^3J = 7.2 Hz
4.11b	H^a	1.02 ppm	triplet	^3J = 7.5 Hz
	H^b	2.24 ppm	pentet	$^3J \approx 7.5$ Hz
	H^c	5.87 ppm	triplet of	^3J = 7.4 Hz
			quartets	^4J = 1.4 Hz
	H^d	1.77 ppm	doublet of	^4J = 1.4 Hz
			triplets	^5J = 0.8 Hz
	H^e	7.80 ppm	triplet	^4J = 1.0 Hz
	H^f	3.41 ppm	triplet of	^3J = 6.8 Hz
			doublets	^4J = 1.0 Hz
	H^g	1.53 ppm	multiplet	
	H^h	1.3 ppm	multiplet	
	H^j	0.91 ppm	triplet	^3J = 7 Hz

4.1.2.3 The Reaction Between Propanal and Isopropylamine

Quantitative formation of the imine 4.9c, N-isopropylpropylidenamine, occurs during a thirty minute period, though the formation of N-isopropyl-2methylpent-2-ene-1-ylidenamine, 4.11c, is only completed after a week, similarly to 4.11a and 4.11b. G.C.-mass spectrometric analysis of the reaction at about 60 % completion are shown in figure 4.7. Two fractions are observed with mass peaks of 99 and 139 indicating that only 4.9c and 4.11c are present. Figure 4.8 contains the ^{1}H NMR spectrum at completion of reaction in which 4.11c is the sole species present. The ^{1}H NMR spectrum of 4.9c is given previously in figure 4.2. The ^{1}H NMR peak assignments are given in table 4.4.

Figure 4.7. G.C.-Mass spectrophotometry analysis at about 60 % completion.

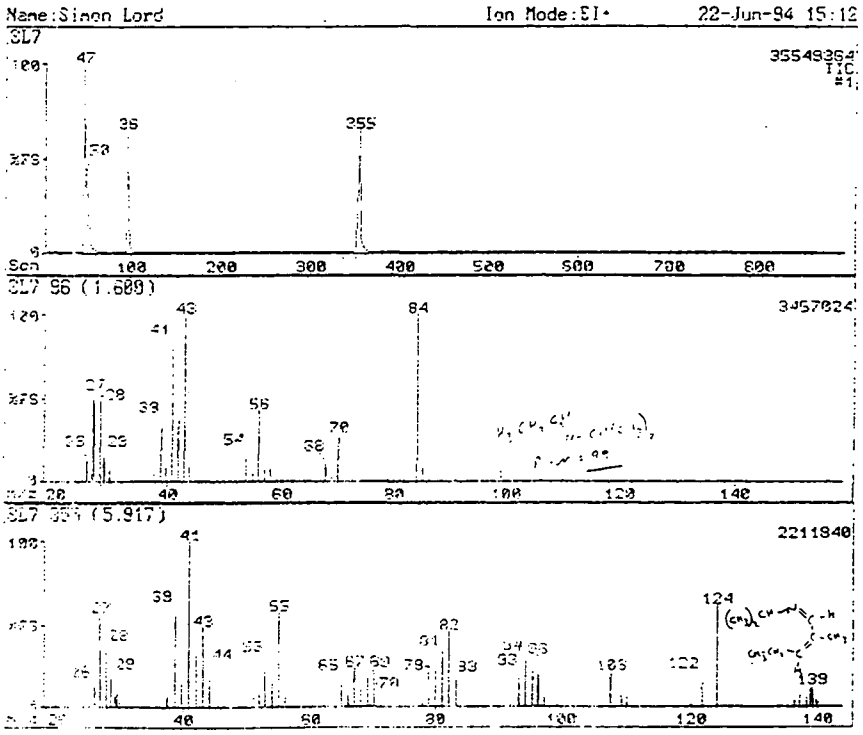

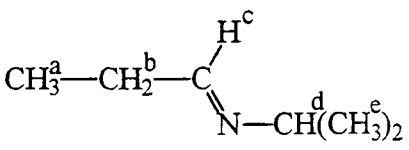

4.9c

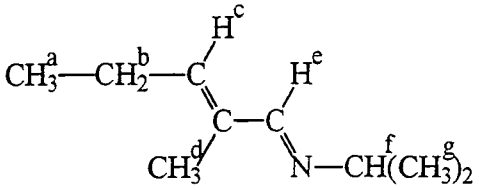

4.11c

Table 4.4. ^1H NMR peak assignments for 4.9c and 4.11c in d_3-acetonitrile.

Compound		δ value	Splitting pattern	Coupling constant
4.9c	H^a	1.01 ppm	triplet	^3J = 7.5 Hz
	H^b	2.14 ppm	quartet of	^3J = 7.5 Hz
			doublets	^3J = 4.3 Hz
	H^c	7.66 ppm	triplet	^3J = 4.3 Hz
	H^d	3.23 ppm	septet	^3J = 6.3 Hz
	H^e	1.07 ppm	doublet	^3J = 6.3 Hz
4.11c	H^a	1.02 ppm	triplet	^3J = 7.5 Hz
	H^b	2.24 ppm	pentet of	$^3J \approx 7.5$ Hz
			quartets	$^4J \approx 0.8$ Hz
	H^c	5.87 ppm	triplet of	^3J = 7.3 Hz
			quartets	^4J = 1.4 Hz
	H^d	1.76 ppm	doublet of	^4J = 1.4 Hz
			triplets	^5J = 0.8 Hz
	H^e	7.83 ppm	broad singlet	
	H^f	3.33 ppm	septet of	^3J = 6.3 Hz
			doublets	^4J = 0.7 Hz
	H^g	1.11 ppm	doublet	$^3J \approx 6.3$ Hz

Figure 4.8. ^1H NMR spectrum in d_3-acetonitrile at completion of reaction.

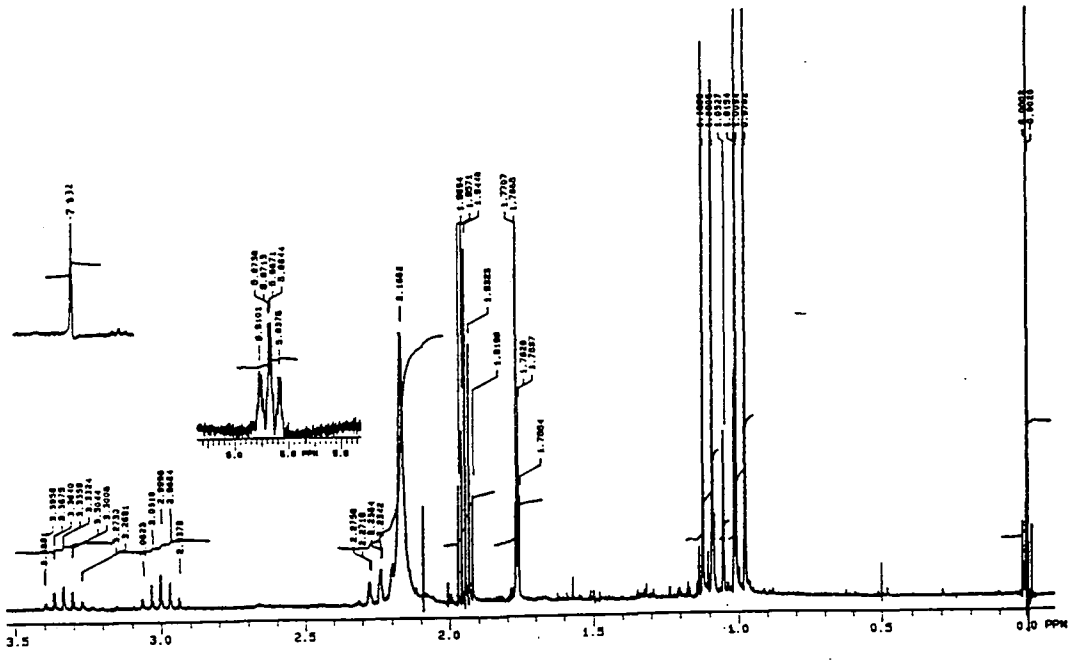

4.1.2.4 The Reaction Between Propanal and Benzylamine

The imine 4.9d, N-benzylpropylidenamine, forms immediately. N-Benzyl-2-methylpent-2-ene-1-ylidenamine, 4.11d, forms slowly over a period of a week. G.C.-mass spectrometric analysis, shown in figure 4.9, indicated the two expected fractions with mass peaks at 147 and 187 corresponding to the compounds 4.9d and 4.11d respectively. However a higher temperature fraction with a mass peak of 195 was also observed. Two extra peaks in the ^1H NMR spectrum had also been unaccounted for with shifts of 8.46 ppm (triplet, J = 1.4 Hz) and 4.77 ppm (doublet, J = 1.4 Hz). This spectrum is shown in figure 4.10. The evidence suggests the formation of the imine, N-benzylbenzylidenamine, 4.14, though only in low concentrations, via the mechanism shown in scheme 4.4. This involves tautomerisation of the 4.9d to the imine 4.15 in which n-propylamine is displaced by benzylamine. The ^1H NMR peak assignments are given in table 4.5. The ^{13}C NMR spectrum of the reaction products is also given in figure 4.11. The conformation of 4.11c (shown on page 127) was confirmed by nOe experiments.

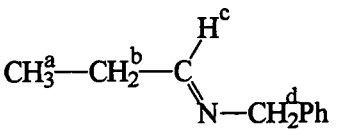

4.9d

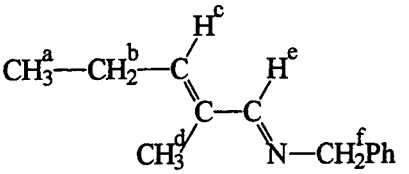

4.11d

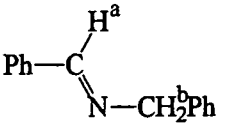

4.14

Table 4.5. ^1H NMR peak assignments for 4.9d and 4.11d in d_3-acetonitrile.

Compound		δ value	Splitting pattern	Coupling constant
4.9d	H^a	1.06 ppm	triplet	^3J = 7.5 Hz
	H^b	2.2 ppm	quartet of	^3J = 7.5 Hz
			doublets	^3J = 4.4 Hz
	H^c	7.63 ppm	triplet	^3J = 4.4 Hz
	H^d	4.50 ppm	singlet	
	phenyl	7.2 - 7.4 ppm		
4.11d	H^a	1.03 ppm	triplet	^3J = 7.5 Hz
	H^b	2.26 ppm	pentet	$^3J \approx$ 7.5 Hz
	H^c	5.95 ppm	triplet of	^3J = 7.4 Hz
			quartets	^4J = 1.4 Hz
	H^d	1.80 ppm	doublet of	^4J = 1.4 Hz
			triplets	^5J = 0.8 Hz
	H^e	7.96 ppm	singlet	
	H^f	4.60 ppm	singlet	
	phenyl	7.1 - 7.4 ppm		
4.14	H^a	8.46 ppm	triplet	^4J = 1.4 Hz
	H^b	4.77 ppm	doublet	^4J = 1.4 Hz
	phenyl	7.1 - 7.4 ppm		

Figure 4.9. G.C.-Mass spectrometry analysis.

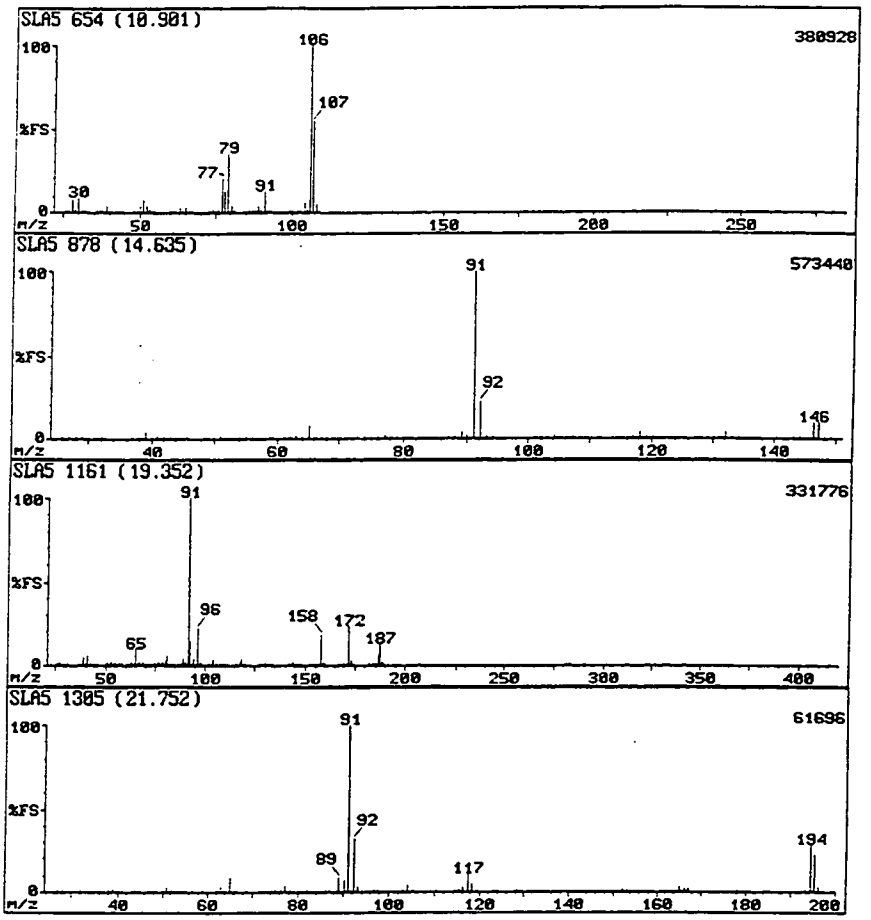

Figure 4.10. ^{1}H NMR spectrum of reaction products in d_3-acetonitrile.

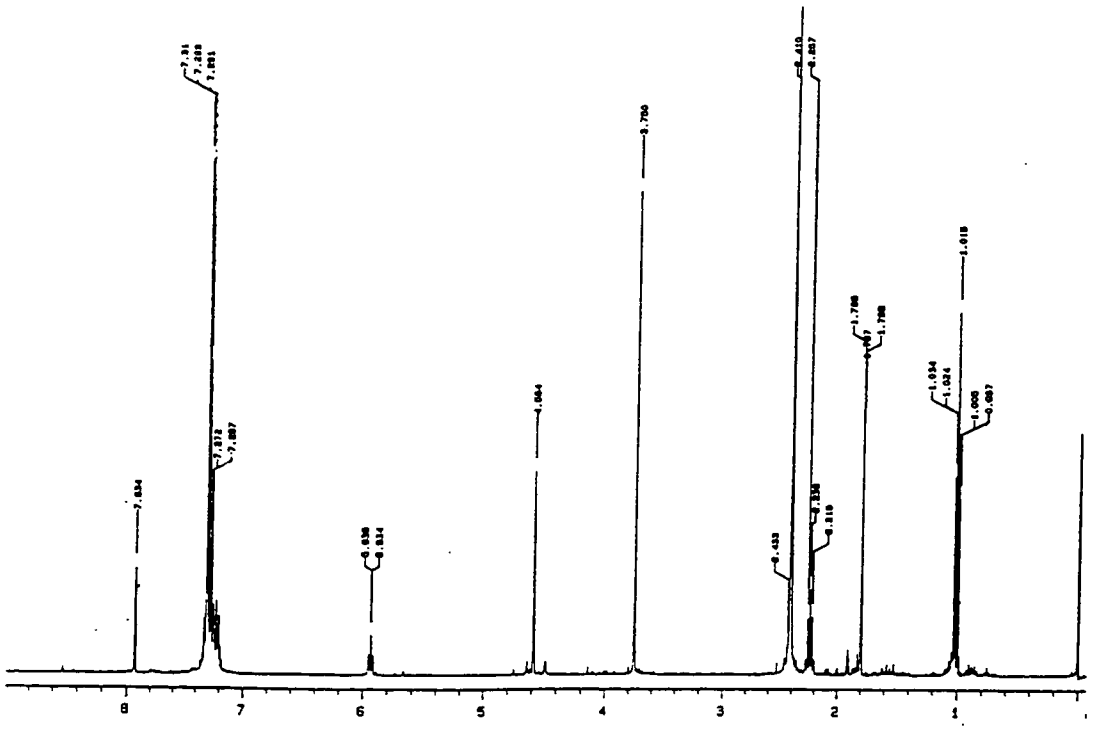

Figure 4.11. ^{13}C NMR spectrum of reaction products in d_3-acetonitrile.

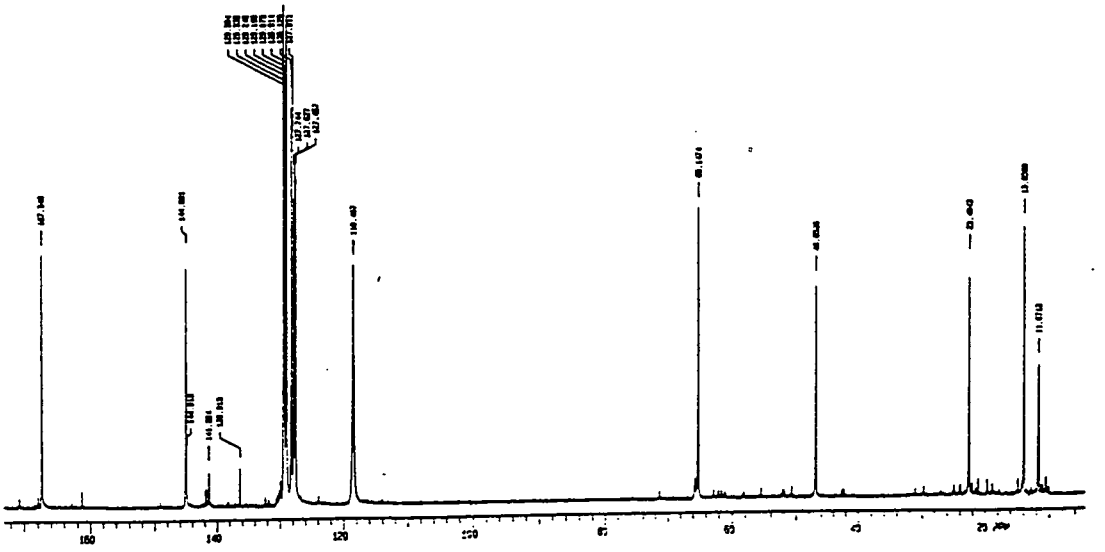

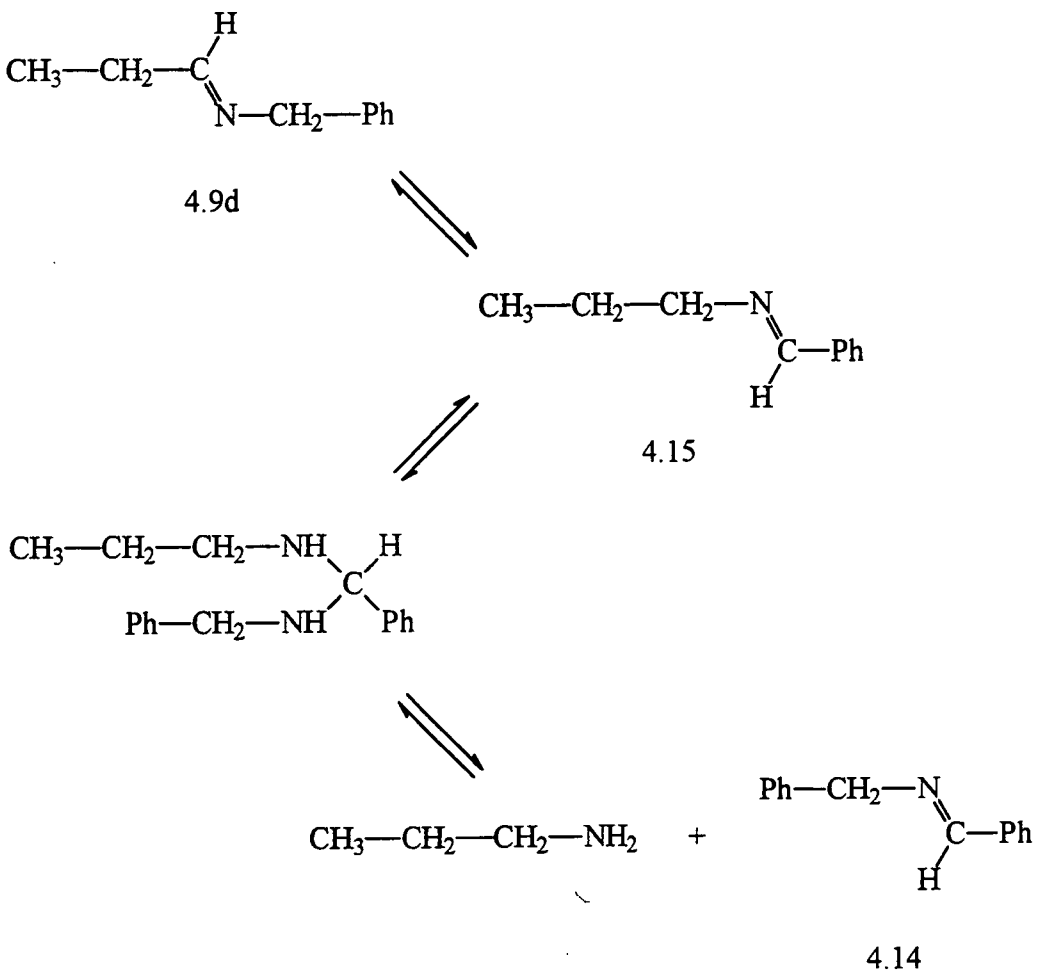

Scheme 4.4

N-Benzyl-2-methylpent-2-ene-1-ylidenamine has also been separately synthesised in order to obtain more information about the compound. It is a golden-yellow liquid, as are 4.11a-c, has a density of 945 g dm^{-3} , and a boiling point of 130 °C at 10 mm Hg, which correlates to 265 °C at 760 mm Hg using pressure-temperature alignment charts. Both ^1H NMR and G.C.-mass spectrometry gave identical results to those shown in figures 4.9 and 4.10. IR spectroscopy gave bands in the regions for conjugated C=C and C=N bonds (1450 and 1630 cm^{-1}) together with both aliphatic and aromatic C-H bonds. The U.V./vis spectrum, contained in figure 4.12, shows a strong U.V. absorbance at λ_{max} = 230 nm and with $\varepsilon = 2.24 \times 10^4$ $dm^3\ mol^{-1}\ cm^{-1}$.

Figure 4.12. U.V./vis spectrum of 4.11d in acetonitrile.

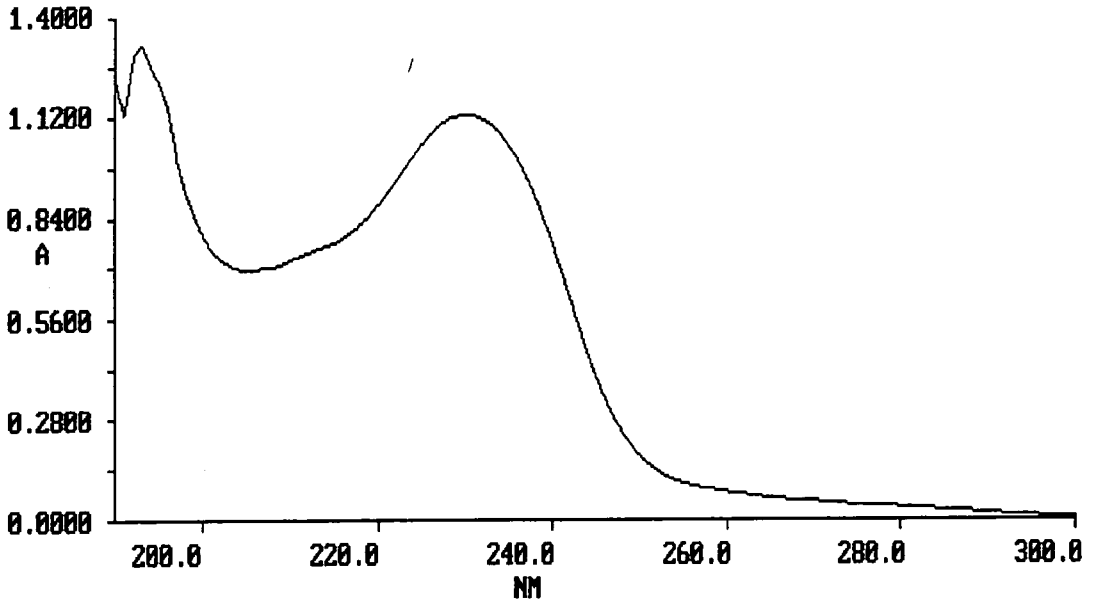

4.1.2.5 Synthesis of N-Benzyl-2-methylpent-2-ene-1-ylidenamine, 4.11d

To 36 ml propanal (0.5 mol) in 400 ml acetonitrile was added 55 ml benzylamine (0.5 mol) and the solution was stirred for 5 days at room temperature. After two hours a yellow tint was observed in the solution and this gradually intensified over the five day period. The acetonitrile was then removed by use of a rotary evaporator and the resulting mixture was fractionally distilled under reduced pressure (10 mm Hg) with use of a Vigreux column. Benzylamine distilled over at 65 °C and N-benzyl-2-methylpent-2-ene-1-ylidenamine distilled over between 128-130 °C as a yellow liquid.

4.2 The Reactions of 2,2,2-Trichloroethanal (Chloral) with Ammonia and Primary Amines

4.2.1 The Reaction Between Chloral (4.16) and Ammonia.

Literature reports[7,8] were found containing synthetic routes to the formation of 2,4,6-tris(trichloromethyl)-1,3,5-hexahydrotriazine, 4.17. However, attempts at isolating this solid proved unsuccessful. The only solid recovered from the reaction was ammonium chloride indicating cleavage of a carbon-chlorine bond since chloral is the only source of chlorine atoms. Further reports[3] have recently been found in support of the fact that the cyclic trimer is not produced.

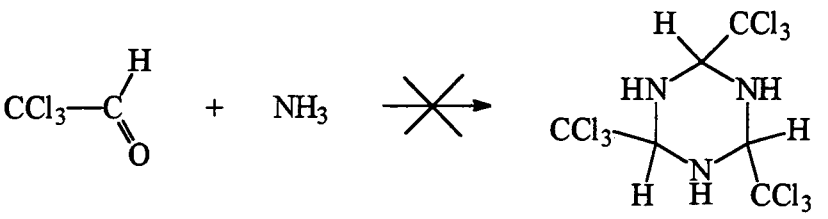

4.16 4.17

4.2.2 The Reactions of Chloral and Primary Amines

Chloral has been reacted with four primary amines, isopropylamine, t-butylamine, benzylamine and aniline. As is seen in similar reactions with propanal, there is no evidence for the formation of the hexahydrotriazine ring structures via trimerisation of the imines. In this series of reactions the carbinolamine intermediates, N-alkyl-2,2,2-trichloro-1-aminoethanols, 4.18a-d, are far more stable than those correspondingly obtained from propanal, forming instantaneously and quantitatively upon mixing chloral with each amine. They then undergo two competitive reactions, forming both the imines, N-substituted-2,2,2-trichloroethylidenamines, 4.19a-d, by loss of water, and the N-substituted formamides, 4.20a-d, by loss of chloroform in a reaction similar to the last step of the haloform reaction. This is shown in scheme 4.5. The ratio of the products 4.19 and 4.20 is seemingly dependent on the water content of the solvent used.

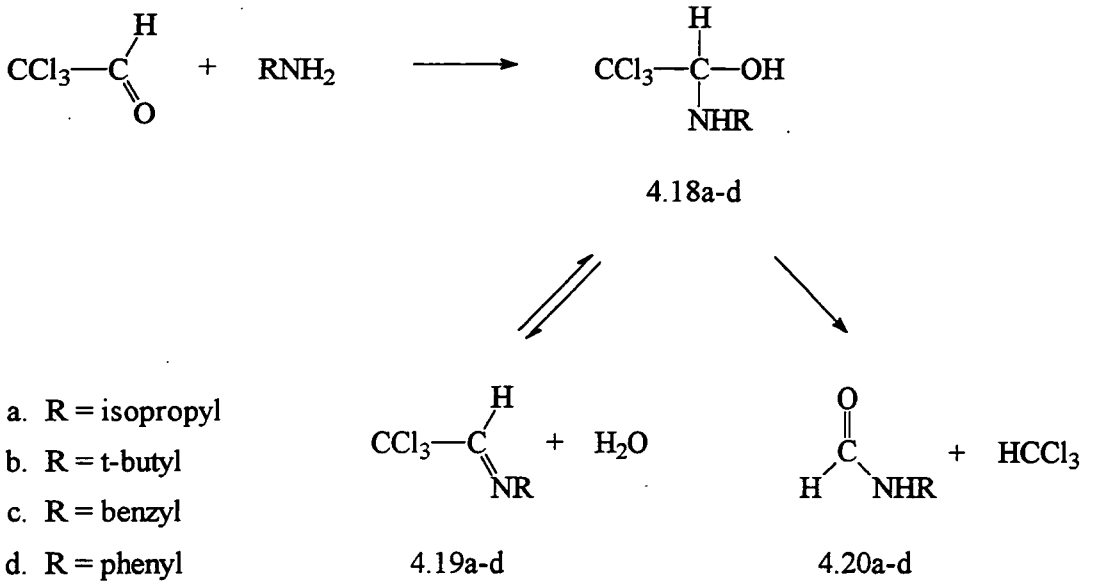

Scheme 4.5

4.2.2.1 The Reaction Between Chloral and Isopropylamine

The progress of this reaction has been followed using a fresh sample of d_3-acetonitrile, and also one containing atmospherically absorbed water. The carbinolamine, N-(isopropyl)-2,2,2-trichloro-1-aminoethanol, 4.18a, forms instantaneously in both cases. In the former run a roughly 3:2 ratio of the imine, N-isopropyl-2,2,2-trichloroethylidenamine, 4.19a, to isopropylformamide, 4.20a, is produced. In the latter the ratio is greater than 5:1 in favour of 4.20a, showing a strong preference for formation of the formamide in the presence of water. Figure 4.13 contains the ^{1}H NMR spectrum of the reaction in dry solvent in its early stages, when 4.18a, 4.19a and 4.20a are all observed. Table 4.6 contains the ^{1}H NMR peak assignments for 4.18a, 4.19a and 4.20a.

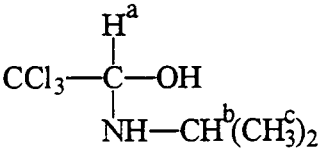

4.18a

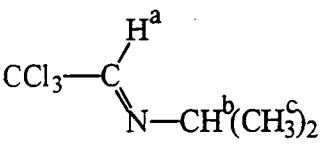

4.19a

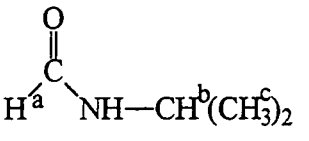

4.20a

Table 4.6. ^{1}H NMR peak assignments for 4.18a, 4.19a and 4.20a in d_3-acetonitrile.

Compound		δ value	Splitting pattern	Coupling constant
4.18a	H^a	4.65 ppm	broad singlet	
	H^b	3.14 ppm	septet	^3J = 6.4 Hz
	H^c	1.06 ppm	doublet	^3J = 6.4 Hz
4.19a	H^a	7.89 ppm	singlet	
	H^b	3.71 ppm	septet	^3J = 6.3 Hz
	H^c	1.18 ppm	doublet	^3J = 6.3 Hz
4.20a	H^a	7.97 ppm	broad singlet	
	H^b	4.00 ppm	septet	^3J = 6.6 Hz
	H^c	1.11 ppm	doublet	^3J = 6.6 Hz

Figure 4.13. ^{1}H NMR spectrum in d_3-acetonitrile showing 4.18a, 4.19a and 4.20a.

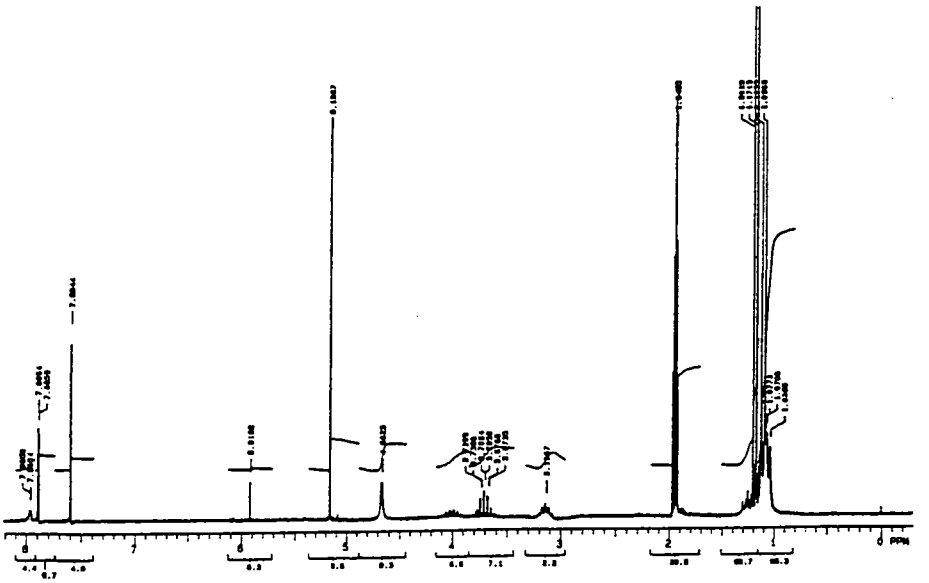

4.2.2.2. The Reaction Between Chloral and t-Butylamine

This reaction was followed using a fresh sample of d_3-acetonitrile, one containing atmospherically absorbed water and one with 10 μl of water added to 1 cm^3 of sample. The latter contains enough water to completely hydrate the 0.2 mol dm^{-3} chloral present in the NMR tube. The carbinolamine, N-(tert-butyl)-2,2,2-trichloro-1-aminoethanol 4.18b forms immediately in all cases. It gives an interesting ^1H NMR spectrum, shown in figure 4.14, in which coupling is seen between the C-H and N-H protons due to the latter's slow exchange.

Figure 4.14. The ^1H NMR spectrum of 4.18b in d_3-acetonitrile.

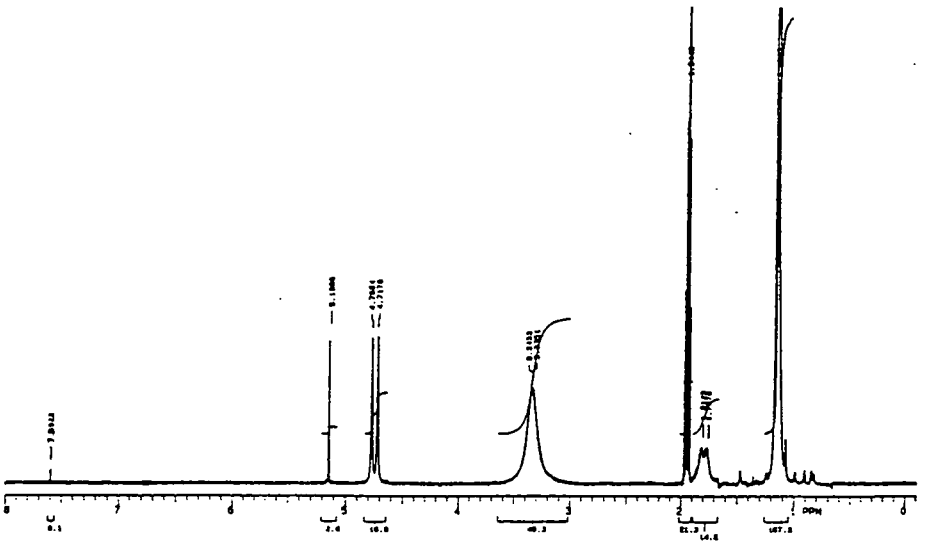

In the run with the completely dry solvent, 4.18b is slowly converted to mainly the imine, N-(tert-butyl)-2,2,2-trichloroethylidienamine, 4.19b, together with a small but observable concentration of chloroform. However there was strangely no sign of an accompanying tert-butylformamide peak, though there was a peak at 5.93 ppm of similar intensity to chloroform. The run containing a trace of water absorbed from the atmosphere gave a ratio of roughly 2:1 in favour of the formamide, 4.20b. The peak at 5.93 ppm was again observed. For the run with hydrated chloral, just peaks for 4.20b, chloroform and the species at 5.93 ppm were observed. Barely a trace of the imine peak was present. In both the water containing runs the integral value of the chloroform peak is roughly equal to the sum of the values for 4.20b and the peak at 5.93 ppm. Figure 4.15 contains a ^1H NMR spectrum showing both 4.19b and 4.20b, the peak assignments for which are given in table 4.7 together with those for 4.18b. Tert-butylformamide shows two sets of peaks due to the restricted rotation about the C-N bond, giving rise to cis and trans isomers.

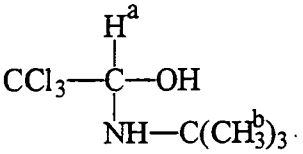

4.18b

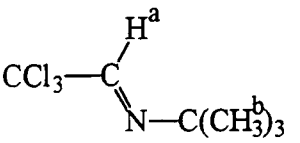

4.19b

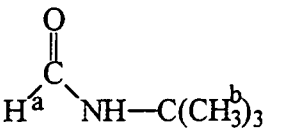

4.20b

Table 4.7. ^1H NMR peak assignments for 4.18b, 4.19b and 4.20b in d_3-acetonitrile.

Compound		δ value	Splitting pattern	Coupling constant
4.18b	H^a	4.74 ppm	doublet	^3J = 10 Hz
	H^b	1.16 ppm	singlet	
	NH	1.79 ppm	broad doublet	^3J = 10 Hz
4.19b	H^a	7.78 ppm	singlet	
	H^b	1.25 ppm	singlet	
4.20b (trans)	H^a	8.22 ppm	doublet	^3J = 12.1 Hz
	H^b	1.28 ppm	singlet	
4.20b (cis)	H^a	7.91 ppm	doublet	^3J = 1.5 Hz
	H^b	1.31 ppm	singlet	

Figure 4.15. ^1H NMR spectrum in d_3-acetonitrile containing bands for both 4.19b and 4.20b.

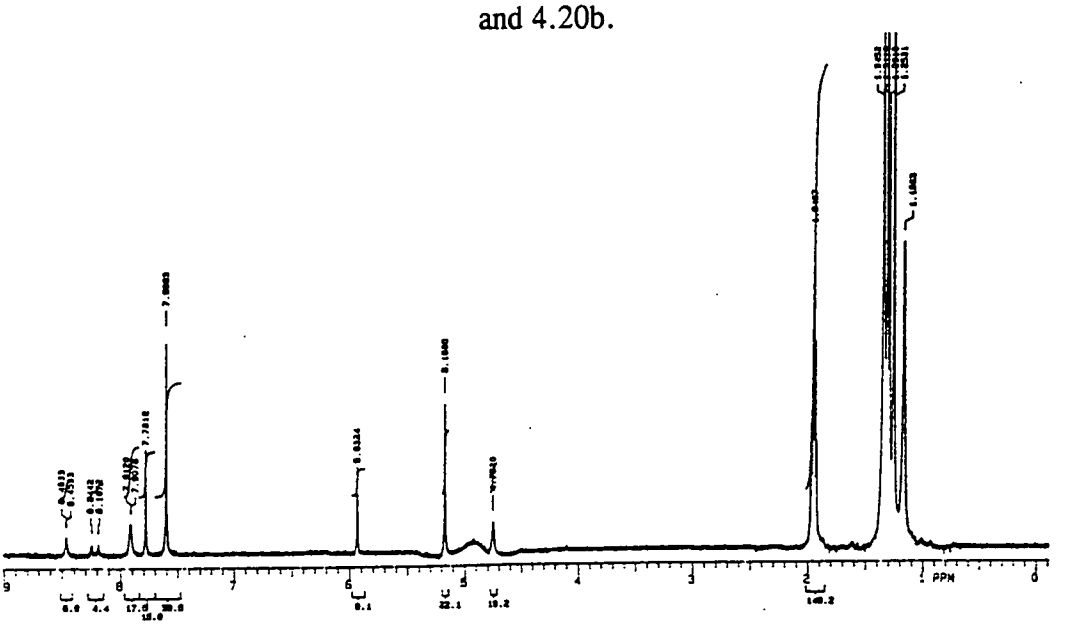

4.2.2.3 The Reaction Between Chloral and Benzylamine

This reaction has been followed both with equimolar reactants and also with chloral in excess. The equilibrium constant for hydration of chloral, contained in table 4.8, is extremely large for a carbonyl compound and is due to the instability from having strongly electron withdrawing groups on the α-carbon The value for propanal is also given and is a typical value for an aldehyde. Thus chloral has the effect of keeping the solvent dry and would be expected to promote the formation of the imine, N-benzyl-2,2,2-trichloroethylidinamine, 4.19c, rather than benzyl formamide, 4.20c.

Table 4.8. Equilibrium constants[9,10] at 25 °C for the reaction

$$R^1R^2C{=}O + H_2O \rightleftharpoons R^1R^2C(OH)_2$$

Aldehyde	$K[H_2O] = \frac{[R^1R^2C(OH)_2]}{[R^1R^2C=O]}$
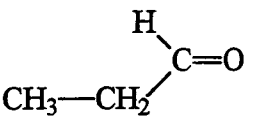	0.71
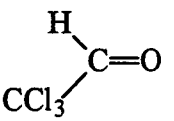	2.8×10^4

The carbinolamine N-benzyl-2,2,2-trichloro-1-aminoethanol, 4.18c, which forms instantaneously, also shows coupling between the C-H and N-H protons. The ^1H NMR also shows that the CH_2 protons in the benzyl functionality are inequivalent, appearing as an AB quartet with $\Delta\nu$ = 35.6 Hz and ^2J = 13.6 Hz. This spectrum is shown in figure 4.16.

The run containing equimolar chloral and benzylamine produced an equilibrium over two days in which the ratio of 4.20c : 4.19c is roughly 10:1, i.e. strongly favouring formation of the formamide. However, in the presence of a 2½ - fold excess of chloral, virtually complete conversion of the carbinolamine to imine occurred within three days, with only a trace of benzylformamide and chloroform, as expected. Figure 4.16 contains the ^1H NMR spectrum from early in the equimolar reaction showing 4.18c, 4.19c and 4.20c, the peak assignments for which are contained in table 4.9

Figure 4.16. ^{1}H NMR spectrum of 4.18c in d_3-acetonitrile.

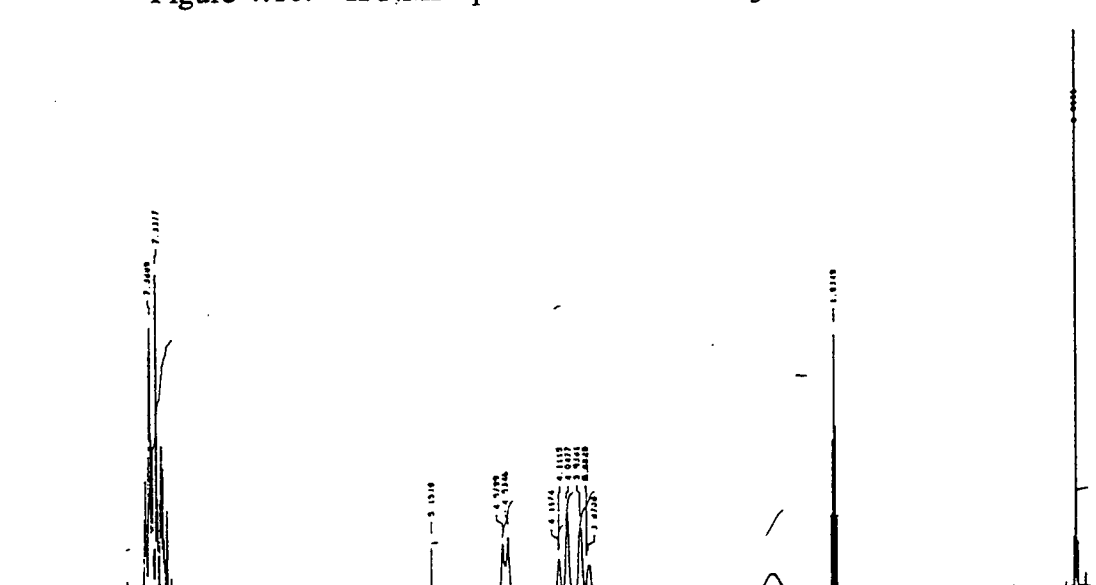

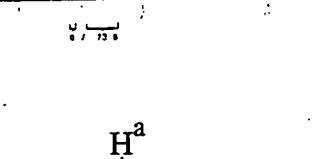

4.18c

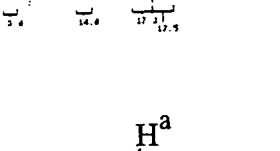

4.19c

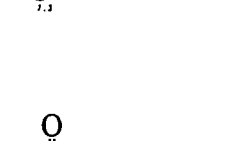

4.20c

Table 4.9. ^{1}H NMR peak assignments for 4.18c, 4.19c and 4.20c in d_3-acetonitrile.

Compound		δ value	Splitting pattern	Coupling constant
4.18c	H^a	4.56 ppm	broad doublet	^3J = 9.1 Hz
	H^b	4.09 ppm	doublet	^3J = 13.8 Hz
	H^c	3.91 ppm	doublet	^3J = 13.8 Hz
	NH	2.4 ppm	v. broad singlet	
	Phenyl	7.2 - 7.5 ppm		
4.19c	H^a	8.01 ppm	triplet	^4J = 1.45 Hz
	H^b	4.81 ppm	doublet	^4J = 1.45 Hz
	Phenyl	7.2 - 7.5 ppm		
4.20c	H^a	8.17 ppm	broad singlet	
	H^b	4.37 ppm	doublet	^3J = 6.3 Hz
	Phenyl	7.2 - 7.5 ppm		

Figure 4.17. ^{1}H NMR spectrum containing peaks for 4.18c, 4.19c and 4.20c in d_3-acetonitrile.

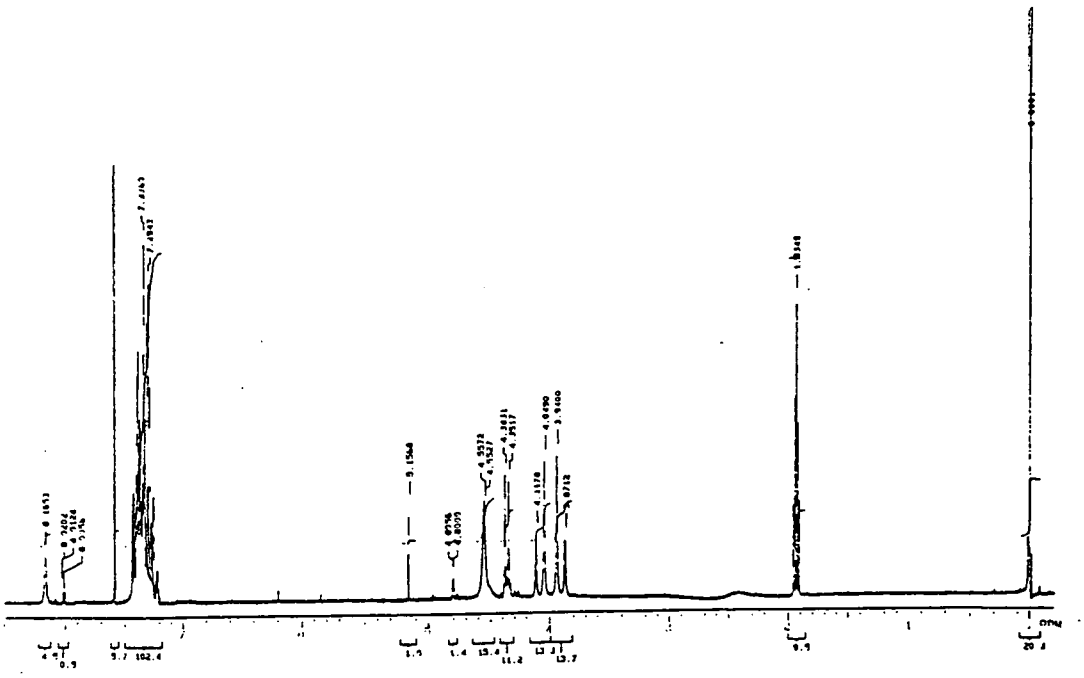

4.2.4 The Reaction Between Chloral and Aniline

The carbinolamine N-phenyl-2,2,2-trichloro-1-aminoethanol, 4.18d, is relatively stable. An equilibrium is slowly produced with the imine, N-phenyl-2,2,2-trichloroethylidenamine, 4.19d, however, this only affords a low imine concentration with the ratio of carbinolamine : imine being 4:1. The ^{1}H NMR spectrum also contained two broad triplets at 5.05 and 5.67 ppm, the latter of which is the dianiline substituted compound N,N'-diphenyl-2,2,2-trichloro-1,1-diaminoethane, 4.21. In the presence of a 1-fold excess of chloral a greater concentration of the imine forms, with the ratio of carbinolamine : imine decreasing to 3:2. This is expected due to chloral's dehydrating properties explained previously. The two triplets at 5.05 and 5.67 ppm are again observed. Only a trace chloroform signal is seen in both sets of reactions. Figure 4.18 contains the ^{1}H NMR spectrum showing the equilibrium set up between 4.18d, 4.19d and 4.21. The peak assignments are given in table 4.10.

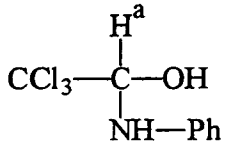

4.18d

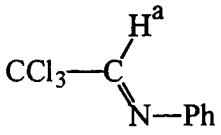

4.19d

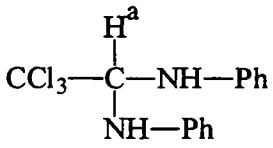

4.21

Table 4.10. ^1H NMR peak assignments for 4.18d, 4.19d and 4.21 in d_3-acetonitrile.

Compound		δ value	Splitting pattern	Coupling constant
4.18d	H^a	5.49 ppm	doublet	^3J = 9.4 Hz
	Phenyl	6.7 - 7.3 ppm		
4.19d	H^a	8.16 ppm	singlet	
	Phenyl	6.7 - 7.5 ppm		
4.21	H^a	5.67 ppm	broad triplet	$^3J \approx 8$ Hz
	Phenyl	6.7 - 7.5 ppm		

Figure 4.18. ^1H NMR spectrum showing 4.18d, 4.19d and 4.21 in d_3-acetonitrile.

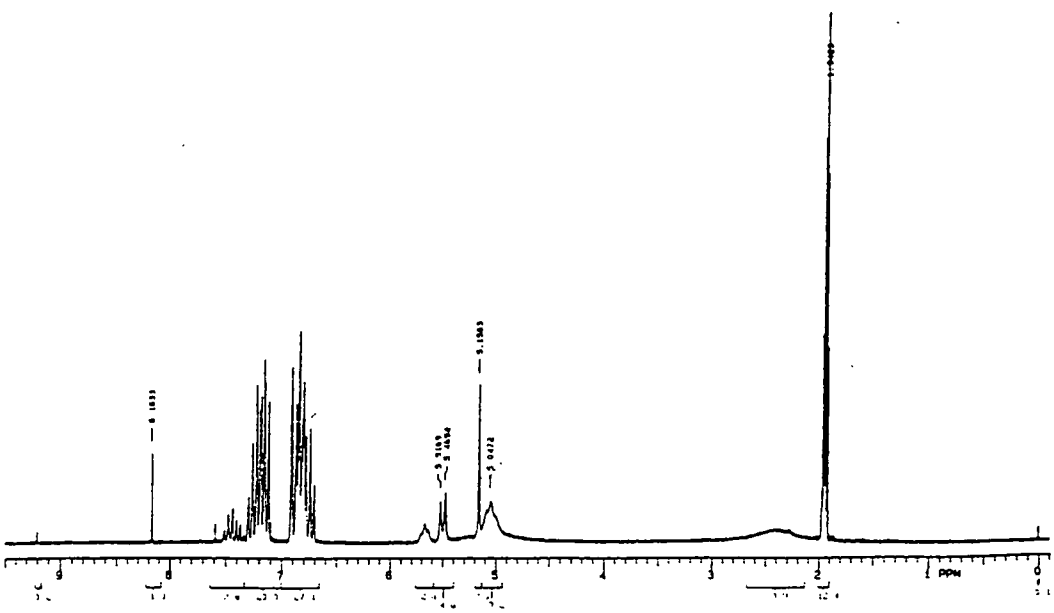

4.3 The Reactions of 2,2-Dichloroethanal with Ammonia and Primary Amines

4.3.1 Dichloroethanal (4.23)

This aldehyde is not commercially available as it readily polymerises[11,12] on standing. Hence it had to be freshly prepared for each reaction. The synthesis is fully described later in the experimental chapter, but involved conversion of the acetal-protected aldehyde 1,1-dichloro-2,2-diethoxyethane, 4.22, to the aldehyde, 4.23, as shown in equation 4.2. Figure 4.19 shows a sample spectrum of the product in which it can be seen that a small quantity of 4.23 has already began the polymerisation process.

$$\underset{\textbf{4.22}}{CHCl_2—CH(OEt)_2} + (PhCO)_2O \xrightarrow{H^+} \underset{\textbf{4.23}}{CHCl_2—CHO} + 2\,PhCOOEt$$

Equation 4.2

2,2-Dichloroethanal readily hydrates in the presence of water. The ^1H NMR bands for this hydrate, 4.22 and 4.23 are given in table 4.11. The spectrum of 4.22 is interesting as the protons in the CH_2 groups are inequivalent due to the steric constraints within the molecule hindering rotation about the carbon-oxygen bond. This produces an AB quartet ($\Delta\nu$ = 19.7 Hz and ^2J = 9.5 Hz) in which each line is split into quartets by the neighbouring CH_3 (^3J = 7 Hz) group thus yielding a sixteen line band.

Figure 4.19. ^1H NMR spectrum of 2,2-dichloroethanal.

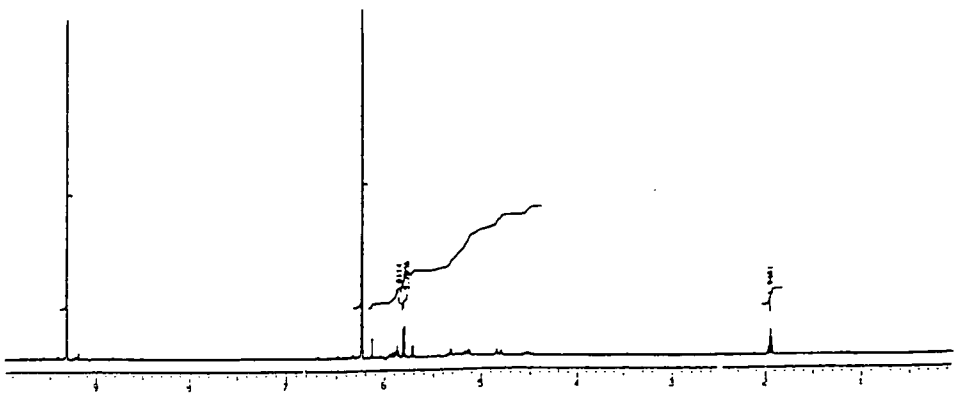

Table 4.11. ^1H NMR peak assignments for 4.22, 4.23 and the hydrate of 4.23.

Compound		δ value	Splitting pattern	Coupling constant
4.22	$C\underline{H}Cl_2$	5.49 ppm	doublet	^3J = 4.4 Hz
	$C\underline{H}(OEt)_2$	4.66 ppm	doublet	^3J = 4.4 Hz
	$O\text{-}C\underline{H}_2\text{-}$	3.71 ppm	AB quartet of quartets	^2J = 9.5 Hz ^3J = 7.0 Hz
	$\text{-}C\underline{H}_3$	1.19 ppm	triplet	^3J = 7.0 Hz
4.23	$C\underline{H}Cl_2$	6.24 ppm	doublet	^3J = 1.7 Hz
	$C\underline{H}O$	9.32 ppm	doublet	^3J = 1.7 Hz
hydrate	$C\underline{H}Cl_2$	5.70 ppm	doublet	^3J = 3.1 Hz
	$C\underline{H}(OH)_2$	5.04 ppm	doublet	^3J = 3.1 Hz

4.3.2 The Reaction between 2,2-Dichloroethanal and Ammonia

Attempts were made to synthesise the ring structure 2,4,6-tris(dichloromethyl)-1,3,5-hexahydrotriazine, 4.26. After acylation of the nitrogen atoms it was hoped that amines (trialkylsilylamines) would react with the C-Cl groups of 4.26 forming three imines that might possibly trimerise forming another ring above the original one, thus producing a cage structure,[13] as shown in scheme 4.6. This could then be nitrated, forming a highly explosive nitramine 4.27.

However, all attempts at producing 4.24 proved unsuccessful. This reaction was also followed using ^1H NMR techniques. The carbinolamine 2,2-dichloro-1-aminoethanol, 4.24, was instantly produced being stable for several hours. The ^1H NMR spectrum contained bands at 5.84 ppm (doublet, ^3J = 2.6 Hz) for the $C\underline{H}Cl_2$ group and at 4.63 ppm (doublet ^3J = 2.6 Hz) for the $C\underline{H}(OH)(NH_2)$ group. The imine 2,2-dichloroethylidenamine, 4.25, however, did not form in observable concentrations. A large number of smaller peaks gradually increased in intensity whilst the main peaks decayed. This coupled with the fact that a brown layer of much higher density formed at the bottom of the NMR tube indicates that the imine may be unstable with respect to polymerisation as is the parent aldehyde.

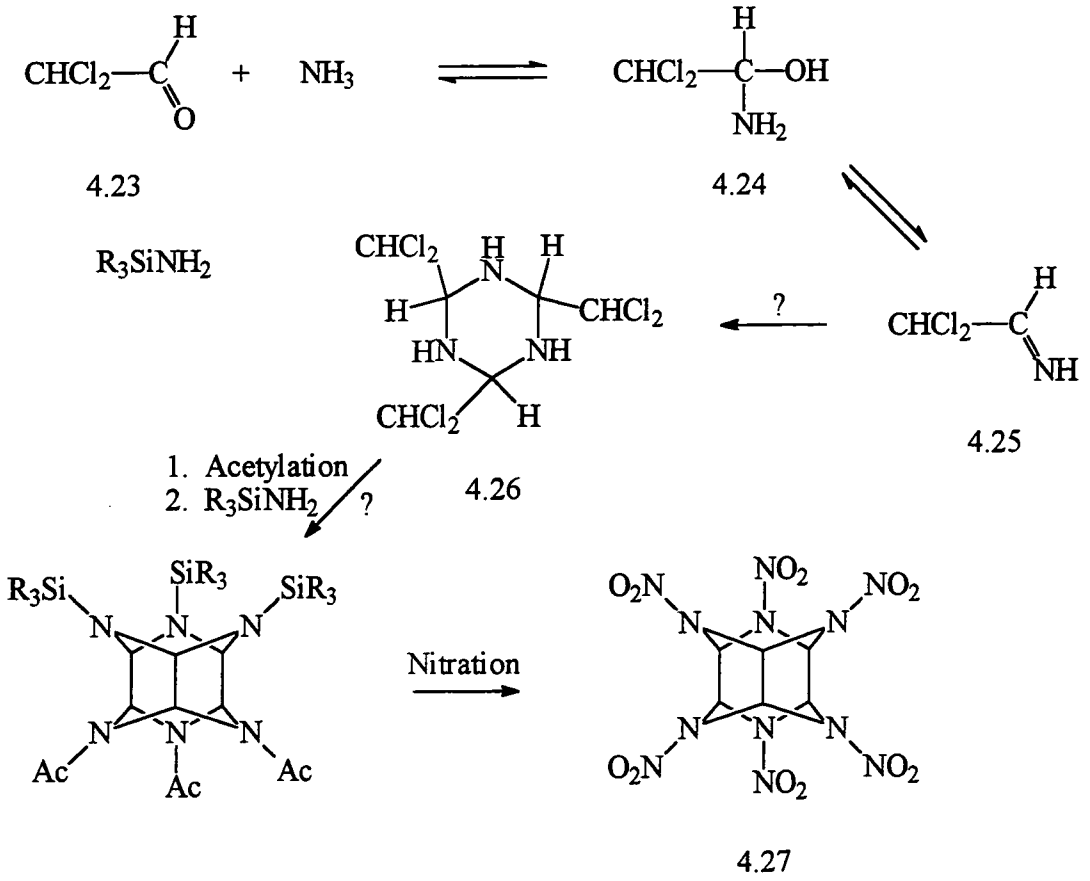

Scheme 4.6

4.3.3 The Reaction Between 2,2-Dichloroethanal and Primary Amines

Three amines, t-butylamine, isopropylamine and benzylamine, have been reacted with 2,2-dichloroethanal, 4.23. The carbinolamine intermediates, N-alkyl-2,2-dichloro-1-aminoethanols, 4.28, in these reactions are unstable with respect to dehydration and are not observed. The imines, N-alkyl-2,2-dichloroethylidenamines, 4.29, are stable forming instantaneously and quantitatively upon mixing. Each imine possesses an α-proton enabling further reaction similar to that of the N-alkylpropylidenamines. However, none contain a second α-proton and hence the last stage of the reaction, deamination, is not possible. The products, 4.30, are N,N'-dialkyl-4,4,2,2-tetrachloro-3-aminobutylidenamines. The mechanism of their formation is given in scheme 4.7.

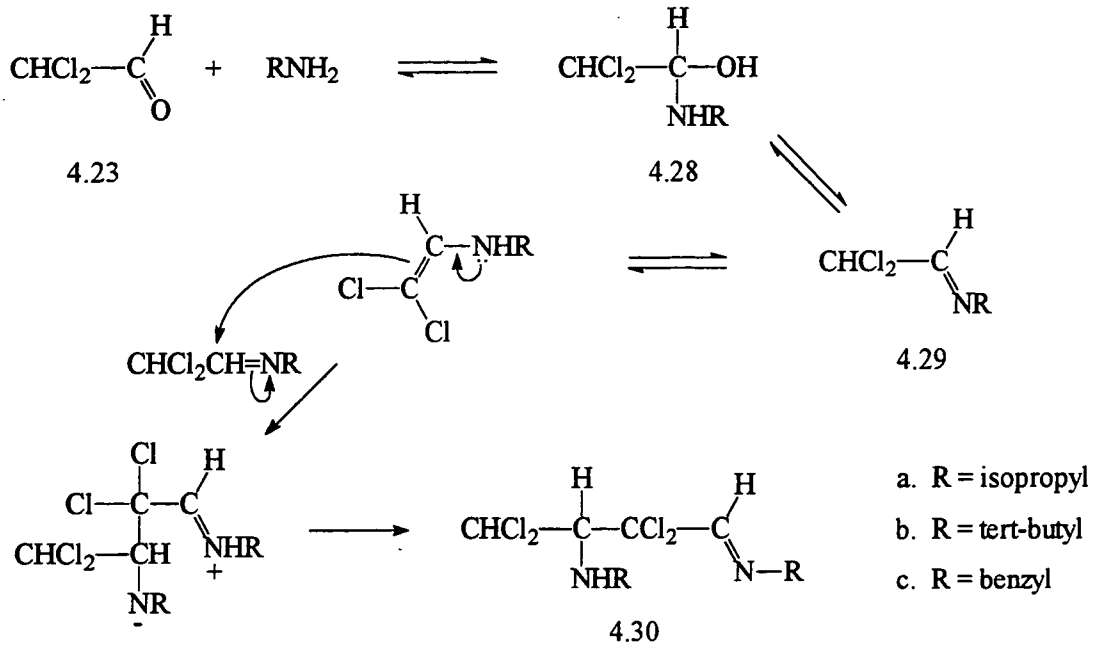

Scheme 4.7

4.3.3.1 The Reaction Between 2,2-Dichloroethanal and Isopropylamine

This reaction resulted in the instant formation of the imine N-isopropyl-2,2-dichloroethylidenamine, 4.29a. Slow formation of N,N'-diisopropyl-4,4,2,2-tetrachloro-3-aminobutylidenamine immediately followed over the period of a day until roughly a 2:1 ratio of 4.30a : 4.29a was produced. However, neither of these two compounds are stable for long periods of time. Their bands in the ^1H NMR spectrum gradually collapse whilst a substantial number of peaks appeared between 4.5 and 6.5 ppm together with one at 9.45 ppm. The ^1H NMR peak assignments for 4.29a and 4.30a are given in table 4.12 and a sample spectrum is shown in figure 4.21. An interesting feature of the compounds 4.30a-c are the very small coupling constants (^3J = 1.8 Hz) for the protons labelled H^a and H^b. This is a low value for hydrogens on adjacent carbon atoms. This is likely to reflect the steric crowding in 4.30a-c which prevents free rotation about the C-C bond. It is known that vicinal coupling constants vary with dihedral angle. A coupling constant of 1.8 Hz corresponds to a dihedral angle of 90 ± 30 °. A run was also carried out using a sample of d_3-acetonitrile containing a small concentration of atmospherically absorbed water. This unexpectedly afforded the carbinolamine, N-isopropyl-2,2-dichloro-1-aminoethanol, 4.28a, initially, the ^1H NMR spectrum of which is shown in figure 4.20. This was slowly converted to the imine, 4.29, over the period of several hours.

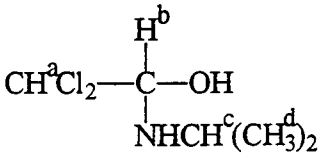

4.28a

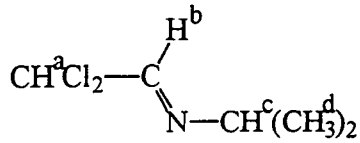

4.29a

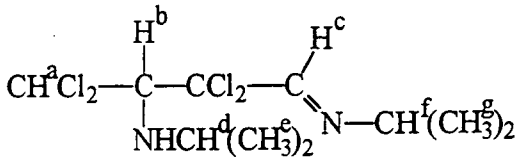

4.30a

Table 4.12. ^{1}H NMR peak assignments for 4.29a and 4.30a in d_3-acetonitrile.

Compound		δ value	Splitting pattern	Coupling constant
4.28a	H^a	5.81 ppm	doublet	^3J = 2.5 Hz
	H^b	4.55 ppm	broad doublet	^3J = 2.5 Hz
	H^c	3.10 ppm	septet	^3J = 6.2 Hz
	H^d	1.06 ppm	doublet	^3J = 6.2 Hz
4.29a	H^a	6.23 ppm	doublet	^3J = 6.3 Hz
	H^b	7.70 ppm	doublet of doublets	^3J = 6.3 Hz ^4J = 0.7 Hz
	H^c	3.50 ppm	septet of doublets	^3J = 6.3 Hz ^4J = 0.7 Hz
	H^d	1.13 ppm	doublet	^3J = 6.3 Hz
4.30a	H^a	6.48 ppm	doublet	^3J = 1.8 Hz
	H^b	4.68 ppm	doublet	^3J = 1.8 Hz
	H^c	7.84 ppm	doublet	^4J = 0.7 Hz
	H^d	3.54 ppm	septet	^3J = 6.3 Hz
	H^e	1.15 ppm	doublet	^3J = 6.3 Hz
	H^f	3.57 ppm	septet of doublets	^3J = 6.3 Hz ^4J = 0.7 Hz
	H^g	1.13 ppm	doublet	^3J = 6.3 Hz

Figure 4.20. ^{1}H NMR spectrum of 4.28a in d_3-acetonitrile.

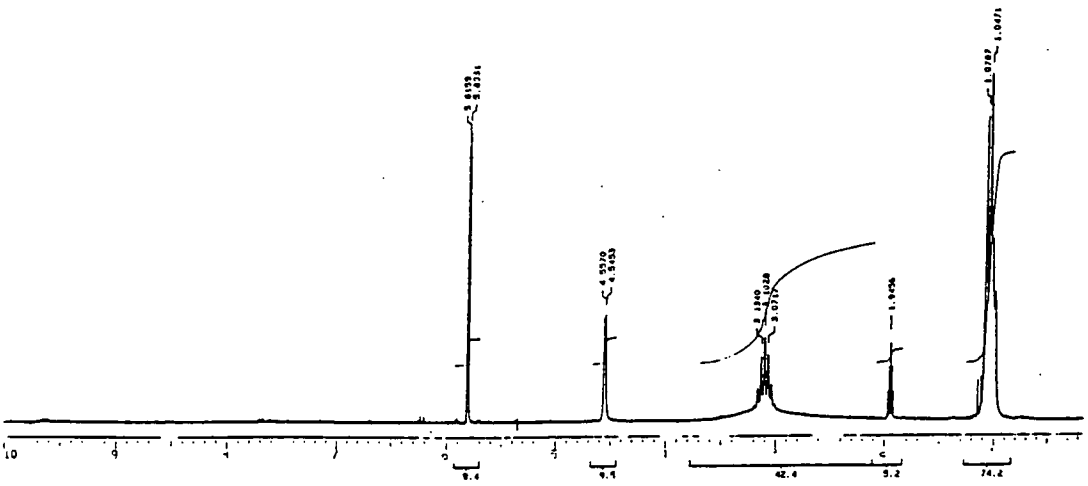

Figure 4.21. ^{1}H NMR spectrum showing 4.29a and 4.30a in d_3-acetonitrile.

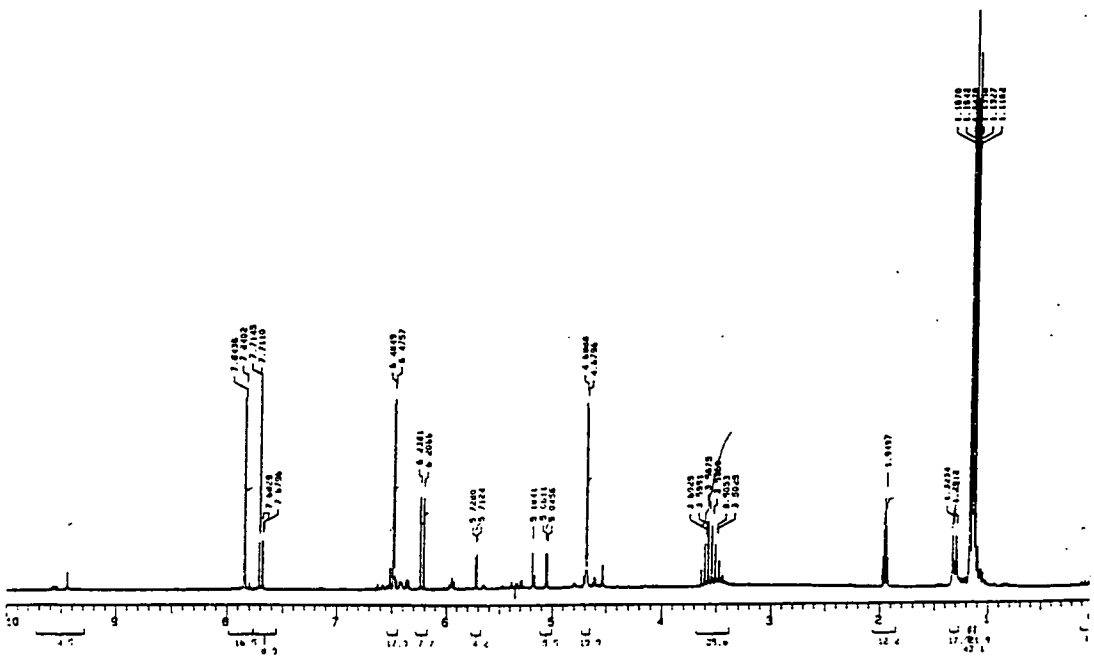

4.3.3.2 The Reaction Between 2,2-Dichloroethanal and t-Butylamine

This reaction instantly afforded the imine N-(tert-butyl)-2,2-dichloroethylidenamine, 4.29b, which was followed by the slow formation of N,N'-di(tert-butyl)-4,4,2,2-tetrachloro-3-aminobutylidenamine, 4.30b, after two days a ratio of 3:2 in favour of 4.30b had been produced. Their bands in the ^1H NMR spectrum gradually collapse in a similar fashion to those of 4.29a and 4.30a. The ^1H NMR peak assignments for 4.29b and 4.30b are given in table 4.13 and a spectrum showing bands for both compounds is given in figure 4.22.

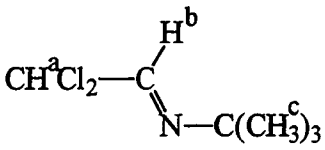

4.29b

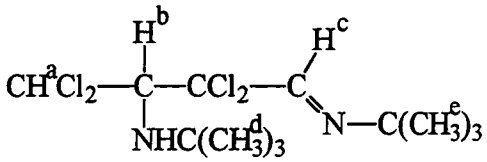

4.30b

Table 4.13. ^1H NMR peak assignments for 4.29b and 4.30b in d_3-acetonitrile.

Compound		δ value	Splitting pattern	Coupling constant
4.29b	H^a	6.21 ppm	doublet	^3J = 6.3 Hz
	H^b	7.61 ppm	doublet	^3J = 6.3 Hz
	H^c	1.13 ppm	singlet	
4.30b	H^a	6.47 ppm	doublet	^3J = 1.8 Hz
	H^b	4.71 ppm	doublet	^3J = 1.8 Hz
	H^c	7.75 ppm	singlet	
	H^d	1.19 ppm	singlet	
	H^e	1.21 ppm	singlet	

Figure 4.22. ^1H NMR spectrum showing 4.29b and 4.30b in d_3-acetonitrile.

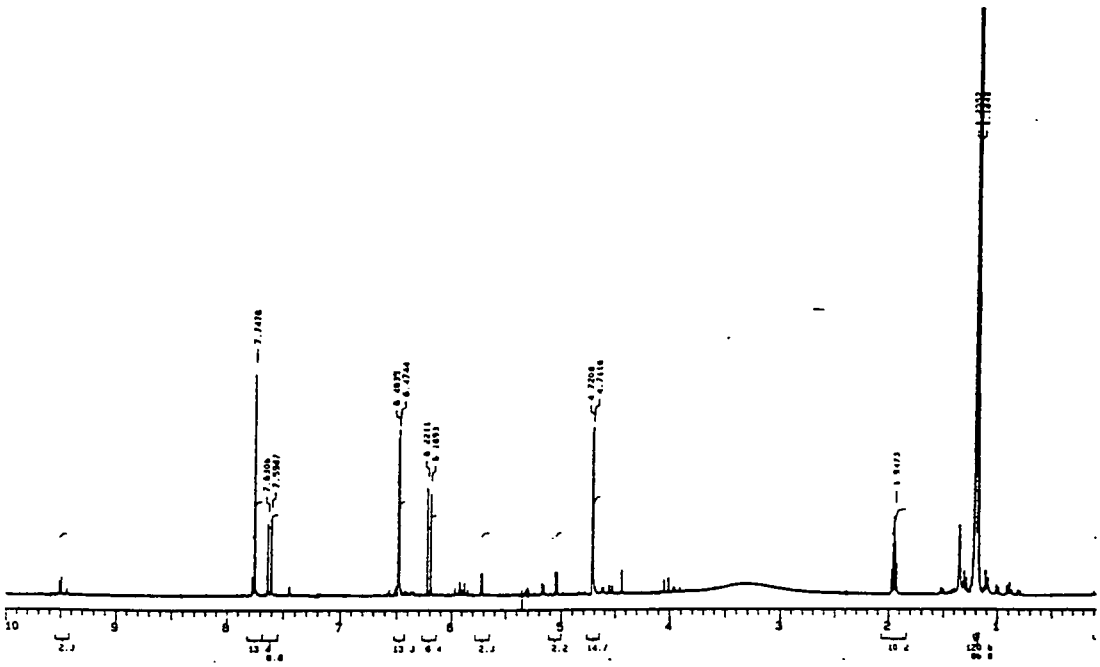

4.3.3.3 The Reaction Between 2,2-Dichloroethanal and Benzylamine

This reaction also gave the imine, N-benzyl-2,2-dichloroethylidenamine, 4.29c, followed by the slower formation of N,N'-dibenzyl-4,4,2,2-tetrachloro-3-aminobutylidenamine, 4.30c. A very small amount of N-benzyl-1-phenylmethylidenamine, 4.14, was also observed. There was evidence for yet another species forming, after a significant concentration of 4.30c had been produced, with bands in the ^1H NMR spectrum at 7.89 ppm (triplet, ^3J = 1.3 Hz) and 6.69 ppm (doublet, ^3J = 1.3 Hz). This compound has not been identified but could be that formed by loss of HCl across the carbons 2 and 3 of 4.30c. This structure would gain extra stabilization by having the alkene and imine in conjugation. Two weeks after the reaction had been initiated a ratio of 3:2:1 for 4.30c : 4.29c : uncharacterised compound had been produced. The ^1H NMR peak assignments for 4.29c and 4.30c are given in table 4.14 and a spectrum showing bands for both compounds is given in figure 4.23.

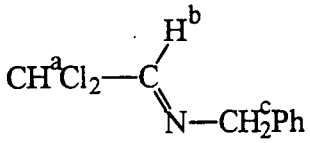

4.29c

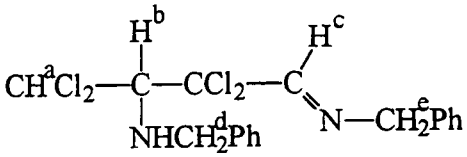

4.30c

Table 4.14. ^1H NMR peak assignments for 4.29c and 4.30c in d_3-acetonitrile.

Compound		δ value	Splitting pattern	Coupling constant
4.29c	H^a	6.30 ppm	doublet	^3J = 6.3 Hz
	H^b	7.82 ppm	doublet	^3J = 6.3 Hz
	H^c	4.66 ppm	singlet	
	Phenyl	7.1 - 7.5 ppm		
4.30c	H^a	6.47 ppm	doublet	^3J = 1.8 Hz
	H^b	4.69 ppm	doublet	^3J = 1.8 Hz
	H^c	7.95 ppm	triplet	^4J = 1.4 Hz
	H^d	4.66 ppm	broad singlet	
	H^e	4.70 ppm	broad singlet	
	Phenyl	7.1 - 7.5 ppm		

Figure 4.23. ^1H NMR spectrum showing 4.29c and 4.30c in d_3-acetonitrile.

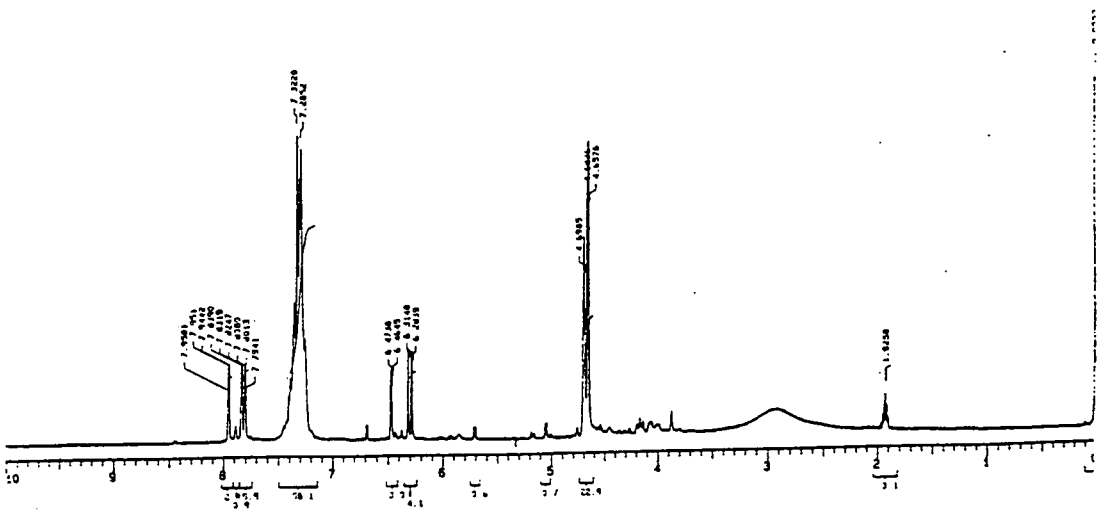

4.4 The Reactions of 2-Chloroethanal with Ammonia and Primary Amines

4.4.1 2-Chloroethanal, 4.31

In its pure form this aldehyde behaves similarly to 2,2-dichloroethanal, polymerising[11] on standing. The introduction of a halogen at the α-position of an aldehyde drastically increases the equilibrium constant for hydration, as seen previously for 2,2,2-trichloroethanal. For 2-chloroethanal the value[9,10] is 37 (cf. that for ethanal, 1.3) so in water 4.31 exists mainly in the hydrated form, in which it is stable to polymerisation. Table 4.15 contains the ^{1}H NMR peak assignments for both 2-chloroethanal and its hydrated form.

Table 4.15. ^{1}H NMR peak assignments for 4.31 and the hydrate in d_3-acetonitrile.

Compound		δ value	Splitting pattern	Coupling constant
4.31	$C\underline{H}_2Cl$	4.25 ppm	doublet	^3J = 1.0 Hz
	$C\underline{H}O$	9.54 ppm	triplet	^3J = 1.0 Hz
hydrate	$C\underline{H}_2Cl$	3.45 ppm	doublet	^3J = 4.7 Hz
	$C\underline{H}(OH)_2$	5.00 ppm	triplet	^3J = 4.7 Hz

4.4.2 The Reaction Between 2-Chloroethanal and Ammonia

This reaction does lead to the formation of the trimeric ring structure 2,4,6-tris(chloromethyl)-1,3,5-hexahydrotriazine, 4.34, via the reaction mechanism shown in scheme 4.8. However, 4.34 has only been synthesised in extremely low yields (ca. 1%). Hence when the reaction was followed by ^{1}H NMR techniques the product bands were only produced with very little intensity. The carbinolamine intermediate 2-chloro-1-aminoethanol, 4.32, was immediately formed upon mixing. The peaks due to this gradually decreased whilst those for 4.34 appeared. The imine 2-chloroethylidenamine, 4.33, was not observed. The ^{1}H NMR peak assignments for 4.32 and 4.34 are given in table 4.16 and the spectrum of 4.34 is shown in figure 4.24.

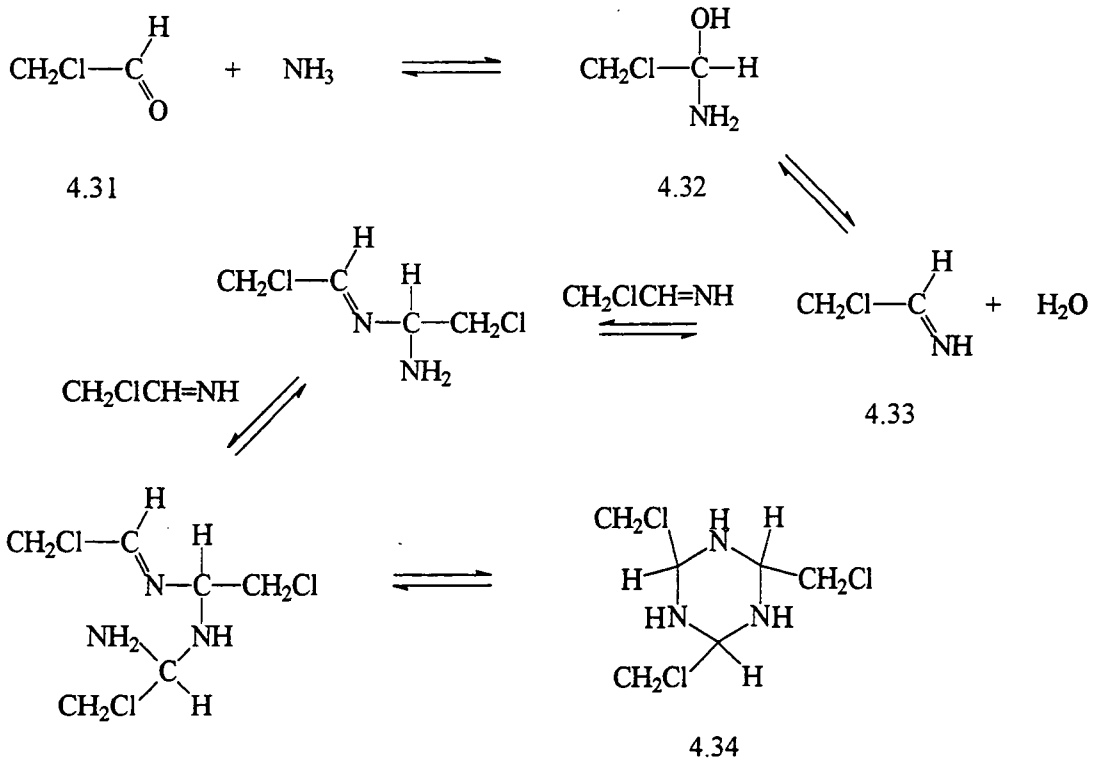

Scheme 4.8

Table 4.16. ^{1}H NMR peak assignments for 4.32 and 4.34 in d_3-acetonitrile.

Compound		δ value	Splitting pattern	Coupling constant
4.32	$C\underline{H}_2Cl$	3.56 ppm	v. broad	^{3}J = 4.4 Hz
	$C\underline{H}(OH)(NH_2)$	4.70 ppm	doublet	^{3}J = 4.4 Hz
			v. broad triplet	
4.34	$C\underline{H}_2Cl$	3.66 ppm	doublet	^{3}J = 4.0 Hz
	NC$\underline{H}$N	4.03 ppm	triplet	^{3}J = 4.0 Hz
	N$\underline{H}$	2.13 ppm	v. broad singlet	

4.4.2.1 Synthesis of 2,4,6-Tris(chloromethyl)-1,3,5-hexahydrotriazine, 4.34

This compound, 4.34, has been synthesised using a similar procedure as used for 4.5 in aqueous media. This involved slowly adding 64 ml of a 50 % wt. solution of 2-chloroethanal in water (0.5 mol) to 120 ml concentrated (16 mol dm^{-3}) aqueous ammonia (2 mol) whilst keeping the temperature below 5 °C with ice-bath cooling. The resultant clear solution was then stored at 0 °C for 5 days. Sodium chloride was added and the mixture stirred at room temperature for one hour, followed by extraction with four 100 ml portions of ether. The combined ether extracts were dried with magnesium sulphate, filtered and the solvent removed by rotary evaporator. The resulting liquid was pumped at 0.1 mbar for 1 hour affording a brown solid, 4.34 (1 % yield). A temperature of below 25 °C was maintained during work-up.

Figure 4.24. ^1H NMR spectrum of 4.34 in d_3-acetonitrile.

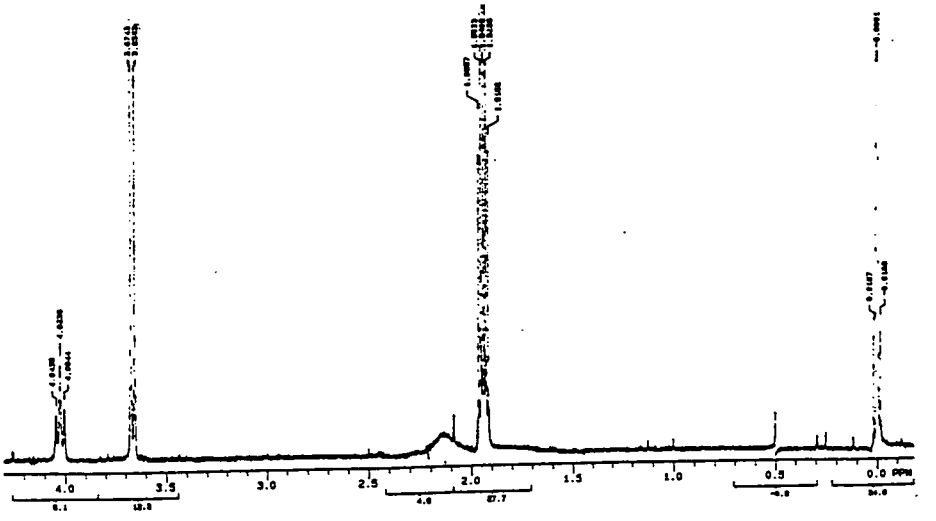

4.4.3 The Reaction Between 2-Chloroethanal and Primary Amines

2-Chloroethanal has been reacted with isopropylamine, tert-butylamine and benzylamine. The carbinolamine intermediates N-alkyl-2-chloro-1-aminoethanols, 4.35, were not observed being less stable than the imines, N-alkyl-2-chloroethylidenamines, 4.36, which formed instantaneously and quantitatively upon mixing.

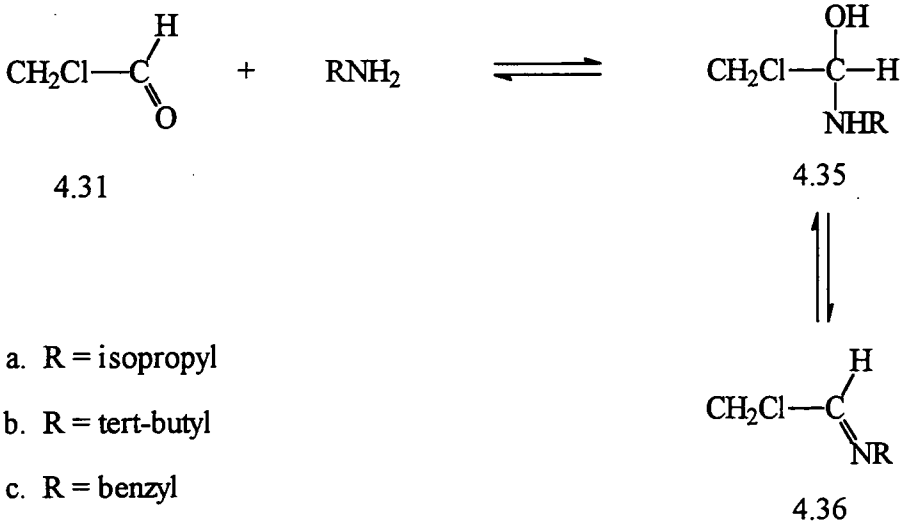

4.31

4.35

4.36

a. R = isopropyl

b. R = tert-butyl

c. R = benzyl

Scheme 4.9

The imines 4.36a-c all react further, however only 4.36a gave a "clean" reaction. This compound has two α-hydrogen atoms and reaction via the aldol-condensation type mechanism occurs as shown in scheme 4.10, yielding N-isopropyl-2,4-dichlorobut-2-ene-1-ylidenamine, 4.37a. This is completed in a four hour period as compared with the week long conversions of N-alkylpropylidenamines, 4.9, to N-alkyl-2-methylpent-2-ene-1-ylidenamines, 4.11. ^{1}H NMR peak assignments for 4.37a are given in table 4.17. The further reaction of 4.36b gave trace bands, contained in table 4.17, similar to those for 4.37a. However they cannot be assigned with complete confidence to the structure 4.37b.

The imine 4.36c showed no evidence for producing the structure 4.37c. Further reaction to N-benzylbenzylidenamine, 4.14, was observed. This was accompanied by a general collapse of all other ^1H NMR signals with the solutions turning a brown colour, as is the case for both the isopropylamine and t-butylamine reactions. This possibly indicates the instability of the imines with respect to polymerisation, similarly to the parent aldehyde.

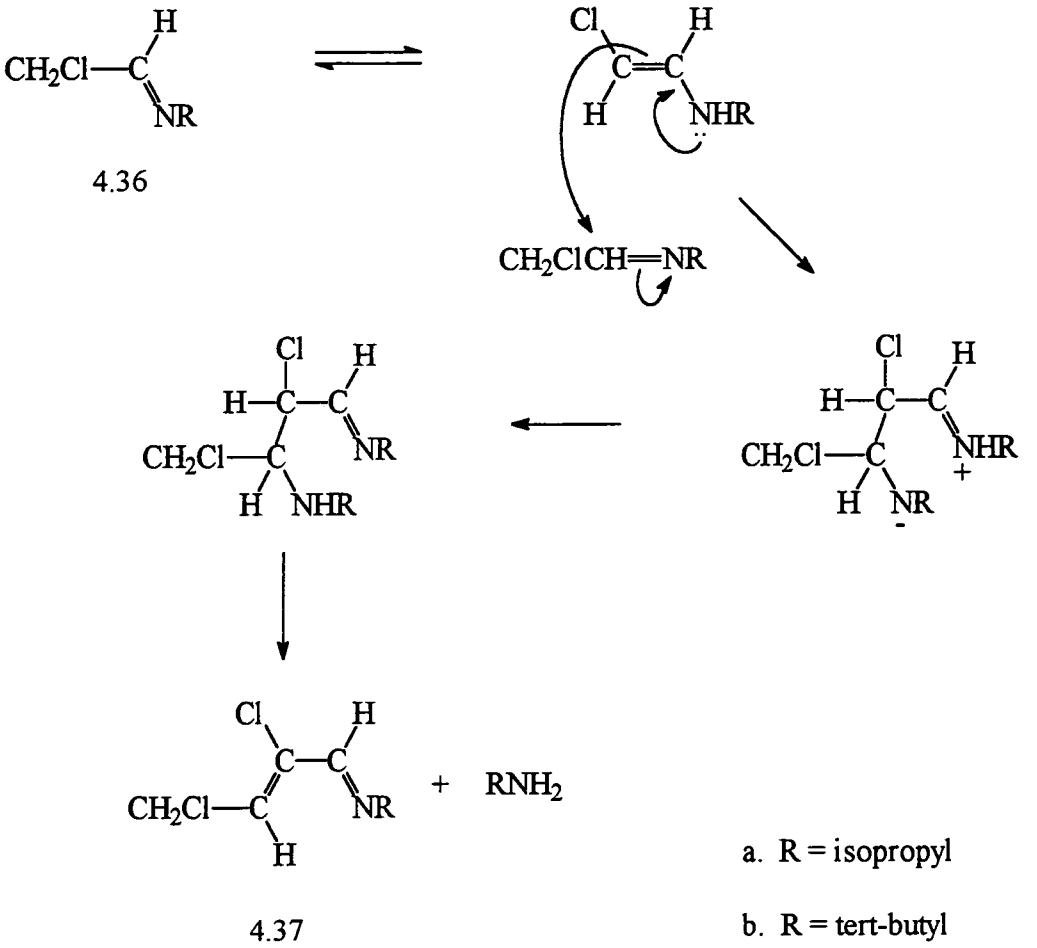

Scheme 4.10

Table 4.17. ^1H NMR peak assignments for 4.36a-c and 4.37a,b in d_3-acetonitrile.

Compound		δ value	Splitting pattern	Coupling constant
4.36a	$C\underline{H}_2Cl$	4.07 ppm	doublet	^3J = 4.9 Hz
	$C\underline{H}$=N	7.66 ppm	triplet of	^3J = 4.9 Hz
			doublets	^4J = 0.6 Hz
	N-$C\underline{H}$	3.41 ppm	septet of	^3J = 6.3 Hz
			doublets	^4J = 0.6 Hz
	$(C\underline{H}_3)_2$	1.11 ppm	doublet	^3J = 6.3 Hz
4.36b	$C\underline{H}_2Cl$	4.08 ppm	doublet	^3J = 4.8 Hz
	$C\underline{H}$=N	7.61 ppm	triplet	^3J = 4.8 Hz
	$(C\underline{H}_3)_3$	1.16 ppm	singlet	
4.36c	$C\underline{H}_2Cl$	4.15 ppm	doublet	^3J = 4.7 Hz
	$C\underline{H}$=N	7.80 ppm	triplet of	^3J = 4.7 Hz
			triplets	^4J = 1.3 Hz
	N-$C\underline{H}_2$	4.60 ppm	broad "singlet"	
	Phenyl	7.2-7.5 ppm		
4.37a	$C\underline{H}_2Cl$	4.43 ppm	doublet	^3J = 7.6 Hz
	$C\underline{H}$=C	6.52 ppm	triplet	^3J = 7.6 Hz
	$C\underline{H}$=N	7.98 ppm	singlet	
	N-$C\underline{H}$	3.44 ppm	septet	^3J = 6.5 Hz
	$(C\underline{H}_3)_2$	1.31 ppm	doublet	^3J = 6.5 Hz
4.37b	$C\underline{H}_2Cl$	4.44 ppm		
	$C\underline{H}$=C	6.55 ppm	*	*
	$C\underline{H}$=N	7.94 ppm		
	$(C\underline{H}_3)_3$	1.21 ppm		

*. Broad bands of low intensity; coupling constants could not be measured.

^1H NMR spectra for 4.36a-c and 4.37a are shown in figures 4.25 - 4.28

Figure 4.25. ^{1}H NMR spectrum of 4.36a in d_3-acetonitrile.

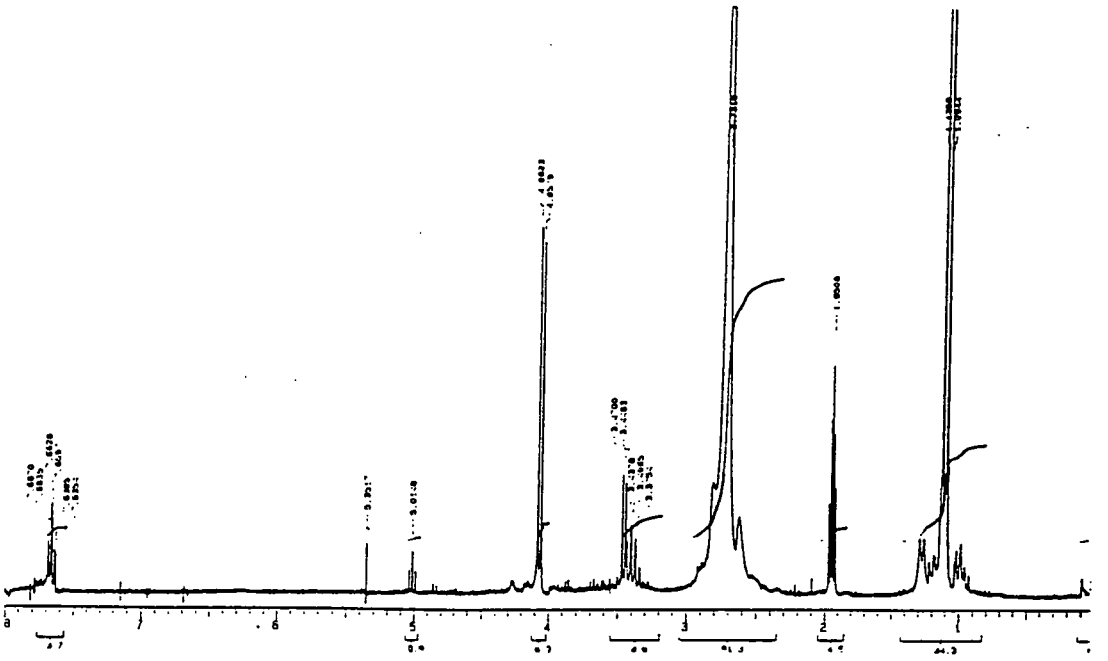

Figure 4.26. ^{1}H NMR spectrum of 4.37a in d_3-acetonitrile.

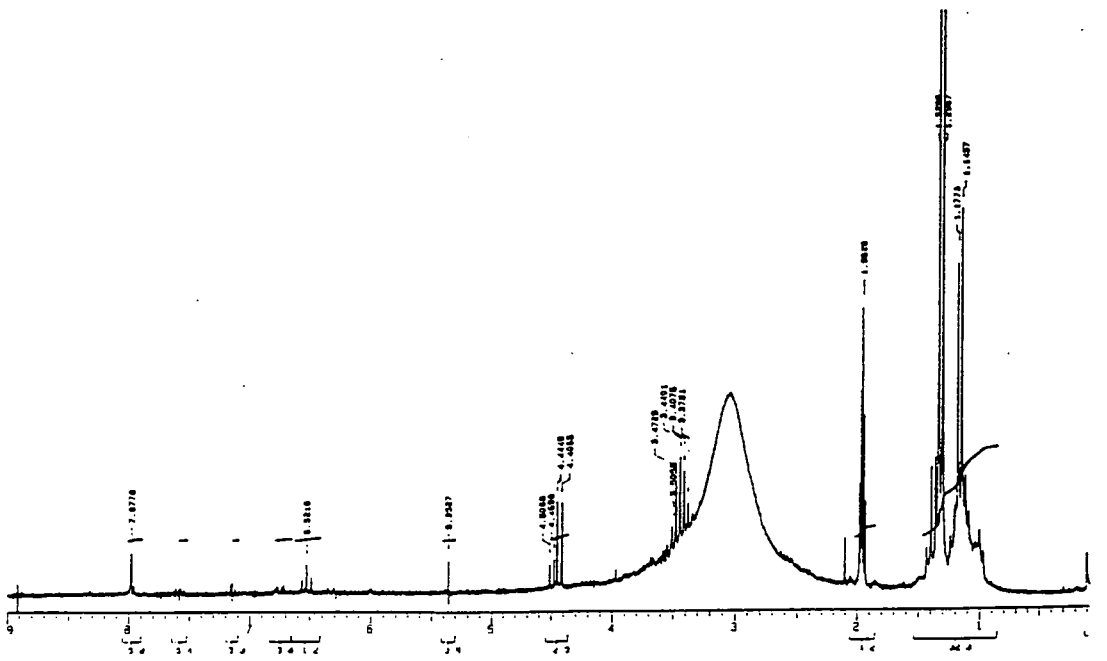

Figure 4.27. ^1H NMR spectrum of 4.36b in d_3-acetonitrile.

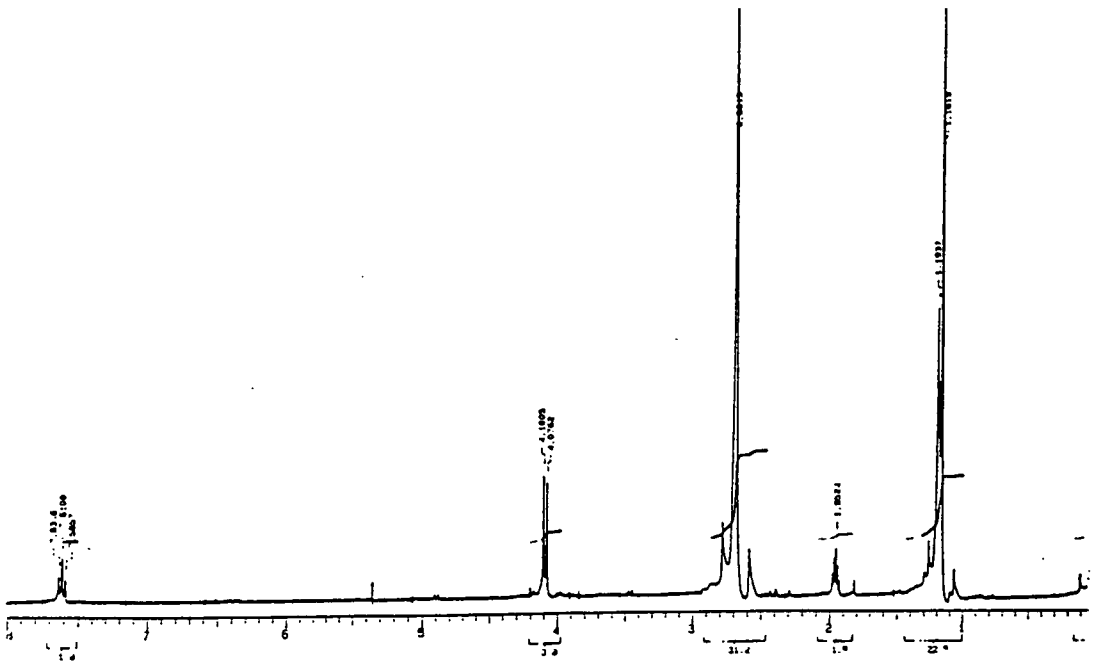

Figure 4.28. ^1H NMR spectrum of 4.36c in d_3-acetonitrile.

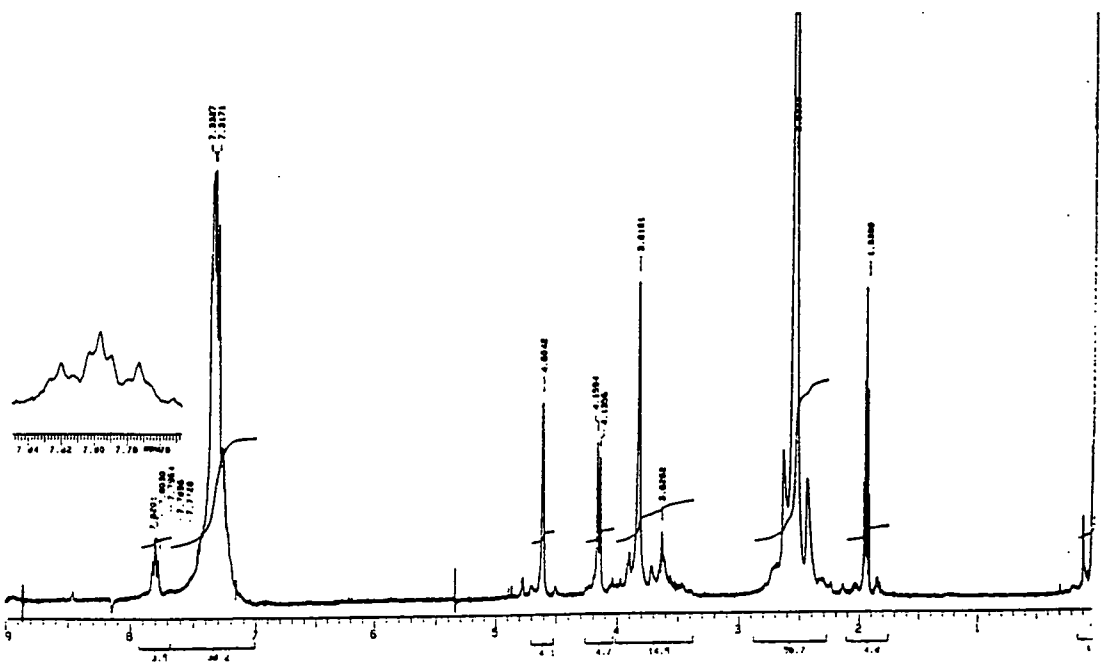

4.5 Summary of Results

4.5.1 Propanal and Ammonia

This reaction yields 2,4,6-triethyl-1,3,5-hexahydrotriazine. None of the intermediates on the reaction pathway form in observable concentrations.

4.5.2 Propanal and Primary Aliphatic Amines

These reactions initially give the imines N-alkylpropylidenamines. These then slowly react to N-alkyl-2-methylpent-2-ene-1-ylidenamines via a reaction mechanism similar to the aldol condensation.

A possible reason for the failure to dimerise and trimerise via C-N bond formation may be the lack of an NH hydrogen in the imines. The first step in the cyclisation is thought to involve N-C bond formation as shown in scheme 4.10.

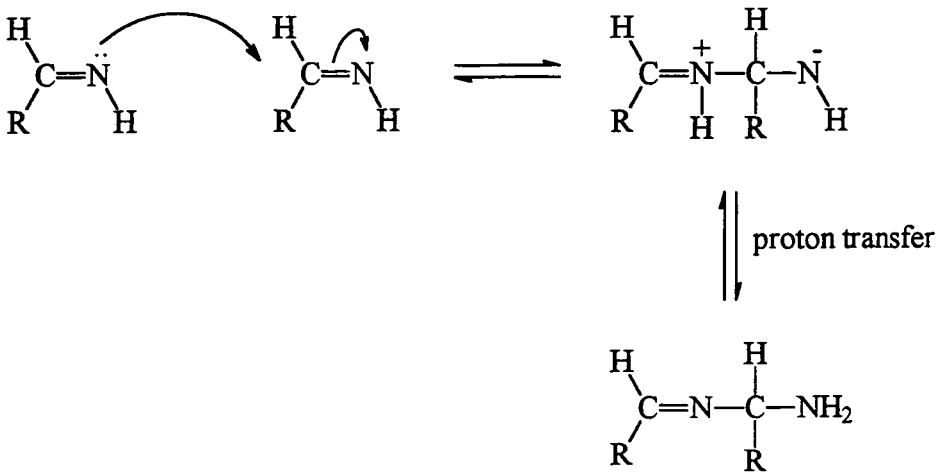

Scheme 4.10

With imines of the structure RHC=NR', formed from primary amines, conversion to a dimeric form by proton- transfer is not possible. Nevertheless it is known that imines, CH_2=NR, formed from formaldehyde,[14-18] may successfully trimerise. These do not possess an amino proton. Thus steric hindrance may be responsible for the failure to trimerise of the imines RCH=NR'.

The alternative pathway, shown in scheme 4.2, eventually yields the observed products by C-C bond formation.

4.5.3 Propanal and Aniline

This initially produces the imine, N-phenylpropylidenamine. This imine, a Schiff's base, does not react along a similar reaction pathway as for aliphatic amines, but in the presence of excess aniline forms N,N-diphenyl-1,1-diaminopropane.

4.5.4 Chloral and Primary Amines

This reaction leads to the formation of the carbinolamines, N-alkyl-2,2,2-trichloro-1-aminoethanols, which are favoured due to the strong electron-withdrawing effect of the trichloromethyl group. This is followed by slower formation of the imines by dehydration or the N-substitutedformamides by loss of chloroform. The former of the subsequent reactions is favoured in dry conditions and the latter with increased water content in the solvent.

4.5.5 2,2-Dichloroethanal and Ammonia

Here the dichloromethyl group promotes formation of the carbinolamine which gradually decomposes to unidentified products. One possible route is polymerisation of the imine.

4.5.6 2,2-Dichloroethanal and Primary Amines

The imines from this reaction are initially formed, being more stable than the carbinolamines. They slowly react further to N,N'-dialkyl-4,4,2,2-tetrachloro-3-aminobutylidenamines via a mechanism similar to the aldol reaction.

4.5.7 2-Chloroethanal and Ammonia

The carbinolamine 2-chloro-1-aminoethanal is formed immediately. This slowly converts to 2,4,6-tris(chloromethyl)-1,3,5-hexahydrotriazine though in very low yields. The intermediate imine is not formed in observable concentrations.
The relatively unsuccessful nature of the trimerisation may be due to the electron-withdrawing effect of the chloromethyl group, which deactivates the imine. Hence the nucleophilicity of the nitrogen is reduced. Also straight chain polymerisation probably competes favourably with the trimerisation route.

4.5.8 2-Chloroethanal and Primary Amines

The imines, N-alkyl-2-chloroethylidenamines, are formed initially and may dimerise by C-C bond formation similarly to the reactions between propanal and primary amines.

4.6 References

1. A. T. Nielsen, R. L. Atkins, A. T. Moore, R. Scott, D. Mallory and J. M. LaBerge, *J. Org. Chem.*, 1973, **38**, 3288.
2. A. T. Nielsen, R. L. Atkins, J. Dipol, and D. W. Moore, *J. Org. Chem.*, 1974, **39**, 1349.
3. E. M. Smolin and L. Rapoport, "The Chemistry of Heterocyclic Compounds; S - Triazines and Derivatives", A. Wiessberger, Ed., Interscience, New York, 1959, Volume 13, Chapter 9.
4. A. R. Katritzky, R. C. Patel and F. G. Ridell, *Angew. Chem. Int. Ed. Engl.*, 1981, **20**, 521.
5. Y. Ogata, and A. Kawasaki, *Tetrahedron*, 1964, **20**, 855, 1573.
6. R. L. Reeves, "The Chemistry of the Carbonyl Group", S. Patai, Ed., Wiley, London, 1966, Volume 1, p. 609.
7. A. Behal and Choay, *Ann. Phys. Chim.*, 1892, **26**, 1.
8. V. Z. El-Hewki and F. Runge, *J. Prakt. Chem.*, 1962, **304**, 297.
9. T. H. Lowry and K. S. Richardson, "Mechanism and Theory in Organic Chemistry", Harper and Row, New York, 3rd. Edition, 1987, p. 664.
10. R. P. Bell, *Adv. Phys. Chem.*, 1966, **4**, 1.
11. L. J. Bellamy and R. L. Williams, *J. Chem. Soc.*, 1958, 3465.
12. Friedrick, *Lieb. Ann. Chem.*, 1881, **206**, 251.
13. R. Millar, Defence Research Agency, Private Communication.
14. E. M. Smolin and L. Rapoport, "The Chemistry of Heterocyclic Compounds; S - Triazines and Derivatives", A. Wiessberger, Ed., Interscience, New York, 1959, Volume 13, Chapter 9.
15. A. G. Giumanini, G. Verardo, E. Zangrando and L. Lassiani, *J. Prakt. Chem.*, 1987, **329**, 1087.
16. B. Mauzé J. Pornet, M. -L. Martin and L. Miginiac, *C. R. Acad. Sci. Paris Ser. C,*, 1970, **270**, 562.
17. J. Graymore, *J. Chem. Soc.*, 1932, 1353.
18. A. G. Giumanini, G. Verardo, L. Randaccio, N. Bresciani-Pahor and P. Traldi, *J. Prakt. Chem.*, 1985, **327**, 739.

Chapter 5

Kinetic Studies of Formation and Decomposition of 2,4,6-Triethyl-1,3,5-Hexahydrotriazine

5.1 Kinetic and Equilibrium Studies

^1H NMR studies indicate that in acetonitrile-water mixtures which are rich in acetonitrile, propanal and ammonia react to give 2,4,6-triethyl-1,3,5-hexahydrotriazine (from now on shortened to TEHT), though there is no evidence for the build up of intermediates in detectable concentrations. A preparative experiment resulted in the formation of TEHT in high yield.

It was decided to make kinetic and equilibrium studies of the reaction between propanal and ammonia to give TEHT.

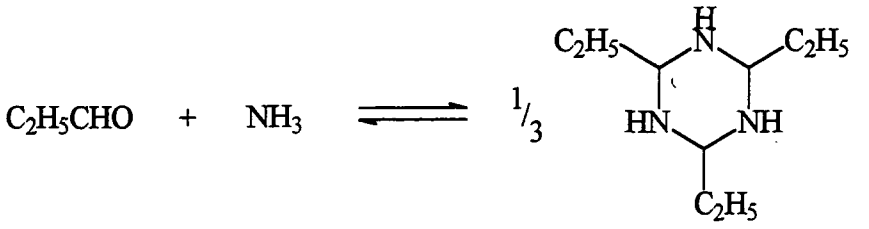

TEHT

Equation 5.1

It is known that in aqueous media propanal is partially hydrated, as shown in equation 5.2. In water the equilibrium constant, K_h , has the value 0.71.

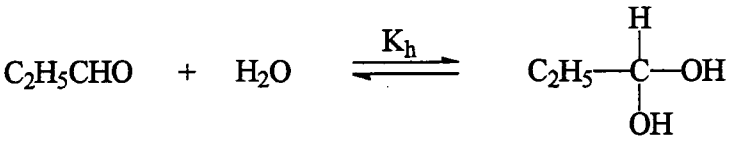

Equation 5.2

Propanal in acetonitrile was found to show an absorbance in the ultra-violet region with λ_{max} at 286 nm and ε = 17.5 $dm^3\ mol^{-1}\ cm^{-1}$. Data in table 5.1 show that with increasing water content the absorption maximum shifts slightly to shorter wavelength. In water the apparent extinction coefficient is reduced due to hydration.

Table 5.1. U.V. data for propanal.

Solvent	λ max /nm	ε max /$dm^3\ mol^{-1}\ cm^{-1}$
acetonitrile	286	17.5
50/50 (v/v) acetonitrile/water	282	15.5
water	279	8.43

In order to eliminate complications due to the presence of the hydrate, measurements were made in acetonitrile rich media where little hydrate should be formed. ^1H N.M.R. spectra confirm that in media containing up to 10 % water, no bands due to hydrate are observed.

In the absence of ammonia the U.V. spectrum indicates that propanal is indefinitely stable. The reaction with ammonia could be conveniently followed by using the reduction with time of absorbance at 286 nm. Initially measurements were made with the ammonia concentration in at least a ten fold excess of the propanal concentration.

Stock solutions of ammonia in acetonitrile/water and propanal in acetonitrile were prepared. The ammonia solution of appropriate concentration was transferred to a 1 cm cell and allowed to reach the temperature of the thermostatted cell compartment of a Perkin-Elmer Lambda 2 spectrophotometer. Reaction was started by the addition of a small volume (0.1 ml) of a stock solution of propanal in acetonitrile.

It was found that the absorbance at 286 nm decreased with time and the data were consistent with first order kinetics. A typical plot is shown in figure 5.1 and the data are collected in table 5.2. Comparison of runs AMALDTD5 and 9 shows that the rate constant is independent of propanal concentration. Plots of k_{obs} versus ammonia concentration at constant water content, figures 5.2 and 5.3, are linear with both positive slopes and intercepts. The positive slope indicates a direct dependence on the ammonia concentration. The positive intercept might indicate that the reactions are reversible equilibria, with the intercept representing the term depending on the reverse rate constant.

Figure 5.1. Plot showing decrease in concentration of propanal with time at 286nm.

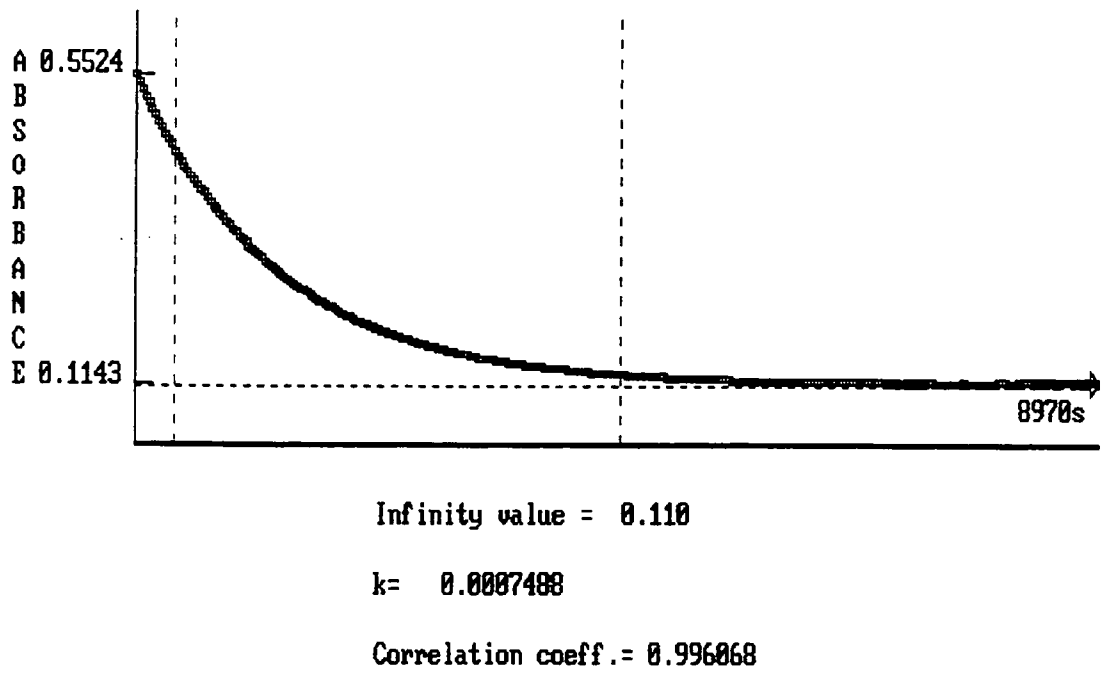

Table 5.2

Reference	$[Propanal]_{stoich}$ / mol dm^{-3}	$[NH_3]_{stoich}$ / mol dm^{-3}	Solvent %water (v/v)	$10^3 \times k_{obs}$ / s^{-1}	Initial abs.	Final abs.	$K_{overall}$
amaldtd1	0.038	0.91	3.4	1.21	0.70	0.093	50
amaldtd2	0.038	0.69	3.3	1.04	0.70	0.127	48
amaldtd3	0.038	0.46	3.1	0.95	0.70	0.188	48
amaldtd4	0.038	0.26	3.0	0.76	0.70	0.299	57
amaldtd5	0.038	0.91	3.4	1.14	0.70	0.078	60
amaldtd9	0.073	0.87	3.4	1.21	1.40	0.108	60
pramtd10	0.04	1.20	20	0.748	0.70	0.110	32
pramtd11	0.04	0.96	20	0.686	0.70	0.159	27
pramtd12	0.04	0.72	20	0.548	0.70	0.198	29
pramtd13	0.04	0.48	20	0.502	0.70	0.287	28

Figure 5.2. Plot of 10^3 k_{obs} vs. [NH_3] in the presence of 3% water.

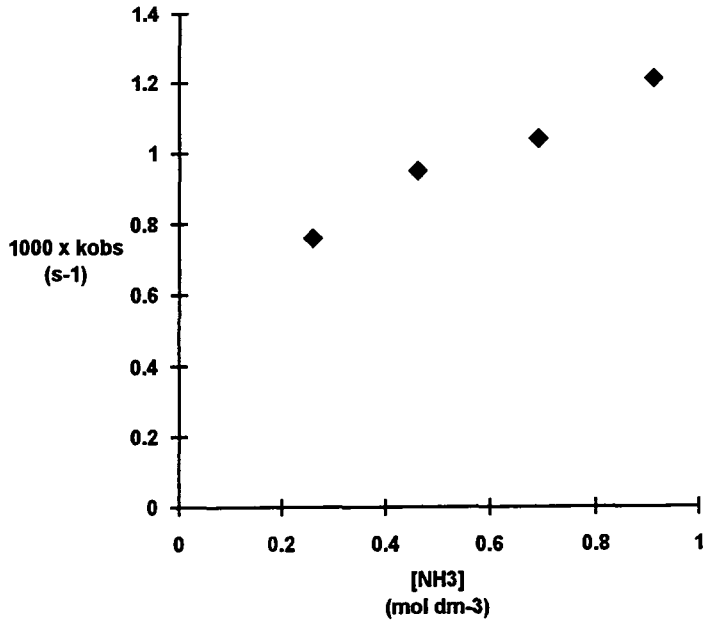

Figure 5.3. Plot of 10^3 k_{obs} vs. [NH_3] in the presence of 20% water.

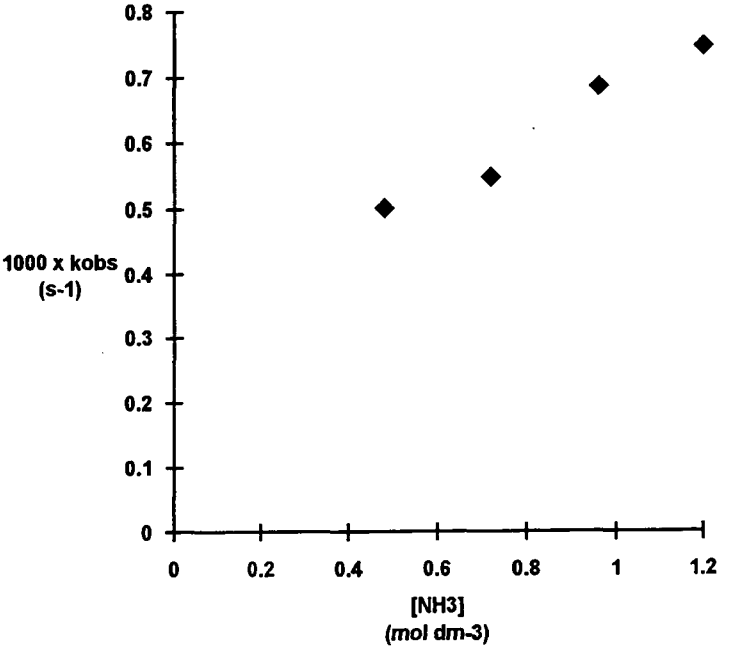

The inital and final absorbance values allow the calculation of an overall equilibrium constant, $K_{overall}$, for the conversion to TEHT. From equation 5.1 we define the equilibrium constant

$$K_{overall} = \frac{[TEHT]^{1/3}}{[C_2H_5CHO]_{free}[NH_3]_{free}} \qquad \text{equation 5.3}$$

It is possible to calculate values for the concentrations using equations 5.4, 5.5 and 5.6.

$$[C_2H_5CHO]_{free} = [C_2H_5CHO]_0 \times \frac{\text{final absorbance}}{\text{initial absorbance}} \qquad \text{equation 5.4}$$

$$[TEHT] = \frac{[C_2H_5CHO]_0 - [C_2H_5CHO]_{free}}{3} \qquad \text{equation 5.5}$$

$$[NH_3]_{free} = [NH_3]_0 - 3[TEHT] \qquad \text{equation 5.6}$$

The results in table 5.2 give values of 50 $\pm$ 5 with 3 % water and 30 $\pm$ 5 with 20 % water. These values are independent of the stoichiometric ammonia concentration or the stoichiometric propanal concentration, indicating the essential correctness of the equilibrium shown in equation 5.1.
Measurements described later, in the presence of added ammonium perchlorate, table 5.3, show that the presence of salt does not affect the equilibrium constant.

For an equilibrium of the type

$$A + B \underset{k_{-1}}{\overset{k_1}{\rightleftharpoons}} C$$

when $[B] >> [A]$, then by standard methods it can be shown that

$$k_{obs} = k_1[B] + k_{-1}$$

where $K_1 = \frac{k_1}{k_{-1}}$

The data in figure 5.2 indicate that this simple picture is not appropriate here. Thus with 3 % water the slope is 0.7 x 10^{-3} dm^3 mol^{-1} s^{-1} and the intercept has the value 0.6 x 10^{-3} s^{-1}. The ratio of these values (1.2 dm^3 mol^{-1}) is not consistent with the value of $K_{overall}$ calculated from absorbance values (50 dm^3 mol^{-1}).

In order to account for this it is necessary to consider the likely mechanism of triazine formation. This is shown below in scheme 5.1.

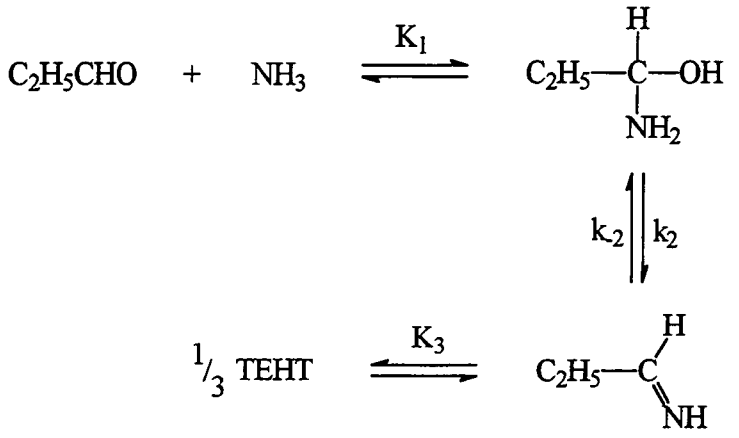

Scheme 5.1

The first and third steps are written as rapid equilibria with the second step (dehydration) being rate-determining. The justification for this is the observation that the rate constant for reaction to give TEHT is dramatically increased by the presence of ammonium perchlorate. This represents acid catalysis of the conversion. It is known from related systems[1,2] that dehydration of carbinolamine is catalysed by acid. Data obtained in the presence of ammonium perchlorate are given in table 5.3. The equilibrium conversion to TEHT was not affected but the rate constants were increased by about an order of magnitude. A typical first order plot is shown in figure 5.4. One problem encountered was the insolubility of ammonium salts in media rich in acetonitrile. It was found that ammonium perchlorate was more soluble than ammonium chloride, but even so the limits of solubility were 0.02 mol dm^{-3} at 20 % water and 0.04 mol dm^{-3} at 50 % water. For a series of runs measurements were made at constant buffer ratio, $[NH_3]$ / $[NH_4+]$ = constant, so as indicated by equation 5.7 the pH should remain constant.

Plots of k_{obs} versus ammonia concentration at constant water content are linear with small or zero intercepts, as shown in figures 5.5 and 5.6.

For the following equilibrium

$$NH_4^+ \underset{}{\overset{K_a}{\rightleftharpoons}} NH_3 + H^+$$

the acid dissociation constant, K_a, is given by

$$K_a = \frac{[NH_3][H^+]}{[NH_4^+]}$$

rearrangement gives

$$[H^+] = \frac{K_a[NH_4^+]}{[NH_3]}$$

Taking logarithms of both side yields

$$pH = pK_a + \log_{10}\left(\frac{[NH_3]}{[NH_4^+]}\right) \qquad \text{equation 5.7}$$

Figure 5.4. Plot showing decrease in concentration of propanal with time at 286 nm in the presence of NH_4ClO_4.

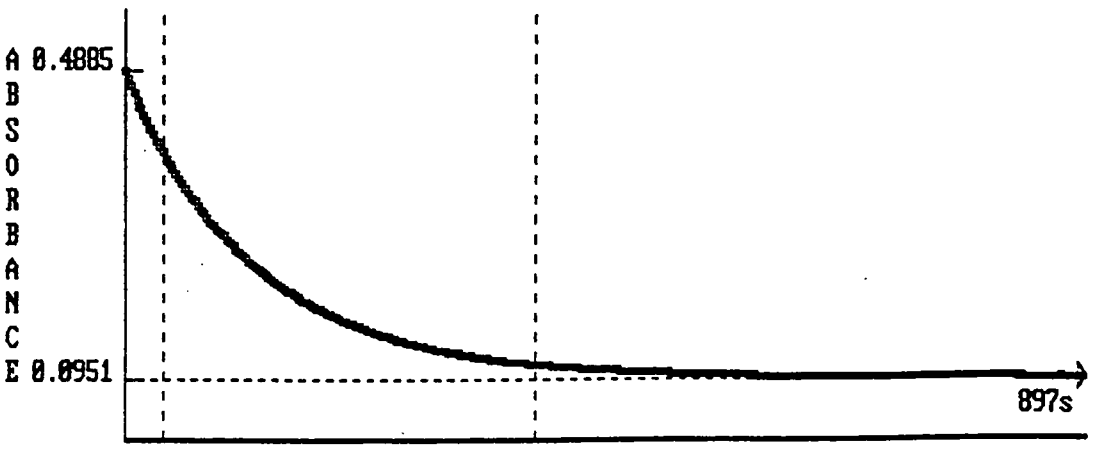

Infinity value = 0.095

k= 0.0079834

Correlation coeff.= 0.996630

Table 5.3

Reference	$[Propanal]_{stoich}$ / mol dm^{-3}	$[NH_3]_{stoich}$ / mol dm^{-3}	$[NH_4ClO_4]$ / mol dm^{-3}	Solvent %water (v/v)	$10^3 \times k_{obs}$ / s^{-1}	Initial abs.	Final abs.	$K_{overall}$
pramtd20	0.04	1.71	0.016	20	10.7	0.70	0.091	26
pramtd17	0.04	1.35	0.013	20	7.98	0.70	0.095	32
pramtd18	0.04	0.90	0.0084	20	4.71	0.70	0.144	31
pramtd21	0.04	0.45	0.0042	20	2.04	0.70	0.252	33
pramtd22	0.04	1.71	0.032	50	9.77	0.60	0.126	16
pramtd23	0.04	1.35	0.026	50	7.67	0.60	0.160	15
pramtd24	0.04	0.90	0.017	50	5.05	0.60	0.194	18
pramtd25	0.04	0.45	0.0085	50	2.70	0.60	0.275	25

Figure 5.5. Plot of 10^3 k_{obs} vs. [NH_3] with added NH_4ClO_4 and in the presence of 20% water.

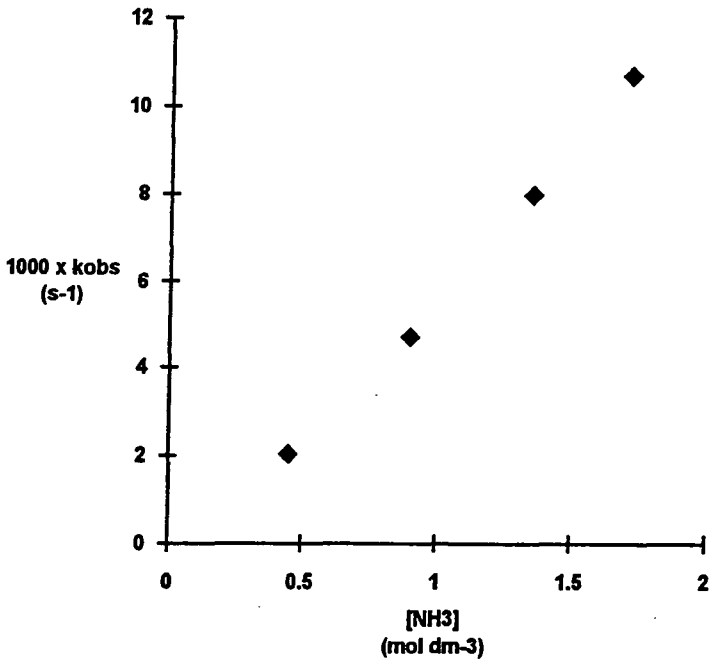

Figure 5.6. Plot of 10^3 k_{obs} vs. [NH_3] with added NH_4ClO_4 and in the presence of 50% water.

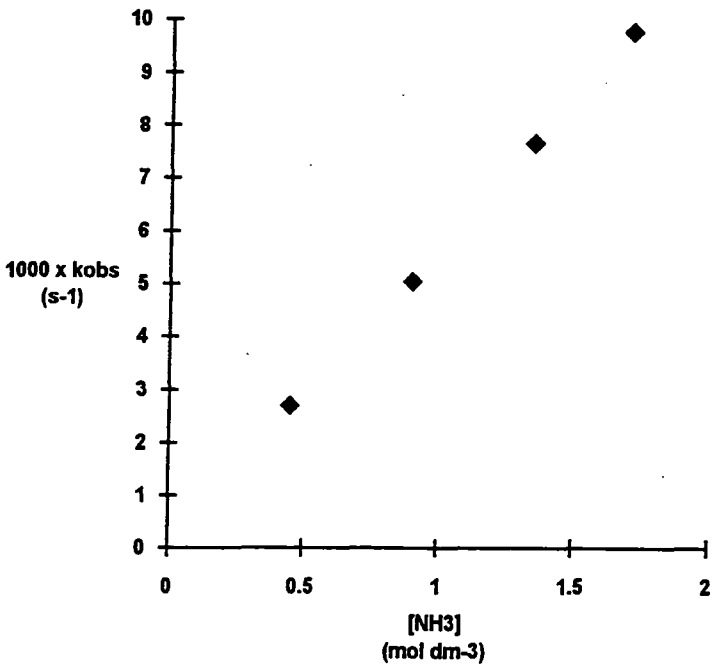

In order to test the reversibility of the reaction it was decided to make measurements of the forward and reverse reaction in solutions of the same solvent composition and keeping the buffer ratio approximately constant. Measurements were made in 20 % water by volume starting from propanal and ammonia and also starting from TEHT. When TEHT was used as the reactant it was found that an increase in absorbance at 286 nm occurred, consistent with formation of propanal. A typical plot is shown in figure 5.7. The data, shown in tables 5.4 and 5.5, indicate that within experimental error a constant value is obtained for the overall equilibrium constant, $K_{overall}$. This is good evidence for the overall equilibrium shown in Scheme 5.1.

Figure 5.7. Plot Showing Increase in Concentration of Propanal with Time at 286nm.

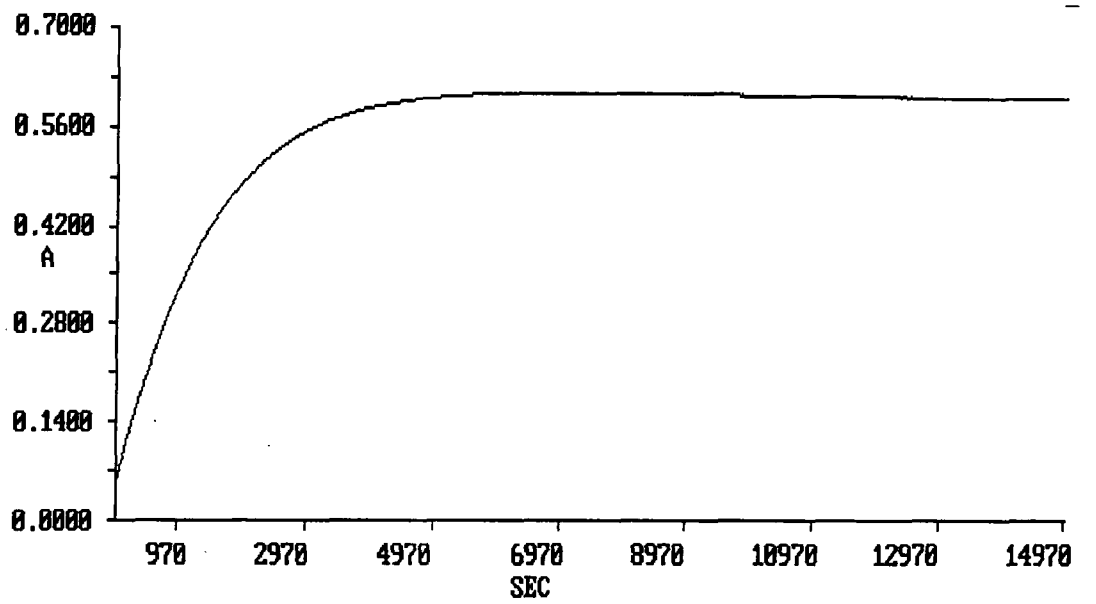

Table 5.4

Reference	$[Propanal]_{stoich}$ / mol dm^{-3}	$[NH_3]_{stoich}$ / mol dm^{-3}	$[NH_4ClO_4]$ / mol dm^{-3}	Initial abs.	Final abs.	$10^3 \times k_{obs}$ / s^{-1}	$K_{overall}$
pramtd31	0.0486	0.96	0.017	0.85	0.156	11.6	27
pramtd32	0.0486	0.72	0.013	0.85	0.197	7.6	28
pramtd33	0.0486	0.48	0.009	0.85	0.280	4.3	29

Table 5.5

Reference	$[TEHT]_{stoich}$ / mol dm^{-3}	$[NH_3]_{stoich}$ / mol dm^{-3}	$[NH_4ClO_4]$ / mol dm^{-3}	Final abs.	$K_{overall}$
tramtd01	0.046	0.0475	1×10^{-3}	1.359	30
tramtd02	0.046	0.095	2×10^{-3}	1.243	26
tramtd03	0.046	0.143	3×10^{-3}	0.971	31
tramtd05	0.0162	0.095	2×10^{-3}	0.618	33
tramtd00	0.046	0	0	1.471	40

5.2 Kinetics

Experimentally it is found that when the extent of conversion of the aldehyde to TEHT is high, then it is possible to get a good fit of the data to first order kinetics (correlation coefficient > 0.99). However when conversion to TEHT is relatively low (as judged by the absorbance at infinity) then the fit with first order kinetics becomes poor. This was noted for runs in 50 % water and also for runs done in pure water.

If the assumption is made that the mechanism of scheme 5.1 is correct, then quite complex kinetics might be expected. In cases such as this it is helpful to identify limiting conditions when simpler kinetic expressions will apply. Here two limitting conditions are :-

i) when the forward reaction is dominant (applies when there is high % conversion to products); and

ii) when the reverse reaction is dominant (applies if TEHT is largely decomposed to reactants).

There is no evidence from U.V. / visible spectroscopy or from N.M.R. spectroscopy for the build up in concentration of intermediates. The assumption is made that step 2 of scheme 5.1 is rate-determining. Then :-

Condition i) if ammonia is in large excess of propanal

$$k_{obs(forward)} = K_1 k_2 [NH_3] \qquad \text{equation 5.8}$$

This approximates to the conditions usually obtained. There seems to be a linear dependence on ammonia concentration. However, this does not explain the intercept in the plots obtained in the absence of ammonium perchlorate.

Condition ii) if the reverse reaction is dominant,

$$-\frac{d[TEHT]}{dt} = \frac{1}{3}\frac{d[propanal]}{dt} = \frac{k_{-2}[imine]}{3} \qquad \text{equation 5.9}$$

where imine = $C_2H_5CH{=}NH$

Now, $K_3 = \frac{[TEHT]^{1/3}}{[imine]}$ or rearranging $[imine] = \frac{[TEHT]^{1/3}}{K_3}$

Substituting this term for [imine] into equation 5.9 gives

$$-\frac{d[TEHT]}{dt} = \frac{k_{-2}[TEHT]^{1/3}}{3K_3}$$

By integration :-

$$-\int_{[TEHT]_0}^{[TEHT]_t} \frac{1}{[TEHT]^{1/3}} d[TEHT] = \int_0^t \frac{k_{-2}}{3K_3} dt$$

$$[TEHT]_t^{2/3} = [TEHT]_0^{2/3} - \frac{2k_{-2}t}{9K_3} \qquad \text{equation 5.10}$$

This indicates that if the reverse reaction is dominant then first order kinetics would not be expected, but a plot of $[TEHT]^{2/3}$ versus time should be linear.

Run TRAMTD05 comes closest to satisfying the condition that the reverse reaction is dominant. Here the TEHT concentration falls from 0.0162 M to 0.00402 M during the course of the reaction. The data did not give first order kinetics. A plot according to equation 5.10 of $[TEHT]^{2/3}$ versus time is shown in figure 5.8. It is not linear as was expected. If TEHT was completely converted to propanal (and ammonia) then we would expect a final absorbance of 0.802. However the infinity value of run TRAMTD05 was 0.609. This is because of reversibility of the reaction. The initial slope of the graph, when the concentration of propanal is low and thus conversion back to TEHT is very small, may give rise to the best value of k_{-2} / K_3.

Figure 5.8. Plot of $[TEHT]^{2/3}$ vs. time for run TRAMTD05.

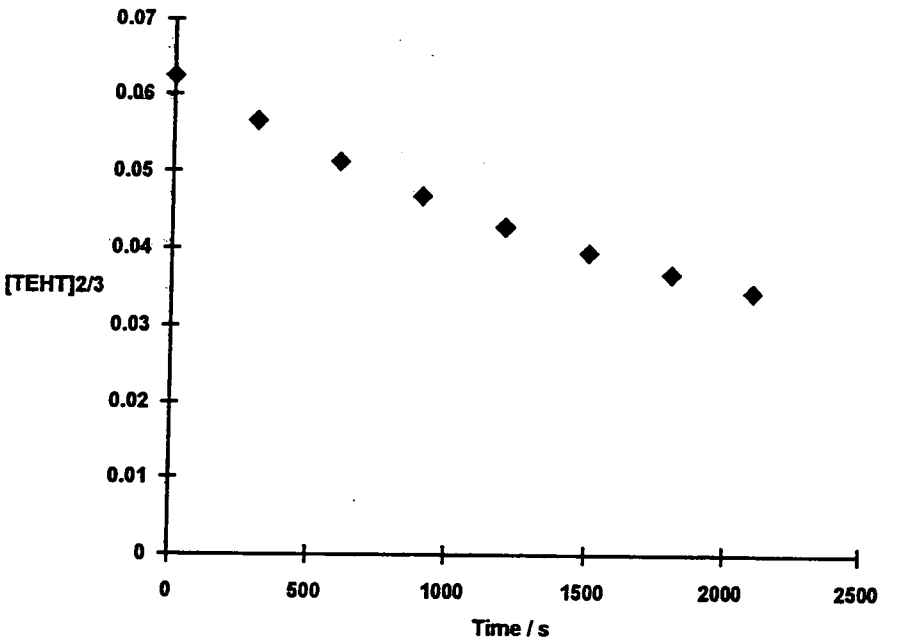

A major problem is to perform the reactions in the forward and reverse directions under similar conditions, so that the rate constants can be used to calculate a value of $K_{overall}$ using equation 5.11.

$$K_{overall} = K_1K_2K_3 = \frac{K_1k_2}{k_{-2}/K_3} = \frac{k_{forward}}{k_{reverse}} \qquad \text{equation 5.11}$$

The runs in table 5.5 were all started at the same buffer ratio $\frac{[NH_3]}{[NH_4^+]} = 47.5$

However, in order to obtain the reverse reaction, the initial concentration of added ammonia had to be very low so that the concentration of ammonium salt was extremely low, and thus subject to uncertainty. Also in the experiments on the reverse reaction the ammonia produced during the decomposition will affect the overall concentration of ammonia present.

5.3 Triethylamine / Triethylammonium Perchlorate Buffered Experiments

A problem obtaining a rate constant for the reverse reaction is that in ammonia / ammonium perchlorate buffers, it is difficult to work with ammonia concentrations which are low enough to eliminate the forward reaction. A solution to this was sought using triethylamine / triethylammonium perchlorate buffers. In these no ammonia was initially present hence the reverse reaction could be isolated. However it was also necessary to measure the rate constants in the forward direction. This, of course, requires the presence of ammonia. It is known[3] that in acetonitrile the pK_a values of triethylamine and ammonia are 18.46 and 16.46 respectively. It is expected that these values will be considerably lower in the presence of added water. Nevertheless since triethylamine is far more basic the ammonia concentration will not be effectively depleted by the equilibrium shown in equation 5.12, which will be essentially in favour of the reactants.

$$NH_3 + NHEt_3^+ \rightleftharpoons NEt_3 + NH_4^+$$

Equation 5.12

Two series of measurements were made, both in 80 / 20 (v / v) acetonitrile / water solvent composition. In the first series the forward reaction was observed using propanal, 0.049 mol dm^{-3}, with a large excess of ammonia. In the second the reverse reaction was measured using TEHT, either 0.02132 or 0.01066 mol dm^{-3}, but with no added ammonia. Two sets of buffer solutions were used; $NHEt_3^+ClO_4^-$ 0.5 mol dm^{-3} with NEt_3 either 0.5 or 0.25 mol dm^{-3}.

5.3.1 Forward Reaction

All measurements were made as a fading reaction at 286 nm following the decrease in propanal concentration. A sufficient excess of ammonia was used to ensure that the kinetics approximated to first order conditions. Data are collected in table 5.6 and a typical first order plot is shown in figure 5.9.

Table 5.6. Rate data for the reaction of propanal, 0.049 mol dm^{-3}, with ammonia in 80 / 20 (v / v) acetonitrile / water with triethylamine / triethylammonium buffers.

Reference	$[NH_3]$ / mol dm^{-3}	Buffer	pH	$k_{obs(f)}$ / s^{-1}	$k_{obs(f)}$ / $[NH_3]$ / dm^3 mol^{-1} s^{-1}	Abs_∞
newtd03	1.0	a	10.9	0.046	0.046	0.105
newtd04	0.8	a	10.8	0.035	0.044	0.154
newtd05	0.6	a	10.7	0.034	0.056	0.177
newtd06	0.4	a	10.6	0.018	0.045	0.257
newtd08	1.0	b	10.4	0.099	0.099	0.132
newtd09	0.8	b	10.5	0.048	0.060	0.155
newtd11	0.6	b	10.4	0.031	0.052	0.189
newtd12	0.4	b	10.4	0.025	0.063	0.246

a. Buffer is 0.5 mol dm^{-3} NEt_3 with 0.5 mol dm^{-3} $NHEt_3{}^+ClO4^-$.

b. Buffer is 0.25 mol dm^{-3} NEt_3 with 0.5 mol dm^{-3} $NHEt_3{}^+ClO4^-$.

Figure 5.9. Plot showing decrease in concentration of propanal with time at 286 nm in the presence of NEt_3 / $NHEt_3{}^+ClO_4^-$.

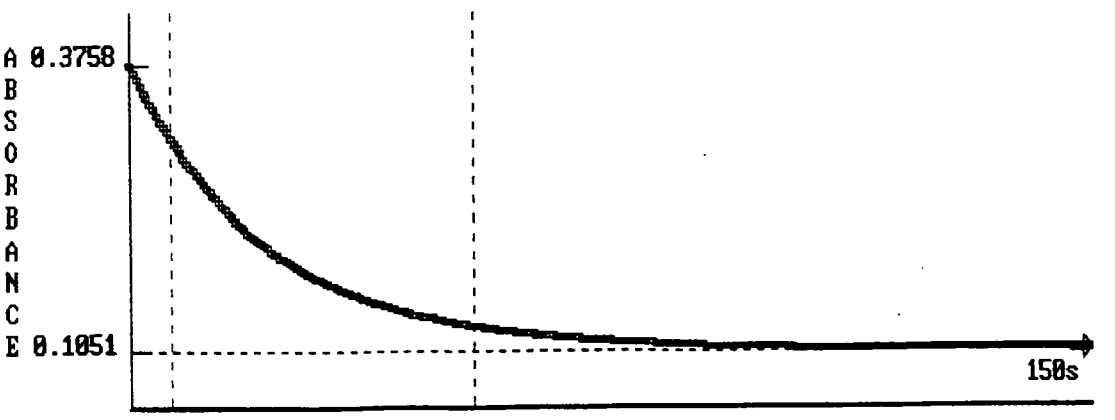

Infinity value = 0.105

k= 0.0463248

Correlation coeff.= 0.990814

Values of $k_{obs(f)}$ / $[NH_3]$ yield values for the product K_1k_2. In buffer a the values are fairly consistent giving 0.045 dm^3 mol^{-1} s^{-1}. In the more acidic buffer b values are higher, indicating the acid catalysis of the reaction, but are rather less consistent. A value of 0.060 dm^3 mol^{-1} s^{-1} has been obtained.

5.3.2 Reverse Reaction

Measurements were made with TEHT concentrations of either 0.02132 mol dm^{-3} or 0.01066 mol dm^{-3} in each of the buffers used to measure the forward reaction. No ammonia was added initially. An example of an absorbance versus time plot showing the increase in propanal concentration is given in figure 5.10. Attempts to fit a first order rate equation to each run were, as expected, unsuccessful.

Figure 5.10. Plot showing formation of propanal.

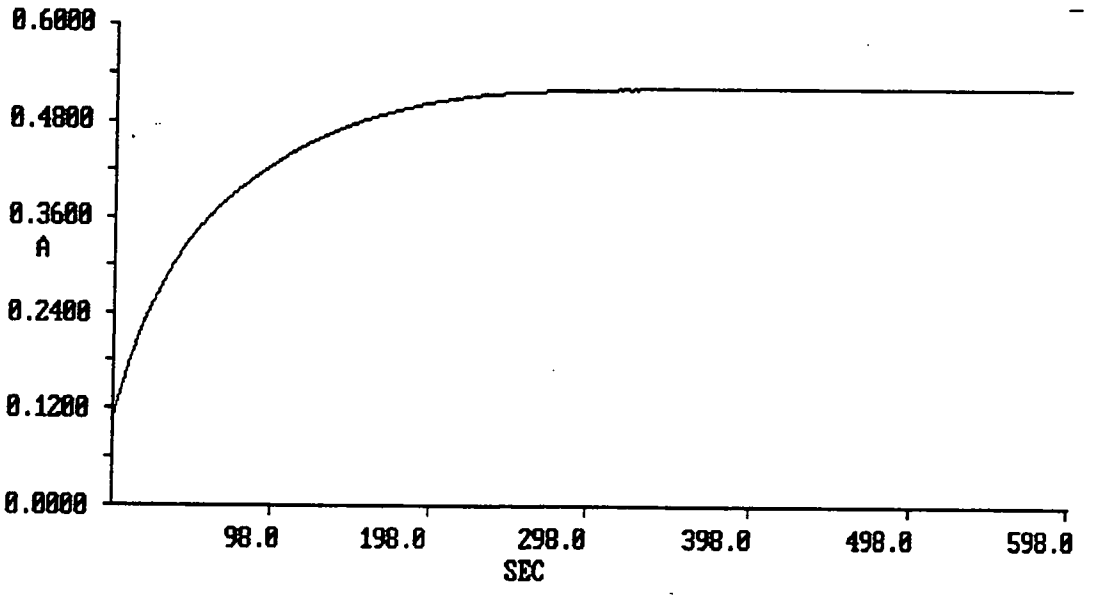

For each kinetic run values of absorbance were taken at fifteen second time intervals and the results used to calculate the absolute concentrations of TEHT remaining. This then allowed graphs of $[TEHT]^{2/3}$ versus time to be plotted so that values for k_{-2} / K_3 could be obtained from the gradient. The results are given in table 5.8. A specimen calculation is shown below.

Run TEHTTD01

$[TEHT]_0 = 0.02032$ mol dm^{-3}.

$\varepsilon_{(TEHT)} = 1.78$ dm^3 mol^{-1} cm^{-1}.

$\varepsilon_{(propanal)} = 16.0$ in buffer a (= 16.9 in buffer b).

$$\begin{aligned} Abs(286nm) &= 1.78[TEHT] + 16.0[propanal] \\ &= 1.78[TEHT] + 16.0x3([TEHT]_0 - [TEHT]) \\ &= 1.78[TEHT] + 1.0809 - 48.0[TEHT] \end{aligned}$$

$$\text{Hence } [TEHT] = \frac{1.0809 - Abs(286nm)}{46.22}$$

Table 5.7. Values of $[TEHT]^{2/3}$ at fifteen second time intervals for run TEHTTD01.

Time / s	Absorbance (286 nm)	10^2 x [TEHT] / mol dm^{-3}	$[TEHT]^{2/3}$ / mol$^{2/3}$ dm^{-2}
0	0.1858	1.8122	0.0690
15	0.3311	1.4978	0.0608
30	0.4264	1.2916	0.0551
45	0.4921	1.1495	0.0509
60	0.5433	1.0387	0.0476
75	0.5873	0.9435	0.0447
90	0.6275	0.8566	0.0419
105	0.6643	0.7769	0.0392
120	0.6986	0.7027	0.0367

Figure 5.11. Plot of $[TEHT]^{2/3}$ vs. time for run TEHTTD01.

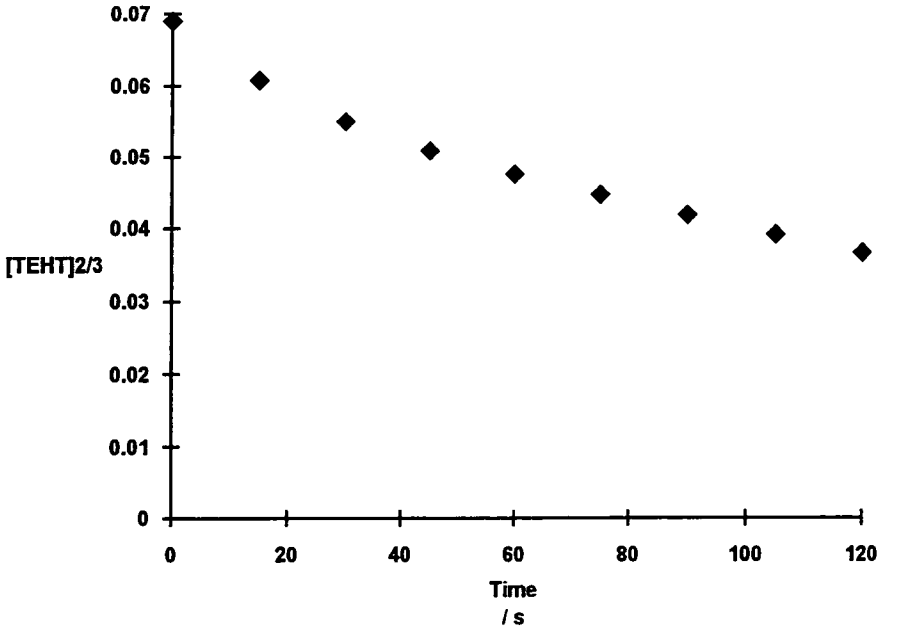

The plot in figure 5.11 shows some curvature but allowed a value for the initial slope, when the reverse reaction is dominant, to be obtained. This value, equal to $-2k_{-2} / 9K_3$ (from equation 5.10), allowed a value for k_{-2} / K_3 1.5 x 10^{-3} $mol^{2/3}$ dm^{-2} s^{-1} to be calculated.

Table 5.8. Rate data for the decomposition of TEHT in 80 / 20 (v / v) acetonitrile / water with triethylamine / triethylammonium buffers.

Reference	$[TEHT]_0$ / mol dm^{-3}	Buffer	k_{-2} / K_3 / $mol^{2/3}$ dm^{-2} s^{-1}
TEHTTD01	0.02132	a	1.50 x 10^{-3}
TEHTTD02	0.02132	b	1.79 x 10^{-3}
TEHTTD03	0.01066	a	1.92 x 10^{-3}
TEHTTD04	0.01066	b	1.71 x 10^{-3}

a. Buffer is 0.5 mol dm^{-3} NEt_3 with 0.5 mol dm^{-3} $NHEt_3{}^+ClO4^-$.

b. Buffer is 0.25 mol dm^{-3} NEt_3 with 0.5 mol dm^{-3} $NHEt_3{}^+ClO4^-$.

Combination via equation 5.11 of the values of k_{-2} / K_3 from table 5.8 with the values of K_1k_2, 0.045 dm^3 mol^{-1} s^{-1} in buffer a and 0.06 dm^3 mol^{-1} s^{-1} in buffer b, obtained from the forward reaction yields values of $K_{overall}$. These are shown in table 5.9.

Table 5.9. Values of $K_{overall}$ calculated from the forward and reverse rate constants for the reaction between propanal and ammonia to yield TEHT in 80 / 20 (v / v) acetonitrile / water with triethylamine / triethylammonium buffers.

Reference	$K_{overall} = \frac{K_1k_2}{k_{-2}/K_3}$ / $mol^{-5/3}$ dm^5
TEHTTD01	30.0
TEHTTD02	33.5
TEHTTD03	23.4
TEHTTD04	35.1

There is admittedly some spread in values of $K_{overall}$ but they yield an average value of 30.5 $mol^{-5/3}$ dm^5. This is in excellent agreement with the values obtained from absorbance measurements in the presence of ammonia / ammonium perchlorate buffers and with no buffers present.

5.4 Summary of Results

The rate data conform to the formation of TEHT being acid catalysed and confirm the essential correctness of the mechanism in scheme 5.1. In this the addition step forming 1-aminopropanol and the trimerisation of the propylidine imine to TEHT are effectively rapid equilibria, with the dehydration step being rate-limiting and subject to acid catalysis. This was shown by the increased rate constant for the reaction in the presence of ammonium perchlorate. It was also noticed in the experiments performed in the two triethylamine / triethylammonium perchlorate buffer systems with the more acidic buffer producing the larger rate constants

The equilibrium measurements show that the equilibrium constant for formation of TEHT, $K_{overall}$, decreases with increasing water content of the solvent. The values obtained were 50 $\pm$ 5 $mol^{-5/3}$ dm^5 with 3 % water, 30 $\pm$ 5 $mol^{-5/3}$ dm^5 with 20 % water and 20 $\pm$ 5 $mol^{-5/3}$ dm^5 with 50 % water. This might be attributed to stabilisation of ammonia relative to acetonitrile.
Calculation of the equilibrium constant from rate data correlated well with the values determined directly giving a value of 30 $\pm$ 6 $mol^{-5/3}$ dm^5.

5.5 References

1. T. H. Lowry and K. S. Richardson, "Mechanism and Theory in Organic Chemisty", Harper and Row, New York, 3rd. Edition, 1987, p. 703.
2. W. P. Jencks, *J. Am. Chem. Soc.*, 1969, **81**, 475.
3. J. F. Coetzee, *Progr. Phys. Org. Chem.*, 1967, **4**, 45.

Chapter 6

Protonation Studies of Dinitropentamethylenetetramine, DPT

6.1 Introduction

Acetylation, nitrosation and nitration of hexamine, 6.1, may lead to the formation of the bicyclononanes 6.2, 6.3 and 6.4 respectively depending on the reaction conditions.

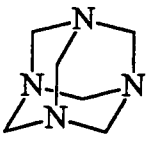

6.1

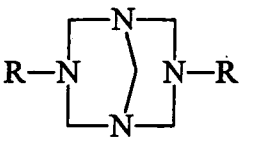

6.2 R = $COCH_3$
6.3 R = NO
6.4 R = NO_2

6.1.1 Formation of Bicyclononanes from Hexamine

The reaction between hexamine and acetic anhydride leads to the formation of either 3,7-diacetyl-1,3,5,7-tetraazabicyclo[3.3.1]nonane, diacetylpentamethylenetetramine DAPT, 6.2, or 1,3,5-triacetyl-1,3,5-hexahydrotriazine (TRAT), 6.5. The production[1] of TRAT is favoured by high temperatures and anhydrous conditions, whereas DAPT is favoured by lower temperatures and the presence of water. This is shown in scheme 6.1.

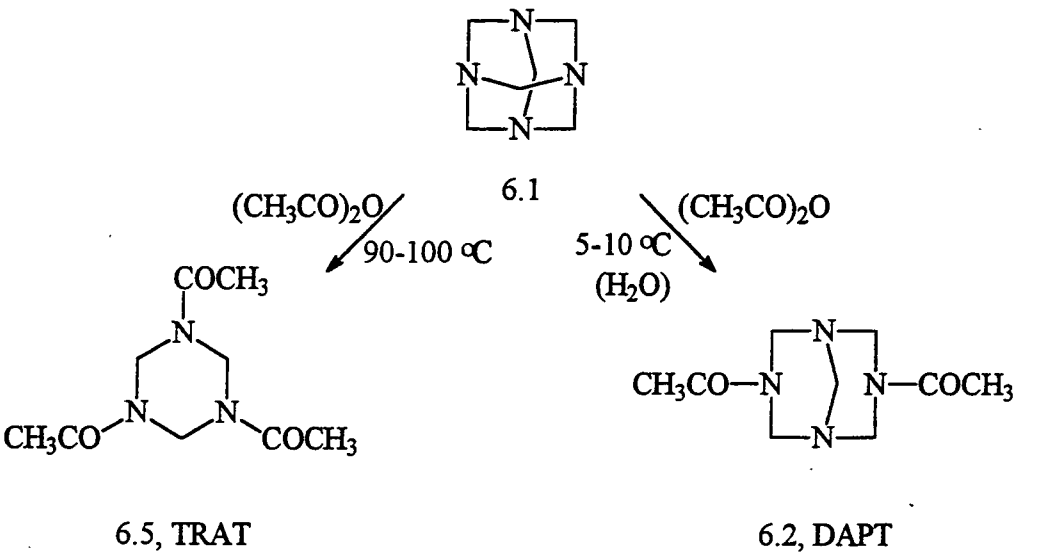

6.5, TRAT

6.2, DAPT

Scheme 6.1

The reaction between hexamine and a mixture of hydrochloric acid and sodium nitrite, leads to the formation of 3,7-dinitroso-1,3,5,7-tetraazabicyclo[3.3.1]nonane (dinitrosopentamethylenetetramine, DNPT), 6.3, or 1,3,5-trinitroso-1,3,5-hexahydrotriazine, 6.6. In highly acidic media, pH 1, only 6.6 is formed, at pH 2 a mixture of 6.3 and DNPT is produced, and between pH 3-6 just DNPT is obtained.[2]

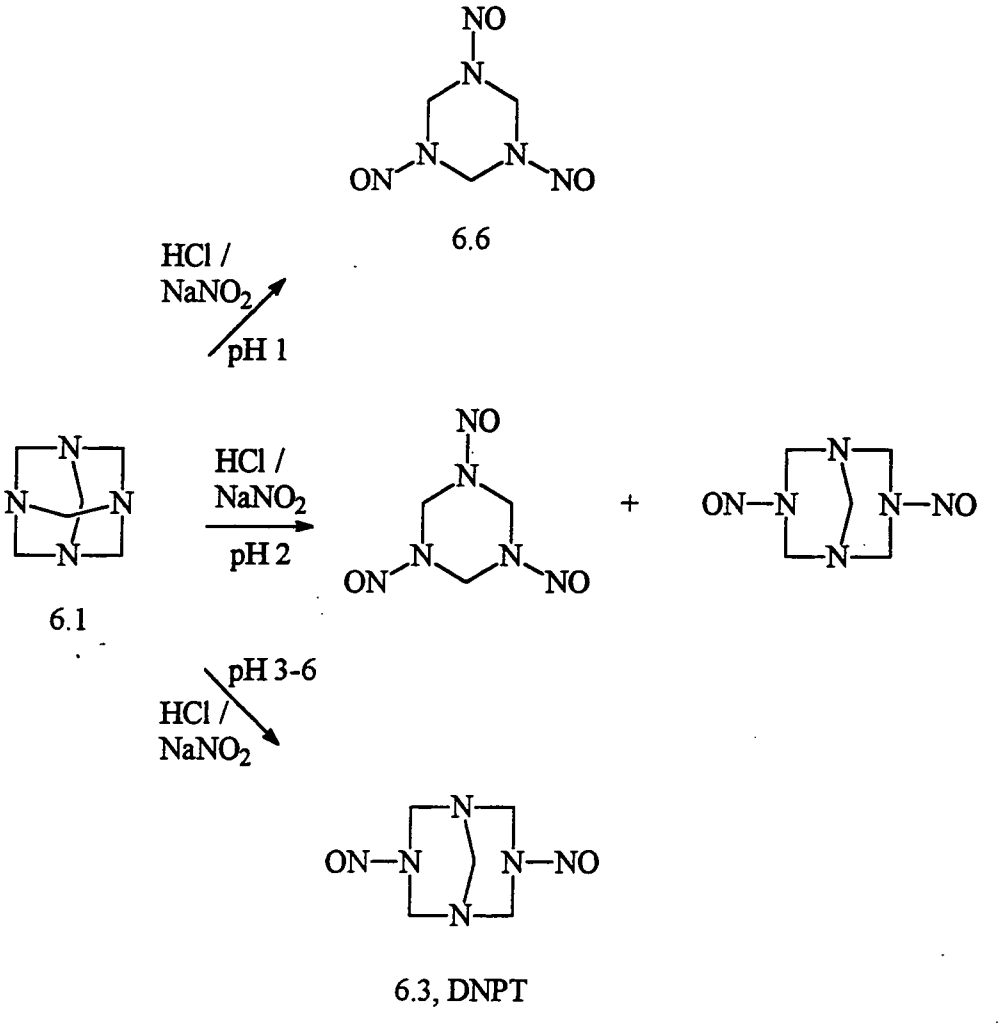

Scheme 6.2

The reaction between hexamine and fuming nitric acid leads to the formation[3] of 3,7-dinitro-1,3,5,7-tetraazabicyclo[3.3.1]nonane (dinitropentamethylenetetramine, DPT), 6.4, along with 1,3,5-trinitro-1,3,5-hexahydrotriazine (RDX), 6.7, equation 6.1.

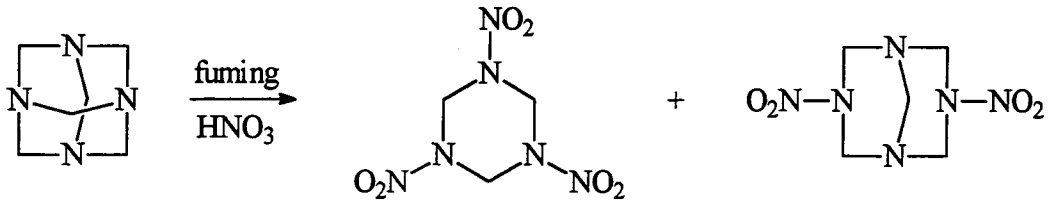

6.1 6.7, RDX 6.4, DPT

Equation 6.1

Two types of mechanism have been postulated[4-8] for the reaction of hexamine with electrophiles. One involves selective cleavage of the methylene bridge group, whilst in the other extensive ring cleavage occurs to species containing single amino - nitrogen fragments which then recombine to form the product.

The use of isotopic labelling has been used to elucidate the mechanisms by which acetylation, nitrosation and nitration proceed. By using mixtures of $^{14}N_4$- and $^{15}N_4$-hexamine and determining the destination of the nitrogen isotopes in the products by mass spectrometry it has been shown that nitrosation involves selective cleavage[9] of the methylene group. This is also the major mechanistic route for acetylation,[1] though the identification of small amounts of $^{14}N_3{}^{15}N$- and $^{14}N^{15}N_3$-DAPT in the product indicates that a small percentage of the reaction occurs through extensive break-up of the cage followed by recombination. Similarly, nitration has been shown[3] to react via the latter mechanism. The more severe reaction conditions used in nitration lead to the extensive break-up of the cage.

6.1.2 Kinetic studies

Studies on the protonation and acid catalysed decomposition of hexamine, DAPT, DNPT and DPT in water have been reported. Hexamine has a pK_a value of 4.89 in water and shows resistance to decomposition in weakly acidic solution.[10] There is also evidence for diprotonation in concentrated acid, with pK_{a2} -1.7, which is followed by decomposition to formaldehyde.

The presence of electron withdrawing groups ($COCH_3$, NO and NO_2) in the bicyclononane derivatives results in a considerable decrease in basicity compared to hexamine. The pK_a values in water have been calculated to be 0.7 for DAPT,[10] 1.1 for DNPT[9] and 0.8 for DPT[11] and are contained in table 6.1. Hence K_a values are a factor of ca. 10^4 smaller for the bicyclononanes than for hexamine.

Table 6.1. pK_a values for hexamine, DAPT, DNPT and DPT in water at 25 °C.

Compound	pK_a
Hexamine	4.89
DAPT	0.7
DNPT	1.1
DPT	0.8

6.2 Synthesis of DPT

DPT has been prepared using a modification[12] of the Hale[13] process. This involved the gradual addition of 10 g (0.071 mol) hexamine with stirring to 35 g fuming (> 95 %) nitric acid at 0 - 10 °C. On dilution of this solution with 100 cm^3 iced - water a white solid, RDX, separated out. This was filtered off and immediately destroyed by placing in aqueous sulphuric acid. The filtrate was neutralized with ammonia solution at 0 °C. DPT precipitated out as white solid, was washed with water and recrystallized from acetone. M. pt. 205 °C (lit.[12] 211.5 °C).

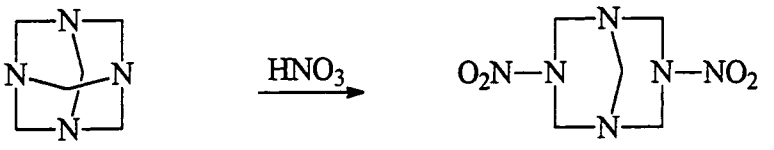

The ^1H N.M.R. spectrum of DPT in d_6-DMSO gave a signal at 4.14 ppm (s, CH_2 bridge) and an AB quartet (J = 13 Hz) for the four equivalent methylene groups with shifts of 4.96 ppm and 5.52 ppm as shown in fig. 6.1. The bands at δ 2.5 and 3.4 are due to the solvent and adventitious water, respectively.

Figure 6.1. ^1H NMR spectrum of DPT in d_6-DMSO.

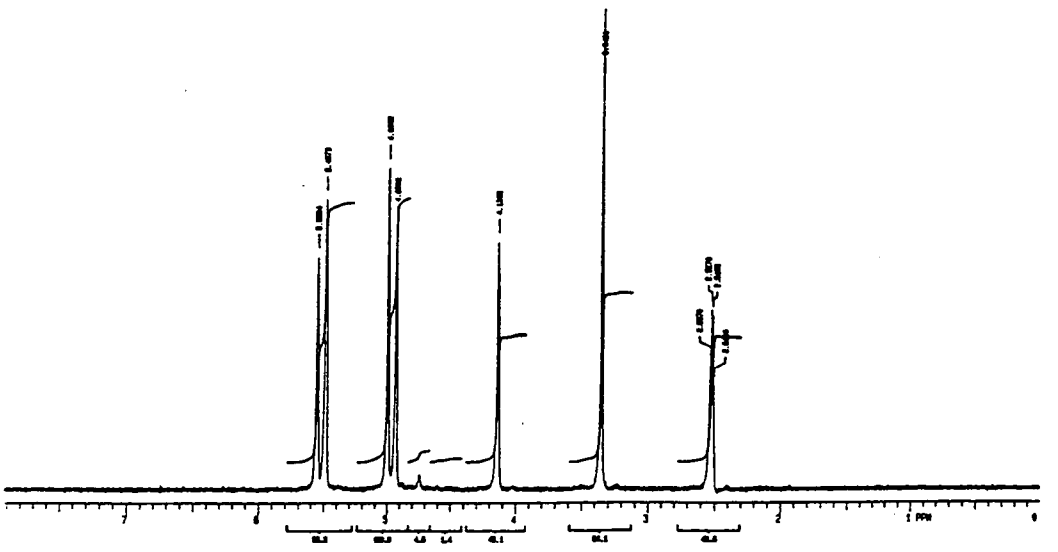

6.3 U.V. Spectrum of DPT

The work of Thorn and Jones[14] on aliphatic nitroamines has resulted in the following guidelines when interpreting U.V. spectra.

i) Primary Nitroamines

In neutral solution ε_{max} for a molecule containing a primary nitroamine function will be observed as approximately 7000 $dm^3\ mol^{-1}\ cm^{-1}$.

ii) Secondary Nitroamines

For compounds containing one secondary nitroamine function per molecule in neutral solution ε_{max} approximates to 5500 $dm^3\ mol^{-1}\ cm^{-1}$. Observation has indicated that for a molecule containing n secondary nitroamine functions ε_{max} approximates to 5500 x n $dm^3\ mol^{-1}\ cm^{-1}$.

The U.V. spectrum of 1 x 10^{-4} M DPT in acetonitrile, as shown in fig. 6.2, gives λ_{max} at 243 nm with ε = 11,500 $dm^3\ mol^{-1}\ cm^{-1}$. This is in good agreement with the 5500 x n formula for secondary nitroamines with n = 2.

Figure 6.2. U.V. spectrum of DPT in acetonitrile at 25 °C.

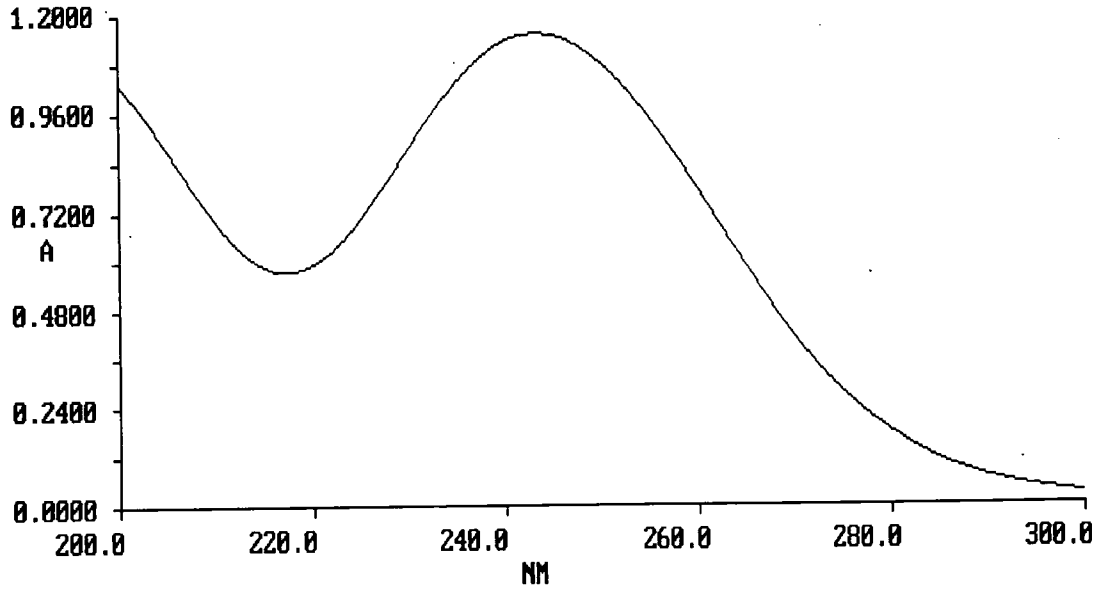

6.4 Protonation of DPT

DPT is stable in acetonitrile for several days. However, upon acidification there is a slight shift of λ_{max} to shorter wavelength accompanied by a slight decrease in absorbance. This initial hypsochromic shift is shown in fig. 6.3. Then follows a slower decomposition process through to nitramide, 6.8, and other products, as shown in equation 6.2. The absorbance gradually increases at 210 nm where nitramide is known to absorb, and decreases above 228 nm where an isosbestic is found. An example of this is shown in figure 6.4.

$$DPT + H^+ \rightleftharpoons DPTH^+ \longrightarrow 2NH_2NO_2 + 2NH_3 + 5CH_2O + H^+$$

6.8

Equation 6.2

Figure 6.3. U.V. spectrum of DPT (a) and DPT in the presence of perchloric acid (b) showing the intial hypsochromic shift.

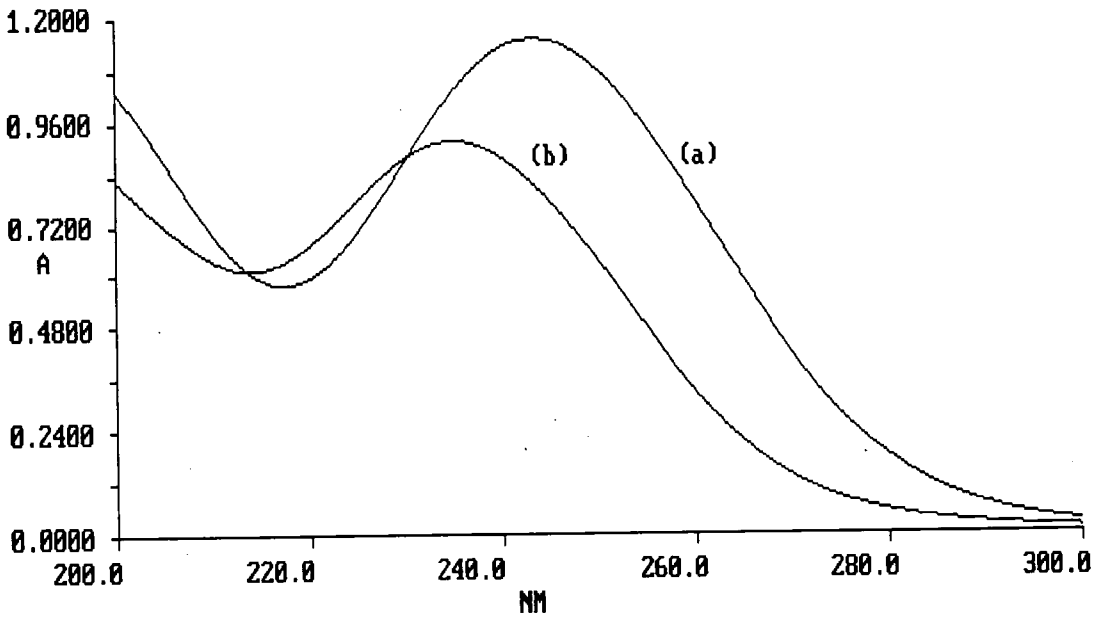

Figure 6.4. Decomposition of DPT in acidic media showing the formation of nitramide at 210 nm.

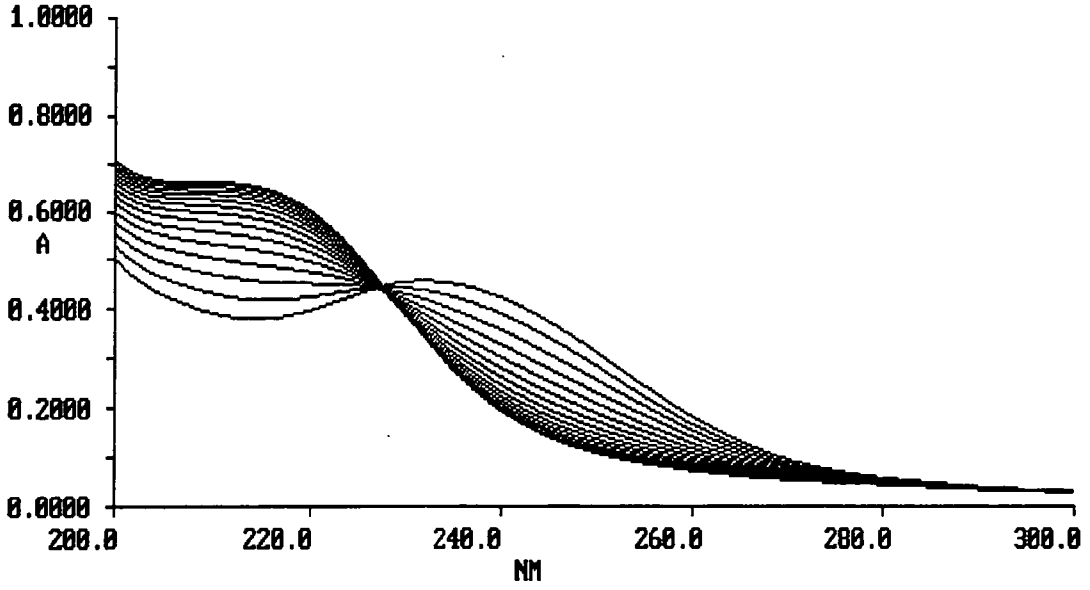

The decomposition in acetonitrile and in acetonitrile containing a low concentration of water has been studied by Crampton and Hamid.[15] An unusual result was that the protonation constant of DPT apparently decreased from a very high value ($> 10^3$) in acetonitrile to a value of ca. 10 in a medium containing 1 % (v/v) water. It was thought to be advisable to check this result.

The initial rapid change in absorbance was studied in several acid concentrations. The equilibrium constant was then calculated using eq. 6.3.

$$K_1 = \frac{[DPTH^+]}{[DPT][H^+]} = \frac{Abs(x) - Abs(y)}{\{Abs(y) - Abs(z)\}[H^+]} \qquad \text{equation 6.3}$$

where :-

Abs (x) = absorbance of DPT (unprotonated) in acetonitrile.

Abs (y) = absorbance of DPT (partially protonated) in acetonitrile containing perchloric acid.

Abs (z) = absorbance of DPT (fully protonated) in acetonitrile containing perchloric acid.

The value of Abs (z) often has to be estimated due to significant decomposition in higher acid concentrations.

In each experimental run the absorbance was measured both at 250 and 270 nm. K_1 values were calculated for both wavelengths. The results are shown in table 6.2. An extra set of runs was also done in the presence of 1.1 % (v/v) added water with the results shown in table 6.3.

Table 6.2. Equilibrium constant for the protonation of DPT[a] in acetonitrile.

10^2 x $[HClO_4]$ / mol dm^{-3}	Total H_2O % by vol.	Abs. at 250 nm	Abs. at 270 nm	$K_{(250)}$ [b] / dm^3 mol^{-1}	$K_{(270)}$ [c] / dm^3 mol^{-1}
0	0.050	1.0795	0.4208		
0.1	0.055	0.7867	0.2294	1869	1926
0.3	0.065	0.689[d]	0.161[d]		
0.6	0.080	0.6900	0.1639	1082	1263
1.0	0.100	0.6719	0.1577	973	1031
2.5	0.175	0.6357[e]	0.1377[e]		

a. The concentration of DPT is 1 x 10^{-4} mol dm^{-3}.

b. Fully protonated absorbance taken as 0.63.

c. Fully protonated absorbance taken as 0.13.

d. These absorbance values appear rather low resulting in inaccurately large equilibrium constants. Thus they were ignored.

e. At this acid concentration it is believed that the slower decomposition stage is significant and this will have reduced the absorbances from their true values.

A major source of error will also arise from the estimation of the fully protonated DPT absorbance (0.63 at 250 nm and 0.13 at 270 nm).

Table 6.3. Equilibrium constant for the protonation of DPT[a] in acetonitrile in the presence of 1.1 % added water.

10^2 x [HClO4] / mol dm^{-3}	Absorbance at 250 nm	Absorbance at 270 nm	$K_{(250)}$[b] / dm^3mol^{-1}	$K_{(270)}$[c] / dm^3mol^{-1}
0	1.107	0.462		
1	1.059	0.425	10.46	13.45
2	1.018	0.400	10.65	12.40
4[d]	0.882	0.315	19.95	22.27
7[d]	0.749	0.216	34.32	53.25
9[d]	0.658	0.188	86.02	80.12

a. The concentration of DPT is 1 x 10^{-4} mol dm^{-3}.

b. Fully protonated absorbance taken as 0.60.

c. Fully protonated absorbance taken as 0.15.

d. At the last three acid concetrations decomposition has become significant, reducing absorbance values and affording inaccurately large equilibrium constants.

Both these sets of results shown in tables 6.2 and 6.3 were obtained using a Perkin-Elmer Lambda 2 spectrophotometer. It has been estimated that the time taken from mixing the DPT and perchloric acid solutions to the machine scanning the mixture is about 14 seconds. Thus, even with a slow decomposition stage, the absorbance values obtained will not solely originate from the initial equilibrium. An attempt was made to minimise these errors by repeating the experiment with 1.1 % added water on a High-Tech Scientific SF-3L stopped-flow spectrophotometer. This reduces the time delay between mixing and obtaining measurements to 2 ms. This short time delay also allowed higher acid concentrations to be used, in which it was hoped to obtain a more accurate fully protonated DPT absorbance. Using the stopped-flow method, changes in voltages were measured at 260 nm. These were converted to absorbances via equation 6.4.

$$\text{Absorbance} = \log_{10}\left\{\frac{Vo}{Vo - \Delta V}\right\} \qquad \text{equation 6.4}$$

In the stopped-flow experiment cells of path length 2 mm are used and all measurements were made in the presence of 5×10^{-5} mol dm^{-3} DPT (c.f. 10 mm cells and 1×10^{-4} mol dm^{-3} DPT when using the Lambda 2 instrument). It can be seen from the Beer - Lambert law, equation 6.5, that reducing the path length, l, by a factor of five and the concentration, c, by a factor of two, then the absorbance will be reduced by a factor of ten.

Beer - Lambert Law $\quad$ Absorbance $= \varepsilon \, . \, c \, . \, l$ $\quad$ equation 6.5

To allow comparison with the earlier experiments all these absorbances have been multiplied by a factor of ten and are shown in table 6.4.

Table 6.4. Equilibrium constant for the protonation of DPT[a] in acetonitrile in the presence of 1.1 % added water (stopped-flow results).

$[HClO_4]$ / mol dm^{-3}	V_o / V	ΔV / V	Absorbance[b] at 260 nm	$K_{(260)}$[c] / dm^3 mol^{-1}	$K_{(260)}$[d] / dm^3 mol^{-1}
0	4.7	0.96	0.9923		
0.01	4.7	0.92	0.9461	7.15	6.64
0.02	4.7	0.92	0.9461	3.58	3.32
0.04	4.7	0.80	0.8103	8.92	8.12
0.07	4.7	0.72	0.7221	9.14	8.18
0.10	4.7	0.60	0.5931	13.62	11.64
0.20	4.7	0.48	0.4679	15.62	12.03

a. The concentration of DPT is 5×10^{-5} mol dm^{-3}.
b. Real values are a factor of 10 smaller as explained above.
c. Fully protonated absorbance taken as 0.30.
d. Fully protonated absorbance taken as 0.25.

The results, contained in table 6.4, calculated with two possible values for the fully protonated form, have some spread in values of K_1. However, they do indicate a value for K_1 of 10 ± 3 dm^3 mol^{-1} in 1.1 % water. These results confirm those reported previously.[15] The major factor causing the decrease in value of K_1 with added water is likely to be the strong hydration of the proton.

6.5 References

1. A. P. Cooney, M. R. Crampton, M. Jones and P. Golding, *J. Heterocycl. Chem.*, 1987, **24**, 1163.
2. W. E. Bachmann and N. C. Deno, *J. Am. Chem. Soc.*, 1951, **73**, 2777.
3. M. R. Crampton, M. Jones, J. K. Scranage and P. Golding, *Tetrahedron*, 1988, **44**, 1679.
4. W. E. Bachmann and J. C. Sheehan, *J. Am. Chem. Soc.*, 1949, **71**, 1812.
5. W. E. Bachmann, W. J. Horton, E. L. Jenner, N. N. MacNaughton and L. B. Scott, *J. Am. Chem. Soc.*, 1951, **73**, 2769.
6. W. E. Bachmann and E. L. Jenner, *J. Am. Chem. Soc.*, 1951, **73**, 2773.
7. E. A. Aristoft, J. A. Graham, R, H. Meen, G. S. Myery and G. F. Wright, *Can. J. Res.*, 1949, **27B**, 520.
8. A. O. Ralph, J. G. MacHutchin and C. A. Winkler, *Can. J. Chem.*, 1951, **29**, 725.
9. M. R. Crampton, J. K. Scranage and P. Golding, *J. Chem. Res.*, 1989, (S) 72.
10. A. P. Cooney, M. R. Crampton and P. Golding, *J. Chem. Soc. Perkin Trans. 2*, 1989, 835.
11. A. P. Cooney, M. R. Crampton, J. K. Scranage and P. Golding, *J. Chem. Soc. Perkin Trans. 2*, 1989, 77.
12. P. Golding, Ministry of defence, Private Communication.
13. G. C. Hale, *J. Am. Chem. Soc.*, 1925, **47**, 2754.
14. R. N. Jones and G. D. Thorn, *Can. J. Res.*, 1949, **27B**, 828.
15. J. Hamid, Ph.D. Thesis, Durham, 1992.

Chapter 7

Experimental Details

7.1 Measurement Techniques

7.1.1 U.V./Vis. Spectrophotometry

All U.V./vis. spectra were obtained from solutions in 1 cm path length quartz cells on a Perkin - Elmer Lambda 2 instrument. This instrument was also used to measure the kinetics of slow reactions ($t_{1/2}$ > 20 s). For rapid reactions (2 ms ≤ $t_{1/2}$ ≤ 20 s) a stopped-flow technique was used (section 7.1.2). Kinetic measurements were usually made under pseudo first order conditions at 298 K. Before reaction the freshly prepared solutions were placed in a water bath thermostatted at 298 K. The Lambda 2 cell holder was also maintained at this temperature with water from the water bath. The absorbance/time data were analysed using a computer fitting program PECSS (Perkin - Elmer Computerised Spectroscopy Software). This program determined the observed rate constants, k_{obs}, using a calculation based on the following derivation.
For a first order process A → B, the rate of formation of product, B, or removal of reactant, A, can be expressed by equation 7.1

$$-\frac{d[A]}{dt} = \frac{d[B]}{dt} = k_{obs}[A] \qquad \text{equation 7.1}$$

Integration of equation 7.1 gives an expression for the observed first order rate constant, k_{obs} (equation 7.2)

$$-\int_{[A]_0}^{[A]_t} \frac{1}{[A]} d[A] = \int_0^t k_{obs}\, dt$$

$$\ln[A]_t - \ln[A]_0 = -k_{obs}t$$

$$k_{obs} = \frac{1}{t}\ln\frac{[A]_0}{[A]_t} \qquad \text{equation 7.2}$$

Where $[A]_0$ and $[A]_t$ are the concentrations of A at times t = 0 and t = t respectively.

Using the Beer - Lambert law ($A = \varepsilon.c.l$, where A is the absorbance, ε is the molar extinction coefficient and l is the path length) and assuming the path length to be 1 cm, expressions for the absorbance at times $t = 0$ and $t = t$ can be derived (equations 7.3 and 7.4).

$$A_0 = \varepsilon_A [A]_0 \qquad \text{equation 7.3}$$

$$A_t = \varepsilon_A [A]_t + \varepsilon_B [B]_t \qquad \text{equation 7.4}$$

Ideally a wavelength is chosen where the absorbance of the reactant A is strong and that of the product B is negligible.

However, since $[B]_t = [A]_0 - [A]_t$, then substituting for $[B]_t$ into equation 7.4 gives:

$$A_t = \varepsilon_A [A]_t + \varepsilon_B [A]_0 - \varepsilon_B [A]_t \qquad \text{equation 7.5}$$

Now $A_\infty = \varepsilon_B [B]_\infty = \varepsilon_B [A]_0$ since $[B]_\infty = [A]_0$

Thus $(A_t - A_\infty) = \varepsilon_A [A]_t - \varepsilon_B [A]_t$

$$[A]_t = \frac{(A_t - A_\infty)}{(\varepsilon_A - \varepsilon_B)} \qquad \text{equation 7.6}$$

Similarly $A_0 = \varepsilon_A [A]_0$

and $A_\infty = \varepsilon_B [B]_\infty = \varepsilon_B [A]_0$

Hence $(A_0 - A_\infty) = \varepsilon_A [A]_0 - \varepsilon_B [A]_0$

$$[A]_0 = \frac{(A_0 - A_\infty)}{(\varepsilon_A - \varepsilon_B)} \qquad \text{equation 7.7}$$

Substituting equations 7.6 and 7.7 into equation 7.2 gives:

$$k_{obs} = \frac{1}{t} \ln \frac{(A_0 - A_\infty)}{(A_t - A_\infty)} \qquad \text{equation 7.8}$$

Rearrangement of equation 7.8 gives the form suitable for a graph:

$$\ln(A_t - A_\infty) = -k_{obs}t + \ln(A_0 - A_\infty) \qquad \text{equation 7.9}$$

Therefore a plot of $\ln(A_t - A_\infty)$ against t should be linear with a slope of $-k_{obs}$. The infinity values A_∞, were determined after a period of ten half lives and the decrease in absorbance followed for at least two half lives.

7.1.2 Stoppped-Flow Spectrometry

For measurement of rate constants too fast to measure by conventional methods a High - Tech SF-3 series stopped-flow spectrometer was used. This is shown schematically in figure 7.1. The two solutions to be reacted, A and B, are stored in reservoirs and are drawn into two identical syringes so that equal volumes are mixed. The syringes are compressed simultaneously by hand, and mixing occurs at point M extremely rapidly. The dead time of this machine is estimated to be 2 ms so reactions with half lives smaller than this cannot be measured by stoppped-flow techniques. The mixture flows into a thermostatted 2 mm path length quartz cell at point O. The plunger of the third syringe will hit a stop and the flow of solution will be stopped. Hitting the stop also triggers the acquisition of data from the reaction. The reaction is observed by passing a beam of monochromatic light of the appropriate wavelength through the cell by fibre optic cable. The light is passed through a photomultiplier and the change in voltage measured due to a change in absorbance of the solution is observed. The software used to run the stopped flow machines also transforms voltage/time data into absorbance/time data. It also calculates the observed rate constants.

The experiments on the protonation of DPT were performed before the instrument was run with the computerised software. The voltage/time data needed manual convertion to absorbance time data using equation 7.10.

$$\text{Absorbance} = \log_{10}\left\{\frac{Vo}{Vo - \Delta V}\right\} \qquad \text{equation 7.10}$$

Figure 7.1. Schematic of a stopped-flow spectrometer.

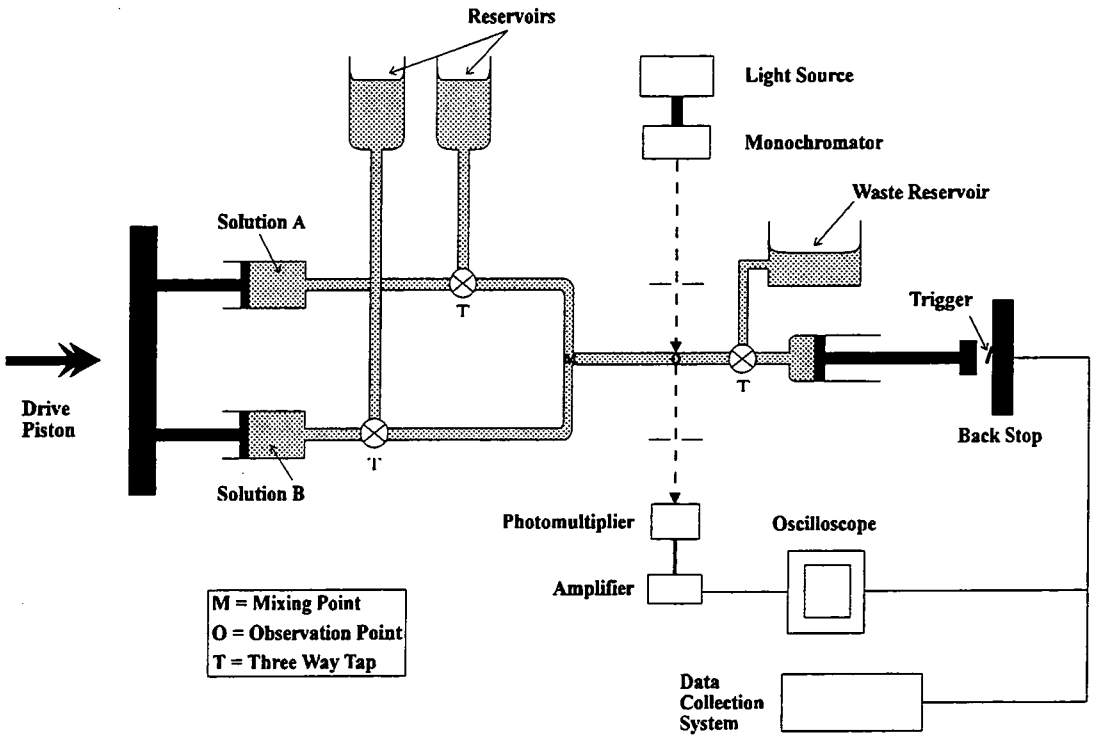

7.1.3 NMR Spectroscopy

All NMR spectra were recorded on either a Bruker AC 250 (250 MHz) machine or the following Varian machines XL 200, VXR 200, Gemini 200 (all 200 MHz) and Gemini 400 (400 MHz).

7.1.4 Mass Spectrometry

Mass spectrophotometric measurements were made with a Fisons V. G. Trio 1000 G.C. - Mass Spectrometer using the electron ionisation technique.

7.1.5 pH Measurements

All pH measurements were performed using a PTI-6 Universal digital pH meter (accurate to 0.02 pH units). The pH meter was calibrated over the range pH 4.0 to 7.0 or pH 7.0 to 10.0 depending on the solution to be measured.

7.2 Materials

7.2.1 Solvents

General purpose acetone and methanol were used for washing all apparatus. Solvents for synthetic work were of the highest grades. Specially dried diethyl ether for extractions was stored over sodium wire. "HiPerSolv Far U.V." grade for HPLC acetonitrile from BDH was used for synthetic and U.V./vis. experiments. However it was found that 1-ethoxy- and 1-phenoxy-2,4,6-trinitrobenzene were only stable in this solvent for short periods of time. For all trinitroaromatic work it was found that 99.9+ % HPLC grade acetonitrile from Aldrich was superior. High purity water was departmentally produced. For N.M.R. experiments acetonitrile-d_3, 99.5 atom % D containing 1 % v/v TMS and dimethyl sulphoxide-d_6 99.9 atom % D were used.

7.2.2 Reagents

All reagents purchased commercially were of the highest grades. Those needed to be synthesised were produced as follows.

DPT

DPT was prepared using a modification[1] of the Hale[2] process. This involved the gradual addition of 10 g (0.071 mol) hexamine with stirring to 35 g fuming (> 95 %) nitric acid at 0 - 10 °C. On dilution of this solution with 100 cm^3 iced - water a white solid, RDX, separated out. This was filtered off and immediately destroyed by placing in aqueous sulphuric acid. The filtrate was neutralized with ammonia solution at 0 °C. DPT precipitated out as white solid, was washed with water and recrystallized from acetone. M. pt. 205 °C (lit.[1] 211.5 °C).

N-benzyl-2-methylpent-2-ene-1-ylidenamine

To 36 ml propanal (0.5 mol) in 400 ml acetonitrile was added 55 ml benzylamine (0.5 mol) and the solution was stirred for 5 days at room temperature. After two hours a yellow tint was observed in the solution and this gradually intensified over the five day period. The acetonitrile was then removed by use of a rotary evaporator and the resulting mixture was fractionally distilled under reduced pressure (10 mm Hg) with use of a Vigreux column. Benzylamine distilled over at 65 °C and N-benzyl-2-methylpent-2-ene-1-ylidenamine distilled over between 128-130 °C as a yellow liquid.

2,4,6-Triethyl-1,3,5-hexahydrotriazine

Method 1

This method, as used by Nielsen and co-workers,[3] involved slow addition (30 mins) of 58 g propanal (1.0 mol) to 250 ml concentrated (16 mol dm^{-3}) aqueous ammonia solution (4 mol), maintaining the temperature below 5 °C with ice-bath cooling. The resultant clear solution was then stored at 0 °C for 5 days. Sodium chloride was added and the mixture stirred at room temperature for one hour, followed by extraction with four 100 ml portions of ether. The combined ether extracts were dried with magnesium sulphate, filtered and the solvent removed by rotary evaporator. The resulting liquid was pumped at 0.1 mbar for 1 hour affording 41.6 g (71 % yield) of clear colourless liquid. A temperature of below 25 °C was maintained during work-up.

Method 2

The second synthetic approach, developed in Durham, involved slow bubbling of dry ammonia gas into 400 ml acetonitrile over 2½ hours. During this period 0.5 mol ammonia gas dissolved in the acetonitrile. To this solution 6.0 g propanal was then added and the mixture left for 15 hours. The solution was dried using magnesium sulphate, filtered and then pumped at 0.1 mbar for 1 hour affording 3.03 g (50 % yield) of product, 4.5.

More recently it has been found that ammonia gas dissolves more efficiently in solvents at temperatures below -33 °C, the boiling point of ammonia. However it must be noted that the freezing point of acetonitrile is -48 °C.

Dichloroethanal

Dichloroethanal was prepared[4] from its diethyl acetal. To 50 g 1,1-dichloro-2,2-diethoxyethane were added 65 g benzoic anhydride and 5 ml concentrated sulphuric acid and the mixture was heated with stirring in an oil bath fitted with a Vigreux column to 210 °C. The product distilled over at 86 °C (lit.[4] 85 - 89 °C). affording 19.9 g (62 % yield) of dichloroethanal.

Pyrrolidinium, piperidinium and n-butylammonium perchlorates

Pyrrolidinium, piperidinium and n-butylammonium perchlorates have all been synthesised using the following method. To 200 ml diethyl ether was added 0.1 moles of amine (7.31 g or 9.88 ml for butylamine, 8.52 g or 9.89 ml for piperidine, 7.11 g or 8.35 ml for pyrrolidine) and the solution cooled to 0 °C using an acetone - carbice bath. This was followed by slow addition of 0.1 mol perchloric acid maintaining the temperature at 0 °C. The salts precipitated out of solution were filtered, washed with cold diethyl ether and dried above an oven. The formation of pyrrolidinium perchlorate was rather unsatisfactory, due to the salt being highly hygroscopic.

7.3 Derivation of Rate Equations

7.3.1 Formation of 3 - Adduct

For formation of the 3 - adduct equation 7.11 applies.

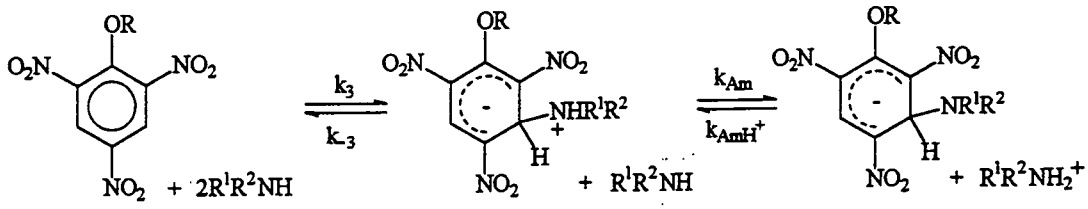

A B C

Equation 7.11

$$\frac{d[C]}{dt} = k_{Am}[Am][B] - k_{AmH^+}[AmH^+][C] \qquad \text{equation 7.12}$$

where Am is the reacting amine species R_1R_2NH.

$$\frac{d[B]}{dt} = k_3[Am][A] + k_{AmH^+}[AmH^+][C] - (k_{-3} + k_{Am}[Am])[B] \qquad \text{equation 7.13}$$

If the zwitterion, B, is treated as a steady - state intermediate then $\frac{d[B]}{dt} = 0$ and

$$[B] = \frac{k_3[Am][A] + k_{AmH^+}[AmH^+][C]}{k_{-3} + k_{Am}[Am]} \qquad \text{equation 7.14}$$

Subtituting for [B] into equation 7.12 and multiplying the $k_{AmH^+}[AmH^+][C]$ term by $\frac{k_{-3} + k_{Am}[Am]}{k_{-3} + k_{Am}[Am]}$ gives

$$\frac{d[C]}{dt} = \frac{k_3 k_{Am}[Am]^2[A] - k_{-3}k_{AmH^+}[AmH^+][C]}{k_{-3} + k_{Am}[Am]} \qquad \text{equation 7.15}$$

During the reaction the sum of the concentrations of the species A, B and C is equal to the initial, stoichiometric concentration of A. So

$$[A]_0 = [A] + [B] + [C]$$

Since B has been regarded as a steady - state intermediate, $[B] \approx 0$

Hence $$[A] = [A]_0 - [C]$$

Substituting for $[A]$ in equation 7.15 yields

$$\frac{d[C]}{dt} = \frac{k_3 k_{Am}[Am]^2[A]_0 - k_3 k_{Am}[Am]^2[C] - k_{-3} k_{AmH^+}[AmH^+][C]}{k_{-3} + k_{Am}[Am]}$$

equation 7.16

At equilibrium $\frac{d[C]}{dt} = 0$ and $[C] = [C]_{eq}$. So

$$0 = \frac{k_3 k_{Am}[Am]^2[A]_0 - k_3 k_{Am}[Am]^2[C]_{eq} - k_{-3} k_{AmH^+}[AmH^+][C]_{eq}}{k_{-3} + k_{Am}[Am]}$$

equation 7.17

Subtracting equation 7.17 from 7.16 gives

$$\frac{d[C]}{dt} = \left(\frac{k_3 k_{Am}[Am]^2 + k_{-3} k_{AmH^+}[AmH^+]}{k_{-3} + k_{Am}[Am]} \right) \left([C]_{eq} - [C] \right)$$

equation 7.18

This can be rewritten in the form

$$\frac{d[C]}{dt} \cdot \frac{1}{\left([C]_{eq} - [C] \right)} = \left(\frac{k_3 k_{Am}[Am]^2 + k_{-3} k_{AmH^+}[AmH^+]}{k_{-3} + k_{Am}[Am]} \right)$$

equation 7.19

The parent, A, does not absorb at the wavelength where the reaction is studied. The concentration of the steady - state intermediate, B, is negligible so that it too does not contribute to the absorbance at that wavelength. Hence the only absorbing species is the product, C. Using the Beer - Lambert law, absorbance = ε.c.l

$$Abs = \varepsilon_C[C].l \qquad \text{equation 7.20}$$

At equilibrium, $$Abs_{eq} = \varepsilon_C[C]_{eq}.l \qquad \text{equation 7.21}$$

Subtracting equation 7.20 from equation 7.21 gives

$$Abs_{eq} - Abs = \varepsilon_C\left([C]_{eq} - [C]\right)l \qquad \text{equation 7.22}$$

Differentiating equation 7.20 yields

$$\frac{dAbs}{dt} = \varepsilon_C l \frac{d[C]}{dt} \qquad \text{equation 7.23}$$

Division of this by equation 7.22 leads to equation 7.24.

$$\frac{dAbs}{dt}.\frac{1}{Abs_{eq} - Abs} = \frac{d[C]}{dt}.\frac{1}{[C]_{eq} - [C]} \qquad \text{equation 7.24}$$

k_{obs} is defined thus

$$k_{obs} = \frac{dAbs}{dt}.\frac{1}{Abs_{eq} - Abs} \qquad \text{equation 7.25}$$

Combination of equations 7.19, 7.24 and 7.25 gives the term for k_{obs}

$$k_{obs} = \left(\frac{k_3 k_{Am}[Am]^2 + k_{-3}k_{AmH^+}[AmH^+]}{k_{-3} + k_{Am}[Am]}\right) \qquad \text{equation 7.26}$$

Equation 7.26 is the general rate expression for formation of the 3 - adducts.

However, in acetonitrile it is known that aliphatic amines interact with their corresponding ammonium ions to produce homoconjugates,[5] as shown in equation 7.27. In the reactions studied the amine concentration is in vast excess over the salt. So the amine concentration will remain effectively unaltered but the final concentration of free ammonium ions will be reduced due to formation of these homoconjugates and a correction is needed for this in equation 7.26.

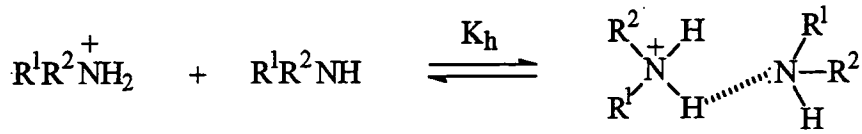

Equation 7.27

Where $$K_h = \frac{[\text{Homoconjugate}]}{[\text{Am}][\text{AmH}^+]_{eq}}$$ equation 7.28

Now, $$[\text{Homoconjugate}] = [\text{AmH}^+]_{stoich} - [\text{AmH}^+]_{eq}$$

Substituting this term for [Homoconjugate] in equation 7.28 and rearranging to obtain a term for $[\text{AmH}^+]_{eq}$ gives

$$[\text{AmH}^+]_{eq} = \frac{[\text{AmH}^+]_{stoich}}{1 + K_h[\text{Am}]}$$ equation 7.29

Substituting this term for $[\text{AmH}^+]$ in equation 7.26 yields equation 7.30, the general rate expression for formation of the 3 - adducts in acetonitrile.

$$k_{obs} = \frac{k_3 k_{Am}[\text{Am}]^2}{k_{-3} + k_{Am}[\text{Am}]} + \frac{k_{-3} k_{AmH^+}[\text{AmH}^+]}{(k_{-3} + k_{Am}[\text{Am}])(1 + K_h[\text{Am}])}$$ equation 7.30

7.3.2 Formation of 1 - Adduct

For formation of the 1 - adduct Scheme 7.1 applies. Formation of the 3 - adduct is rapid compared to that of the 3 - adduct.

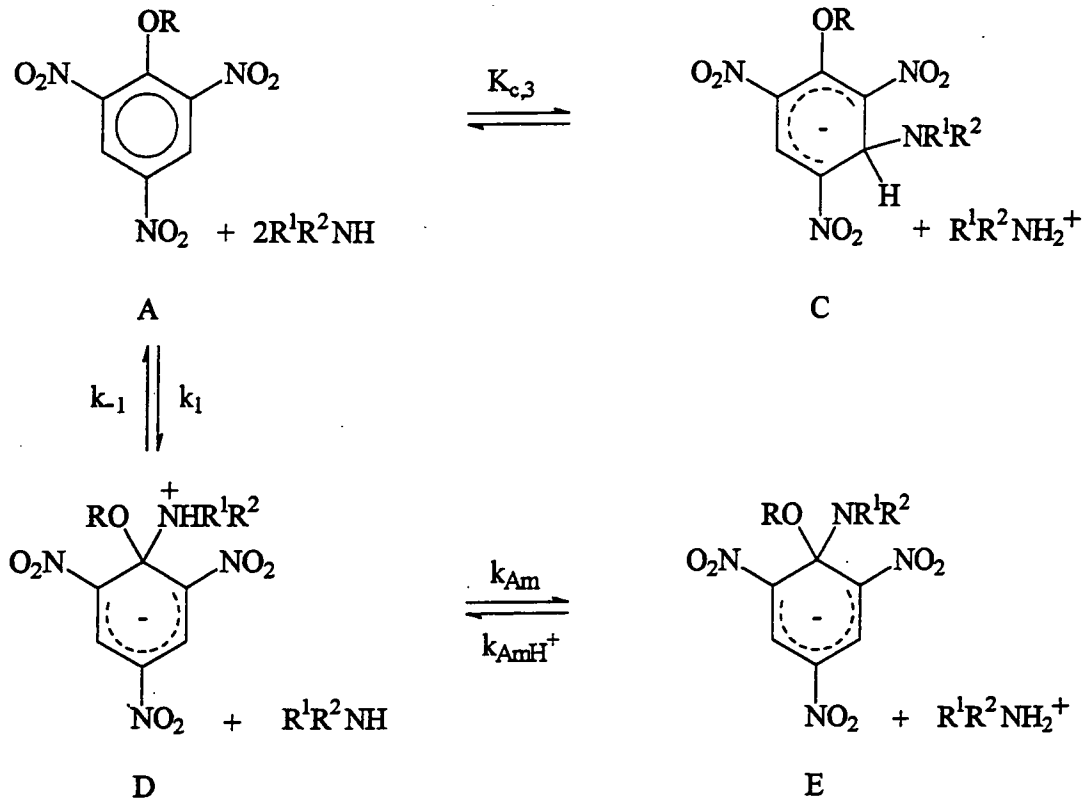

Scheme 7.1

Equation 7.31 is the rate expression for the formation of the 1 - adduct. It is derived in an analogous way to the corresponding equation for formation of the 3 - adduct.

$$\frac{d[E]}{dt} = \frac{k_1 k_{Am}[Am]^2[A] - k_{-1}k_{AmH^+}[AmH^+][E]}{k_{-1} + k_{Am}[Am]} \qquad \text{equation 7.31}$$

Now, $$[A]_0 = [A] + [C] + [E]$$ equation 7.32

and the overall equilibrium constant for formation of the 3 - adduct is

$$K_{c,3} = \frac{[C][AmH^+]}{[A][Am]^2}$$

This can be rewritten as

$$[C] = \frac{K_{c,3}[A][Am]^2}{[AmH^+]}$$ equation 7.33

Substituting for $[C]$ in equation 7.32 and rearranging to get a term for $[A]$ gives

$$[A] = \frac{[A]_0 - [E]}{1 + \frac{K_{c,3}[Am]^2}{[AmH^+]}}$$ equation 7.34

Substituting this term for $[A]$ in equation 7.31 yields

$$\frac{d[E]}{dt} = \frac{k_1 k_{Am}[Am]^2([A]_0 - [E])}{(k_{-1} + k_{Am}[Am])\left(1 + \frac{K_{c,3}[Am]^2}{[AmH^+]}\right)} - \frac{k_{-1}k_{AmH^+}[AmH^+][E]}{(k_{-1} + k_{Am}[Am])}$$

equation 7.35

At equilibrium $\frac{d[E]}{dt} = 0$ and $[E] = [E]_{eq}$. So

$$0 = \frac{k_1 k_{Am}[Am]^2([A]_0 - [E]_{eq})}{(k_{-1} + k_{Am}[Am])\left(1 + \frac{K_{c,3}[Am]^2}{[AmH^+]}\right)} - \frac{k_{-1}k_{AmH^+}[AmH^+][E]_{eq}}{(k_{-1} + k_{Am}[Am])}$$

equation 7.36

Subtracting equation 7.36 from 7.35 gives

$$\frac{d[E]}{dt} = \left(\frac{k_1 k_{Am}[Am]^2}{\left(k_{-1} + k_{Am}[Am]\right)\left(1 + \frac{K_{c,3}[Am]^2}{[AmH^+]}\right)} + \frac{k_{-1}k_{AmH^+}[AmH^+]}{\left(k_{-1} + k_{Am}[Am]\right)} \right) \left([E]_{eq} - [E]\right)$$

equation 7.37

This can be rewritten in the form

$$\frac{d[E]}{dt} \cdot \frac{1}{\left([E]_{eq} - [E]\right)} = \left(\frac{k_1 k_{Am}[Am]^2}{\left(k_{-1} + k_{Am}[Am]\right)\left(1 + \frac{K_{c,3}[Am]^2}{[AmH^+]}\right)} + \frac{k_{-1}k_{AmH^+}[AmH^+]}{\left(k_{-1} + k_{Am}[Am]\right)} \right)$$

equation 7.38

Both C and E are absorbing species at the wavelength used in the reaction. So, using the Beer - Lambert law, absorbance = ε.c.l

$$\frac{Abs}{l} = \varepsilon_E[E] + \varepsilon_C[C]$$ equation 7.39

From equation 7.32 it can be seen that

$$[C] = [A]_0 - [A] - [E]$$

Substituting this term for $[C]$ and the term for $[A]$ from equation 7.34 into equation 7.39, followed by rearrangement gives

$$\frac{Abs}{l} = [E]\left(\varepsilon_E - \frac{\varepsilon_C K_{c,3}[Am]^2[AmH^+]}{[AmH^+] + K_{c,3}[Am]^2} \right) + \frac{\varepsilon_C [A]_0 K_{c,3}[Am]^2[AmH^+]}{[AmH^+] + K_{c,3}[Am]^2}$$

equation 7.40

This can be simplified to the form

$$\frac{Abs}{l} = [E]Y + Z \qquad \text{equation 7.41}$$

where $Y = \varepsilon_E - \dfrac{\varepsilon_C K_{c,3}[Am]^2[AmH^+]}{[AmH^+] + K_{c,3}[Am]^2}$

and $Z = \dfrac{\varepsilon_C [A]_0 K_{c,3}[Am]^2[AmH^+]}{[AmH^+] + K_{c,3}[Am]^2}$

At equilibrium

$$\frac{Abs_{eq}}{l} = [E]_{eq} Y + Z \qquad \text{equation 7.42}$$

Subtracting equation 7.41 from 7.42 and multiplying both sides by l yields

$$Abs_{eq} - Abs = l([E]_{eq} - [E])Y \qquad \text{equation 7.43}$$

Differentiating equation 7.41 and multiplying both sides by l yields

$$\frac{dAbs}{dt} = l.Y\frac{d[E]}{dt} \qquad \text{equation 7.44}$$

Division of this by equation 7.43 leads to equation 7.45.

$$\frac{dAbs}{dt} \cdot \frac{1}{Abs_{eq} - Abs} = \frac{d[E]}{dt} \cdot \frac{1}{[E]_{eq} - [E]} \qquad \text{equation 7.45}$$

The definition of k_{obs} is

$$k_{obs} = \frac{dAbs}{dt} \cdot \frac{1}{Abs_{eq} - Abs} \qquad \text{equation 7.46}$$

Hence, combining equations 7.38, 7.45 and 7.46 yields the overall rate expression for formation of the 1-adducts.

$$k_{obs} = \frac{k_1 k_{Am}[Am]^2}{(k_{-1} + k_{Am}[Am])\left(1 + \frac{K_{c,3}[Am]^2}{[AmH^+]}\right)} + \frac{k_{-1} k_{AmH^+}[AmH^+]}{(k_{-1} + k_{Am}[Am])}$$

equation 7.47

In acetonitrile a correction for $[AmH^+]$ is needed in the final term due to the formation of homoconjugates. This is shown between equations 7.27 and 7.29 in the derivation of the rate expression for the 3 - adducts. Substituting the term for $[AmH^+]$ from equation 7.29 into equation 7.47 yields equation 7.48, the general rate expression for formation of the 1 - adducts in acetonitrile.

$$k_{obs} = \frac{k_1 k_{Am}[Am]^2}{(k_{-1} + k_{Am}[Am])\left(1 + \frac{K_{c,3}[Am]^2}{[AmH^+]}\right)} + \frac{k_{-1} k_{AmH^+}[AmH^+]_{st}}{(k_{-1} + k_{Am}[Am])(1 + K_h[Am])}$$

equation 7.48

7.3.3 Formation of the Picramides

For formation of the picramides equation 7.49 applies. This involves acid catalysed expulsion of the ethoxy leaving group from the 1 - adduct

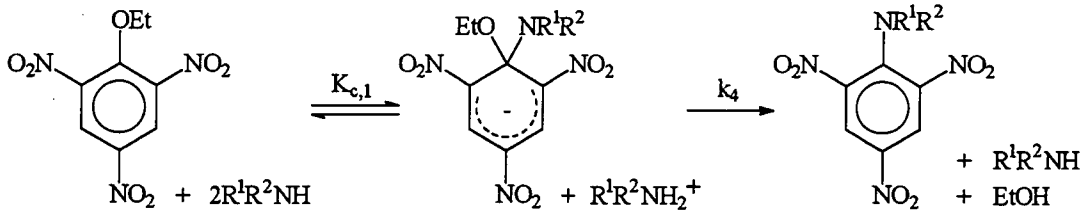

A E F

Equation 7.49

The reaction is followed by measuring the formation of the picramide, F. So

$$\frac{d[F]}{dt} = k_4[AmH^+][E] \qquad \text{equation 7.50}$$

Now, $$[A]_0 = [A] + [E] + [F] \qquad \text{equation 7.51}$$

and the overall equilibrium constant for formation of the 1 - adduct is

$$K_{c,1} = \frac{[E][AmH^+]}{[A][Am]^2}$$

Which can be rewritten in the form

$$[A] = \frac{[E][AmH^+]}{K_{c,1}[Am]^2} \qquad \text{equation 7.52}$$

Substituting for $[A]$ in equation 7.51 and rearranging to get a term for $[E]$ gives

$$[E] = \frac{K_{c,1}[Am]^2}{K_{c,1}[Am]^2 + [AmH^+]}\left([A]_0 - [F]\right) \qquad \text{equation 7.53}$$

Substituting for [E] in equation 7.50 gives

$$\frac{d[F]}{dt} = \frac{k_4 K_{c,1}[Am]^2[AmH^+]}{K_{c,1}[Am]^2 + [AmH^+]}\left([A]_0 - [F]\right) \qquad \text{equation 7.54}$$

At equilibrium $\frac{d[F]}{dt} = 0$ and $[F] = [F]_{eq}$. So

$$0 = \frac{k_4 K_{c,1}[Am]^2[AmH^+]}{K_{c,1}[Am]^2 + [AmH^+]}\left([A]_0 - [F]_{eq}\right) \qquad \text{equation 7.55}$$

subtracting equation 7.55 from 7.54 yields

$$\frac{d[F]}{dt} = \frac{k_4 K_{c,1}[Am]^2[AmH^+]}{K_{c,1}[Am]^2 + [AmH^+]}\left([F]_{eq} - [F]\right) \qquad \text{equation 7.56}$$

This can be rewritten in the form

$$\frac{d[F]}{dt} \cdot \frac{1}{\left([F]_{eq} - [F]\right)} = \frac{k_4 K_{c,1}[Am]^2[AmH^+]}{K_{c,1}[Am]^2 + [AmH^+]} \qquad \text{equation 7.57}$$

The picramide, F, is the only absorbing species at the wavelength which the reaction is followed. So, using the Beer - Lambert law, absorbance = ε.c.l

$$Abs = \varepsilon_F [F].l \qquad \text{equation 7.58}$$

At equilibrium

$$Abs_{eq} = \varepsilon_F [F]_{eq}.l \qquad \text{equation 7.59}$$

Subtracting equation 7.58 from 7.59 gives

$$Abs_{eq} - Abs = \varepsilon_F\left([F]_{eq} - [F]\right).l \qquad \text{equation 7.60}$$

Differentiating equation 7.58 yields

$$\frac{dAbs}{dt} = l.\varepsilon_F \frac{d[F]}{dt} \qquad \text{equation 7.61}$$

Division of this by equation 7.60 gives

$$\frac{dAbs}{dt} \cdot \frac{1}{Abs_{eq} - Abs} = \frac{d[F]}{dt} \cdot \frac{1}{([F]_{eq} - [F])} \qquad \text{equation 7.62}$$

The definition of k_{obs} is

$$k_{obs} = \frac{dAbs}{dt} \cdot \frac{1}{Abs_{eq} - Abs} \qquad \text{equation 7.63}$$

Hence, combining equations 7.57, 7.62 and 7.63 yields the overall rate expression for formation of the 1-adducts.

$$k_{obs} = \frac{k_4 K_{c,1} [Am]^2 [AmH^+]}{K_{c,1} [Am]^2 + [AmH^+]} \qquad \text{equation 7.64}$$

In acetonitrile a correction for $[AmH^+]$ is needed to the formation of homoconjugates. This is shown between equations 7.27 and 7.29 in the derivation of the rate expression for the 3 - adducts. Substituting the term for $[AmH^+]$ from equation 7.29 into equation 7.64 yields equation 7.65, the general rate expression for formation of the picramides in acetonitrile.

$$k_{obs} = \frac{k_4 K_{c,1} [Am]^2 [AmH^+]_{st}}{K_{c,1} [Am]^2 (1 + K_h [Am]) + [AmH^+]_{st}} \qquad \text{equation 7.65}$$

7.4 References

1. P. Golding, Ministry of defence, Private Communication.
2. G. C. Hale, *J. Am. Chem. Soc.*, 1925, **47**, 2754.
3. A. T. Nielsen, R. L. Atkins, A. T. Moore, R. Scott, D. Mallory and J. M. LaBerge, *J. Org. Chem.*, 1973, **38**, 3288.
4. J. Böeseken, F. Tellegen and M. Plusjé, *Rec. Trav. Chim.*, 1938, **57**, 73.
5. J. F. Coetzee and G. R. Padmanabhan, *J. Am. Chem. Soc.*, 1965, **87**, 5005.

APPENDIX

Research Colloquia, Seminars, Lectures and Conferences Attended

A.1 First Year Induction Course (October 1992)

The course consists of a series of one hour lectures on the services available in the department.

1. Introduction, research resources and practicalities.
2. Safety matters.
3. Electrical appliances and hands on spectroscopic services.
4. Departmental computing.
5. Chromatography and high pressure operations.
6. Elemental analysis.
7. Mass spectrometry.
8. Nuclear magnetic resonance spectroscopy.
9. Glassblowing techniques.

A.2 Research Colloquia, Seminars and Lectures Arranged by Durham University Chemistry Department 1992-1995. (*denotes lectures attended)

1992

October 15 Dr. M. Glazer & Dr. S. Tarling, Oxford University & Birbeck College, London.
It Pays to be British! - The Chemist's Role as an Expert Witness in Patent Litigation.

October 20 Dr. H. E. Bryndza, Du Pont Central Research.
Synthesis, Reactions and Thermochemistry of Metal (Alkyl) Cyanide Complexes and Their Impact on Olefin Hydrocyanation Catalysis.

* October 22 Prof. A. Davies, University College London.
The Ingold-Albert Lecture The Behaviour of Hydrogen as a Pseudometal.

October 28 Dr. J. K . Cockcroft, University of Durham.
Recent Developments in Powder Diffraction.

October 29 Dr. J. Emsley, Imperial College, London.
The Shocking History of Phosphorus.

November 4 Dr. T. P. Kee, University of Leeds.
Synthesis and Co-ordination Chemistry of Silylated Phosphites.

* November 5 Dr. C. J. Ludman, University of Durham.
Explosions, A Demonstration Lecture.

November 11 Prof. D. Robins, Glasgow University
Pyrrolizidine Alkaloids : Biological Activity, Biosynthesis and Benefits.

November 12 Prof. M. R. Truter, University College, London.
Luck and Logic in Host - Guest Chemistry.

November 18 Dr. R. Nix, Queen Mary College, London.
Characterisation of Heterogeneous Catalysts.

November 25 Prof. Y. Vallee, University of Caen.
Reactive Thiocarbonyl Compounds.

November 25 Prof. L. D. Quin, University of Massachusetts, Amherst.
Fragmentation of Phosphorous Heterocycles as a Route to Phosphoryl Species with Uncommon Bonding.

November 26 Dr. D. Humber, Glaxo, Greenford.
AIDS - The Development of a Novel Series of Inhibitors of HIV.

* December 2 Prof. A. F. Hegarty, University College, Dublin.
Highly Reactive Enols Stabilised by Steric Protection.

* December 2 Dr. R. A. Aitken, University of St. Andrews.
The Versatile Cycloaddition Chemistry of $Bu_3P.CS_2$.

* December 3 Prof. P. Edwards, Birmingham University.
The SCI Lecture - What is a Metal?

December 9 Dr. A. N. Burgess, ICI Runcorn.
The Structure of Perfluorinated Ionomer Membranes.

1993

January 20 Dr. D. C. Clary, University of Cambridge.
Energy Flow in Chemical Reactions.

January 21 Prof. L. Hall, Cambridge.
NMR - Window to the Human Body.

January 27 Dr. W. Kerr, University of Strathclyde.
Development of the Pauson-Khand Annulation Reaction : Organocobalt Mediated Synthesis of Natural and Unnatural Products.

* January 28 Prof. J. Mann, University of Reading.
Murder, Magic and Medicine.

February 3 Prof. S. M. Roberts, University of Exeter.
Enzymes in Organic Synthesis.

February 10 Dr. D. Gillies, University of Surrey.
NMR and Molecular Motion in Solution.

* February 11 Prof. S. Knox, Bristol University.
The Tilden Lecture Organic Chemistry at Polynuclear Metal Centres.

February 17 Dr. R. W. Kemmitt, University of Leicester.
Oxatrimethylenemethane Metal Complexes.

February 18 Dr. I. Fraser, ICI Wilton.
Reactive Processing of Composite Materials.

February 22 Prof. D. M. Grant, University of Utah.
Single Crystals, Molecular Structure, and Chemical-Shift Anisotropy.

February 24 Prof. C. J. M. Stirling, University of Sheffield.
Chemistry on the Flat-Reactivity of Ordered Systems.

* March 10 Dr. P. K. Baker, University College of North Wales, Bangor.
Chemistry of Highly Versatile 7-Coordinate Complexes.

* March 11 Dr. R. A. Y. Jones, University of East Anglia.
The Chemistry of Wine Making.

* March 17 Dr. R. J. K. Taylor, University of East Anglia.
Adventures in Natural Product Synthesis.

* March 24 Prof. I. O. Sutherland, University of Liverpool.
Chromogenic Reagents for Cations.

* May 13 Prof. J. A. Pople, Carnegie-Mellon University, Pittsburgh, USA.
The Boys-Rahman Lecture Applications of Molecular Orbital Theory.

* May 21 Prof. L. Weber, University of Bielefeld.
Metallo-phospha Alkenes as Synthons in Organometallic Chemistry.

* June 1 Prof. J. P. Konopelski, University of California, Santa Cruz.
Synthetic Adventures with Enantiomerically Pure Acetals.

June 2 Prof. F. Ciardelli, University of Pisa.
Chiral Discrimination in the Stereospecific Polymerisation of Alpha Olefins.

June 7 Prof. R. S. Stein, University of Massachusetts.
Scattering Studies of Crystalline and Liquid Crystalline Polymers.

June 16 Prof. A. K. Covington, University of Newcastle.
Use of Ion Selective Electrodes as Detectors in Ion Chromatography.

June 17 Prof. O. F. Nielsen, H. C. Orsted Institute, University of Copenhagen.
Low-Frequency IR and Raman Studies of Hydrogen Bonded Liquids.

* September 13 Prof. Dr. A. D. Schlüter, Freie Universität Berlin, Germany.
Synthesis and Characterisation of Molecular Rods and Ribbons.

September 13 Dr. K. J. Wynne, Office of Naval Research, Washington, USA.
Polymer Surface Design for Minimal Adhesion.

September 14 Prof. J. M. DeSimone, University of North Carolina, Chapel Hill, USA.
Homogeneous and Heterogeneous Polymerisations in Environmentally Responsible Carbon Dioxide.

September 28 Prof. H. Ila, North Eastern Hill University, India.
Synthetic Strategies for Cyclopentanoids via Oxoketene Dithioacetals.

October 4 Prof. F. J. Feher, University of California, Irvine, USA.
Bridging the Gap between Surfaces and Solution with Sessilquioxanes.

* October 14 Dr. P. Hubberstey, University of Nottingham.
Alkali Metals : Alchemist's Nightmare, Biochemist's Puzzle and Technologist's Dream.

* October 20 Dr. P. Quayle, University of Manchester.
Aspects of Aqueous ROMP Chemistry.

October 21 Prof. R. Adams, University of South Carolina, USA.
Chemistry of Metal Carbonyl Cluster Complexes : Development of Cluster Based Alkyne Hydrogenation Catalysts.

October 27 Dr. R. A. L. Jones, Cavendish Laboratory, Cambridge.
Perambulating Polymers.

November 10 Prof. M. N. R. Ashfold, University of Bristol.
High Resolution Photofragment Translational Spectroscopy : A New Way to Watch Photodissociation.

November 17 Dr. A. Parker, Rutherford Appleton Laboratory, Didcot.
Applications of Time Resolved Resonance Raman Spectroscopy to Chemical and Biochemical Problems.

* November 24 Dr. P. G. Bruce, University of St. Andrews.
Structure and Properties of Inorganic Solids and Polymers.

November 25 Dr. R. P. Wayne, University of Oxford.
The Origin and Evolution of the Atmosphere.

* December 1 Prof. M. A. McKervey, Queen's University, Belfast.
Synthesis and Applications of Chemically Modified Calixarenes.

* December 8 Prof. O. Meth-Cohn, University of Sunderland.
Friedel's Folly Revisited - A Super Way to Fused Pyridines.

December 16 Prof. R. F. Hudson, University of Kent.
Close Encounters of the Second Kind.

1994

January 26 Prof. J. Evans, University of Southampton.
Shining Light on Catalysts.

February 2 Dr. A. Masters, University of Manchester.
Modelling Water Without Using Pair Potentials.

February 9 Prof. D. Young, University of Sussex.
Chemical and Biological Studies on the Coenzyme Tetrahydrofolic Acid.

February 16 Prof. K. H. Theopold, University of Delaware, USA.
Paramagnetic Chromium Alkyls : Synthesis and Reactivity.

February 23 Prof. P. M. Maitlis, University of Sheffield.
Across the Border : From Homogeneous to Heterogeneous Catalysis.

* March 2 Dr. C. Hunter, University of Sheffield.
Noncovalent Interactions between Aromatic Molecules.

March 9 Prof. F. Wilkinson, Loughborough University of Technology.
Nanosecond and Picosecond Laser Flash Photolysis.

* March 10 Prof. S. V. Ley, University of Cambridge.
New Methods for Organic Synthesis.

March 25 Dr. J. Dilworth, University of Essex.
Technetium and Rhenium Compounds with Applications as Imaging Agents.

* April 28 Prof. R. J. Gillespie, McMaster University, Canada.
The Molecular Structure of some Metal Fluorides and Oxofluorides : Apparent Exceptions to the VSEPR Model.

* May 12 Prof. D. A. Humphreys, McMaster University, Canada.
Bringing Knowledge to Life.

* October 5 Professor N. L. Owen, Brigham Young University, Utah.
Determining Molecular Structure - the INADEQUATE NMR Way.

* October 19 Professor N. Bartlett, University of California.
Some Aspects of (AgII) and (AgIII) Chemistry.

October 26 Dr. G. Rumbles, Imperial College.
Real or Imaginary 3rd Order Non-Linear Optical Materials.

November 2 Dr. P. G. Edwards, University of Wales, Cardiff.
The Manipulation of Electronic and Structural Diversity in Metal Complexes - New Ligands for New Properties.

* November 9 Dr. G. Hogarth, University College, London.
New Vistas in Metal Imido Chemistry.

* November 16 Professor M. Page, University of Huddersfield.
Four Membered Rings and B-Lactamase.

* November 23 Dr. J. Williams, University of Loughborough.
New Approaches to Asymmetric Catalysis.

* November 30 Professor P. Parsons, University of Reading.
Applications of Tandem Reactions in Organic Synthesis.

December 7 Professor D. Briggs, ICI and University of Durham.
Surface Mass Spectrometry.

1995

January 25 Dr. D. A. Roberts, Zeneca Pharmaceuticals.
The Design and Synthesis of Inhibitors of the Renin - Angiotensin System.

February 1 Dr. T. Cosgrove, Bristol University.
Polymers do it at Interfaces.

February 8 Dr. D. O'Hare, Oxford University.
Synthesis and Solid State Properties of Poly- Oligo- and Multidecker Metallocenes.

* February 15 Professor W. Motherwell, University College, London.
New Reactions for Organic Synthesis.

February 22 Professor E. Schaumann, University of Clausthal.
Silicon- and sulphur-mediated ring opening reactions of epoxide.

* March 1 Dr. M. Rosseinsky, Oxford University.
Fullerene Intercalation Chemistry.

April 26 Dr. M. Schroder, University of Edinburgh.
Redox Active Macrocyclic Complexes: Rings, Stacks and Liquid Crystals.

May 3 Professor E. W. Randall, Queen Mary and Westfield College.
New Perspectives in NMR imaging.

May 24 Dr. P. Beer, Oxford University.
Anion Complexation Chemistry.

A.3 Conferences Attended

4th European Symposium on Organic Reactivity and 2nd Newcastle Meeting on Molecular Mechanisms in Bioorganic Processes, Newcastle, England, July 11 - 16, 1993.

International Union of Pure and Applied Chemistry.
12th conference on physical organic chemistry, Padova, Italy, August 28-September 2, 1994.
Poster presented: "Condensation Reactions of Amines and Carbonyl Compounds Leading to Cyclic Derivatives."

Royal Society of Chemistry Organic Reaction Mechanisms.
Seminars at :
SmithKline Beecham, Welwyn Garden City, September, 1993; and
Zeneca, Huddersfield, Yorkshire, September, 1994.